

Market Design for Integrated Energy Systems of the Future

Anubhav Ratha

PhD Thesis, March 2022, Kongens Lyngby, Denmark



DANMARKS TEKNISKE UNIVERSITET
Center for Electric Power and Energy (CEE)
DTU Electrical Engineering

**Market Design for Integrated Energy Systems of
the Future**

Dissertation, by Anubhav Ratha

Supervisors:

Professor Pierre Pinson, Technical University of Denmark

Associate Professor Jalal Kazempour, Technical University of Denmark

Senior Researcher Ana Virág, VITO, Belgium

DTU – Technical University of Denmark, Kongens Lyngby – March 2022

Market Design for Integrated Energy Systems of the Future

This thesis was prepared by:

Anubhav Ratha

Supervisors:

Professor Pierre Pinson, Technical University of Denmark

Associate Professor Jalal Kazempour, Technical University of Denmark

Senior Researcher Ana Virág, VITO, Belgium

Dissertation Examination Committee:

Associate Professor Spyros Chatzivasileiadis

Department of Electrical Engineering, Technical University of Denmark, Denmark

Professor Miguel F. Anjos

School of Mathematics, University of Edinburgh, United Kingdom

Associate Professor Alexandre Street

Electrical Engineering Department, Pontifical Catholic University, Rio de Janeiro, Brazil

Center for Electric Power and Energy (CEE)

DTU Electrical Engineering

Elektrovej, Building 325

DK-2800 Kgs. Lyngby

Denmark

Tel: (+45) 4525 3500

Fax: (+45) 4588 6111

E-mail: cee@elektro.dtu.dk

Release date: March 2022

Edition: 1.0

Class: Internal

Field: Electrical Engineering

Remarks: The dissertation is presented to the Department of Electrical Engineering of the Technical University of Denmark in partial fulfillment of the requirements for the degree of Doctor of Philosophy.

Copyrights: 2018 – 2022

ISBN: 000-00-00000-00-0

*Life can only be understood backwards,
but it must be lived forwards.*

— Søren Kierkegaard

Preface

This thesis was prepared at the Department of Electrical Engineering of the Technical University of Denmark (DTU) in partial fulfillment of the requirements for acquiring the degree of Doctor of Philosophy in Engineering. The Ph.D. project was funded by a research grant from Flemish Institute of Technological Research (VITO), Belgium and an internal DTU scholarship.

This dissertation summarizes the work carried out by the author during his Ph.D. project. It started on 1st December 2018 and was completed on 31st March 2022. During this period, he was hired by the Technical University of Denmark as a Ph.D. student at the Center for Electric Power and Energy (CEE) at the Department of Electrical Engineering.

The thesis is composed of four chapters which summarize the four attached scientific papers, three of which have been peer-reviewed and published, whereas one of them is currently under review.



Anubhav Ratha
31 March 2022

Acknowledgements

My Ph.D. journey over the last three years was a challenging yet enriching experience. This journey was possible only due to the support and guidance of numerous people, including my supervisors, colleagues, close friends, and family.

First, I am deeply grateful to my DTU Ph.D. supervisors Pierre Pinson and Jalal Kazempour for allowing me the opportunity to work with them. Thank you both for providing me with the freedom to pursue different research directions yet being always available for constructive discussions whenever I needed them. Thank you, Pierre, for your empathetic leadership and your guidance beyond academic matters, inspiring me and shaping me for the better. Thank you, Jalal, for your dedication and commitment to our research, and for always encouraging me to push my limits. You both taught me to believe in myself and the positive personal and professional values you instilled will stay with me.

Next, I am immensely thankful to my VITO Ph.D. supervisor Ana Virág for her advice and support, and for nudging me to broaden my horizons whenever I got too enchanted by the mathematical intricacies. Thank you, Ana, for hosting me during my stay in Belgium and for welcoming me to the E-Markets team at VITO. Thanks to Hélène and Shahab for our fruitful collaborations. Your challenging questions and insightful comments have greatly enriched my research journey.

I would like to thank all former and current members of the ELMA group at DTU for making my Ph.D. journey a memorable one through our friendships. It is a privilege to be a part of such a friendly and supportive research group. Unwinding together at conferences and social events is as integral a part of our culture as is our collaboration. A special thanks goes to Anna and Vladimir for introducing me to the Ph.D. student life at DTU and for making our collaboration a pleasurable and unique learning experience for me. Thanks to Yannick and Linde for our engaging (and ongoing) research discussions, which started towards the end of my Ph.D. journey. I am indebted to Andreas, Anna, Linde, Liyang, and Yannick for painstakingly proofreading parts of my thesis and providing me with valuable feedback. Thank you, Peter, for translating my abstract into Danish. Not every Ph.D. student has the honor of being a part of two great research teams. I am thankful to members of the VITO E-Markets team for making me feel at home in Belgium. Thanks to Anibal for your insightful comments on improving my thesis.

Next, I would like to thank my close friends in Denmark and all over the world. Thank you, Andreas, Valeska, Jochen, Eléa, and Amandine, for the happy times we spent together in these last years and for many more to come. Thanks to Tiago and Ana for our friendly discussions over a wide range of topics. Thank you, Anita and Vineet, for always being there to lend an understanding ear. Thanks to Aurabind and Arjav for your unwavering support over the years.

A special thanks to Satabdee for your support and for sharing your excitement and enthusiasm for research with me; it rekindled my passion for research whenever I needed a boost.

Last, but not least, my family has been an unwavering source of support, confidence, and encouragement throughout this journey. Thank you *Papa* for your wise counsel and for your relentless pursuit of research which inspires me continuously. Thank you *Mum* for your unconditional love and understanding, and for seeing the best in my abilities at times when I couldn't. *I dedicate my research work and this Ph.D. thesis to both of you.* I am grateful to my siblings – my sister, Mitali, my brother, Anurag, and my brother-in-law, Manas – for always being there for me, no matter what, and for motivating me to keep moving forward. A special thanks to my nephew, Arnav, for providing me with much-needed pleasurable distractions, the joy of watching you grow up has rejuvenated me throughout the years.

Vi ses,
Anubhav

Kgs. Lyngby, Denmark, March 2022

Table of Contents

Preface	i
Acknowledgements	iii
Table of Contents	v
List of Figures	vii
List of Tables	vii
Abstract	ix
Resumé	xi
1 Introduction	1
1.1 Context and motivation	1
1.2 Challenges in harnessing cross-carrier flexibility	2
1.3 Research directions	3
1.3.1 Flexibility-centric electricity markets	3
1.3.2 Uncertainty-aware coordination among energy systems	5
1.4 Scientific contributions	6
1.5 Thesis structure	8
1.6 List of publications	9
2 Flexibility-centric Electricity Markets	11
2.1 Beyond linear markets for energy systems	11
2.1.1 Nonlinearities and non-convexities in electricity markets	13
2.1.2 Towards conic markets for electricity	14
2.2 A general conic market for electricity	15
2.2.1 Towards a multi-period and multi-commodity electricity market	16
2.2.2 SOCP-based market clearing as centrally-solved optimization	17
2.2.3 Economic interpretations and equilibrium analysis	19
2.3 Case study: An uncertainty-aware electricity market	22
2.3.1 Adjustment policies: A flexibility service	23
2.3.2 Endogenous pricing of uncertainty: A simple example	26
2.3.3 Uncertainty-aware SOCP-based electricity market	28
2.4 Future perspectives	31
3 Uncertainty-Aware Coordination Among Energy Systems	33
3.1 Uncertainty propagation in integrated energy systems	33

3.1.1	Centralized electricity and natural gas dispatch under uncertainty	34
3.1.2	Challenges in studying uncertainty propagation	36
3.1.3	Towards uncertainty-aware integrated electricity and gas systems	37
3.2	Affine policies for harnessing cross-carrier flexibility	39
3.2.1	Towards a tractable SOCP problem	39
3.2.2	Numerical results	44
3.3	Stochastic control and pricing in natural gas networks	47
3.3.1	Towards an analytical gas network response model	47
3.3.2	Towards pricing the mitigation of uncertainty propagation	53
3.3.3	Numerical results	57
3.4	Future perspectives	60
4	Conclusions and Perspectives	61
4.1	Key findings	61
4.2	Perspectives for future research	62
Bibliography		65
Collection of relevant publications		75
[Paper A]	Moving from Linear to Conic Markets for Electricity	77
[Paper B]	Exploring Market Properties of Policy-based Reserve Procurement for Power Systems	129
[Paper C]	Affine Policies for Flexibility Provision by Natural Gas Networks to Power Systems	139
[Paper D]	Stochastic Control and Pricing for Natural Gas Networks	149

List of Figures

1.1	Illustration of the challenges in harnessing cross-carrier flexibility and the research directions adopted in this thesis	3
2.1	Illustration of commodities traded in an uncertainty-aware electricity market	24
2.2	Day-ahead dispatch and market prices for the deterministic benchmark and proposed uncertainty-aware market framework	28
2.3	Allocation of adjustment policies with chosen degrees of unbiasedness parameters . .	29
2.4	Spatial prices of energy in the 24-node network and optimal prices under the various RES paradigms	29
2.5	Expected in-sample market-clearing cost comparison with increasing RES share	30
2.6	Out-of-sample market-clearing cost comparison for the 50% RES paradigm	31
3.1	Illustration of a coupled electricity and natural gas system.	33
3.2	Uncertainty-aware coordinated electricity and natural gas dispatch	39
3.3	Expected day-ahead dispatch cost and ex-ante violation probability for various levels of reliability criteria set by the central system operator	45
3.4	Normalized relaxation gaps for the convex relaxations of the non-convex gas flow equations under uncertainty	46
3.5	Equivalence between uncertainty- and variance-aware gas-market clearing optimization to an equilibrium problem	53
3.6	Expected cost vs. pressure variance for various assignments of control policies	58
3.7	Effect of variance-agnostic and variance-aware gas system optimization on the variance of state variables	58
3.8	Comparison of total payments for the various gas system agents under different market-clearing frameworks	59

List of Tables

2.1	Comparison between expected market clearing costs for the deterministic benchmark and the proposed market-clearing framework	27
-----	--	----

Abstract

Global energy decarbonization relies on electricity systems with large shares of uncertain and variable renewable energy sources. Electrification of energy end uses such as transportation and space heating are further increasing the stochasticity of demand. As a result, system operators must procure additional operational flexibility to maintain a supply-demand balance in the presence of production and consumption forecast errors. Beyond flexible resources within the electricity system, short-term coordination among the various energy systems (e.g., electricity, natural gas, and district heating), provides additional flexibility which remains largely untapped. Harnessing this cross-carrier flexibility is appealing since it does not require large infrastructure investments, rather relying on effective coordination among the various actors in the energy systems. Furthermore, establishing this coordination in a market-based framework is essential to harness cross-carrier flexibility in a long-term and sustainable manner.

In this context, the objective of this thesis is to improve the market-based coordination among energy systems at operational time scales to incentivize, steer, and harness cross-carrier flexibility in competitive settings. The thesis contributes by developing new market-clearing frameworks for energy systems, relying on stochastic optimization techniques. Moreover, new commodities representing flexibility services, such as policy-based reserves, adjustment policies, and variance minimization services, are proposed which contribute towards a cost-efficient and reliable harnessing of cross-carrier flexibility. Using tools from mechanism design and game theory, the proposed market frameworks are evaluated for their ability to satisfy the desired economic properties of competitive markets, such as efficiency, cost recovery, and revenue adequacy.

To account for the heterogeneous flexibility providers in the integrated energy system, this thesis introduces a novel *flexibility-centric* electricity market-clearing framework. The proposed forward market admits participants with second-order cone strategy sets and revisits the classical spatial price equilibrium problem in a second-order cone programming context. Generalizing over the existing linear programming-based electricity markets, conic markets enable participants to accurately express the nonlinearities in their costs and constraints through conic bids, and the network operators to model a physically-accurate flow of energy in the networks. The inclusion of second-order cone constraints makes electricity markets uncertainty-, asset-, and network-aware, thereby incentivizing heterogeneous flexibility providers across the integrated energy system to participate in a market-based flexibility procurement. Under the assumption of perfect competition, it is analytically proven that moving towards conic electricity markets does not incur the loss of any desired economic properties inherent to the linear markets.

Harnessing cross-carrier flexibility is expected to propagate short-term uncertainty across the energy system boundaries. This adversely impacts the reliability and price competitiveness of the coupled energy systems due to network congestion and the resulting price spikes. To address that, a new *uncertainty-aware coordination* framework is proposed to model and mitigate the uncertainty propagation in coupled electricity and natural gas systems. Flexible assets in

both systems as well as the network flexibility provided by short-term storage of gas in pipelines are employed in mitigating the adverse effects of uncertainty propagating from the electricity to the gas side. Convexification strategies are adopted to manage the non-convexities underlying the gas system model in stochastic settings. An efficient pricing scheme is developed which endogenously considers uncertainty and the variance of state variables in the energy systems. In contrast to deterministic coordination among energy systems, market participants are remunerated (penalized) for their contribution to mitigating (aggravating) the adverse impacts of uncertainty.

Resumé

Den globale dekarbonisering er afhængig af elsystemer med store andele af usikre og variable vedvarende energikilder. En øget elektrificering til f. eks. transport og rumopvarmning øger efterspørgslen yderligere samt gør den mere stokastisk. Heraf følger det, at systemoperatører er nødt til at fremskaffe yderligere fleksibilitet i den daglige operationelle drift for at opretholde balancen mellem udbud og efterspørgsel som følge af prognoseusikkerheder af produktion og forbrug. Ud over fleksible ressourcer i elnettet giver kortsigtet koordinering mellem de forskellige energisystemer (f.eks. el, naturgas og fjernvarme) yderligere fleksibilitet, som er stort set udnyttet indtil nu. At udnytte denne fleksibilitet på tværs af operatører er tiltalende, da det ikke kræver store infrastrukturinvesteringer, men snarere er afhængigt af effektiv koordinering mellem de forskellige aktører i energisystemerne. Desuden er etableringen af denne koordinering i en markedsbaseret ramme afgørende for at udnytte fleksibiliteten på tværs af energisystemerne på en langsigtet og bæredygtig måde.

I denne kontekst er formålet med denne afhandling at forbedre den markedsbaserede koordinering mellem energisystemer på operationelle tidsskalaer for at tilskynde til, styre og udnytte tværgående fleksibilitet i et markedsbaseret miljø. Specialet bidrager ved at udvikle nye teknikker til at cleare markeder for energisystemer, baseret på stokastiske optimeringsteknikker. Desuden foreslås nye produkter, der repræsenterer fleksibilitetsydeler, såsom regelbaserede reserver, tilpasningsydeler og ydelser til minimering af varians, som bidrager til en omkostningseffektiv og pålidelig udnyttelse af fleksibilitet på tværs af energisystemer. Ved brug af mekanisme design og spilteori evalueres de foreslædede teknikker til at cleare markeder for deres evne til at tilfredsstille de ønskede økonomiske egenskaber på konkurrenceprægede markeder, såsom effektivitet, omkostningsdækning og indtægtstilstrækkelighed.

For at tage højde for de heterogene fleksibilitetsudbydere i det integrerede energisystem, introducerer denne afhandling en ny fleksibilitetscentreret ramme for clearing af elmarkedet. Det foreslæde forward marked tillader deltagelse med strategier af konisk form af andenordens grad, og det klassiske prisligevægtsproblem i en andenordens konisk programmerings kontekst bliver revideret. Ved at generalisere over de eksisterende elmarkeder baseret på lineær programmering gør markeder baseret på konisk programmering deltagerne i stand til nøjagtigt at udtrykke ikke-lineariteter i deres omkostninger og begrænsninger gennem koniske bud, og netværksoperatørerne kan modellere en nøjagtig fysisk strøm af energi i nettet. Inkluderingen af andenordens koniske begrænsninger gør elmarkederne usikkerheds-, aktiv- og netværksbevidste, hvilket giver incitament til heterogene fleksibilitetsudbydere på tværs af det integrerede energisystem til at deltage i markedsbaserede fleksibilitetsydeler. Under antagelsen om perfekt konkurrence er det analytisk bevist, at bevægelse mod koniske elmarkeder ikke medfører tab af ønskede økonomiske egenskaber, der er forbundet med de lineære markeder.

Udnyttelse af tværgående fleksibilitet i energisystemet forventes at propagere kortsigtet usikkerhed på tværs af energisystemets grænser. Dette påvirker de kobledes energisystemers pålidelighed

og priskonkurrenceevne negativt på grund af overbelastning af nettet og de deraf følgende prisstigninger. For at imødegå dette foreslås en ny usikkerhedsbevidst koordinationsramme for at modellere og afbøde præpareringen af usikkerhed i koblede el- og naturgassystemer. Fleksible aktiver i begge systemer såvel som netværksfleksibiliteten ved korttidsopbevaring af gas i rørledninger bruges til at afbøde de negative virkninger af usikkerhed, der forplanter sig fra elektriciteten til gassiden. Konvekse strategier er vedtaget for at håndtere de ikke-konveksiteter, der ligger til grund for gassystemmodellen i et stokastisk miljø. Der udvikles en effektiv prissætning, som endogent tager højde for usikkerhed og variansen af tilstandsvariable i energisystemerne. I modsætning til deterministisk koordinering mellem energisystemer bliver markedsdeltagere honoreret (straffet) for deres bidrag til at afbøde (forværre) de negative virkninger af usikkerhed.

CHAPTER 1

Introduction

1.1 Context and motivation

To address the challenge of climate change, countries are reducing their dependence on fossil fuels. This global energy transition is supported primarily by the increasing shares of uncertain and variable renewable energy sources (RES), such as wind and solar power production, in the electricity (or electric power) system [1]. Meanwhile, energy end uses, e.g., transportation and space heating, are undergoing electrification, which not only increases the volume of electricity demand but also its uncertainty and variability across time and space. Stochastic production and consumption must match in real-time to ensure a continuous supply-demand balance in the electricity grid. Any imbalance, if left uncorrected, may lead to large-scale cascading blackouts [2]. An adaptive, flexible operation of the electricity system is therefore crucial to achieving CO₂ emission reduction targets while ensuring reliable supply to consumers. This motivates electricity system operators to procure additional *operational flexibility*¹ to maintain the supply-demand balance in presence of the errors associated with production and consumption forecasts.

As a parallel development, various energy systems, such as electricity, natural gas, and district heating (or cooling) systems are becoming interdependent with increasing physical, operational, and economic interactions among them. Leveraging the synergies from this integration of energy systems has recently received significant attention as a source of operational flexibility [4, 5]. These synergies arise from the flexible operation of so-called *boundary agents*, who operate at the interface of the energy systems. Examples of such boundary agents include gas-fired power plants (using natural gas as fuel to produce electricity), combined heat and power (CHP) plants (typically, burning gas to produce heat and electricity), heat pumps (using electricity to provide heating), and the upcoming power-to-gas units (using electricity to produce hydrogen or natural gas). Energy conversion enabled by the flexible operation of boundary agents also allows the short-term storage of natural gas in pipelines and of hot (cold) water in the heating (cooling) supply networks. This form of network flexibility can be utilized to balance variability from RES in the electricity system.

In general, harnessing the existing *cross-carrier flexibility*² is appealing compared to investing in new flexibility options within the electricity system [6], such as setting up large-scale energy storages or expanding the transmission grids, or building new flexible power plants. Coordination among energy systems in the short-term (for instance, in the day-ahead of operation time scale) unlocks a significant amount of flexibility for the electricity system at low capital investment on infrastructure [7]. A holistic approach towards the coordinated operation of these energy systems is therefore regarded as the next step in their evolution, transforming them from the current practice of systems operating in silos towards an integrated energy system [8, 9].

¹In the context of this thesis, operational flexibility, or simply flexibility, refers to the capability of a system to modify its output or state in response to a signal. In electricity systems under uncertainty, the quantification of forecast errors (estimated or realized) could be such a signal. See [3] for a discussion on the various definitions of flexibility in the literature.

²Operational flexibility from energy system integration is termed as ‘cross-carrier flexibility’, referring to its origin from energy systems involving energy carriers other than electricity, e.g., natural gas, hot or cold water.

1.2 Challenges in harnessing cross-carrier flexibility

To leverage energy system integration for flexibility, physical coupling among the energy systems should be supported by coordinated planning and control [10–12] as well as coordination among the market structures [7].

Currently, markets in the various energy systems operate independently and asynchronously, i.e., energy products are traded as commodities in separate, pool-based wholesale forward markets which operate with different time scales and temporal resolutions. These forward markets ensure the security of energy supply and price competitiveness. Apart from the physically delivered commodities, long-term financial products are traded in futures markets, wherein the inherent risks and price volatility can be mitigated via hedging. This thesis focuses on the short-term wholesale forward markets of energy, which are typically cleared 12 to 36 hours ahead of the actual delivery of energy, i.e., at the day-ahead stage³. At these time scales, the markets are cleared under uncertainty about the production and consumption forecasts. In the specific context of electricity markets, procuring operational flexibility, e.g., cross-carrier flexibility, is crucial to the mitigation of uncertainty during the subsequent real-time operation stage.

Considering the multiple uncoupled markets to which boundary agents are exposed, market-based coordination among energy systems exists via the trading and operating strategies of such agents. However, such ad-hoc, agent-driven coordination is neither cost-optimal for the integrated system nor does it allow for a reliable harnessing of cross-carrier flexibility. Moreover, due to the sequential and separate nature of the energy markets, limited information exchange among the energy markets leads to a potential misrepresentation of the actual costs and constraints faced by the agents. Therefore, the cross-carrier flexibility potential is either over-estimated or remains under-utilized. Market mechanisms and products that enable *market-based coordination* among the actors in the various energy systems are crucial for optimally harnessing the available cross-carrier flexibility in a long-term and sustainable manner [19].

To that end, this thesis addresses some of the challenges associated with establishing market-based coordination among energy systems at operational time scales. Establishing market-based coordination faces challenges on technical, operational, economic, and regulatory fronts.

First, technical challenges arise from the mathematical complexity of modeling the energy system assets, especially while considering uncertainty. This is further exacerbated by the propagation of short- and long-term uncertainty among the energy systems, due to their interdependencies [20]. Second, there are operational challenges rooted in the different flow dynamics of energy vectors within the various networks, i.e., gas or water molecules and electrons. This makes the reliable operation of integrated energy systems a complex control problem spread over multiple geographical and temporal scales [7]. At the same time, the slower flow dynamics of gas and heat networks as compared to the electricity system enables these networks to provide network flexibility in the form of short-term energy storage [21, 22]. Third, there exist economic challenges in establishing efficient markets while taking the preferences and operational constraints of a variety of market actors into account. Thus, technology-agnostic and non-discriminatory markets, which do not favor any specific actor (or group of actors) based on their asset types, location, etc.,

³Interested readers are referred to [13] for a comprehensive introduction to electricity markets, while [14] provides the specific context of market integration of weather-dependent RES. Introduction to the natural gas system and markets can be found in [15, 16] and [17] provides an introduction to the district heating market in the Danish context. A discussion on the sequence of energy market clearings can be found in [18, Chapter 2].

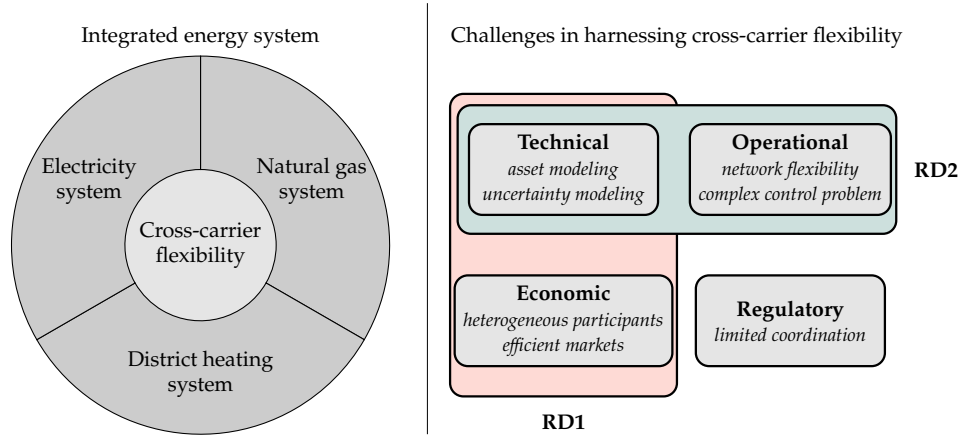


Figure 1.1: Illustration of the challenges in harnessing cross-carrier flexibility and the research directions (**RD1** and **RD2**) adopted in this thesis to address them. **RD1:** Flexibility-centric electricity markets, **RD2:** Uncertainty-aware coordination among energy systems.

are necessary yet challenging to achieve [23, 24]. Finally, regulatory challenges stem from the historically independent operations of these energy systems with limited coordination among the system operators and markets. While this operational paradigm continues to evolve with the coupling of energy systems due to the boundary agents, existing (and foreseen) regulatory barriers force these agents to make decisions with limited information.

Overcoming these various challenges with well-designed market-based coordination schemes paves the way to (i) increase the economic efficiency of the overall integrated energy system, (ii) enable the market actors to meet their operational goals, and eventually, (iii) lead to the right price signals for sustainable business models to unlock cross-carrier flexibility. To achieve these goals, a rethinking of existing market structures is necessary. Considering the multidimensional challenges involved, this thesis adopts a multidisciplinary research approach. In particular, concepts from energy system modeling are combined with control theory, stochastic programming, mechanism design, and game theory to develop and analyze new market-clearing frameworks and products to improve the market-based coordination for harnessing cross-carrier flexibility.

1.3 Research directions

As illustrated in Figure 1.1, this thesis presents the findings of two research directions addressing the aforementioned challenges. Focusing on the technical and economic challenges, the first direction, **RD1**, rethinks electricity markets such that flexibility is unlocked by steering the operation of heterogeneous market actors, i.e., those facing a variety of nonlinear physical costs and constraints. The second research direction, **RD2**, addresses the technical and operational challenges. A methodology is proposed for uncertainty-aware coordination between the electricity and natural gas systems, focusing on endogenous modeling of uncertainty and its propagation via boundary agents. A pricing scheme is developed to provide flexible agents with efficient financial remuneration for mitigating uncertainty. The following elaborates on these research directions.

1.3.1 Flexibility-centric electricity markets

Since the liberalization of the electricity sector, electricity markets in many countries typically have sought a *spatial price equilibrium*⁴ by solving a linear programming (LP) market-clearing problem.

⁴A spatial price equilibrium is a set of commodity prices and trade flows that satisfy partial equilibrium conditions over a network while accounting for the transportation costs and constraints associated with the trade flows [25].

When network constraints are fully taken into account, solutions to this problem include optimal production and consumption quantities and the spatially-differentiated nodal energy prices, also known as locational marginal prices (LMPs) [26, 27].

However, the LP framework is inadequate to match the following developments in electricity systems under the green transition. First, a majority of supply bids in the electricity markets are expected to arise from weather-dependent RES which incur a near-zero marginal production cost and are non-dispatchable, i.e., their real-time production can not be planned with a high degree of certainty [13, 28]. Consequently, short-term electricity markets are exposed to uncertainty, which should be endogenously considered in the market-clearing problem with more advanced uncertainty modeling tools than those available within the LP framework. Second, mitigating uncertainty requires a market-based procurement of operational flexibility, e.g., cross-carrier flexibility, from a variety of flexibility providers within the integrated energy system. These flexibility providers largely have nonlinear operational costs and constraints. Approximating these costs and constraints by linear functions renders it unattractive for these agents to provide flexibility. Third, with the inexact linear approximations that model power flows in the electricity network, markets may procure flexibility that cannot be physically delivered. This may lead to increased curtailment of RES and in the worst cases, risk disturbing the supply-demand imbalance.

Extending the spatial price equilibrium beyond the LP framework to more general convex optimization frameworks overcomes these limitations to a great extent. First, it enables physically accurate modeling of costs and constraints of the assets and energy flows in the networks comprising the integrated energy system. For instance, recent work by [29] extends electricity markets by the inclusion of quadratic costs faced by flexible power producers. Similarly, [30] proposes a pricing scheme for electricity networks considering a physically accurate nonlinear model for flows in electricity networks. Second, the extension beyond the LP framework provides opportunities to introduce a more accurate characterization of uncertainty and risk within the market-clearing framework. In that context, recent works [31, 32] propose stochastic electricity markets, involving nonlinear constraints, which outperform existing stochastic market clearing alternatives within the LP framework [33–35].

As reflected by this growing research focus (see, e.g., [36] for a recent comprehensive survey), it is clear that the prevalent LP-based electricity markets should evolve to meet future energy system needs. This evolution should be guided by several key considerations. Electricity markets do not need to fundamentally drift away from the goal of seeking a spatial price equilibrium, rather should be broadened to reflect the physical realities of the market participants and the network [23]. Existing economic interpretations and desired properties of the spatial price equilibrium must be retained while the electricity market design is extended to allow uncertainty modeling and mitigation in a cost-efficient way. Furthermore, electricity markets must evolve such that flexibility provision is rewarded appropriately [24]. This is crucial since revenues from flexibility products and services are expected to become more prominent for the market participants, as the average value of LMPs is suppressed while their volatility increases with higher shares of weather-dependent RES [37]. Prior works [29–32] adopt a limited view of addressing only one of the previously-discussed shortcomings of LP-based markets, lacking a broader rethinking of electricity markets to make them future-proof.

To this end, one of the research goals of this thesis is to propose a *flexibility-centric* electricity market-clearing framework. Such a market framework admits an endogenous consideration of

uncertainty and provides non-discriminatory access to a wide variety of heterogeneous flexibility sources within the integrated energy system to mitigate it. At the same time, the optimal production and consumption quantities are obtained while considering an accurate model for the flow of electricity in the network required to fulfill the energy and flexibility trades.

1.3.2 Uncertainty-aware coordination among energy systems

Harnessing operational flexibility from market-based coordination of integrated energy systems leads to increased interdependence. On the one hand, this necessitates that energy markets are cleared while taking system-coupling constraints into account. Recent research works have focused on that, e.g., clearing the electricity market while ensuring gas network constraints are met [38] or clearing the heat market while considering the flexibility needs of the coupled electricity system [39]. On the other hand, the interdependence also propagates short-term uncertainty from the electricity system to the coupled natural gas and district heating systems. This is evident from the increasing volumes of natural gas traded in short-term forward markets such as Gaspoint Nordic as opposed to the conventional long-term supply contracts, typical to the gas industry [40]. Further evidence is from China where electricity-agnostic heat dispatch of CHPs leads to constraint violations in the electricity system and curtailment of wind power production by up to 20% [41].

In particular, natural gas and electricity systems have become highly coupled due to the recent proliferation of gas-fired power plants, driven by their fast commissioning along with access to cheap gas supply⁵ [43, 44]. Gas-fired power plants have a lower CO₂ footprint and emit less particulate matter compared to conventional coal power plants while having the ability to rapidly change their production set points to provide operational flexibility. Consequently, natural gas is regarded as a ‘transition fuel’ in the evolving generation mix on the path towards decarbonization of electricity systems [45]. However, in providing operational flexibility to the electricity system, the natural gas system increasingly faces challenges caused by the short-term uncertainty in gas withdrawals [20]. Specifically, the gas demand from gas-fired power plants differs from traditional gas demands due to its time-varying and unpredictable nature. This leads to an increase in the frequency of network congestion and price spikes, thereby reducing the affordability of gas and reliability of the natural gas system [46].

The harnessing of cross-carrier flexibility should therefore be augmented by the consideration of *uncertainty propagation* among energy systems. Studying uncertainty propagation entails several aspects. First, the analytical and computational issues arising from nonlinearities and non-convexities inherent to the asset and network models of energy systems should be resolved. Second, probabilistic methods should be deployed to model various sources of uncertainty within the integrated energy system [47]. Third, recourse actions necessary to mitigate the uncertainty should be quantified and allocated among the flexibility providers. Next, the flexibility provided should be remunerated in a market-based, economically-efficient manner to ensure a reliable operation in the long term [48]. Finally, the impact of uncertainty propagation on the variance of state variables of the coupled network should be quantified, e.g., how does unpredictable gas uptake needed for the flexible operation of gas-fired power plants translate to changes in flow rates and nodal pressures in the gas system. Prior works, e.g., [49–51], have largely neglected these crucial aspects of uncertainty propagation across the energy system boundaries.

⁵Interestingly, as of March 2022, various geo-political reasons combined with a series of market trends and mishaps have led to historically high natural gas prices [42]. Therefore, some of the statements made in this thesis need rethinking based on future developments in this context.

Therefore, the second research goal of this thesis is to develop a methodology to steer the available cross-carrier flexibility while accounting for the uncertainty propagation among the energy systems. This involves developing uncertainty-aware models for flexibility providers, studying the impact of uncertainty propagation on operational constraints, and finally, developing market-clearing mechanisms that endogenously reward uncertainty and variance mitigation.

1.4 Scientific contributions

The primary objective of this thesis is to address challenges associated with harnessing cross-carrier flexibility by improving market-based coordination among energy systems. Aligned with the research directions introduced in Section 1.3, this is enabled (i) by proposing and analyzing a novel flexibility-centric design of electricity markets in [\[Paper A\]](#) and [\[Paper B\]](#), and (ii) by developing a new methodology for modeling and mitigating uncertainty propagation among the integrated energy systems in [\[Paper C\]](#) and [\[Paper D\]](#).

Towards flexibility-centric markets, [\[Paper A\]](#) proposes a new multi-period and multi-commodity forward electricity market-clearing framework which admits heterogeneous market participants with second-order cone (SOC) strategy sets. The resulting market-clearing problem takes the form of a second-order cone programming (SOCP) problem, which is a generalization of classical LP problems, within the convex optimization realm. Admitting SOC strategy sets in the market enables participants to express the SOC-representable nonlinearities in their costs and constraints. The multi-period market allows flexibility providers to reflect temporally-coupled costs and constraints in their market participation strategies. Multiple commodities in the market move the trades beyond electricity, i.e., towards endogenous consideration of a variety of possible flexibility services as additional commodities. The proposed SOCP-based electricity market-clearing framework results in scientific contributions from various perspectives.

From an operational perspective, the generic nature of the proposed market framework provides non-discriminatory access for flexibility providers within the integrated energy system. Moreover, admitting SOC constraints in the market-clearing problem enables a physically realistic representation of flows in the energy networks. Physical equations governing the steady-state flow of energy, when represented by SOC constraints, typically improve over the linear approximations used in LP-based markets [\[52\]](#). Leveraging the multi-commodity feature, system operators can introduce new flexibility products tailored to effectively harness various kinds of operational flexibility, as required to mitigate the adverse impacts of uncertainty during real-time operation. From a market design⁶ perspective, the proposed market-clearing framework is the first work to study spatial price equilibrium in a conic optimization framework. This is relevant to competitive settings beyond energy markets that involve physical or non-physical systems, where cost- and constraint-related nonlinearities are currently handled by linear approximations. In addition, desired economic properties of the market equilibrium, e.g., existence, uniqueness, market efficiency, cost recovery for the market participants, and revenue adequacy in the market, are analytically proven to hold under the assumption of perfect competition [\[27\]](#). This demonstrates that the economic principles and properties underlying the existing LP-based markets are retained while the electricity markets seek a conic spatial price equilibrium.

⁶In the context of this thesis, *market design* refers to auction-based marketplaces involving non-cooperative players who make simultaneous decisions under perfect but incomplete information about the game underlying the market clearing [\[53\]](#). This implies that players know their own strategy sets and cost functions perfectly, however the costs and strategy sets of their competitors are unknown to them [\[54\]](#). In this setting, classical concepts from mechanism design literature, e.g., [\[55, 56\]](#), are adopted in the thesis to evaluate the proposed market-clearing frameworks.

Considering the relevance of endogenous pricing of uncertainty, [Paper B] studies a specific variant of the general market framework proposed in [Paper A]. In [Paper B], a day-ahead stochastic electricity market-clearing mechanism is proposed wherein energy and flexibility in the form of operating reserves are procured jointly. Compared to the current practice of sequential, separate markets for procuring energy and flexibility adopted by a majority of electricity markets [57], the proposed co-optimization leads to a lower expected cost of system operation while providing guarantees for reliable operation despite the uncertain RES production. These cost savings arise from an optimal dimensioning of the amount of flexibility procured, enabled by considering uncertainty endogenous to the joint market clearing.

A new class of flexibility products, called *policy-based reserves* based on affine control policies [58] are studied. These policies are rules, agreed at the day-ahead market stage, that govern how flexibility providers respond to forecast error realizations during or close to real-time operation. Contrary to the capacity-based reserves, policy-based reserves, when considered in the joint market-clearing setting, tightly couple the flexibility provider's actual operational constraints with the delivery of the flexibility service. Consequently, the flexibility procured is priced dynamically, consistent with actual flexibility needs in the electricity system. While a market for energy and reserves based on affine policies within a robust optimization framework was proposed in [59], [Paper B] optimizes these policies in a chance-constrained optimization framework [60]. Employing chance-constrained optimization enables analytical proofs of the desired economic properties, built on mathematical tools from game theory and equilibrium analysis [61, 62].

Numerical results in [Paper A] and [Paper B] illustrate how the market redesign, coupled with the policy-based reserves, equip the electricity system operator with a tool to procure a risk-adjusted amount of flexibility from various flexibility providers in the integrated energy system. However, the adaptive response by agents in delivering flexibility leads to the propagation of short-term uncertainty across the energy system boundaries, which is addressed in [Paper C] and [Paper D].

Towards studying uncertainty propagation in integrated energy systems, [Paper C] develops a stochastic co-optimization of electricity and natural gas systems. In addition to the flexibility providers in both energy systems, network flexibility from short-term storage of gas in the pipelines of the gas network, i.e., *linepack flexibility*, is considered. Optimal recourse actions in the form of affine control policies are allocated such that the state variables in the gas system, i.e., nodal pressures and flows in pipelines, are adjusted to effectively harness the linepack flexibility. This ensures the availability of fuel for the withdrawals by gas-fired power plants to mitigate the uncertainty from RES in the coupled electricity system. The study of uncertainty propagation is modeled in a distributionally-robust chance-constrained optimization framework, which generalizes chance-constrained optimization by providing stronger reliability guarantees against unknown distributions. While a co-optimization of electricity and gas systems is not practical due to the regulatory barriers, the framework developed is relevant to system operators since it can be regarded as an ideal benchmark for market-based coordination among energy systems focused on uncertainty propagation.

From a methodological perspective, [Paper C] develops novel convexification approaches for nonlinear and non-convex flow dynamics of the gas network under uncertainty. These approaches are required to attain computational tractability of the stochastic co-optimization problem under the nonlinear and non-convex constraints. Out-of-sample simulations illustrate the trade-off faced by system operators between the expected day-ahead cost of operation and the robustness of the

solution against adverse uncertainty realizations. Furthermore, state variables in the gas system were found particularly susceptible to constraint violations that worsen the relaxation errors induced by the convexification step. Thus, establishing a strong analytical dependency between the random forecast errors and the response of the gas system is crucial to mitigate their effects.

To that end, [Paper D] establishes affine control policies such that gas system state variables admit closed-form analytical expressions involving nominal and recourse components. The recourse components depend on the actions of the controllable flexibility providers, i.e., gas suppliers and active pipelines hosting compressors or valves that provide pressure regulation. A linearization strategy is adopted to address the non-convexities in the gas system as opposed to convex relaxations in [Paper C]. The closed-form analytical characterization of state variables developed in [Paper D] results in scientific contributions from different perspectives.

From an operational perspective, system operators are provided with the confidence that the gas network state remains feasible during the real-time operation stage with a very high (preset) probability. Real-time constraint feasibility of the gas system is guaranteed, up to the quality of forecasts available at the day-ahead stage. *A priori* worst-case performance metrics defining the upper bounds on feasibility errors are provided. Further, analytical expressions for state variables enable a variance penalization scheme so that system operators can trade off the expected cost of operation with the variance of the state variables anticipated due to the uncertainty propagation.

From a market design perspective, a market-clearing framework for gas systems is developed, which is not only uncertainty-aware but also variance-aware⁷. In contrast to prevalent deterministic gas markets, the endogenous consideration of uncertainty and variance leads to an efficient pricing scheme for flexibility services mitigating these economic externalities. Consequently, market participants are remunerated (or penalized) for their contribution towards mitigating (or aggravating) uncertainty and variance. Leveraging a combination of LP and SOCP duality theory, the market-clearing outcomes are analytically proven to satisfy the desired economic properties, cost recovery and revenue adequacy, in expectation.

1.5 Thesis structure

This thesis introduces the main concepts underlying the research directions pursued and summarizes the contributions of the scientific publications during the Ph.D. project. While **Chapters 2-3** summarize the methodology and scientific contributions, the scientific publications attached in the Appendix provide details on relevant literature, methodology, and simulation results.

Focusing on the first research direction, **Chapter 2** discusses the contributions of this thesis towards harnessing cross-carrier flexibility enabled by flexibility-centric electricity markets. The first part introduces a general energy market-clearing problem and its relation to spatial price equilibrium. The need to move beyond linear markets for energy systems is motivated, considering the nonlinearities inherent to the asset and network models in these systems. The second part discusses the multi-period and multi-commodity conic electricity market, highlighting the methodological and theoretical contributions of [Paper A]. The last part discusses numerical results from [Paper A] and [Paper B] in the context of a specific variant of the general conic market, a two-commodity uncertainty-aware electricity market that entails endogenous pricing of uncertainty.

⁷While uncertainty-awareness refers to the mitigation of uncertain gas withdrawals by gas-fired power plants, variance-awareness refers to the ability to control the variance of state variables in the gas system with high fidelity.

Addressing the second research direction, **Chapter 3** presents the framework developed for studying uncertainty propagation from the electricity to the natural gas systems. The first part of the chapter introduces a general nonlinear and non-convex framework for studying uncertainty propagation in a coupled electricity and natural gas system in a centralized coordination paradigm. The challenges associated with studying uncertainty propagation are highlighted. The second part summarizes the methodological and numerical contributions of [**Paper C**] in developing and validating the convexification strategies which enable a tractable reformulation of the original non-convex problem. The last part discusses the contributions of [**Paper D**] in establishing a gas network response model to the uncertainty propagated and introduces an efficient pricing scheme for mitigation of uncertainty and variance of gas system state variables.

Chapter 4 concludes the thesis, summarizing its main contributions and discussing future research directions.

Notation: In the interest of notational coherence, mathematical formulations in this thesis have been adjusted compared to the original formulations in the scientific publications. The set of real and non-negative real numbers are denoted by \mathbb{R} and \mathbb{R}_+ . Upper case alphabets with a script typeface, such as \mathcal{A} , represent sets, while vectors are denoted by lower case boldface and matrices by upper case boldface alphabets. For a vector v , operator v^\top denotes its transpose, $\|v\|$ denotes its Euclidean norm and $\text{diag}(v)$ returns a diagonal matrix with vector v as the leading diagonal. The k -th element of vector v is retrieved as the scalar v_k whereas the operator $[\cdot]_k$ extracts the k -th element of a vector expression. $\mathbf{0}$ and $\mathbf{1}$ are vectors of zeros and ones. For a matrix $M \in \mathbb{R}^{p \times q}$, $[M]_{(:,k)} \in \mathbb{R}^p$ retrieves its k -th column while $[M]_{(k,:)} \in \mathbb{R}^{1 \times q}$ retrieves its k -th row. The operator $\text{tr}(M)$ returns the trace of the matrix M , while the expression $M \succ 0$ indicates its positive-definiteness. Arithmetic operators \leqslant , $=$, and \geqslant on vectors and matrices are understood element-wise. Operation \circ is the element-wise product while \otimes denotes the Kronecker product.

1.6 List of publications

The relevant publications which are summarized in this thesis are listed as follows:

- [**Paper A**] A. Ratha, P. Pinson, H. Le Cadre, A. Virag and J. Kazempour, "Moving from Linear to Conic Markets for Electricity," submitted to *European Journal of Operational Research*, (under review, first round), 2021.
- [**Paper B**] A. Ratha, J. Kazempour, A. Virag and P. Pinson, "Exploring Market Properties of Policy-based Reserve Procurement for Power Systems," in *2019 IEEE 58th Conference on Decision and Control (CDC)*, 2019, pp. 7498-7505, doi: 10.1109/CDC40024.2019.9029777.
- [**Paper C**] A. Ratha, A. Schwele, J. Kazempour, P. Pinson, S. Shariat Torbhagan and A. Virag, "Affine Policies for Flexibility Provision by Natural Gas Networks to Power Systems," in *Electric Power Systems Research*, Volume 189, 2020, doi: 10.1016/j.epsr.2020.106565.
- [**Paper D**] V. Dvorkin, A. Ratha, P. Pinson and J. Kazempour, "Stochastic Control and Pricing for Natural Gas Networks," in *IEEE Transactions on Control of Network Systems (Early Access)*, 2021, doi: 10.1109/TCNS.2021.3112764.

The following publications have also been prepared during the Ph.D. study, but have been omitted from the thesis because they are not directly related to the primary objective.

[Pub. E] A. Ratha, P. Pinson, H. Le Cadre and J. Kazempour, "Statistical Learning in Strategic Environments: An Energy Market Perspective," (Working paper).

[Pub. F] Y. Werner, A. Ratha and J. Kazempour, "Network-Aware Procurement of Reserves in Electricity Markets" (Working paper).

CHAPTER 2

Flexibility-centric Electricity Markets

This chapter presents the contributions of this thesis towards proposing a novel electricity market-clearing framework based on SOC constraints. Including SOC constraints improve uncertainty-, asset-, and network-awareness of the electricity market, which among other advantages within the electricity system, helps unlock cross-carrier flexibility. Using an illustrative energy market-clearing problem, Section 2.1 motivates the move beyond LP-based markets by highlighting nonlinearities and non-convexities in energy systems. Leveraging the market framework developed in [Paper A], Section 2.2 formulates a multi-period, multi-commodity conic electricity market and provides theoretical results associated with the market equilibrium. An uncertainty-aware variant of the general conic market is presented in Section 2.3 and numerical results based on [Paper A] and [Paper B] are discussed. Finally, Section 2.4 discusses future research perspectives.

2.1 Beyond linear markets for energy systems

Energy markets seek to achieve a spatial price equilibrium with optimal prices and trade flows that satisfy partial equilibrium conditions over a network [63, 64]. Historically, such problems rely on LP theory to derive the marginal prices [65], leading to linear energy markets. However, the LP framework is limiting in energy systems as it fails to accurately represent the operational characteristics of physical assets and the network. These limitations are highlighted in the following via an illustrative market-clearing problem.

Consider a pool-based energy market with market participants (buyers and sellers) collected in a set $\mathcal{I} = \{1, 2, \dots, I\}$, where $I \geq 2$. Let $\mathbf{q}_i \in \mathcal{Q}_i$ denote the decision vector of the i -th participant drawn from a strategy set \mathcal{Q}_i . Let each participant incur a cost function $c_i(\mathbf{q}_i)$, increasing in \mathbf{q}_i . Assume a sign convention: $c_i(\mathbf{q}_i) \geq 0$ applies to sellers, indicating a convex cost of selling, whereas $c_i(\mathbf{q}_i) \leq 0$ applies to buyers, indicating a concave utility of buying. In a two-sided auction framework, price-quantity sell offers and buy bids are matched by an auctioneer to maximize the social welfare, contingent on the spatial constraints¹. In its abstract form, this network-based market clearing is given by a centrally-solved optimization problem

$$\min_{\mathbf{q}_i} \sum_{i \in \mathcal{I}} c_i(\mathbf{q}_i) \quad (2.1a)$$

$$\text{s.t. } \mathbf{q}_i \in \mathcal{Q}_i, \forall i \quad (2.1b)$$

$$f^M(\{\mathbf{q}_i\}_{i \in \mathcal{I}}) \in \mathcal{F}^M \quad (2.1c)$$

$$f^N(\{\mathbf{q}_i\}_{i \in \mathcal{I}}) \in \mathcal{F}^N, \quad (2.1d)$$

¹Not all energy markets involve such two-sided auctions. For instance, due to limited competition and the critical nature of the heat supply, the heat market in the Greater Copenhagen area is organized based solely on least-cost dispatch considering technical limits of the heat producers and the district heating network, such that heat producers compete on production costs while the retail prices are predetermined and fixed [66].

where a market operator (acting as the auctioneer) minimizes social disutility (or maximizes social welfare) in (2.1a) subject to the individual constraints of each participant (2.1b) and coupling constraints (2.1c) - (2.1d) involving decision vectors of multiple participants.

The continuous, vector-valued functions $f^M(\cdot)$ and $f^N(\cdot)$ comprising the coupling constraints ensure that the allocations $\{q_i\}_{i \in \mathcal{I}}$ are in feasible sets \mathcal{F}^M and \mathcal{F}^N , respectively. The function $f^M(\cdot)$ typically encodes information about the location of participants within the network and their preferences on quantities to trade. Accordingly, the set \mathcal{F}^M contains allocations $\{q_i\}_{i \in \mathcal{I}}$ that are *market-feasible*, implying that the market-clearing conditions, e.g., supply-demand balance, are satisfied. The function $f^N(\cdot)$ transforms the participant-specific quantities bought or sold to physical flows in the network required to fulfill the trades during physical delivery. Therefore, the set \mathcal{F}^N contains allocations that are *network-feasible*, i.e., allocations resulting in energy flows in the network that remain within the network limits. Such network limits include flow capacities, physical bounds on state variables, network operator's safety limit prescriptions, etc. While marginal prices are determined from shadow prices associated with (2.1c), shadow prices associated with (2.1d) can be interpreted as prices that arise from reaching network limits². In energy systems, the set of network-feasible allocations \mathcal{F}^N is generally larger than the set of market-feasible allocations \mathcal{F}^M . As a result, possibly multiple optimal solutions to problem (2.1) are obtained contingent to market feasibility in (2.1c) and a minimum of social disutility (2.1a) subject to individual constraints (2.1b).

Convexity of the centrally-solved market-clearing problem (2.1) is highly desirable since it enables deriving *globally optimal* prices and quantities leveraging Lagrangian duality [68, Chapter 5] as opposed to locally optimal solutions. Economic interpretations for such pool-based markets arise from the equivalence of the optimization problem (2.1) with a spatial price equilibrium involving non-cooperative players [69]: market participants, a network operator, and a market operator³. In classical game theory, the existence of Nash equilibria in such equilibrium problems is given under common assumptions of convexity and compactness of the players' strategy sets and continuity of their cost functions [71]. With the optimization-equilibrium problem equivalence, the uniqueness of the market-clearing outcomes, i.e., optimal quantities and prices, are conditioned on the strict convexity of cost functions comprising the objective function (2.1a) [72, Chapter 16]. In energy systems, satisfying these assumptions requires convex approximations and relaxations due to the nonlinearity and non-convexity of the physical characteristics of participants and the network⁴.

In the specific case of the electricity system, based on a number of simplifying assumptions, many countries adopt an LP-based market-clearing problem to obtain the optimal quantities and prices. However, the limitations due to these assumptions are now exacerbated in electricity systems under the green transition, wherein appropriately harnessing and remunerating flexibility is essential. In the context of problem (2.1), these assumptions and their limitations in addressing the nonlinearities and non-convexities faced by electricity markets are discussed.

²For instance, [Paper D] employs the gas network operator's prescribed variance criteria to obtain a price for high variance of state variables (nodal pressures and gas flows) in the network. See [32, 67] for applications of such variance minimization technique to power flows in electricity network.

³The separation of roles of the network operator and the market operator may be virtual since energy markets around the world adopt various organizational structures to assign these roles. For instance, electricity markets in the United States adopt a consolidation of these roles into an independent system operator (ISO), see e.g., [70], whereas markets in Europe typically have separate entities responsible for operating the network and the market, respectively.

⁴As an example, the steady-state flow of gas in pipelines is governed by non-convex Weymouth equations. However, in the interest of simplicity, short-term trades in natural gas markets rely on simple entry-exit models in the EU that ignore the network constraints and transportation path [15].

2.1.1 Nonlinearities and non-convexities in electricity markets

The nonlinearities and non-convexities are highlighted below from the perspective of market participants, modeling energy flow in the network, and accounting for uncertainty.

Participants cost functions and strategy sets

Market participants in (2.1) face cost (utility) functions $c_i(\cdot)$ which are typically modeled as quadratic functions, given the operational characteristics of the physical assets producing (consuming) energy [13]. Ramping costs incurred from frequent adaptations in the operational state to provide flexibility are also modeled as quadratic functions [29]. In LP-based electricity markets, these costs and utilities are usually accounted for via linear or piecewise-linear approximations. Such linear approximations may fail to fully capture the costs of these participants, thereby deterring them from market participation and flexibility provision. Cost functions aside, an LP-based market only admits participants with polyhedral strategy sets \mathcal{Q}_i in (2.1b). Whereas, the feasible operating regions of various assets are typically nonlinear. When an inner (outer) polyhedral approximation is enforced, their feasibility sets are shrunk (expanded), thereby undermining (over-estimating) the amount of flexibility that can be harnessed. Apart from nonlinearities, non-convexity of \mathcal{Q}_i also arises from integrality constraints associated with the commitment status of power producers [73]. This non-convexity is resolved in practice by solving a unit-commitment problem as a mixed-integer linear programming (MILP) problem prior to the actual market clearing⁵ from which optimal prices and quantities are derived [74].

Nonlinear and non-convex network constraints

Representing energy flow dynamics, (2.1d) is governed by nonlinear and non-convex functions, even under steady-state conditions [75]. To attain convexity, electricity markets generally adopt a linearized direct current (DC) approximation of the nonlinear and non-convex alternating current (AC) power flow equations, relying on a number of assumptions [76]. In that case, the feasibility set \mathcal{F}^N reduces to a polyhedron, whereas the function $f^N(\cdot)$ is an affine function including the power flow distribution factor (PTDF) matrix together with an incidence matrix mapping the location of market participants w.r.t. the power lines. However, the network flows at the resulting market equilibrium are typically not feasible w.r.t. the AC power flows in the lines [77]. Furthermore, with increasing decentralization of the electricity system, a significant portion of energy trades are expected to occur within the distribution grid, by so-called "prosumers" of electricity [78], via decentralized market structures [79]. The assumptions underlying the linearization of power flows suffer severe inaccuracies for such decentralized market structures operating in the playing field of the distribution grid. Accurate operational modeling of flexible assets must be augmented by a physically accurate representation of the network constraints as the flexible resources are likely to be dispersed across the electricity network. With the inexact linear approximation, the market-clearing outcomes for the delivery of flexibility services are not feasible in the real world.

Nonlinearities in modeling uncertainty and risk

With increasing shares of weather-dependent RES, electricity markets are exposed to significant uncertainty which needs to be accounted for by stochastic market-clearing practices. This implies

⁵European markets usually do not solve a unit commitment problem, while admitting complex bid structure to enable market participants to internalize their commitment decisions and costs associated within the bids.

that the variable q_i in (2.1) is no longer deterministic and rather adopts the structure of a stochastic variable $q_i(\xi)$, where ξ represents the uncertainty faced by the market participants. Classical approaches within the LP framework include scenario-based stochastic programs [33, 34, 80] and robust optimization techniques [35, 59], which are unsuitable in practical settings as they suffer from computational intractability and solution conservativism, respectively. Options beyond the LP framework include chance-constrained programming, which admits nonlinear yet convex, computationally tractable⁶ and analytically expressible uncertainty models [31, 82]. Moreover, uncertainty propagation across the energy systems while harnessing cross-carrier flexibility leads to increased variance of state variables in the coupled system. Modeling this variance also requires the use of nonlinear constraints [67, 83].

Non-convexities aside, a nonlinear yet convex market-clearing problem beyond the LP framework alleviates these limitations to a large extent. For instance, within the realm of convex optimization, the SOCP framework based on second-order cones generalizes the LP framework [68]. The choice of LP in the early stages of electricity markets was motivated by the simplicity of economic interpretations and the computational capabilities available at the time to solve large-scale LP problems. However, recent mathematical and computational advances in conic programming [84, 85] have made SOCP markets a practical option. Leveraging these developments, [**Paper A**] proposes and analyzes a conic electricity market-clearing mechanism based on the SOCP framework. SOCP-based electricity markets enable a more accurate representation of physical assets and the network as well as uncertainty while retaining the advantages of LP in terms of optimality, economic interpretations, and computational ease. In what follows, the contributions of [**Paper A**] are briefly outlined in the context of prior works.

2.1.2 Towards conic markets for electricity

The market-clearing framework proposed in [**Paper A**] is *uncertainty-aware* by design since it admits a chance-constrained stochastic market clearing based on a conic reformulation of the probabilistic constraints [60]. More details on these constraints are given in Section 2.3. Regarding participants' strategies, the market framework in [**Paper A**] allows participants to express their SOC-representable nonlinearities via convex strategy sets Q_i formed by an intersection of polyhedra and second-order cones [86, 87]. Further, participants are allowed to submit convex quadratic cost functions $c_i(\cdot)$ in (2.1a), since such functions are admissible in SOCP problems by constraint reformulation [85]. These characteristics enable electricity markets to be *asset-aware*. Finally, convex quadratic relaxations to the non-convex AC power flow equations have been proposed utilizing the SOC relaxation [88–90], which improve the physical accuracy of power flow models over linear approximations. The network feasibility set \mathcal{F}^N in (2.1d) may thus be formed by an intersection of polyhedra and second-order cones, instead of being restricted to polyhedral sets. This leads to *network-aware* electricity markets, potentially reducing the re-dispatch of market participants to ensure network feasibility [91]. To summarize, SOCP-based markets improve the uncertainty-, asset-, and network-awareness of electricity markets.

Beyond energy markets, conic constraints in an equilibrium context were first discussed in [92], focusing on mitigation of financial risk. In contrast, [**Paper A**] approaches the spatial price

⁶Theoretically, an optimization problem is considered computationally tractable if it can be solved in polynomial time. However, as discussed in [81], tractability in practice refers to the reformulation of problems as linear or conic programs, solvable using off-the-shelf solvers.

equilibrium problem with conic constraints to alleviate the simplifications and approximation errors induced by linearization in markets underlying physical systems and networks, e.g., energy networks [26, 93, 94], water networks [95], telecommunication networks [96], supply chain and logistics networks [97], etc.

In the context of electricity markets, SOC constraints have recently gained interest in market proposals based on chance-constrained programming [31, 32]. The single-period stochastic market clearing proposed in [31] discusses the internalization of uncertainty in the price formation process, highlighting the advantages of chance-constrained electricity markets over scenario-based stochastic markets in terms of potential acceptability in a real-world implementation. The work in [32] showed that SOC reformulations of chance constraints also enable an analytical characterization of the risk faced by electricity markets in mitigating the uncertain RES, leading to risk- and variance-aware electricity prices. In regards to asset-awareness, [29] study quadratic costs of deliverability in unit commitment problems, essential to modeling ramping costs while providing flexibility. Finally, towards network-awareness, considering the SOC relaxation of power flows in distribution systems, pricing schemes based on conic duality were proposed in a deterministic setting in [30], and extended in [98] to include uncertainty modeled via chance constraints.

Previous works have focused on only one of the three aspects, i.e., uncertainty-, asset-, or network-awareness of the markets, whereas integration of large shares of RES in electricity markets requires a combined approach. This thesis generalizes the prior works, such that heterogeneous market participants with nonlinear (and potentially inter-temporal constraints) and quadratic costs could participate in multiple commodity trades in an electricity market aimed at harnessing flexibility in a network-aware, cost-efficient manner. Consequently, flexibility providers take a central role in the proposed market design, transforming electricity markets from energy-centric to flexibility-centric.

Remark 1 (Addressing non-convexities). Non-convexity of participants' strategy sets in (2.1) implies that the optimal quantity allocations and prices do not necessarily support social welfare-maximizing equilibrium, i.e., producers may not recover their costs [99]. This is resolved in practice by out-of-market payments, called uplift payments, which are in turn minimized by adopting a convex hull pricing scheme, see [100, 101] for details⁷. Neglecting cost recovery of participants, similar to the two-step unit commitment approach using MILP [74], these non-convexities can be practically incorporated as an extension to the proposed framework in [Paper A], rendering the problem as a mixed-integer second-order cone program (MISOCP), e.g., see [31]. Commercial nonlinear programming (NLP) and conic solvers can already solve MISOCP problems, adopting a variety of algorithms [104]. However, further computational advances are needed prior to adoption in real-world electricity markets.

2.2 A general conic market for electricity

In addition to uncertainty-, asset-, and network-awareness of the electricity market framework proposed in [Paper A], its generality is augmented by considering multiple time periods and involving trades over multiple commodities, as will be discussed in Section 2.2.1. The general conic market is formulated in Section 2.2.2, while Section 2.2.3 presents the market-clearing problem as a spatial price equilibrium and discusses the economic properties underlying the market equilibrium.

⁷To alleviate the computational issues associated with computing convex hull prices in real-world electricity markets, [102] develops a SOCP reformulation of the Lagrangian dual of the unit commitment problem under linear network flow approximations. This was recently further generalized in [103] to include AC power flows via convex relaxations such as the SOC relaxation. These approaches align well with the proposal of moving towards conic electricity markets in [Paper A], as they indicate the readiness of the electricity markets to admit nonlinearities in the market-clearing problem.

2.2.1 Towards a multi-period and multi-commodity electricity market

The optimization problem (2.1) is extended over discrete periods within a finite horizon, e.g., a day-ahead electricity market cleared hourly with the periods collected in a set $\mathcal{T} = \{1, 2, \dots, T\}$, where $T = 24$. Let $\mathcal{P} = \{1, 2, \dots, P\}$ denote the set of P hourly-traded commodities in the market. The P commodities are of two kinds: energy and flexibility services. While energy represents the quantity bought or sold in MWh at a given period, flexibility services refer to the exchanges that facilitate a reliable operation of the electricity system during the real-time stage, e.g., ensuring supply-demand balance, managing network congestion, providing voltage control, etc. Section 2.3 discusses such a flexibility service called *adjustment policies*, focusing on real-time supply-demand balance. The following introduces the context of heterogeneous participants in a multi-period and multi-commodity SOCP-based electricity market. Further notation is developed to add specifics to the illustrative example (2.1).

Including heterogeneous market participants

The market framework proposed in [Paper A] admits several types of heterogeneous participants: (i) dispatchable (and flexible, to varying degrees) power producers such as gas-fired power plants, hydro power plants, etc., (ii) non-dispatchable power producers such as weather-dependent RES, (iii) flexible energy consumers, and finally, (iv) actors that trade the flexibility services only, e.g., firms operating (physical or virtual) energy storage or power-to-gas units. To enable for a multi-period market framework, let the decision vector of the i -th participant $\mathbf{q}_i \in \mathbb{R}^{K_i T}$ be comprised of subvectors $\mathbf{q}_{it} \in \mathbb{R}^{K_i}$ where $K_i \geq P$ denotes the number of decision variables at period t . This implies that in addition to possible contributions towards trades involving the P commodities, participants may have $K_i - P$ state variables involved in their operational constraints. This segregation enables a variety of flexibility providers to accurately reflect their operational constraints in the proposed conic market, via a bid structure that takes their state variables into account. Cost functions $c_{it}(\mathbf{q}_{it}) : \mathbb{R}^{K_i} \mapsto \mathbb{R}$ in (2.1a) denote the participant's time-separated costs. This cost structure preserves the convexity of (2.1a) while enabling the participation of flexibility providers, such as energy storage units, who could change roles from sellers (while discharging) to buyers (while charging). For compactness of notation, subvectors $\mathbf{q}_{ip} \in \mathbb{R}^T$ denote the trades towards the p -th commodity for the participant i over all T hours. Finally, the market participants may face inter-temporal operational constraints that link their strategies across multiple periods, e.g., constraints that limit the rate of change in quantities across subsequent periods, constraints that couple the decisions over time periods. Such constraints affect the strategy set \mathcal{Q}_i , however, they are admissible in the market as long as the \mathcal{Q}_i are convex and conic.

Including SOC constraints

Any linear or convex quadratic inequalities involving the decision vector \mathbf{q}_i in (2.1) can be represented by SOC constraints of the general form

$$\|\mathbf{A}_{ij} \mathbf{q}_i + \mathbf{b}_{ij}\| \leq \mathbf{d}_{ij}^\top \mathbf{q}_i + e_{ij}, \quad \forall j \in \mathcal{J}_i, \quad (2.2)$$

where the set \mathcal{J}_i collects the J_i SOC constraints faced by participant i [86]. Each constraint in (2.2) admits parameters $\mathbf{A}_{ij} \in \mathbb{R}^{m_{ij} \times K_i T}$, $\mathbf{b}_{ij} \in \mathbb{R}^{m_{ij}}$, $\mathbf{d}_{ij} \in \mathbb{R}^{K_i T}$ and $e_{ij} \in \mathbb{R}$, corresponding to a $(m_{ij} + 1)$ -dimensional second-order cone $\mathcal{C} \subseteq \mathbb{R}^{m_{ij}+1}$. While the parameters embody the structural and geometrical information for each constraint, the dimensions reflect the relationships

among the decision variables. As illustrated in [Paper A], these parameters and dimensions are not identical among the various participants or even among various SOC constraints of a single participant. The feasibility region for (2.2) is formed by the Cartesian product of J_i second-order cones $\mathcal{C}_i = \prod_{j \in \mathcal{J}_i} \mathcal{C}_{ij} = \mathcal{C}_{i1} \times \cdots \times \mathcal{C}_{iJ_i}$, which is convex.

Ensuring market and network feasibility in the multi-commodity market

In the multi-commodity setup, market feasibility as given by (2.1c) can be rewritten as

$$\sum_{i \in \mathcal{I}} \mathbf{G}_{ip} \mathbf{q}_{ip} = \mathbf{0}_T, \quad \forall p \in \mathcal{P}, \quad (2.3)$$

where $\mathbf{G}_{ip} \in \mathbb{R}^{T \times T}$ represents a commodity-specific *coupling matrix* for each participant. For the commodity representing energy, typically, identity matrices form this coupling matrix for electricity producers and consumers. However, in the context of integrated energy system, these coupling matrices may crucially encode energy conversion efficiencies for flexibility providers. From a market design perspective, the market feasibility modeling approach in (2.3) enables defining new flexibility services that may involve trades among a subset of participants, i.e., \mathbf{G}_{ip} might be null matrices for some commodities for some participants.

In modeling network feasibility, a linear PTDF formulation of power flows is adopted for simplicity of exposition⁸. Let the electricity network be represented by a directed graph $(\mathcal{N}, \mathcal{L})$ comprised of nodes $\mathcal{N} = \{1, 2, \dots, N\}$ and a set of power lines \mathcal{L} collecting pairs of connected nodes (n, n') . Let subsets $\mathcal{I}_n \subseteq \mathcal{I}$, $\forall n \in \mathcal{N}$ collect the participants located at various nodes. The network feasibility constraint (2.1d) for each market-clearing period is

$$\left| \sum_{n \in \mathcal{N}} [\Psi]_{(:,n)} \left(\sum_{i \in \mathcal{I}_n} \sum_{p \in \mathcal{P}} [\mathbf{G}_{ip} \mathbf{q}_{ip}]_t \right) \right| \leq \bar{s}, \quad \forall t, \quad (2.4)$$

where $\Psi \in \mathbb{R}^{L \times N}$ denotes the PTDF matrix of the electricity network and $s \in \mathbb{R}^L$ denotes the power line capacity limits. The absolute value operator enforces symmetric limits on line capacities, but the formulation in (2.4) can be altered to include capacity limits that depend on the flow direction. While the summation over all commodities in (2.4) reflects that all commodities share the common physical network for trade fulfillment, alternative formulations can be envisioned, e.g., flexibility services may be purely financial instruments to hedge risk in electricity markets [105, 106].

2.2.2 SOCP-based market clearing as centrally-solved optimization

Adapting the illustrative problem in (2.1) to the multi-period and multi-commodity conic electricity market setting leads to a market-clearing problem

$$\min_{\mathbf{q}_i} \sum_{i \in \mathcal{I}} \sum_{t \in \mathcal{T}} \left(\mathbf{q}_{it}^\top \text{diag}(\mathbf{c}_{it}^Q) \mathbf{q}_{it} + \mathbf{c}_{it}^L^\top \mathbf{q}_{it} \right) \quad (2.5a)$$

$$\text{s.t. } \|\mathbf{A}_{ij} \mathbf{q}_i + \mathbf{b}_{ij}\| \leq \mathbf{d}_{ij}^\top \mathbf{q}_i + e_{ij}, \quad \forall j \in \mathcal{J}_i, \quad \forall i : (\boldsymbol{\mu}_{ij}, \nu_{ij}) \quad (2.5b)$$

$$\mathbf{F}_i \mathbf{q}_i = \mathbf{h}_i, \quad \forall i : (\boldsymbol{\gamma}_i) \quad (2.5c)$$

$$\sum_{i \in \mathcal{I}} \mathbf{G}_{ip} \mathbf{q}_{ip} = \mathbf{0}_T, \quad \forall p : (\boldsymbol{\lambda}_p) \quad (2.5d)$$

$$\left| \sum_{n \in \mathcal{N}} [\Psi]_{(:,n)} \left(\sum_{i \in \mathcal{I}_n} \sum_{p \in \mathcal{P}} [\mathbf{G}_{ip} \mathbf{q}_{ip}]_t \right) \right| \leq \bar{s}, \quad \forall t : (\underline{\boldsymbol{\varrho}}_t, \bar{\boldsymbol{\varrho}}_t) \quad (2.5e)$$

⁸Example EC.3 in [Paper A] illustrates an extension to include the SOC-based convex relaxation of the non-convex AC power flow equations.

where the objective function is comprised of linear and quadratic cost (utility) terms $\mathbf{c}_{it}^L, \mathbf{c}_{it}^Q \in \mathbb{R}^{K_i}$, respectively. Aside from the inequalities, constraint (2.5c) with parameters $\mathbf{F}_i \in \mathbb{R}^{R_i \times K_i T}$ and $\mathbf{h}_i \in \mathbb{R}^{R_i}$ models the R_i participant-specific equality constraints that may arise in modeling temporal or spatial dynamics underlying the physical asset models. For instance, in the integrated energy system, modeling network flexibility from linepack involves such spatial dynamics, whereas energy evolution equations in energy storage units model temporal dynamics via such linear equality constraints.

The Lagrange multipliers associated with the constraints in (2.5) are shown in parentheses next to them. For the SOC constraints (2.5b), a tuple of dual variables comprised of Lagrange multiples $\mu_{ij} \in \mathbb{R}^{m_{ij}}$ and $\nu_{ij} \in \mathbb{R}_+$ arise from dualization of the SOC constraints as detailed in Appendix A [**Paper A**]. Participant-specific equality constraints (2.5c) have dual variable $\gamma_i \in \mathbb{R}^{R_i}$ associated with them. The shadow prices $\lambda_p \in \mathbb{R}^T$ linked to market feasibility conditions in (2.5d) for the P commodities are interpreted as the system-wide commodity prices. Finally, the dual variables $\underline{\varrho}_t, \bar{\varrho}_t \in \mathbb{R}_+^L$ in (2.5e) are the shadow prices associated with the line flow limits.

Objective function reformulation and strict convexity

For computational tractability and analytical simplicity, the objective function (2.5a) is reformulated by defining auxiliary variables $\mathbf{z}_i \in \mathbb{R}^T, \forall i$, as discussed in detail in Example EC.1 in [**Paper A**]. As a result, the final SOCP-based market-clearing problem writes as

$$\min_{\mathbf{q}_i, \mathbf{z}_i} \sum_{i \in \mathcal{I}} \sum_{t \in \mathcal{T}} \left(z_{it} + \mathbf{c}_{it}^L{}^\top \mathbf{q}_{it} \right) \quad (2.6a)$$

$$\text{s.t. } \left\| \mathbf{C}_{it}^Q \mathbf{q}_{it} \right\|^2 \leq z_{it}, \forall t, \forall i \quad (2.6b)$$

$$(2.5b) - (2.5e), \quad (2.6c)$$

where the constraint (2.6b) is a special form of the general SOC constraint, called the rotated SOC constraint [85]. The matrix parameter \mathbf{C}_{it}^Q is a factorization of the original quadratic cost matrix, such that, $\text{diag}(\mathbf{c}_{it}^Q) = \mathbf{C}_{it}^Q{}^\top \mathbf{C}_{it}^Q$. Observe that (2.6a) is strictly convex if every market participant incurs a non-zero quadratic cost at each hour. Mathematically, this implies that strict convexity of (2.6a) is guaranteed only if the quadratic cost matrix is positive definite, i.e., $\text{diag}(\mathbf{c}_{it}^Q) \succ 0, \forall t, \forall i$.

Conic market bids

Rethinking the market-clearing framework provides an opportunity to introduce a new bid format. In the interest of generality, a common bid format for supply offers and demand bids is adopted and jointly referred to as bids. A conic market bid \mathcal{B}_i by participant i is a tuple

$$\mathcal{B}_i := \left(n_i, \{ \mathbf{A}_{ij}, \mathbf{b}_{ij}, \mathbf{d}_{ij}, e_{ij} \}_{j \in \mathcal{J}_i}, \mathbf{F}_i, \mathbf{h}_i, \{ \mathbf{G}_{ip} \}_{p \in \mathcal{P}}, \{ \mathbf{c}_{it}^Q, \mathbf{c}_{it}^L \}_{t \in \mathcal{T}} \right), \quad (2.7)$$

where $n_i \in \mathcal{N}$ is the electricity network node at which the participant i is located. Parameters $\mathbf{A}_{ij}, \mathbf{b}_{ij}, \mathbf{d}_{ij}, e_{ij}, \forall j \in \mathcal{J}_i$ are associated with the J_i SOC constraints; $\mathbf{G}_{ip}, \forall p \in \mathcal{P}$ are the coupling matrices for the P commodities; \mathbf{F}_i and \mathbf{h}_i correspond to the R_i equality constraints; and finally, $\mathbf{c}_{it}^Q, \mathbf{c}_{it}^L, \forall t \in \mathcal{T}$ represent the temporally-separated quadratic and linear bid prices. In contrast to classical price-quantity bids prevalent in LP-based electricity markets, e.g., [107], the conic bids enable participants to explicitly reflect the physical nonlinearities in their costs and operational constraints. Furthermore, market participation in terms of supply (or demand) quantity towards a specific commodity is decoupled from the costs and constraints associated with the state

variables of the market participants. Compared to the price-quantity bids, the proposed bid format requires a more complex exchange of information between the market participants and the market operator. However, the additional modeling fidelity available to heterogeneous market participants (including flexibility providers) can be argued to outweigh the increased complexity of communication. In practice, a simple bid transformation software layer could convert the standard price-quantity bids by participants into the conic bid format, prior to the market clearing in (2.6). Section EC.1 of [Paper A] uses modeling examples to illustrate the parameters constituting the conic market bids by heterogeneous market participants.

2.2.3 Economic interpretations and equilibrium analysis

Given the convexity of the centrally-solved market-clearing problem (2.6), a combination of linear and conic Lagrangian duality theory is leveraged to derive the spatially-differentiated prices of the various commodities. The first step is to establish strong duality for the primal market-clearing problem (2.6) and its dual problem, formulated in Appendix A of [Paper A]. In what follows, key theoretical results on the spatial price equilibrium underlying the problem (2.6) are summarized, while all proofs can be found in Appendix B of [Paper A].

Deriving prices for commodities

Unlike duality in LP problems where merely the feasibility of primal and dual problems guarantees strong duality, SOCP problems require *essentially strict feasibility* of primal and dual problems for strong duality to hold [87]. [Paper A] proves the existence of strong duality for problem (2.6) by relying on the existence of finite bounds on the Euclidean norm of participants' decision vectors \mathbf{q}_i , $\forall i$, as formalized in the following.

Lemma 1 (Boundedness). *Given the feasibility of problem (2.6), there exist sufficiently large finite scalar bounds $\bar{D}_i^Q \in \mathbb{R}_+$ on the Euclidean norm of decision vectors \mathbf{q}_i , given by $\|\mathbf{q}_i\| \leq \bar{D}_i^Q$, $\forall i$, such that the optimal solution to problem (2.6) remains unchanged with addition of the norm bounds.*

The existence of such bounds is justified for the physical assets involved in the electricity market. Lemma 1 enables proving essentially strict feasibility of the dual problem to (2.6) using a variant of the Big-M method [108], while essentially strict feasibility of the primal market is proven using a variation of Phase-I method [68]. Conventionally, in a market-clearing context, the existence of strictly feasible or even merely feasible solutions is assumed while studying the equilibrium. However, in the interest of generality and wider acceptance of the electricity market redesign proposed in [Paper A], these issues are addressed theoretically at the market design stage.

Theorem 1 (Conic Spatial Prices). *Given that the set of feasible solutions to the primal problem (2.6) is non-empty and Lemma 1 holds, the following conditions are met at the optimal solution:*

- (i) *Strong duality holds for the primal market-clearing problem (2.6) and its dual problem.*
- (ii) *Optimal trade allocations \mathbf{q}_{ip}^* , $\forall i \in \mathcal{I}$ for the $p \in \mathcal{P}$ commodities are obtained and the market clears with optimal nodal prices $\boldsymbol{\Pi}_p^* \in \mathbb{R}^{N \times T}$ for the p -th commodity given by*

$$\boldsymbol{\Pi}_p^* = \boldsymbol{\Lambda}_p^* - \boldsymbol{\Psi}^\top (\bar{\boldsymbol{\rho}}^* - \underline{\boldsymbol{\rho}}^*), \quad \forall p \in \mathcal{P}, \quad (2.8)$$

where $\underline{\boldsymbol{\rho}}^$, $\bar{\boldsymbol{\rho}}^* \in \mathbb{R}^{L \times T}$ and $\boldsymbol{\Lambda}_p^* \in \mathbb{R}^{N \times T}$ are auxiliary variables with stacked columns of optimal Lagrangian multipliers $\underline{\boldsymbol{\varrho}}_t^*$, $\bar{\boldsymbol{\varrho}}_t^*$, $\forall t$ and $\boldsymbol{\lambda}_p^*$, $\forall n$, respectively, over the T market-clearing periods, i.e.,*

$$\bar{\boldsymbol{\rho}}^* = [\bar{\boldsymbol{\varrho}}_1^* \cdots \bar{\boldsymbol{\varrho}}_T^*], \quad \underline{\boldsymbol{\rho}}^* = [\underline{\boldsymbol{\varrho}}_1^* \cdots \underline{\boldsymbol{\varrho}}_T^*], \quad \text{and} \quad \boldsymbol{\Lambda}_p^* := \mathbb{1}_N^\top \otimes \boldsymbol{\lambda}_p^*.$$

The structure of the conic spatial prices in Theorem 1 is analogous to the LMPs in the LP-based markets. It comprises of a nodal price component Λ_p^* and a network price component that is non-zero only if congestion arises due to power flows required for the physical fulfillment of the commodity trades. The proof relies on deriving the sensitivity of the partial Lagrangian function for (2.6) to commodity demands. A partial Lagrangian function of (2.6) is obtained by considering only the coupling constraints (2.5d) - (2.5e) while relaxing the participant-specific constraints.

Interpretation as a spatial price equilibrium problem

To study the equilibria underlying the market-clearing problem (2.6), the following actors in the market are considered: market participants, a market operator acting as a *price setter*, and a network operator acting as a *spatial arbitrageur*. While the market operator collects the bids (2.7) from the market participants and is responsible for clearing the market, the network operator is responsible for the physical fulfillment of the trades, collecting a non-zero congestion rent whenever trades lead to network congestion.

To better illustrate the spatial price equilibrium resulting from interactions among these actors in the multi-period and multi-commodity setting, a few auxiliary variables need to be defined. First, for each participant, let $\mathbf{W}_{ip} \in \mathbb{R}^{N \times T}$ denote the hourly quantities of p -th commodity transacted (bought or sold) at all the N nodes of the network. Second, let the variable $\mathbf{y}_t \in \mathbb{R}^N$ denote net power injection at the N network nodes w.r.t. all commodities and all market participants. Finally, to decompose the trades across the commodities, let a commodity-specific net nodal injection variable $\mathbf{Q}_p^{\text{inj}} \in \mathbb{R}^{N \times T}$ be defined as

$$\mathbf{Q}_p^{\text{inj}} := \begin{bmatrix} \sum_{i \in \mathcal{I}_1} (\mathbf{G}_{ip} \mathbf{q}_{ip})^\top & \sum_{i \in \mathcal{I}_2} (\mathbf{G}_{ip} \mathbf{q}_{ip})^\top & \cdots & \sum_{i \in \mathcal{I}_N} (\mathbf{G}_{ip} \mathbf{q}_{ip})^\top \end{bmatrix}^\top. \quad (2.9)$$

The spatial price equilibrium is formed by the individual profit-maximizing problems of the I market participants (2.10), the congestion rent maximization problem of the network operator (2.11), and the market-clearing conditions upheld by the market operator (2.12). In (2.10), the prices Π_p given by Theorem 1 appear as parameters whereas the price components, i.e., $\underline{\varrho}_t$, $\bar{\varrho}_t$, and λ_p , are shadow prices in the network operator's problem (2.11) and the market operator's equalities (2.12), respectively. The market-clearing condition (2.12a) ensures that net injection at each node at each period is balanced by transport service provided by the network operator, such that the shadow price $\omega_t \in \mathbb{R}^N$ is interpreted as the price of transmitting power from an arbitrary hub to each of the N nodes. Condition (2.12b) ensures the system-wide balance of traded commodities, as discussed previously.

Theorem 2 (Spatial Price Equilibrium). *The centrally-solved market-clearing problem (2.6) is equivalent to a competitive spatial price equilibrium comprised of market participants, $i \in \mathcal{I}$, each solving the profit maximization (2.10), the network operator solving the congestion rent maximization (2.11), and the market operator clearing the market by enforcing the equalities (2.12).*

The proof for Theorem 2 relies on the equivalence of the Karush-Kuhn-Tucker (KKT) optimality conditions of the two problems. As a corollary to Theorem 2, the existence of an equilibrium is proven based on showing convexity and compactness of strategy sets and continuity of the payoff functions in (2.10) and (2.11) due to [71, Theorem 1]. Lastly, observe that while the market-clearing allocations \mathbf{q}_i^* are unique, conditioned on the strict convexity of the objective function (2.6a), no such guarantees on the uniqueness of the prices Π_p^* can be given since the dual problem to (2.6)

Market participant profit maximization, $\forall i \in \mathcal{I}$:

$$\max_{\mathbf{q}_i, \mathbf{z}_i, \mathbf{W}_{ip}} \underbrace{\sum_{p \in \mathcal{P}} \text{tr}(\boldsymbol{\Pi}_p^\top \mathbf{W}_{ip})}_{\text{transaction revenues}} - \underbrace{\sum_{t \in \mathcal{T}} \left(z_{it} + \mathbf{c}_{it}^L \top \mathbf{q}_{it} \right)}_{\text{cost (utility) of production (consumption)}} - \underbrace{\sum_{t \in \mathcal{T}} \boldsymbol{\omega}_t^\top \left(\sum_{p \in \mathcal{P}} ([\mathbf{W}_{ip}]_{(:,t)} - \mathbb{1}_{n_i} [\mathbf{G}_{ip} \mathbf{q}_{ip}]_t) \right)}_{\text{transport cost for trade fulfillment}} \quad (2.10a)$$

$$\text{s.t. } \left\| \mathbf{C}_{it}^Q \mathbf{q}_{it} \right\|^2 \leq z_{it}, \forall t \quad (2.10b)$$

$$\|\mathbf{A}_{ij} \mathbf{q}_i + \mathbf{b}_{ij}\| \leq \mathbf{d}_{ij}^\top \mathbf{q}_i + e_{ij}, \forall j \in \mathcal{J}_i \quad (2.10c)$$

$$\mathbf{F}_i \mathbf{q}_i = \mathbf{h}_i \quad (2.10d)$$

$$\mathbf{W}_{ip}^\top \mathbf{1} = \mathbf{G}_{ip} \mathbf{q}_{ip}, \forall p \in \mathcal{P} \quad (2.10e)$$

Network operator congestion rent maximization:

$$\max_{\mathbf{y}_t} \sum_{t \in \mathcal{T}} \boldsymbol{\omega}_t^\top \mathbf{y}_t \quad (2.11a)$$

$$\text{s.t. } -\bar{\mathbf{s}} \leq \Psi \mathbf{y}_t \leq \bar{\mathbf{s}} \quad : (\underline{\boldsymbol{\varrho}}_t, \bar{\boldsymbol{\varrho}}_t) \quad (2.11b)$$

Market clearing constraints:

$$\sum_{p \in \mathcal{P}} [\mathbf{Q}_p^{\text{inj}}]_{(:,t)} = \mathbf{y}_t, \forall t \quad : (\boldsymbol{\omega}_t) \quad (2.12a)$$

$$\sum_{i \in \mathcal{I}} \mathbf{G}_{ip} \mathbf{q}_{ip} = \mathbf{0}, \forall p \in \mathcal{P} \quad : (\boldsymbol{\lambda}_p) \quad (2.12b)$$

(formulated in Appendix A of [Paper A]) does not have a strictly convex objective function. The conditions on the uniqueness of the allocations at equilibrium closely correspond to those in prevalent LP-based markets⁹, see [110] for example.

Satisfaction of desired economic properties

In classical mechanism design theory, competitive markets are evaluated for their ability to satisfy certain economic properties [27, 69, 111]: efficiency of the market, cost recovery of market participants, revenue adequacy of the market operator, and incentive compatibility of bids. Assuming a finite number of participants competing in the market, these properties cannot be satisfied simultaneously without additional assumptions [55, 56]. Further, the satisfaction of these properties relies on the choice of payment mechanism adopted, i.e., how the auctioneer (market operator) characterizes rules for collecting payments from buyers and distributes them to the sellers. In [Paper A], aligned with a majority of electricity markets worldwide, a marginal pricing or uniform pricing scheme is adopted for pricing of commodities, implying that all accepted bids are cleared at a common price at a given location in the network. Under the uniform pricing scheme and assuming perfect competition (i.e., all market participants are price takers), the following theorem formalizes theoretical results of [Paper A] on the satisfaction of economic properties.

Theorem 3 (Economic Properties). *The market-clearing problem (2.6) results in allocations \mathbf{q}_i^* , $\forall i \in \mathcal{I}$ and spatial commodity prices $\boldsymbol{\Pi}_p^*$, $\forall p \in \mathcal{P}$ such that at optimality the following hold:*

⁹If the strict convexity assumption is dropped, [109] provides conditions on network connectivity, PTDF matrix parameters, and the structure of participants' cost functions under which unique equilibrium allocations are obtained in a market with linear constraints. Further research is needed to study these conditions for the proposed SOCP-based market.

- (i) **Market efficiency:** Under the perfect competition assumption, social welfare is maximized, i.e., no participant has incentives to unilaterally deviate from the market-clearing outcomes.
- (ii) **Cost recovery:** Let the bids \mathcal{B}_i for each market participant $i \in \mathcal{I}$ be such that $e_{ij} \geq \| \mathbf{b}_{ij} \|$, $\forall j \in \mathcal{J}_i$ and $\mathbf{h}_i = \mathbf{0}$. Then, the optimal allocations \mathbf{q}_i^* , $\forall i \in \mathcal{I}$ and optimal spatial commodity prices Π_p^* , $\forall p \in \mathcal{P}$ ensure cost recovery for the market participants.
- (iii) **Revenue adequacy:** The market operator does not incur financial deficit at the end of the market-clearing horizon, i.e.,

$$\sum_{p \in \mathcal{P}} \sum_{i \in \mathcal{I}} \text{tr}(\Pi_p^{*\top} \mathbf{W}_{ip}^*) - \sum_{t \in \mathcal{T}} \boldsymbol{\omega}_t^{*\top} \mathbf{y}_t^* \geq 0.$$

The property of market efficiency in Theorem 3 is proven under the assumption of perfect competition involving rational and self-interested participants and relies on the equivalence of optimization and the equilibrium as given by Theorem 2. Cost recovery for each participant is proven using strong duality of their individual profit maximization problem (2.10) in combination with Cauchy-Schwarz inequality, conditioned on specific aspects of participants' strategy sets defined by the SOC constraints (2.5b) and linear equalities (2.5c). In particular, the condition $e_{ij} \geq \| \mathbf{b}_{ij} \|$, $\forall j \in \mathcal{J}_i$ relates the parameters of SOC constraints (2.5b) and holds true in most practical settings, except for participants having a non-zero lower bound on their decision variables. This practical issue of cost recovery not being guaranteed for such market participants also exists in LP-based electricity markets. The condition $\mathbf{h}_i = \mathbf{0}$ requires homogeneity of the linear equality constraint (2.5c), i.e., $\mathbf{q}_i = \mathbf{0}$ should be feasible for the participants. The revenue adequacy condition is satisfied when the net payments made to the operator towards all commodity trades is at least as large as the payments made to the network operator towards transmission services. Revenue adequacy (and budget balance¹⁰) of the market operator is proven using the KKT optimality conditions of the market-clearing problem (2.6). Finally, incentive compatibility of the bids is generally satisfied for uniform pricing scheme only while considering an infinite number of market actors, i.e., the incentive of an individual participant to deviate from price-taking, perfectly competitive behavior while submitting their bids tends to zero as the number of participants goes to infinity [113]. Akin to the prevalent LP-based markets, the proposed conic market mechanism achieves incentive compatibility at the limit. This implies that if a very large number of participants compete in the market, then they bid according to their true preferences.

2.3 Case study: An uncertainty-aware electricity market

This section discusses the modeling details and numerical results associated with an uncertainty-aware electricity market, a variant of the general conic electricity market proposed in [Paper A]. This specific variant focuses on the redesign of electricity markets to endogenously model the uncertainty, while introducing a new flexibility service, called adjustment policies, to mitigate it. Such uncertainty faced by a day-ahead electricity market could arise, for instance, from imperfect forecasts of the power production from weather-dependent RES or from imperfect load forecasts

¹⁰Budget balance condition in mechanism design is a refinement of the revenue adequacy property, which is reached when the market operator does not accrue any surplus revenue at the optimal market-clearing outcomes, i.e., the statement (iii) in Theorem 3 is satisfied with an equality. From an economic perspective, this is an improvement over surplus-generating outcomes, since the auctioneer's (market operator's) surplus represents a loss in social welfare (sum of utilities of participants), which can be viewed as the cost of truthfulness [112].

for consumers. An uncertainty-aware market clearing takes the form of a stochastic program. The illustrative market-clearing problem (2.1) is rewritten as the following stochastic program:

$$\min_{\tilde{q}_i(\xi)} \mathbb{E}^{\mathbb{P}_\xi} \left[\sum_{i \in \mathcal{I}} c_i(\tilde{q}_i(\xi)) \right] \quad (2.13a)$$

$$\text{s.t. } \tilde{q}_i(\xi) \in \mathcal{Q}_i, \forall i \quad (2.13b)$$

$$f^M(\{\tilde{q}_i(\xi)\}_{i \in \mathcal{I}}) \in \mathcal{F}^M \quad (2.13c)$$

$$f^N(\{\tilde{q}_i(\xi)\}_{i \in \mathcal{I}}) \in \mathcal{F}^N. \quad (2.13d)$$

The participants' strategies $\tilde{q}_i(\xi)$ are stochastic variables such that optimal allocations from (2.13) depend on realizations of a continuous random variable $\xi \sim \mathbb{P}_\xi$, where \mathbb{P}_ξ is a probability distribution function. The objective (2.13a) is to minimize the expected social disutility w.r.t. the probability distribution \mathbb{P}_ξ . Although it involves a finite number of variables, due to the presence of an infinite number of constraints based on the possibly infinitely many realizations of ξ , problem (2.13) is a semi-infinite program [114]. Computational intractability aside, such semi-infinite programs complicate the economic interpretations associated with Lagrangian duality [115].

In a market setting, the intractability of such stochastic programs is typically resolved using robust optimization techniques [116], scenario-based methods, and chance-constrained optimization approach [117]. Scenario-based approximations replace the random variable ξ with samples corresponding to finitely many scenarios sampled from \mathbb{P}_ξ , each scenario associated with a known probability such that all probabilities add up to 1. Robust optimization approaches approximate the infinite set from which ξ draws to a finite, well-defined convex uncertainty set, e.g., polyhedral, ellipsoid, etc., over which the objective is to minimize cost against the worst-case realization within the uncertainty set. However, in practical market settings, these approaches suffer from computational intractability due to a large number of scenarios needed to represent uncertainty accurately and conservatism of the worst-case optimal solution, respectively. Chance-constrained programming offers a promising alternative to approximate the stochastic market clearing (2.13) by providing computational tractability and analytical reformulations under mild conditions, e.g., feasibility region formed by (2.13b) - (2.13d) is polyhedral [117].

In Section 2.3.1 adjustment policies are introduced, while discussing the chance-constrained optimization framework adopted to optimize them. Considering a single-period, single-node electricity system, Section 2.3.2 draws numerical results from [Paper B] to demonstrate how introducing this flexibility service results in endogenous pricing of uncertainty and remunerates agents for its mitigation. Section 2.3.3 presents results from [Paper A] where the approach is generalized to consider a network with heterogeneous market participants that face inter-temporal constraints. The numerical results justify the move towards conic markets for uncertainty management by comparing it with LP-based uncertainty-aware market alternatives.

2.3.1 Adjustment policies: A flexibility service

An electricity market under uncertainty, such as (2.13), can be seen as a two-stage problem: day-ahead market-clearing followed by the real-time operation stage. Since the day-ahead market makes decisions prior to the realization of uncertainty, it should account for recourse actions by flexibility providers in response to uncertainty. In [Paper A] and [Paper B], a flexibility service called adjustment policies is proposed and analyzed. Adjustment policies embody the recourse actions in uncertainty-aware electricity markets and are activated during or close to

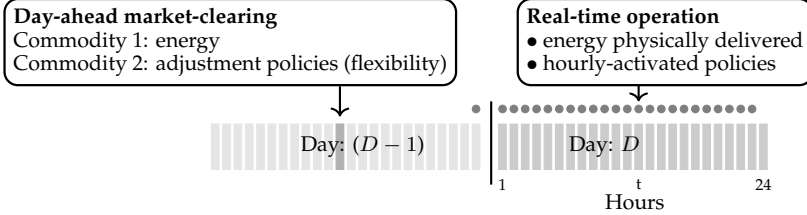


Figure 2.1: Illustration of commodities traded in an uncertainty-aware electricity market. Reproduced from [Paper A].

real-time operation stage when uncertainty is revealed. These policies are in *per unit* (or represent percentages) and characterize the contribution of each flexibility provider towards the mitigation of potential real-time imbalance in the electricity system. Optimal adjustment policies are obtained while making look-ahead decisions at the day-ahead market stage by jointly clearing energy and flexibility in a two-commodity chance-constrained electricity market. Figure 2.1 illustrates the market-clearing timeline of the uncertainty-aware electricity market. The setting in [Paper B] focuses solely on power producers as flexibility providers. Whereas, [Paper A] generalizes the market with SOC constraints that enables heterogeneous flexibility providers within (and possibly beyond) the electricity system (e.g., flexible generators, energy storage, flexible consumers, etc.) to submit bids for energy and flexibility. In addition to the payments for energy, flexibility providers are paid upfront for the flexibility services, i.e., at the day-ahead stage, while the actual activation of flexibility occurs closer to real-time when uncertainty is revealed.

While more general nonlinear but convex recourse decisions could potentially be admitted in the proposed market framework based on [118], [Paper A] and [Paper B] employ affine adjustment policies since they provide a computationally-tractable approximation of the stochastic program (2.13) that can be solved without requiring an iterative solution approach. Such affine policies stem from the theory of linear decision rules (LDR), which are well-studied in the field of operations research to make an operational decision under uncertainty [58, 119, 120].

From historical data and forecasts to affine adjustment policies

At the day-ahead market-clearing stage, typically the market operator has access to load and RES generation forecasts for the hours of physical delivery the next day. In addition to the forecasts, it is reasonable to assume that the market operator has historical measurements of these uncertain parameters, such that a model of the stochastic process driving this uncertainty can be constructed. Using a single-period electricity market for simplicity of notation, the following further illustrates the adjustment policies within the chance-constrained optimization framework.

Let the set $\mathcal{W} = \{1, 2, \dots, W\}$ collect the W independent sources of uncertainty faced by the market operator and the vector $\xi \in \mathbb{R}^W$ denote the random forecast errors. The set $\mathcal{W} \subseteq \mathcal{I}$ could, for instance, denote a set of weather-dependent RES. Assume that ξ follows a probability distribution \mathbb{P}_ξ which is sufficiently parameterized by its first- and second-order moments, i.e., mean $\mu \in \mathbb{R}^W$ and covariance $\Sigma \in \mathbb{R}^{W \times W}$. The moments of the error distribution are estimated by the market operator having access to a finite number of historical measurements. Without loss of generality, the stochastic power production $\tilde{q}_i \in \mathbb{R}_+$ during real-time operation can be modeled as

$$\tilde{q}_i = q_i - \xi_i, \quad \forall i \in \mathcal{W}, \quad (2.14a)$$

where q_i denotes a nominal production quantity, usually given by the best available forecast at the time of bid submission and ξ_i is the i -th element of the forecast error vector ξ . To mitigate this uncertainty, the stochastic power production by a flexible power producer during real-time operation is modeled as an affine recourse function of the uncertainty,

$$\tilde{q}_i = q_i + g_i(\xi), \quad \forall i \in \mathcal{F}, \quad (2.14b)$$

where $\mathcal{F} \subseteq \mathcal{I}$ collects the set of flexible power producers and $g_i : \mathbb{R}^W \mapsto \mathbb{R}$. Since [Paper A] and [Paper B] employ global uncertainty characterizations¹¹, i.e., flexibility providers respond to the net uncertainty faced by the system, we have $g_i(\xi) = \mathbf{1}^\top \xi$, where $\mathbf{1} \in \mathbb{R}^W$ is a vector of ones.

Under the chance-constrained optimization framework, the market operator allocates adjustment policies to flexibility providers while allowing them to violate their operational constraints with a small probability $\varepsilon \in (0, 1)$, typically $\varepsilon \ll 1$. For instance, a chance constraint limiting the total production, i.e., sum of nominal and adjustment, is written as

$$\mathbb{P}_\xi(q_i + \alpha_i(\mathbf{1}^\top \xi) \leq \bar{Q}_i) \geq (1 - \varepsilon), \quad \forall i \in \mathcal{F}, \quad (2.14c)$$

where α_i is the adjustment policy allocated to producer i . This probabilistic non-convex constraint admits a convex analytical approximation based on [60, 117] and reformulates as a $(W + 1)$ -dimensional SOC constraint

$$r_\varepsilon \|\mathbf{X}\mathbf{1}^\top \alpha_i\| \leq \bar{Q}_i - q_i - \mathbf{1}^\top \boldsymbol{\mu} \alpha_{i1}, \quad (2.14d)$$

where $\mathbf{X} \in \mathbb{R}^{W \times W}$ denotes a factorization of the covariance matrix such that $\Sigma = \mathbf{X}\mathbf{X}^\top$. For instance, such a factorization can be obtained in a computationally efficient manner using Cholesky decomposition, resulting in \mathbf{X} having a lower-triangular structure. Parameter $r_\varepsilon \in \mathbb{R}_+$ is a safety parameter chosen by the market operator relying on the knowledge of the distribution \mathbb{P}_ξ , such that r_ε increases as ε reduces. For instance, when ξ is normally distributed, the safety parameter r_ε is given by the inverse cumulative distribution function of the standard Gaussian distribution evaluated at $(1 - \varepsilon)^{\text{th}}$ quantile, where $\varepsilon < 0.5$. Constraint (2.14d) is represented by the general SOC constraint (2.2), for some fixed j , with parameters

$$\mathbf{A}_{ij} = [\mathbf{0} \quad \mathbf{X}\mathbf{1}], \quad \mathbf{b}_{ij} = \mathbf{0}, \quad \mathbf{d}_{ij} = -1/r_\varepsilon [1 \quad \mathbf{1}^\top \boldsymbol{\mu}]^\top \quad \text{and} \quad e_{ij} = \bar{Q}_i/r_\varepsilon.$$

Further modeling details involving the SOC reformulations of chance constraints of participants with inter-temporal constraints, e.g., energy storage, as well as joint chance constraints, as opposed to the individual constraint example in (2.14c), are provided in Section EC.2 of [Paper A].

Optimizing policies in chance-constrained programs

A few intermediate steps are followed to reach the final tractable form of the chance-constrained electricity market-clearing problem. First, the chance constraints on participants' linear inequalities as well as the power flows in the network are analytically reformulated as SOC constraints of varying dimensions, following a procedure similar to above. The expectation term in the objective function involving the costs of the participants, as in (2.13a), is expanded and reformulated as a rotated SOC as discussed in Section 2.2.2. The resulting market-clearing problem is a

¹¹It is possible to have adjustment policies that exhibit higher fidelity of uncertainty response, e.g., in gas networks, [Paper D] employs nodal response to uncertainty, i.e., adjustment policies of flexibility providers are individually tuned to each uncertainty source, considering their location in network as well as potential network congestion.

tractable SOCP problem solved centrally by the market operator using off-the-shelf commercial conic solvers, such as MOSEK, Gurobi, CPLEX, etc. At the optimal solution, nominal dispatch of the participants and adjustment policies are obtained. Each flexibility provider is allocated an adjustment policy at a given market-clearing period while ensuring a least-cost delivery of flexibility considering participant's individual constraints as well as the coupled market and network feasibility constraints. A description of intermediate steps and the formulation of the final SOCP-based market-clearing problem is provided in Section EC.2 of [Paper A].

2.3.2 Endogenous pricing of uncertainty: A simple example

To demonstrate the endogenous pricing of uncertainty enabled by the proposed market framework, [Paper B] considers a simple single-period, single-node electricity market setting. Only flexible power producers with limits on minimum and maximum production capacity and available flexible capacity are considered as flexibility providers. Electricity demand is considered inflexible and inelastic, while wind farms are the sources of uncertainty in the system. The hourly market is simulated over a clearing horizon of 24 hours, considering 1000 realizations of the uncertain power production from the wind farms. Further details on modeling of the market participants, e.g., their cost and constraint parameters, are in [Paper B]. The market framework entails a chance-constrained co-optimization of energy and adjustment policies wherein adopting the following assumptions result in an LP-based electricity market:

Assumption 1. The forecast errors are spatially and temporally uncorrelated, i.e., the covariance matrix Σ is a diagonal matrix with variances of individual uncertainty sources in the diagonal.

Assumption 2. The adjustment policies characterizing the flexibility provided by flexible power producers are non-negative.

Assumption 3. The forecast errors are assumed to follow a zero-mean Gaussian distribution, such that $\xi \sim \mathcal{N}(0, \Sigma)$.

In Assumption 1, while spatial independence of forecast errors is realistic for electricity markets over large geographical area [82], the absence of temporal correlation enables the study of a single-period electricity market by decoupling the market-clearing hours. Assumption 2 implies that during the real-time operation, flexible power producers adapt their production aligned with the overall system imbalance, i.e., if $\mathbf{1}^\top \xi \geq 0$ indicates a deficit in real-time production from RES as compared to the day-ahead forecast, all power producers increase their production. While it appears intuitive that this should always hold true, considering the network topology and congestion due to energy flows and flexibility provision, it might be beneficial for flexibility providers to respond in opposition to system needs provided it leads to higher social welfare¹². The Gaussianity of forecast errors in Assumption 3, coupled with Assumption 2, enables exact analytical reformulation of chance constraints into linear inequalities. The resulting LP-based market facilitates easier economic interpretations using LP duality theory and represents a soft change compared to prevalent LP-based markets while introducing uncertainty-awareness. However, Assumptions 1-3 introduce restrictions that potentially limit practical adoption, and are therefore dropped in [Paper A] while introducing a multi-period market involving network constraints.

¹²Considering inflexible and inelastic demand, the market-clearing problem involving social welfare maximization is equivalent to a cost minimization problem for sellers since buyers exhibit an infinite utility. Hereafter, in this thesis, we use cost minimization as a proxy for social welfare maximization.

Table 2.1: Comparison between expected market clearing costs (averaged over 1000 scenarios) for the deterministic benchmark and the proposed market-clearing framework.

Costs [k€]	Deterministic MRR = 200 MW	Uncertainty-aware		
		$\gamma = 0.5$	$\gamma = 1.0$	$\gamma = 3.0$
Operations	401.4	398.2	400.9	408.0
Reserves	70.2	0.6	2	38.1
Total	471.6	398.6	402.9	446.1
Change [%]	-	-15.5%	-14.6%	-5.4%

Comparison with a deterministic benchmark

To illustrate the effectiveness of the proposed uncertainty-aware market framework in [Paper B], it was evaluated against a benchmark deterministic co-optimization of energy and reserve procurement via out-of-sample simulations¹³. In the absence of currently operational joint clearing of energy and reserves in European electricity markets, this benchmark reflects a natural extension to the prevalent sequential market-clearing approach. The market operator enforces an exogenously-determined minimum reserve requirement (MRR) to procure flexibility from the flexibility providers. As detailed in [Paper B], for the system parameters considered, an MRR of 200 MW was empirically evaluated to be an optimal choice to compare against the proposed market framework. At lower values, the expected cost of operation in the deterministic benchmark was higher and had high variability associated with it, due to load shedding needed during the real-time operation stage. Whereas higher MRR values correspond to over-dimensioning of the reserves such that the total system operation cost increases.

Table 2.1 compares the expected day-ahead market clearing costs for the deterministic benchmark and the proposed uncertainty-aware market averaged over the 1000 wind forecasts realization scenarios. The parameter γ represents the *degree of unbiasedness* of the Gaussian distribution assumed by the chance constraints as compared to the distribution from which actual realization scenarios are drawn, such that $\gamma = 1$ indicates that historical forecast errors distribution perfectly represent the actual probability distribution. For values of $\gamma < 1$, the uncertainty-aware market underestimates the actual uncertainty, resulting in lower costs of day-ahead reserve procurement, whereas for values of γ larger than 1, the problem overestimates the actual wind forecast errors and thus allocates affine adjustment policies for reserves such that the cost of reserves is higher. For the deterministic benchmark, the cost of reserves is higher than the uncertainty-aware market, even for the case of $\gamma = 3$ which reflects the case when the chance constraints are reformulated using a distribution of uncertainty that is three times as dispersed as the actual realization. This demonstrates the robustness of the uncertainty-aware market, given Assumption 3 holds, against large forecast errors as compared to the deterministic benchmark.

Optimal dispatch, price of uncertainty and adjustment policies

Figure 2.2(a) and 2.2(b) compare the optimal dispatch of power producers to meet the inflexible demand. While reserve capacity is scheduled in the deterministic benchmark, in the uncertainty-aware market explicit reserve capacity procurement is replaced by adjustment policies. Optimal day-ahead price for energy and flexibility (only available for the uncertainty-aware market) are

¹³Here, the notion of out-of-sample (OOS) simulations refers to different covariance matrices of the Gaussian distribution from which scenarios of actual wind realizations are drawn. In contrast, stochastic programming literature typically considers random scenarios drawn from other distributions as OOS.

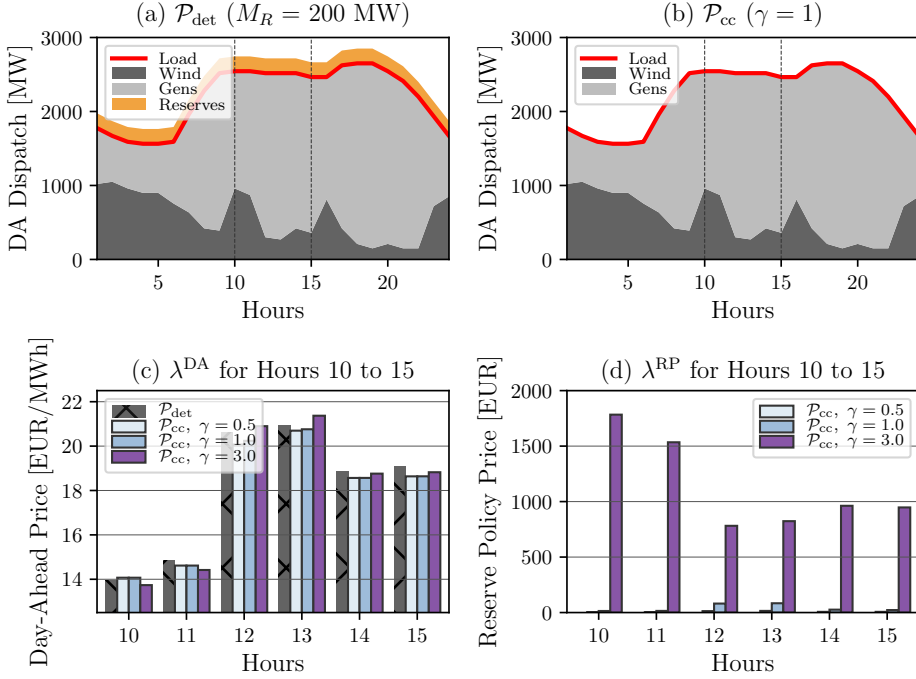


Figure 2.2: Day-ahead (DA) dispatch and market prices for the deterministic benchmark (\mathcal{P}_{det}) and proposed uncertainty-aware market framework (\mathcal{P}_{cc}). Reproduced from [Paper B].

shown in Figure 2.2(c) and Figure 2.2(d), respectively. Hours with higher wind power production forecasts result in lower day-ahead prices for both the market mechanisms due to the zero marginal cost of wind farms. Moreover, as Figure 2.2(d) shows, higher values of γ result in higher prices associated with allocating adjustment policies, signifying the overestimation of actual wind forecast realizations by the market-clearing problem. Figure 2.3 shows the optimal allocation of adjustment policies among the flexible power producers, labeled G1 through G12. The more expensive producer G4 is allocated with an adjustment policy only in hours with high wind share and with higher values of γ . In general, the uncertainty-aware framework provides the market operator with a high-fidelity tool to optimally procure a risk-adjusted amount of flexibility from providers.

2.3.3 Uncertainty-aware SOCP-based electricity market

Next, Assumptions 1-3 are dropped while considering a two-commodity energy and flexibility market admitting heterogeneous participants: flexible power producers and energy storage units. Market clearing outcomes are studied for various wind energy share paradigms, ranging from 10% to 60% of total energy demand from consumers met by wind power producers¹⁴. As before, wind farms bid at zero costs to ensure bid acceptance, while energy storage units bid with costs lower than the cheapest flexible power producer. To highlight the impact of network congestion on spatial prices, two network configurations are studied: (i) without any network bottlenecks and (ii) with network bottlenecks induced by reducing the capacity of three transmission lines, highlighted in blue in Figure 2.4(a). Further details on the participants, wind share paradigms, and network topology are in [Paper A]. The resulting SOCP problem leads to commodity trades such that an uncertainty-aware spatial price equilibrium is reached.

¹⁴These wind energy share paradigms represent the ongoing green transition of electricity systems across the world, supported by uncertain and variable RES.

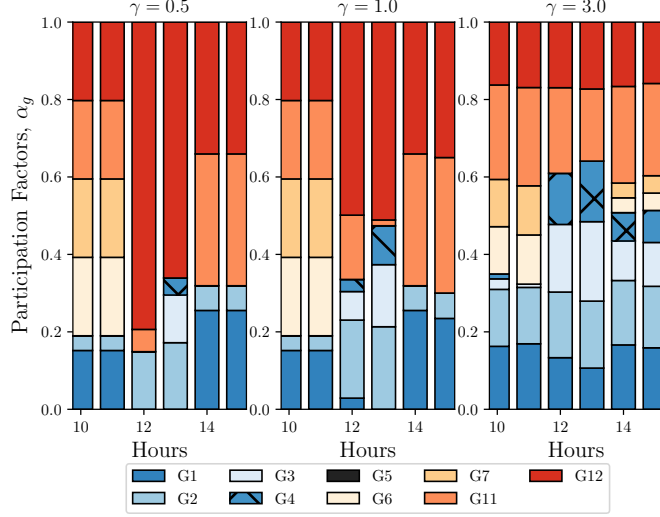


Figure 2.3: Allocation of adjustment policies with the various chosen degrees of unbiasedness, γ . Reproduced from [Paper B].

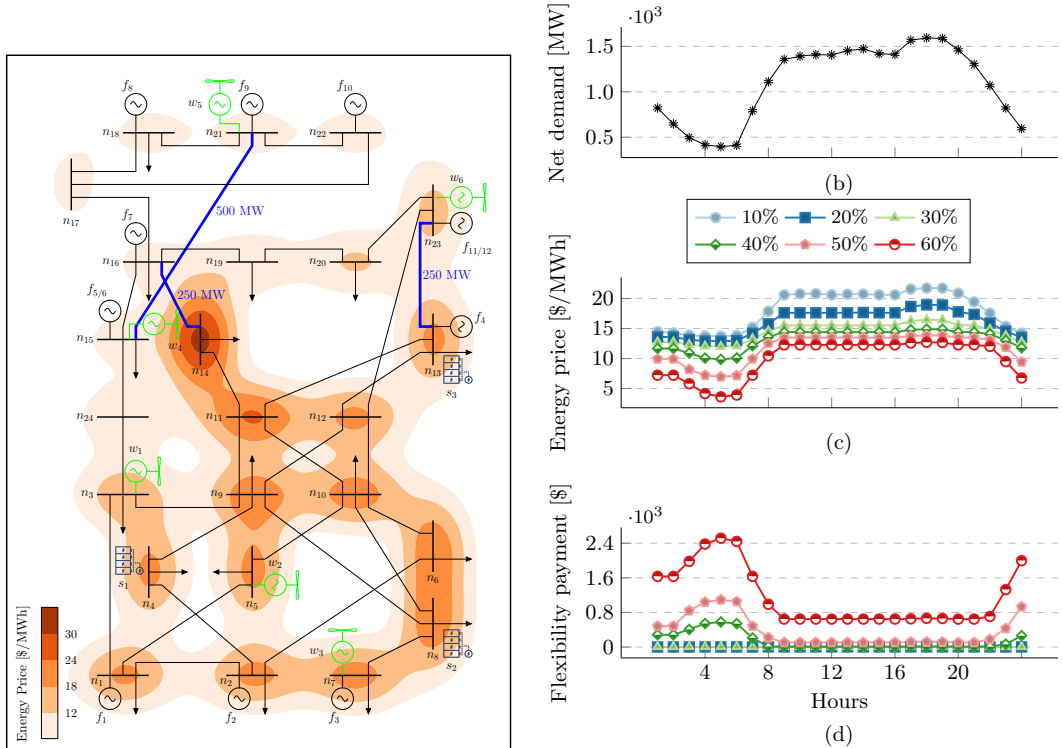


Figure 2.4: (a) Electricity network visualizing spatial prices of energy for the configuration with bottlenecks at hour 23 under the 50% RES paradigm, (b) expected net demand for the 50% RES paradigm, (c) system-wide prices for energy, and (d) the total hourly flexibility payments for various RES paradigms. Reproduced from [Paper A].

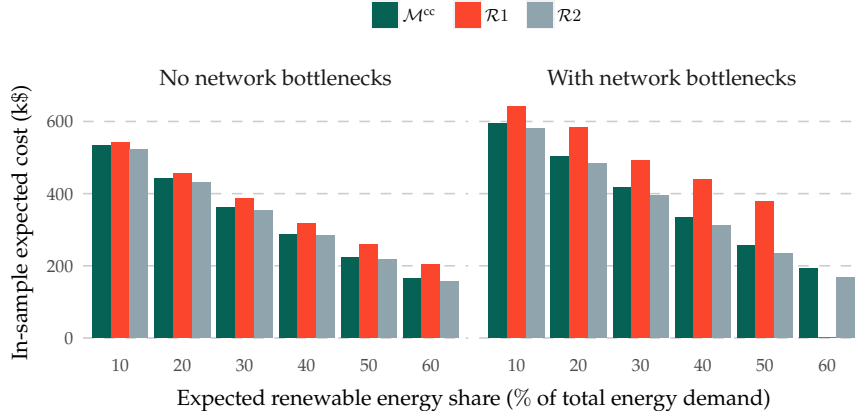


Figure 2.5: Expected in-sample market-clearing cost comparison, with increasing RES shares, among the proposed SOCP-based market \mathcal{M}^{cc} and LP-based benchmarks: deterministic market $\mathcal{R}1$ and scenario-based stochastic market $\mathcal{R}2$. Reproduced from [Paper A].

Impact of congestion and uncertainty on prices

The density plot in Figure 2.4(a) shows the day-ahead energy price at various network nodes at hour 23 under the 50% RES paradigm. Figure 2.4(b) shows the day-ahead forecast for the net demand (energy demand less the wind power forecasts) for the 50% RES paradigm, while Figures 2.4(c) and 2.4(d) show the prices of energy and payments towards adjustment policies, respectively. In addition to the difference among the hours as discussed in Section 2.3.2, increasing uncertainty in the day-ahead market leads to lower energy prices coupled with higher payments towards procurement of flexibility services, thereby sending right market signals towards increased participation of flexibility providers over the long run. Observe that, since the adjustment policies are in per unit, the hourly flexibility payments in Figure 2.4(d) are total payments made by the market operator towards procuring the flexibility service, which is then allocated among the flexibility providers based on the policy allocated to them. In particular, as exhaustively covered in [Paper A], the payment follows a differentiated pricing scheme depending on a number of factors: (i) level of uncertainty perceived by the market operator (quantified by forecast error covariance matrix and day-ahead forecast), (ii) network topology, i.e., location of a flexibility provider w.r.t. uncertainty sources and network congestions, and (iii) whether other flexibility providers are available, i.e., how scarce is flexibility at a given hour.

Comparison with LP-based benchmarks: In-sample and out-of-sample costs

To highlight the improvements in social welfare while moving towards the SOCP-based uncertainty-aware market, it is compared against two uncertainty-aware market-clearing references available within the LP domain. First reference market, $\mathcal{R}1$ is a deterministic market framework based on MRR, similar to that considered in [Paper B], while the second reference market $\mathcal{R}2$ solves a scenario-based stochastic market-clearing problem. Further details on the benchmarks as well as the parameters considered in these numerical experiments are provided in [Paper A]. Figure 2.5 shows the expected in-sample cost comparison between the proposed SOCP-based market framework, denoted by \mathcal{M}^{cc} and the LP-based benchmarks, $\mathcal{R}1$ and $\mathcal{R}2$. Here, in-sample refers to evaluating the market-clearing outcomes against an identical set of samples used to construct the uncertainty model for the chance-constrained program, referring to $\gamma = 1$ in the previously-discussed context of [Paper B]. Due to its exogenous consideration of uncertainty, $\mathcal{R}1$

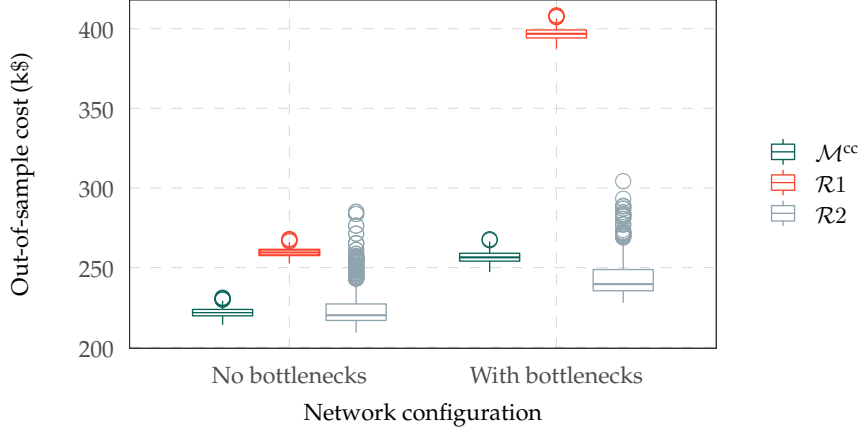


Figure 2.6: Out-of-sample market-clearing cost comparison for the 50% RES paradigm among the proposed SOCP-based market \mathcal{M}^{cc} and LP-based benchmarks: deterministic market $\mathcal{R}1$ and scenario-based stochastic market $\mathcal{R}2$. Reproduced from [Paper A].

leads to higher cost (and eventually infeasibility in the case with network bottlenecks for RES share of 60%) due to over-dimensioning of reserves procured. While \mathcal{M}^{cc} and $\mathcal{R}2$ lead to comparable costs, the market outcomes of $\mathcal{R}2$ do not provide any guarantees on the feasibility of the market beyond these scenarios considered¹⁵.

To further compare the performance of these market frameworks, out-of-sample simulations are performed by considering 500 uncertainty realizations distinct from those considered in the reformulation of the chance constraints during the real-time operation stage. While the LP benchmarks $\mathcal{R}1$ and $\mathcal{R}2$ involve a real-time market allowing adjustments (at a premium) up to the flexible capacity limits defined in the day-ahead market stage, the SOCP-market \mathcal{M}^{cc} strictly adheres to the activation of the adjustment policies. To account for potential infeasibility during the real-time stage, contingency actions, i.e., wind power curtailment and load shedding, are allowed with a high penalty. Figure 2.6 shows the distribution of out-of-sample costs for the various market frameworks for the 50% RES paradigm¹⁶. The deterministic market framework $\mathcal{R}1$ performs poorly compared to others, as in the in-sample case. Further, the scenario-based market framework $\mathcal{R}2$ exhibits a high variability from the expected in-sample cost, and as further discussed in [Paper A], requires frequent contingency actions as compared to \mathcal{M}^{cc} . The numerical results demonstrate the uncertainty-aware SOCP-based market framework outperforms the LP-based benchmarks in terms of social welfare and its reduced variability.

2.4 Future perspectives

While the discussion in this chapter focuses primarily on electricity markets, the theoretical results and methodology developed are of potential interest in competitive settings that involve physical or non-physical systems, where cost- and constraint-related nonlinearities are currently managed by adopting approximation techniques via linearization. In particular, within the integrated energy system context, the flexibility-centric redesign of electricity markets presented in this chapter

¹⁵An analytical lower bound on the number of scenarios necessary to provide identical feasibility guarantees for \mathcal{M}^{cc} and $\mathcal{R}2$ is given in [121, Theorem 5]. Based on the parameters and participant characteristics considered in [Paper A], it corresponds to 80,000 scenarios, therefore imposing serious computational limitations on practical adoption of $\mathcal{R}2$.

¹⁶For each box, the central line indicates the median, the ends indicate the 25th and 75th percentiles, whereas the whiskers extend up to 1.5 times the interquartile range and rings denote outliers.

contributes towards a cost-efficient harnessing of cross-carrier flexibility. A SOCP-based electricity market provides a crucial step in generalizing the prevalent LP-based markets, such that a variety of heterogeneous flexibility providers are incentivized to reflect their nonlinearities via conic bids, ensuring cost recovery beyond the linear approximations of their feasibility sets. Further, a physically accurate representation of flows in the network is also enabled by this step in the evolution of electricity markets. Finally, as demonstrated by numerical experiments, SOCP-based markets allow an endogenous characterization of uncertainty faced at the day-ahead stage, thereby improving social welfare. Beyond the uncertainty-aware variant simulated in the experiments, the general conic market proposal opens pathways for future research involving one or more attributes of uncertainty-, asset-, and network-awareness. For instance, studying coordination between transmission and distribution system operators to harness flexibility in uncertainty- and network-aware settings. In the integrated energy system context, as covered in Chapter 3, combining these attributes paves the way for a reliable and resilient system operation in the coupled energy systems, while harnessing cross-carrier flexibility.

CHAPTER 3

Uncertainty-Aware Coordination Among Energy Systems

This chapter summarizes the contributions of this thesis towards enabling uncertainty-aware coordination among energy systems. In addition to the operational costs and constraints of the flexibility providers within the integrated energy system, consideration of uncertainty and its propagation across system boundaries is crucial for harnessing cross-carrier flexibility. Section 3.1 presents a general uncertainty-aware centralized coordination framework for electricity and natural gas systems, discusses the challenges associated with it, and how this thesis addresses them. Based on [Paper C], Section 3.2 discusses the specific methodology and numerical results associated with harnessing cross-carrier flexibility under uncertainty propagation. Focusing on the impact of uncertainty propagation on state variables, Section 3.3 discusses the uncertainty- and variance-aware gas market framework proposed in [Paper D]. Lastly, Section 3.4 discusses future research perspectives.

3.1 Uncertainty propagation in integrated energy systems

The increasing interdependence among energy systems leads to the propagation of uncertainty among them. The challenges with uncertainty propagation are particularly severe for coupled electricity and natural gas systems. This is because the green energy transition of the electricity system is supported primarily by the operational flexibility provided by gas-fired power plants. Figure 3.1 illustrates a coupled electricity and gas system. On the one hand, cross-carrier flexibility is harnessed via the flexible operation of gas-fired power plants and short-term storage of natural gas in pipelines, i.e., linepack flexibility. On the other hand, adapting to the supply fluctuations from weather-dependent RES in the electricity system induces unforeseen changes in the operational status of the assets and network in the natural gas system. Naturally, the propagation of uncertainty can be studied in both directions, e.g., considering renewable biogas sources which induce uncertain supply injections into the electricity system or the impact of

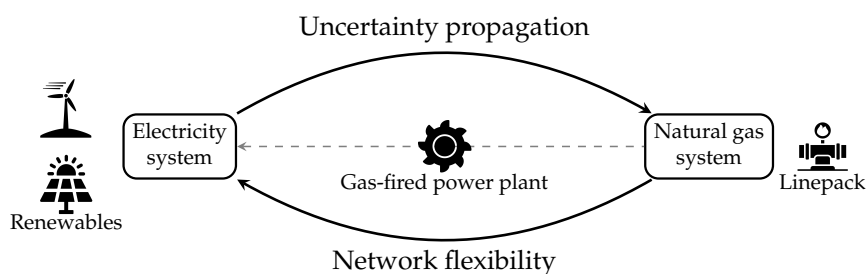


Figure 3.1: Illustration of a coupled electricity and natural gas system.

upcoming power-to-gas units leveraging surplus electricity production from RES. However, for simplicity of exposition, this thesis studies uni-directional uncertainty propagation, i.e., how the operational constraints of assets and the network in the coupled natural gas system are impacted by the uncertainty propagated from the electricity system¹.

As discussed in Chapter 1, electricity and natural gas systems are typically dispatched sequentially in separate markets. Nevertheless, this chapter presents a methodology assuming centralized dispatch as a first step towards studying uncertainty propagation. Such an uncertainty-aware, centralized dispatch can be regarded as an ideal benchmark for market-based coordination among the electricity and gas systems, providing upper bounds on the amount of cross-carrier flexibility harnessed and uncertainty propagation mitigated.

3.1.1 Centralized electricity and natural gas dispatch under uncertainty

Consider a stochastic centralized dispatch of a coupled electricity and natural gas system formulated as problem (3.1), to be solved by a central system operator ahead of real-time operation, e.g., at the day-ahead stage. From an uncertainty modeling perspective, the problem is a distributionally-robust chance-constrained (DRCC) program. It generalizes the stochastic market-clearing problem (2.13) as the uncertainty faced by the central system operator is no longer assumed to follow a specific distribution. Instead, the objective function (3.1a) adopts a min-max structure such that the total expected system cost over the market-clearing horizon is minimized while the uncertain variable, ξ , is drawn from the worst probability distribution within a family of distributions, collected in an ambiguity set² \mathcal{P} . A robust joint chance constraint (3.1b) involves a set of linear inequalities that are simultaneously satisfied with a probability or reliability level of at least $(1 - \varepsilon)$ over all probability distributions \mathbb{P}_ξ contained in the family \mathcal{P} . The parameter $\varepsilon \in (0, 1)$ denotes a preset constraint violation probability encapsulating the system operator's risk preference. Modeling the impact of uncertainty on state variables of a physical system using such joint chance constraints aligns naturally with the well-established reliability metrics used by system operators to characterize risk. The equality constraints (3.1c) are expected to hold *almost surely* (*a.s.*), given the uncertainty. The uncertainty-aware coordination problem is written as:

$$\min_{\tilde{\chi}, \tilde{\vartheta}, \tilde{\kappa}} \max_{\mathbb{P}_\xi \in \mathcal{P}} \mathbb{E}^{\mathbb{P}_\xi} \left[\sum_{t \in \mathcal{T}} \left(\sum_{i \in \mathcal{I}} c_i^E(\tilde{\chi}_{it}) + \sum_{k \in \mathcal{K}} c_k^G(\tilde{\vartheta}_{kt}) \right) \right] \quad (3.1a)$$

$$\text{s.t. } \min_{\mathbb{P}_\xi \in \mathcal{P}} \mathbb{P}_\xi \begin{bmatrix} f^{\text{EN}}(\tilde{\chi}_t, \tilde{\kappa}_t) \leq 0 \\ h^\chi(\tilde{\chi}_t) \leq 0, \quad h^\vartheta(\tilde{\vartheta}_t) \leq 0 \\ h^\varrho(\tilde{\varrho}_t) \leq 0, \quad h^\varphi(\tilde{\varphi}_t) \leq 0 \\ h^\kappa(\tilde{\kappa}_t) \leq 0, \quad h^\psi(\tilde{\psi}_t) \leq 0 \end{bmatrix} \geq 1 - \varepsilon, \quad \forall t \in \mathcal{T}, \quad (3.1b)$$

$$\min_{\mathbb{P}_\xi \in \mathcal{P}} \mathbb{P}_\xi \begin{bmatrix} f^{\text{EM}}(\tilde{\chi}_t, \tilde{\kappa}_t, \delta_t^E) = 0 \\ f^{\text{GM}}(\tilde{\chi}_t, \tilde{\vartheta}_t, \tilde{\kappa}_t, \tilde{\varphi}_t, \delta_t^G) = 0 \\ f^{\text{GN}}(\tilde{\varphi}_t, \tilde{\varrho}_t, \tilde{\kappa}_t) = 0 \\ f_t^{\text{LP}}(\tilde{\psi}, \tilde{\varphi}) = 0 \end{bmatrix} \stackrel{\text{a.s.}}{=} 1, \quad \forall t \in \mathcal{T}, \quad (3.1c)$$

¹Aligned with this focus, the framework presented in this thesis represents the gas network with a higher modeling granularity, i.e., consideration of state variables, whereas the state variables of the electricity network, e.g., bus voltage magnitudes and phases, power losses, etc. are ignored by assuming lossless DC power flows in lines.

²Ambiguity sets are typically built using approaches that leverage historical observations or estimated empirical distributions. For instance, by fitting observations to known probability distributions, by collecting distributions described by empirically estimated moments of uncertainty (moment-based ambiguity sets), by using probabilistic distance metrics such as Wasserstein distance measured w.r.t. the empirical distribution (metric-based ambiguity sets), etc. See [122] for an extensive review.

where the dependency of the stochastic variables on the uncertainty is omitted from representation to reduce notational clutter. The gas network is represented by a directed graph $(\mathcal{M}, \mathcal{E})$ with gas nodes denoted by $\mathcal{M} = \{1, 2, \dots, M\}$ and pipelines denoted by $\mathcal{E} = \{1, 2, \dots, E\}$. Each element of the set \mathcal{E} is formed by a pair of connected nodes (m, m') . The graph may contain cycles, whereas parallel pipelines and self-loops should not exist. The set of pipelines hosting pressure regulation assets such as compressors or valves are called active pipelines and denoted by $\mathcal{E}_a \subseteq \mathcal{E}$. For the electricity system, as in Chapter 2, a directed graph $(\mathcal{N}, \mathcal{L})$ denotes the electricity network with N nodes and L power lines. Parameters $\delta_t^E \in \mathbb{R}^N$ and $\delta_t^G \in \mathbb{R}^M$ denote the inflexible, inelastic nodal demand of electricity and gas at the respective nodes of the energy systems. Stochastic variables $\tilde{\chi}_t(\xi) \in \mathbb{R}_+^I$ and $\tilde{\vartheta}_t(\xi) \in \mathbb{R}_+^K$ indicate the electricity and natural gas injected by the electricity producers and gas suppliers, collected in sets $\mathcal{I} = \{1, 2, \dots, I\}$ and $\mathcal{K} = \{1, 2, \dots, K\}$, respectively. Variables $\tilde{\varrho}_t(\xi) \in \mathbb{R}_+^M$, $\tilde{\varphi}_t(\xi) \in \mathbb{R}^E$, and $\tilde{\psi}_t(\xi) \in \mathbb{R}_+^E$ denote the state variables of the natural gas system, i.e., the nodal gas pressures, gas flows in pipelines, and the amount of linepack available in the pipelines. Finally, the variable $\tilde{\kappa}_t(\xi) \in \mathbb{R}^E$ denotes active, continuous control actions in regulating gas pressure in the network, i.e., by the operation of compressors and valves.

The terms in objective function (3.1a), $c_i^E(\tilde{\chi}_{it})$ and $c_k^G(\tilde{\vartheta}_{kt})$ denote the convex, twice-differentiable cost functions of electricity and natural gas injection over the $\mathcal{T} = \{1, 2, \dots, T\}$ periods. The set of linear inequalities comprising the robust joint chance constraint (3.1b) is formed by the power flow limits in the electricity system, $f^{\text{EN}}(\tilde{\chi}_t, \tilde{\kappa}_t) \leq 0$, and bounds on the variables, denoted by functions taking the form $h^{(\cdot)}(\cdot) \leq 0$. These functions represent the possibly multiple (but finite) number of linear inequalities on the variables. Apart from physical bounds on the variables, these inequalities may include system operator's operational constraints, e.g., ensuring uni-directional gas flows in active pipelines, maintaining a minimum linepack amount at the end of dispatch horizon, etc. Linear equality constraints $f^{\text{EM}}(\tilde{\chi}_t, \tilde{\kappa}_t, \delta_t^E) = 0$ and $f^{\text{GM}}(\tilde{\chi}_t, \tilde{\vartheta}_t, \tilde{\kappa}_t, \tilde{\varphi}_t, \delta_t^G) = 0$ represent the electricity and gas market-clearing conditions, i.e., supply-demand balance, respectively. Observe that the gas market-clearing condition is the crucial constraint which couples the decisions between the two systems, such that the fuel consumed by gas-fired power plants is considered as variable gas withdrawals. The pressure regulation variable $\tilde{\kappa}_t(\xi)$ appears in both the types of balancing constraints to account for compressors and valves that may operate by consuming electricity or natural gas. The flows of natural gas in the network is governed by the nonlinear and non-convex equality $f^{\text{GN}}(\tilde{\varphi}_t, \tilde{\varrho}_t, \tilde{\kappa}_t) = 0$, representing the steady state flow of gas in pipelines as a function of nodal pressure and its regulation. Lastly, the linear equality $f_t^{\text{LP}}(\tilde{\psi}, \tilde{\varphi}) = 0$ represents the temporal dynamics of natural gas linepack.

Similar to problem (2.13), problem (3.1) is a semi-infinite program due to the possibly infinite number of constraints owing to the stochastic variables. The chance-constrained stochastic programming problem (2.13) admits computationally-tractable and convex reformulations under mild conditions. In practice, however, the assumption of a known probability distribution can be restrictive. On the contrary, optimal solutions to DRCC programs, such as (3.1), provide stronger reliability guarantees against the possible uncertainty realizations drawing from an unknown distribution. This is of special relevance to the study of uncertainty propagation as the robustness of the solution against uncertainty is desirable. Moreover, the conservativeness of the solution associated with considering the worst-case distribution in the objective function can be adjusted by refining the ambiguity set and by an appropriate choice the joint constraint violation probability through data-driven approaches [122]. Despite its modeling advantages, the structure of problem (3.1) poses analytical and computational challenges that must be resolved to achieve tractability.

In addition to the tractability issues stemming from the choice of a generic uncertainty model in (3.1), studying uncertainty propagation as such brings additional challenges. For instance, the non-convexity associated with gas flow equations in (3.1c) needs to be addressed. Similarly, analytical characterizations of the impact of uncertainty propagation on the state variables in the coupled gas network must be obtained. In what follows, these challenges are further elaborated upon and the specific methodological contributions of [Paper C] and [Paper D] are presented in the context of prior works.

3.1.2 Challenges in studying uncertainty propagation

Modeling flow dynamics in networks

Under steady-state conditions and adopting simplifying assumptions, the physical equations governing the flow of gas in pipelines are represented by nonlinear equalities in (3.1c) that are inherently non-convex³. In deterministic settings, i.e., when all parameters are known with certainty, problem (3.1) is solved by overcoming non-convexity, typically using convex SOC relaxations [125] or linearization around exogenously-determined discrete operating points [126]. Without circumventing non-convexity and without considering the uncertainty propagation perspective, a deterministic gas network optimization can be solved using specialized algorithmic solvers [124] or general-purpose nonlinear solvers [127]. However, the consideration of uncertainty in the nonlinear and non-convex setting of problem (3.1) brings significant challenges since establishing a convex analytical dependency of the optimization variables on the uncertainty is not straightforward. Beyond steady-state conditions, a transient model of gas flows in the pipelines is described by a system of nonlinear partial differential equations, for which no analytical solution is available even in deterministic settings. While computationally-intensive numerical methods must be deployed to solve them, deriving meaningful market-clearing prices in presence of such algorithms can be challenging. Nevertheless, for studying uncertainty propagation with a focus on its market-based mitigation, it is sufficient to model gas flows under steady-state conditions. This is because all time derivatives in the partial differential equations can be assumed to be zero for the temporal resolution under which markets typically operate, i.e., hourly or quarter-hourly periods⁴.

Analytical characterization of uncertainty response

As problem (3.1) is solved at the day-ahead stage, recourse decisions are necessary to guide the integrated energy system towards mitigation of uncertainty during the subsequent real-time operation periods. From an uncertainty propagation perspective, recourse actions, if optimally decided, provide a network response model in the natural gas system such that an analytical dependency between the network state and the random forecast errors is established. Classically, within the DRCC framework, recourse actions based on linear decision rules have been proposed [129]. Considering the nonlinearity and non-convexity of the steady-state gas flow equation in (3.1c), linear decision rules provide a tractable approximation of the nonlinear dynamics of state variables in the natural gas system. Nonlinear decision rules, e.g., quadratic decision rules proposed in [118], potentially provide a tighter approximation of the stochastic problem, albeit at

³Also known as the Weymouth equation, these non-convex equalities are obtained by ignoring friction and geographical tilt in pipelines as well as neglecting any variations in ambient temperature and in gas injections under steady-state conditions [123, 124].

⁴This assumption is supported by recent work in [128] who show that these transients rarely survive in large, real-world gas networks beyond a time step of 3 minutes.

higher modeling and computational complexity. Nonetheless, if linear decision rules are chosen in the interest of their modeling simplicity, the solutions to problem (3.1) should be validated via rigorous in-sample and out-of-sample simulation studies. These simulation studies are aimed at characterizing the sub-optimality and approximation errors w.r.t the original non-convex stochastic problem, induced by the adoption of linear decision rules. Another critical aspect underlying uncertainty propagation among energy systems is analyzing and managing the impact of uncertainty from the electricity side on the state variables of the natural gas system, i.e., nodal pressures, flows in the pipelines, and consequently, the amount of linepack available. For that, simulations aside, analytical expressions characterizing the uncertainty-dependence of these state variables are necessary.

Convex approximation of robust joint chance constraints

Due to the presence of robust joint chance constraints (3.1b), the problem (3.1) typically admits a non-convex feasible region and is notoriously difficult to solve, even when the family of distributions \mathcal{P} is a singleton set, i.e., when the chance constraints are not distributionally robust and the inequalities forming them are linear [130]. Tractable convex approximations and reformulations that exploit the structure of the problem (3.1) are essential to attain solvability. Several approaches towards achieving tractability for such problems are summarized in [131] and extensively surveyed in [122]. Relevant to this thesis, a classical approach uses Bonferroni's inequality to conservatively approximate (3.1b) by replacing it with N_{\leq} individual robust chance constraints deriving violation probabilities from the vector $\hat{\epsilon} \in \mathbb{R}_+^{N_{\leq}}$, such that $\mathbf{1}^\top \hat{\epsilon} = \varepsilon$, as in [60]. This approach is similar to how non-robust joint chance constraints are treated and provides an inner convex approximation of the robust joint chance constraint (3.1b), which could be improved upon via an optimal selection [130] of $\hat{\epsilon}$. Nevertheless, even a sub-optimal selection of $\hat{\epsilon}$, e.g., $\hat{\epsilon}_k = \frac{\varepsilon}{N_{\leq}}, \forall k = 1, 2, \dots, N_{\leq}$ provides a joint constraint feasibility guarantee [130], which is crucial to studying uncertainty propagation. Similarly, a naive outer convex approximation of non-convex robust joint constraint is obtained by relaxing the requirement of simultaneous satisfaction of the N_{\leq} linear inequalities in (3.1b). While it does not provide guarantees on joint constraint satisfaction, this approach can still be useful in studying complex, temporally-coupled physical systems, as described by problem (3.1), under uncertainty. In such cases, it is essential to analyze the solution to problem (3.1) through out-of-sample simulations focusing on actual constraint violations.

3.1.3 Towards uncertainty-aware integrated electricity and gas systems

A large number of prior works, e.g., see [21, 38, 50, 132], have studied the harnessing of cross-carrier flexibility from integrated electricity and gas systems in deterministic settings. Recently, the research focus has shifted towards uncertainty-aware coordination among these energy systems to reflect the reality of high shares of weather-dependent RES in the electricity system. Within the uncertainty-aware coordination framework, stochastic programs based on scenarios [51, 133], robust optimization techniques [134–136], and chance-constrained optimization [137, 138] have been adopted. While scenario approaches face computational tractability issues stemming from a large number of scenarios required to represent uncertainty adequately, robust optimization techniques suffer from obtaining overly conservative operational costs [139]. Besides, from an uncertainty propagation perspective, the major drawback of robust and scenario-based programs is their ignorance of the gas system state within the prescribed uncertainty set or beyond the chosen scenarios. This provides barriers to achieving an analytical characterization of a gas system

uncertainty response model, which is crucial to establish a market-based framework for mitigation of uncertainty propagation. Lastly, the scenario-based and robust optimization approaches lead to poor performance of the day-ahead decisions when faced with uncertainty realizations beyond those forming the uncertainty set and scenario set, respectively. As an alternative, chance-constrained optimization yields an optimal uncertainty response across the entire forecast error distribution (or a family of such distributions in the DRCC setting). Furthermore, the convex analytical reformulations admitted by the probabilistic chance constraints provide opportunities to establish an analytical dependency between uncertainty and the state of the natural gas system.

Overcoming the previously-discussed challenges, this thesis employs chance-constrained optimization to develop a methodology to analyze and mitigate the uncertainty propagation. First, [Paper C] develops a unified framework to harness cross-carrier flexibility by allocating affine recourse policies to flexible agents (e.g., flexible power producers, natural gas suppliers) and state variables of the gas system which govern linepack flexibility. A tractable convex approximation of problem (3.1) is obtained by considering a moment-based ambiguity set \mathcal{P} that contains all multivariate distributions from which random variable ξ could be drawn, such that they are described by a known mean and covariance. Empirical estimates of these statistical moments are obtained from the historical measurements of forecast errors related to the uncertainty, thereby resulting in day-ahead and recourse decisions consistent with the available information on uncertainty. The non-convexity of gas flow equations and inter-temporal constraints associated with linepack flexibility in (3.1c) are managed by applying suitable convex relaxation techniques and reformulations involving the separation of uncertainty coefficients, respectively.

While [Paper C] develops the first methodology to study uncertainty propagation using a tractable approximation of the non-convex problem (3.1), the affine policies allocated to gas system state variables fail to capture the impacts of uncertainty propagation in the gas network, governed by nonlinear physical equations. Consequently, numerical results indicate that state variables are prone to constraint violations, thereby worsening the errors induced by the convex approximation.

To address that, [Paper D] develops a chance-constrained gas system optimization framework wherein control policies for flexibility providers, i.e., gas suppliers and active pipelines in the gas system, are optimized such that the state variables admit closed-form analytical expressions involving nominal and random components. This is achieved by adopting a linearization strategy for convexification of the non-convex gas flow equations in (3.1c). The linearization strategy coupled with the affine control policies ensures that the random state variables are given by affine functions of the control inputs for flexible gas injections and pressure regulation, thereby capturing the dependency of the uncertain network state on the system operator's decisions. As a result, constraint feasibility of state variables during real-time operation is guaranteed, up to the quality of the available day-ahead forecasts. Additionally, the variance of state variables under uncertainty can be explicitly penalized to reflect system operator's preference on the network state during the real-time operation stage. Overall, the analytical characterization of uncertainty and variance mitigation enables efficient pricing of these flexibility services in addition to the natural gas commodity, leveraging a combination of LP and SOCP duality. Consequently, flexibility providers are efficiently remunerated for their contribution towards uncertainty and variance mitigation during the real-time operation stage, such that they recover the costs incurred in providing these services while the gas market operator remains revenue adequate. The satisfaction of these desired economic properties is crucial to the real-world adoption of the proposed stochastic control and pricing approach.

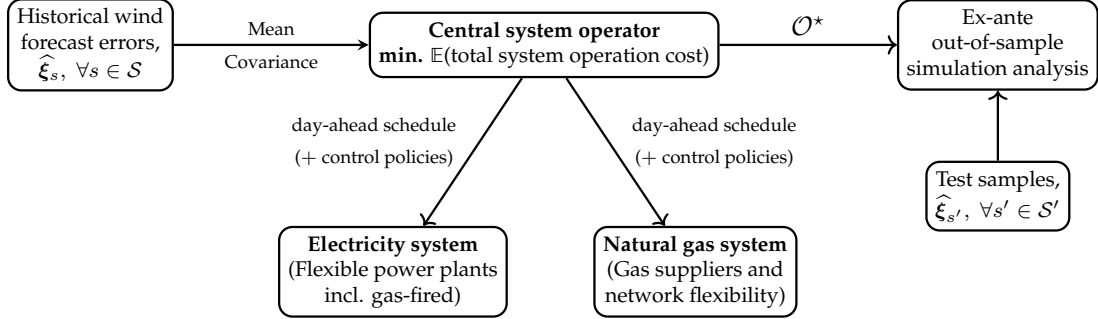


Figure 3.2: Uncertainty-aware coordinated electricity and natural gas dispatch

In summary, the stochastic control and market for natural gas systems developed in [Paper D] provides system operators with tools to efficiently control the uncertainty propagation, while incentivizing competing agents to provide flexibility services. The final SOCP market-clearing problem involves an additional *variance minimization service*, thereby extending the two-commodity uncertainty-aware conic electricity market discussed in Chapter 2.3 to a three-commodity coupled electricity and natural gas market that takes uncertainty propagation into account.

The uncertainty-aware coordination framework developed in [Paper C] and [Paper D], elaborated in the next sections, paves the way for market mechanisms incentivizing the active participation of gas system agents and the gas network to provide cross-carrier flexibility while mitigating uncertainty propagation.

3.2 Affine policies for harnessing cross-carrier flexibility

In the following, Section 3.2.1 outlines the methodology developed in [Paper C] to provide a tractable convex approximation of problem (3.1). Section 3.2.2 presents numerical results focusing on the trade-off between expected system operation cost and mitigation of the uncertainty propagated while discussing the quality of the convex approximation to problem (3.1).

3.2.1 Towards a tractable SOCP problem

Figure 3.2 summarizes the DRCC framework proposed in [Paper C] to study uncertainty propagation and its mitigation. A centralized, uncertainty-aware dispatch is solved at the day-ahead stage by a central system operator responsible for both the electricity and natural gas systems. The power produced by wind farms during the real-time operation stage is the sole uncertainty source considered. An ambiguity set constructed using the statistical moments derived from historical measurements, collected in a set $\mathcal{S} = \{1, 2, \dots, S\}$, is used to quantify the uncertainty faced by the system operator. Aside from the modeling assumptions discussed so far, e.g., steady-state flow of gas in pipelines and lossless DC approximation of power flows, the computational tractability of problem (3.1) is achieved under the following technical assumptions:

Assumption 4. The true probability distribution underlying the uncertainty is uniquely described by its first- and second-order moments.

Assumption 5. The directions of gas flows in all pipelines in the gas system are predetermined and considered to be fixed at the day-ahead stage by the central system operator.

Assumption 6. The pressure regulation actions in the active pipelines in the gas system are considered lossless, i.e., the pressure regulation does not consume any electricity or gas.

Assumption 4 is essential to the definition of moment-based ambiguity sets to characterize the distributional robustness of problem (3.1). Choosing this ambiguity set renders the DRCC program (3.1) robust against a set of log-concave distributions, which includes common distributions that forecast errors in energy systems are often modeled to obey, e.g., Gaussian, Weibull, beta distribution, etc. [140]. Assumption 5 is adopted to enable the approximation of problem (3.1) as a convex problem. Otherwise, integer variables are necessary to model flow directions. This introduces additional non-convexities and complexities associated with characterizing recourse actions in presence of integer variables. Lastly, Assumption 6 is a technical assumption adopted to simplify the modeling of pressure regulation. Modeling electricity-based pressure regulation introduces bi-directional uncertainty propagation which is out of the scope of this thesis, whereas gas-based pressure regulation introduces challenges in convexification of the gas flow equations. Assumptions 5-6 are dropped in [Paper D] by using a linearization strategy that circumvents these challenges.

Referring to Figure 3.2, the set \mathcal{O}^* collects the solution to the central dispatch problem. It is comprised of an optimal day-ahead schedule and control policies allocated to agents in both energy systems. The solution quality is evaluated via out-of-sample analysis, using a set of realizations comprising the test dataset $\mathcal{S}' = \{1, 2, \dots, S'\}$, distinct from those used to estimate the statistical moments. The out-of-sample simulations are performed by fixing the day-ahead decisions while their performance is evaluated against the test dataset, without re-optimization performed to ensure real-time feasibility of the problem. Therefore, they are referred to as *ex-ante* simulations. The following introduces some additional notation and describes the intermediate steps involved in obtaining the final tractable SOCP form of the non-convex DRCC problem (3.1).

Moment-based ambiguity set

For the T periods considered, let $\xi \in \mathbb{R}^{WT}$ denote the uncertain forecast errors for wind farms $\mathcal{W} = \{1, 2, \dots, W\}$, where \mathcal{W} collects the W wind farms in the electricity system. Let the ambiguity set describing the uncertainty ξ be defined such that it contains all multivariate probability distributions supported by a mean $\mu \in \mathbb{R}^{WT}$ and covariance $\Sigma \in \mathbb{R}^{WT \times WT}$, given as

$$\mathcal{P} = \{\mathbb{P}_\xi \in \mathcal{P}^0(\mathbb{R}^{WT}) : \mathbb{E}^{\mathbb{P}_\xi}[\xi] = \mu, \mathbb{E}^{\mathbb{P}_\xi}[\xi\xi^\top] = \Sigma\}, \quad (3.2)$$

where \mathcal{P}^0 denotes all probability distributions in \mathbb{R}^{WT} . Without losing generality, forecast errors are considered to follow a zero-mean distribution, i.e., $\mu = \mathbf{0}$ and that the true covariance matrix Σ can be empirically estimated from historical measurements. The structure of the positive semi-definite covariance matrix, Σ is such that its diagonal blocks, comprised of sub-matrices, $\Sigma_t \in \mathbb{R}^{W \times W}, \forall t \in \mathcal{T}$, capture the spatial correlation among the forecast errors in period t , while the off-diagonal blocks contain information about spatio-temporal correlation of the uncertain parameters. The ambiguity set \mathcal{P} defined in (3.2) can be extended to include uncertainty regarding the moments. When the system operator is less confident about the empirical moment estimates, further robustification of problem (3.1) can be achieved by considering these moments to be inexact but contained in well-described uncertainty sets, e.g., ellipsoidal [141]. Conversely, the system operator may impart expert knowledge about the uncertainty to shrink the ambiguity set \mathcal{P} , e.g., by including higher-order statistical moments [81], or by introducing structural restrictions on probability distributions such as symmetry [142] or uni-modality [143].

Affine policies as recourse actions

For the flexible producers of electricity and natural gas, recourse actions defined in the form of affine policies characterize their response to wind forecast errors realized during the real-time stage. The real-time production governed by affine policies is

$$\tilde{\chi}_t(\xi) = \chi_t + (\mathbb{1}^\top \xi_t) \alpha_t, \quad \forall t, \quad (3.3a)$$

$$\tilde{\vartheta}_t(\xi) = \vartheta_t + (\mathbb{1}^\top \xi_t) \beta_t, \quad \forall t, \quad (3.3b)$$

where $\chi_t \in \mathbb{R}^I$ and $\vartheta_t \in \mathbb{R}^K$ are the nominal quantities produced by the electricity producers and gas suppliers, respectively, at period t . Adopting a global uncertainty characterization, these flexibility providers respond to the net uncertainty faced by the system through policies $\alpha_t \in \mathbb{R}^I$ and $\beta_t \in \mathbb{R}^K$, respectively.

Given the simplified representation of flows in the electricity network adopted in [Paper C] using PTDFs, the changes in the power flows in the lines are given by the responses of producers α_t , contingent to the balancing constraints satisfied for the spatial configuration of wind farms, demands, and power producers. Therefore, the electricity market clearing in (3.1c) takes the form

$$\mathbb{1}^\top (\chi_t + (\mathbb{1}^\top \xi_t) \alpha_t) + \mathbb{1}^\top (\mathbf{W}_t - \xi_t) = \mathbb{1}^\top \delta_t^E, \quad \forall t, \quad (3.4)$$

where $\mathbf{W}_t \in \mathbb{R}^W$ is the best available point forecast of electricity production from wind farms at the day-ahead stage. Since the support of ξ_t spans \mathbb{R}^W , the infinite-dimensional equality (3.4) is met almost surely by matching the zero- and first-order coefficients of uncertainty [129], resulting in a set of deterministic equalities

$$\mathbb{1}^\top \chi_t + \mathbb{1}^\top \mathbf{W}_t = \mathbb{1}^\top \delta_t^E, \quad \forall t, \quad (3.5a)$$

$$\mathbb{1}^\top \alpha_t = 1, \quad \forall t. \quad (3.5b)$$

The power flows in the lines during the real-time stage are constrained by the capacity limits applied to both the nominal flows, i.e., considering perfect forecasts of wind farm production, and changes to it induced by the real-time adjustments in the production schedule to mitigate the uncertainty. Given the recourse actions, the resulting individual robust chance-constrained inequalities are approximated by SOC constraints, as discussed later in this section.

For further clarity of notation, the set of electricity producers in \mathcal{I} is partitioned into two disjoint subsets, \mathcal{G} collecting all gas-fired power plants and \mathcal{C} collecting all non-gas power producers. The uncertainty response of the the coupled natural gas system is therefore characterized by the recourse actions allocated to flexible gas suppliers (3.3b) and the real-time adjustments to fuel demand from the gas-fired power producers $k^G \circ \alpha_t, \forall i \in \mathcal{G}$. Here, the parameter $k^G \in \mathbb{R}^{|\mathcal{G}|}$ collects the fuel conversion factor of the gas-fired power producers. In turn, the state variables of the gas system, i.e., nodal pressures, flows in pipelines, and the amount of linepack available at a given period are physically described by the nonlinear, non-convex, and time-coupled equations in (3.1c) governing the flows in the gas network and the evolution of linepack over the T periods. Providing an accurate analytical characterization of changes in state variables under this complex setting is not straightforward. Focusing on first developing the methodology of uncertainty propagation, [Paper C] approximates this analytical characterization via affine functions in the interest of achieving simplicity of modeling. Therefore, the nodal pressures and flows in the gas

network at the real-time stage are approximated as affine functions of uncertainty:

$$\tilde{\varrho}_t(\xi) = \varrho_t + (\mathbb{1}^\top \xi_t) \eta_t, \quad \forall t, \quad (3.6a)$$

$$\tilde{\varphi}_t(\xi) = \varphi_t + (\mathbb{1}^\top \xi_t) \zeta_t, \quad \forall t, \quad (3.6b)$$

where variables $\varrho_t, \eta_t \in \mathbb{R}^M$ denote the nominal and stochastic components of the nodal gas pressures, respectively, while $\varphi_t, \zeta_t \in \mathbb{R}^E$ represent the nominal and stochastic components of the flows in pipelines. While not directly controllable, the auxiliary recourse variables η_t and ζ_t approximate the real-time feasibility of the state variables given the controllable recourse actions α_t and β_t . This implies that real-time feasibility of network state is guaranteed to the extent that the convex relaxation strategy adopted for the non-convex gas flow equations is tight⁵.

Convexification strategies for state equations of the gas system

Under the assumption of lossless pressure regulation provided by active pipelines, the flow of gas in pipelines at the real-time stage, represented by $f^{GN}(\tilde{\varphi}_t, \tilde{\varrho}_t, \tilde{\kappa}_t) = 0$ in (3.1c), is given by a set of stochastic quadratic equalities

$$\tilde{\varphi}_{et}(\xi) |\tilde{\varphi}_{et}(\xi)| = k_e^W \left((\tilde{\varrho}_{mt}(\xi))^2 - (\tilde{\varrho}_{m't}(\xi))^2 \right), \quad \forall e = (m, m') \in \mathcal{E}, \quad \forall t, \quad (3.7)$$

where parameters $k^W \in \mathbb{R}_+^E$ encode the friction coefficient and geometry of the gas pipelines. The absolute value operator in the left-hand side of (3.7) preserves the direction of gas flows in the pipelines. Given Assumption 5, this operator can be dropped since the gas flow directions are known, thereby reducing the left-hand side of (3.7) to $(\tilde{\varphi}_{et}(\xi))^2$. Under the policies given by (3.6), the equalities in (3.7) are expanded and equivalently replaced by three separate equalities formed by zero-, first-, and second-order coefficients of ξ on both sides, resulting in equalities, defined by $\forall e = (m, m') \in \mathcal{E}, \forall t$,

$$\varphi_{et}^2 = k_e^W (\varrho_{mt}^2 - \varrho_{m't}^2) \quad (3.8a)$$

$$\zeta_{et}^2 = k_e^W (\eta_{mt}^2 - \eta_{m't}^2) \quad (3.8b)$$

$$\zeta_{et} \varphi_{et} = k_e^W (\eta_{mt} \varrho_{mt} - \eta_{m't} \varrho_{m't}). \quad (3.8c)$$

While the equalities (3.8) are deterministic and thus, finite-dimensional, they remain non-convex. [Paper C] circumvents this by adopting an inner SOC relaxation of (3.8a)-(3.8b) obtained by equivalently writing these equalities as two-sided quadratic inequalities, wherein the non-convex quadratic inequalities are dropped. A similar strategy cannot be applied to (3.8c) since both the resulting inequalities are non-convex due to the presence of bilinear terms. Therefore, a McCormick relaxation [145] is adopted, i.e., rectangular envelopes based on the known (and estimated) upper and lower bounds of the variables provide an outer approximation of (3.8c) by a set of linear inequalities.

Apart from the gas flow equations, the stochastic linear equality $f_t^{LP}(\tilde{\psi}, \tilde{\varphi}) = 0$ in (3.1c) governing the evolution of linepack stored in the gas pipelines is reformulated as a set of deterministic equalities adopting a similar coefficient matching. These convexification strategies for the state equations of the gas system under uncertainty propagation are discussed in detail in [Paper C].

⁵As elaborated upon in Section 3.3, adopting a linearization strategy, [Paper D] provides guarantees for real-time network feasibility (up to linearization accuracy) for the gas system while focusing on a single-period (no linepack flexibility) setting and considering a variant of problem (3.1) involving non-robust joint chance constraints. Recently, [144] proposed an improvement over [Paper C] and [Paper D] by applying recourse actions based on multi-stage linear decision rules to this problem, thus enabling these guarantees in multi-period settings.

SOC reformulation of robust joint chance constraints

The robust joint chance constraints (3.1b) are approximated as SOC constraints following a two-step process. First, the requirement of simultaneous satisfaction of the N_{\leq} equalities comprising (3.1b) is relaxed by considering N_{\leq} robust individual chance constraints. This results in an outer approximation of the feasible region of constraint (3.1b), wherein the tightness of the approximation is adjusted by choosing the individual constraint violation probabilities, $\hat{\varepsilon}$. Second, under the availability of first- and second-order moments, standard results based on a variant of Chebyshev's inequality are used to provide deterministic SOC approximation of the non-convex individual chance constraints [146, Theorem 2.2]. For instance, given the recourse action in (3.3b) and the zero-mean assumption, a robust individual chance constraint denoting an upper bound on the k -th gas supplier's injection

$$\min_{\mathbb{P}_{\xi} \in \mathcal{P}} \mathbb{P}_{\xi}[\vartheta_{kt} + (\mathbb{1}^T \xi_t) \beta_{kt} \leq \bar{\vartheta}_k] \geq (1 - \hat{\varepsilon}_k), \quad \forall t, \quad (3.9)$$

is reformulated as a SOC constraint of the form

$$\sqrt{\frac{1 - \hat{\varepsilon}_k}{\hat{\varepsilon}_k}} \|\beta_{kt} \mathbb{1}^T \mathbf{X}_t\| \leq \bar{\vartheta}_k - \vartheta_{kt}, \quad \forall t, \quad (3.10)$$

where \mathbf{X}_t is a factorization of the covariance matrix such that $\Sigma = \mathbf{X} \mathbf{X}^\top$ and $\bar{\vartheta}_k \in \mathbb{R}_+$ denotes the maximum gas injection capacity of the supplier. A similar approximation strategy is applied to all robust individual constraints comprising (3.1b). This SOC approximation is known to provide overly conservative solutions as $\hat{\varepsilon}_k \rightarrow 0$ and approaches infeasibility for $\hat{\varepsilon}_k \approx 0$. Recently, [147] proposed an exact reformulation of such robust individual chance constraints, alleviating this conservatism. However, such reformulation is applicable to double-sided linear inequalities, e.g., stochastic variables admitting affine recourse actions that are bounded both above and below, whereas constraint (3.1b) typically also includes single-sided linear inequalities such as directionality of gas flows and pressure regulation provided by active pipelines. In [Paper C], the issues related to high conservatism and potential infeasibility of the SOC approximations of robust individual chance constraints are addressed by an appropriate choice of $\hat{\varepsilon}$.

Objective function reformulation

The work in [Paper C] assumes linear functions to model the cost of power and gas injections in the objective function (3.1a). Given the recourse actions defined in (3.3) for the electricity producers and gas suppliers, the objective function (3.1a) rewrites as

$$\min_{\mathcal{V}} \max_{\mathbb{P}_{\xi} \in \mathcal{P}} \mathbb{E}^{\mathbb{P}_{\xi}} \left[\sum_{t \in \mathcal{T}} \left(\sum_{i \in \mathcal{I}} c_i^E^\top (\chi_{it} + (\mathbb{1}^T \xi_t) \alpha_{it}) + \sum_{k \in \mathcal{K}} c_k^G^\top (\vartheta_{it} + (\mathbb{1}^T \xi_t) \beta_{kt}) \right) \right], \quad (3.11)$$

where the set of variables is comprised of nominal and recourse variables collected in a set $\mathcal{V} = \{\chi, \vartheta, \rho, \varphi, \psi, \alpha, \beta, \eta, \zeta\}$. Moreover, under the zero-mean forecast error assumption, the expectation operator is applied to eliminate the uncertainty-dependent terms of the objective function, and consequently, the maximization term in the objective function (3.11) is no longer applicable. Therefore, the objective (3.11) reduces to the following deterministic linear cost

$$\min_{\mathcal{V}} \left[\sum_{t \in \mathcal{T}} \left(\sum_{i \in \mathcal{I}} c_i^E^\top \chi_{it} + \sum_{k \in \mathcal{K}} c_k^G^\top \vartheta_{it} \right) \right]. \quad (3.12)$$

Observe that, unlike the quadratic cost functions discussed in Chapter 2, the objective function (3.12) does not explicitly penalize the recourse actions. Rather, the cost of mitigation of uncertainty is implicitly captured by the risk-aware SOC constraints approximating the probabilistic constraints⁶.

Adopting the affine recourse actions, followed by the convex relaxation of the state equations in the gas system, convexification of robust joint chance constraints (3.1b), and reformulation of the objective function, the infinite-dimensional problem (3.1) is approximated by a SOCP problem, provided in Appendix A of [Paper C]. This SOCP problem is solved using off-the-shelf commercial solvers and provides a tractable methodology to study the uncertainty-aware coordination in a coupled power and natural gas system.

3.2.2 Numerical results

The methodology developed in [Paper C] is evaluated by studying the optimal solution (nominal dispatch decisions and recourse actions) for a coupled power and natural gas system with high share of power production from wind farms. The ambiguity set in (3.2) is constructed using wind forecast scenarios developed for wind farms in Western Denmark [148]. For the robust individual chance constraints, an identical constraint violation probability, $\hat{\varepsilon}(\cdot)$, is chosen for simplicity. Wind forecast error datasets used to build the ambiguity set and in out-of-sample simulations as well as the parameters related to the network, production, and consumption in the electricity and gas systems are given in [Paper C] and an online appendix to the paper.

For a given choice of constraint violation probability, solving the tractable SOCP approximation of problem (3.1) results in optimal dispatch and affine policies allocated to the power producers and gas suppliers. As exhaustively covered in [Paper C], these allocations depend not only on the available capacity and cost structure of electricity producers and gas suppliers but also on the network constraints of both the systems. In particular, a spatially-optimal, cost-efficient delivery of energy and flexibility is achieved under uncertainty. Furthermore, considering the fuel demand from gas-fired power plants to provide flexibility in hours with high wind shares, linepack flexibility is effectively utilized by dispatching the cheapest gas suppliers in the hours with low gas demand, storing the excess gas in the pipelines. This enables a cost-efficient mitigation of the uncertainty propagated from the electricity system to the gas side, leveraging linepack flexibility.

Trade-off between expected operation cost and robustness to uncertainty

From an uncertainty mitigation perspective, studying the trade-off between the expected operation cost and the choice of constraint violation probability (a proxy for robustness to uncertainty) is crucial. While the optimal day-ahead decisions are fixed, out-of-sample simulations are performed using a test dataset comprised of $S' = 1,000$ wind realizations scenarios. For a chosen individual constraint violation probability $\hat{\varepsilon}$, the ex-ante joint constraint violation probability is

$$\Gamma_{\hat{\varepsilon}} = \frac{1}{S'} \sum_{s' \in S'} \mathbb{I}_{s'}, \quad (3.13)$$

where the indicator function $\mathbb{I}_{s'}$ admits a value of 1 if at least one of the N_{\leq} inequalities comprising the robust joint chance constraint (3.1b) is violated for the scenario s' . The probability $\Gamma_{\hat{\varepsilon}}$ shows the

⁶This choice of cost functions renders it difficult to derive meaningful prices for the mitigation of the uncertainty propagated. As discussed in Section 3.3, [Paper D] overcomes this issue by modeling the cost function of gas injections and pressure regulation losses as quadratic cost functions.

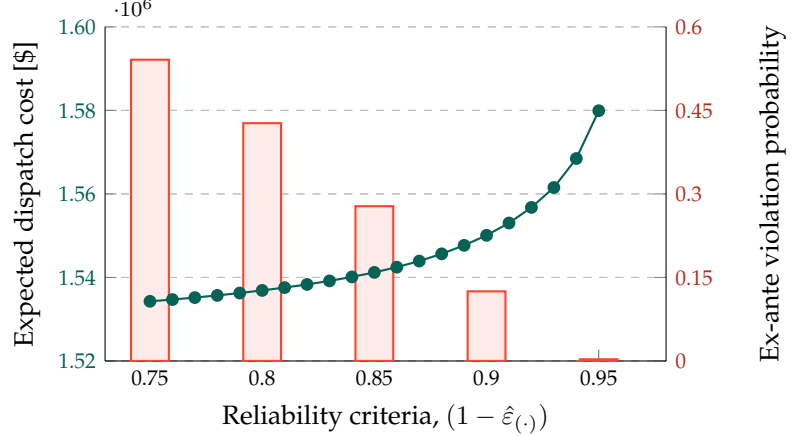


Figure 3.3: Expected day-ahead dispatch cost (line plot, referring to the left y-axis) and ex-ante violation probability (bars, referring to the right y-axis) with the reliability criteria set by the central system operator, $(1 - \hat{\varepsilon})$. Adapted from [Paper C].

proportion of the ex-ante scenarios that have at least one constraint violated beyond the numerical tolerance of the optimization solver employed.

For a range of reliability levels, $(1 - \hat{\varepsilon})$, prescribed by the central system operator, Figure 3.3 shows the expected cost of day-ahead dispatch (line plot with filled circles as markers, referring to the left-hand y-axis) and the ex-ante out-of-sample violation probability $\Gamma_{\hat{\varepsilon}}$ observed (bars, referring to the right-hand y-axis). The expected cost of dispatch at the day-ahead stage increases with higher confidence requirement levied by the system operator. Due to the outer approximation approach adopted for tractability of robust joint chance constraints, the values of $\Gamma_{\hat{\varepsilon}}$ are observed to be generally higher than the individual constraint violation probabilities chosen. However, with a relatively high expected cost, for reliability criteria $(1 - \hat{\varepsilon}) = 0.95$, an ex-ante joint constraint violation probability observed is 0.003, which indicates a better robustness to uncertainty than modeled. Considering the large number of chance constraints involved in the case study, SOC approximations based on Chebyshev's inequality leads to infeasibility for reliability criteria set at $(1 - \hat{\varepsilon}) > 0.95$.

Further results discussed in [Paper C] dive deeper into the observed ex-ante violation probability $\Gamma_{\hat{\varepsilon}}$, studying how they correspond to constraint violations in individual groups of constraints comprising (3.1b) for various prescribed levels of $\hat{\varepsilon}$. In particular, it is observed that the available linepack flexibility in the natural gas system was not depleted while mitigating the uncertainty propagated from the electricity. On the other hand, constraints modeling gas flow directions as fixed by the system operator before solving problem (3.1), as formalized in Assumption 5, are violated with a high frequency.

Tightness of convex relaxations

Beyond the out-of-sample simulations, the tightness of the convex relaxations adopted for the original stochastic non-convex gas flow equations (3.7) is studied to characterize the impact of uncertainty propagation on state variables. For the equalities in (3.8), a normalized root mean square relaxation gap parameter is computed, accounting for each equality constraint of the form

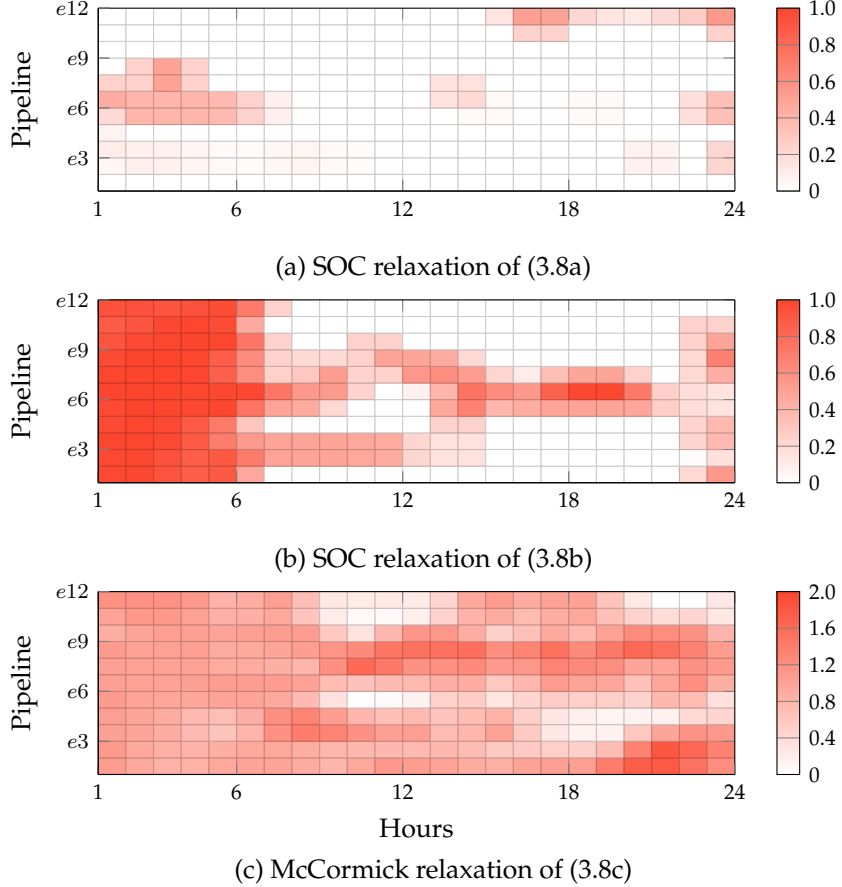


Figure 3.4: Normalized relaxation gaps for the convex relaxations of the non-convex equality (3.7). Adapted from [Paper C].

$A_{et} = B_{et}, \forall e \in \mathcal{E}, \forall t$ relaxed as $A_{et} \leq B_{et}$, such that

$$\Xi = \left[\frac{1}{T} \frac{1}{E} \sum_{t \in \mathcal{T}} \sum_{e \in \mathcal{E}} \left(\frac{B_{et}^* - A_{et}^*}{B_{et}^*} \right)^{\frac{1}{2}} \right]. \quad (3.14)$$

Here, the superscript $*$ indicates the expression at the left-hand or right-hand side evaluated at the optimum. For $\hat{\varepsilon} = 0.05$, a Ξ -value of 0.78, 1.67, and 2.87 was observed for the equalities obtained by separating the terms that are uncertainty-independent (3.8a), quadratically- (3.8b), and linearly-dependent (3.8c) on uncertainty, respectively. The heatmaps in Figure 3.4 decompose the Ξ -value obtained for the three equalities in (3.8) for the various pipelines and time periods. While the relaxation is sufficiently tight for the uncertainty-independent terms of the original equation, shown in Figure 3.4(a), it is unsatisfactory for the uncertainty-dependent terms⁷. In particular, the equality obtained by matching the second-order coefficients of uncertainty (3.8b), exhibits high relaxation gaps in the early hours of the simulation horizon. On the one hand, this can be explained by the non-radial and cyclical topology of the gas network considered in the case study. On the other hand, the network topology effect is exacerbated by the uncertainty propagation from the electricity side. This mandates excess gas injections in the early hours to have sufficient linepack flexibility to cater to the gas withdrawal demands by gas-fired power

⁷Several works (see, e.g., [149], [150], [151]) have proposed approaches to improve the exactness of such SOC and McCormick relaxations of non-convex quadratic equalities based on an iterative tightening of the variable bounds or via augmenting the relaxation with tighter convex quadratic envelopes.

plants to provide flexibility to the coupled electricity system. Finally, McCormick relaxation of the non-convex equality corresponding to first-order coefficients of uncertainty (3.8c) exhibits poor relaxation exactness. In addition to the sub-optimal, loose bounds on the variables that influence the tightness of McCormick relaxation, this can be attributed to adversely negative values of the auxiliary recourse variables η and ζ that model the uncertainty response of state variables, i.e., pressures and flows, respectively.

In summary, the numerical results of [Paper C] underscore the importance of establishing a strong analytical dependency between the state variables and the uncertainty faced by the natural gas system to effectively mitigate it without adversely impacting the operational constraints. In particular, considering the relaxation gaps induced, the convex relaxation approach adopted in [Paper C] towards reaching a tractable reformulation of problem (3.1) needs rethinking. Further, the assumption of uni-directional gas flows adopted to circumvent integrality constraints is restrictive while studying uncertainty propagation. Section 3.3 discusses the methodology and results from [Paper D], which bypasses the simplifying assumptions adopted in [Paper C].

3.3 Stochastic control and pricing in natural gas networks

To establish a strong convex dependency between uncertainty propagated from the electricity system and the resulting changes in state variables of the coupled gas system, [Paper D] develops optimal control policies for gas injections and pressure regulation rates to provide real-time control inputs for the gas system operators. Dropping Assumptions 5-6, [Paper D] models the bi-directional flow of gas in pipelines and considers active pipelines that consume natural gas to provide pressure regulation. Lastly, to alleviate the conservatism associated with the SOC reformulation of robust joint chance constraints, [Paper D] considers a variant of problem (3.1) that involves non-robust joint chance constraints⁸.

In the following, Section 3.3.1 outlines the methodological contributions of [Paper D] with a specific focus on the linearization strategy adopted for convexification of the non-convex gas flow equations under uncertainty. Section 3.3.2 presents the analytical results underlying the proposed pricing for uncertainty and variance mitigation in the natural gas system. Lastly, the numerical results in Section 3.3.3 highlight the ability of the optimal control actions in mitigating uncertainty and variance propagated to natural gas systems.

3.3.1 Towards an analytical gas network response model

As discussed in Section 3.1.2, problem (3.1) can be solved to optimality under deterministic settings. Using best-available forecasts for the uncertainty, [Paper D] solves a deterministic, non-convex equivalent of the stochastic problem (3.1) to obtain a stationary point. This stationary point forms the basis for linearization of the nonlinear, non-convex Weymouth equation denoted by $f^{\text{GN}}(\tilde{\varphi}_t, \tilde{\varrho}_t, \tilde{\kappa}_t) = 0$. The modeling in [Paper D] ignores linepack flexibility and rather focuses on pressure regulation provided by lossy compressors and valves to mitigate the impact of uncertainty propagation. For simplicity of notation, each node is assumed to host a single gas supplier or demand and the subscripts t are dropped hereafter.

⁸However, [Paper D] provides theoretical results on the analytical gas network response model that hold for a variety of probability distributions that uncertainty of electricity demand and generation from weather-dependent RES are commonly modeled to obey [140].

Convexification of gas flow equations via linearization

For clarity of exposition, the following introduces some additional notation, augmenting the gas system variables. First, let $\tilde{\pi}(\xi) \in \mathbb{R}_+^M$ denote the squared nodal pressures in the gas system, such that $\tilde{\pi}_m(\xi) = (\tilde{\varrho}_m(\xi))^2$, $\forall m \in \mathcal{M}$. Next, let the topology of the gas network graph be described by a node-edge incidence matrix $\mathbf{A} \in \mathbb{R}^{M \times E}$, such that

$$\mathbf{A}_{k\ell} = \begin{cases} +1, & \text{if } k = m \\ -1, & \text{if } k = m' \\ 0, & \text{otherwise} \end{cases}, \quad \forall \ell = (m, m') \in \mathcal{E}.$$

The non-convex quadratic gas flow equations (3.7) can be rewritten in a vector form as

$$\tilde{\varphi}(\xi) \circ |\tilde{\varphi}(\xi)| = \text{diag}[\mathbf{k}^W](\mathbf{A}^\top \tilde{\pi}(\xi) + \tilde{\kappa}(\xi)), \quad (3.15)$$

where $\text{diag}[\mathbf{k}^W]$ is a diagonal matrix collecting the pipeline constants. Let the equalities in (3.15) be denoted as $f^{\text{GN}}(\tilde{\varphi}, \tilde{\pi}, \tilde{\kappa}) = 0$ and approximated, following a first-order Taylor series expansion, as

$$f^{\text{GN}}(\tilde{\varphi}, \tilde{\pi}, \tilde{\kappa}) \approx f^{\text{GN}}(\dot{\varphi}, \dot{\pi}, \dot{\kappa}) + \mathcal{J}(\dot{\varphi})(\tilde{\varphi} - \dot{\varphi}) + \mathcal{J}(\dot{\pi})(\tilde{\pi} - \dot{\pi}) + \mathcal{J}(\dot{\kappa})(\tilde{\kappa} - \dot{\kappa}) = 0, \quad (3.16)$$

where $\mathcal{J}(\mathbf{x}) \in \mathbb{R}^{E \times n}$ denotes the Jacobian of (3.15) w.r.t. an arbitrary vector $\mathbf{x} \in \mathbb{R}^n$ and $(\dot{\varphi}, \dot{\pi}, \dot{\kappa})$ is a stationary point retrieved by solving a deterministic variant of problem (3.1), by setting $\tilde{\delta}^G(\xi) = \delta^G$. Since $f^{\text{GN}}(\dot{\varphi}, \dot{\pi}, \dot{\kappa}) = 0$ at the stationary point, after rearrangement of terms, equation (3.16) provides an affine relation between the gas flows, nodal pressures, and pressure regulation around the stationary point:

$$\begin{aligned} \tilde{\varphi} - \dot{\varphi} &= \mathcal{J}(\dot{\varphi})^{-1} \mathcal{J}(\dot{\pi})(\dot{\pi} - \tilde{\pi}) + \mathcal{J}(\dot{\varphi})^{-1} \mathcal{J}(\dot{\kappa})(\dot{\kappa} - \tilde{\kappa}) \\ \Leftrightarrow \tilde{\varphi} &= \underbrace{\mathcal{J}(\dot{\varphi})^{-1} (\mathcal{J}(\dot{\pi})\dot{\pi} + \mathcal{J}(\dot{\kappa})\dot{\kappa}) + \dot{\varphi}}_{g_1(\dot{\varphi}, \dot{\pi}, \dot{\kappa})} - \underbrace{\mathcal{J}(\dot{\varphi})^{-1} \mathcal{J}(\dot{\pi})\tilde{\pi}}_{\mathbf{G}_2(\dot{\varphi}, \dot{\pi})} - \underbrace{\mathcal{J}(\dot{\varphi})^{-1} \mathcal{J}(\dot{\kappa})\tilde{\kappa}}_{\mathbf{G}_3(\dot{\varphi}, \dot{\kappa})} \\ \Leftrightarrow \tilde{\varphi} &= g_1(\dot{\varphi}, \dot{\pi}, \dot{\kappa}) + \mathbf{G}_2(\dot{\varphi}, \dot{\pi})\tilde{\pi} + \mathbf{G}_3(\dot{\varphi}, \dot{\kappa})\tilde{\kappa}. \end{aligned} \quad (3.17)$$

Here, parameters $g_1 \in \mathbb{R}^E$, $\mathbf{G}_2 \in \mathbb{R}^{E \times M}$, and $\mathbf{G}_3 \in \mathbb{R}^{E \times E}$ encode the sensitivity of gas flow rates to the nodal pressures and pressure regulation rates. These sensitivities are well-defined unless the stationary point $(\dot{\varphi}, \dot{\pi}, \dot{\kappa})$ is a bifurcation point for the non-convex problem. The system of equations defined by (3.17) is rank-deficient since $\text{rank}(\mathbf{G}_2) = M - 1$, thereby resulting in infinitely many solutions. However, as the gas network graph is connected, $E \geq M - 1$ holds necessarily, and therefore, a unique solution can be retrieved by choosing a reference network node⁹, $r \in \mathcal{M}$, such that $\tilde{\pi}_r = \dot{\pi}_r$.

Given the uniquely-characterized linearization (3.17) of the non-convex equality (3.15), the original deterministic non-convex problem and its deterministic convex approximation counterpart produce equivalent solutions at the stationary point. Consequently, the deterministic convex approximation can be used as a proxy to develop a stochastic gas system optimization problem with probabilistic linear equalities and inequalities. While the stochastic gas system optimization problem is presented in the following, formulations of the deterministic non-convex problem and its convex approximation can be found in [Paper D].

⁹In practice, a node with a large and constant gas injection is typically selected as a reference node [136]. However, any node that does not host a variable gas injection or extraction and is not a receiving node for active pipelines is a potential candidate.

Chance-constrained gas system optimization

Let the set of active pipelines \mathcal{E}_a be partitioned into disjointed subsets \mathcal{E}_c , hosting compressors and \mathcal{E}_v , hosting valves. Let a sign convention be adopted such that $\tilde{\kappa}_e(\xi) \geq 0$, $\forall e \in \mathcal{E}_c$ and $\tilde{\kappa}_e(\xi) \leq 0$, $\forall e \in \mathcal{E}_v$. While compressors increase the pressure at the receiving node of the active pipeline compared to the sending node, activation of valves reduces the pressure along the active pipeline. Active pipelines provide these pressure regulation services by consuming gas. Let the matrix parameter $\mathbf{B} \in \mathbb{R}^{M \times E}$ relate the active pipelines to their sending nodes while accounting for the losses $b_e \in \mathbb{R}_+$ incurred while providing pressure regulation services, i.e.,

$$\mathbf{B}_{ke} = \begin{cases} b_e, & \text{if } k = m, k \in \mathcal{E}_c \\ -b_e, & \text{if } k = m, k \in \mathcal{E}_v, \quad \forall e = (m, m') \in \mathcal{E}. \\ 0, & \text{otherwise} \end{cases}$$

Consequently, the gas supply-demand balance $f^{\text{GM}}(\tilde{\chi}, \tilde{\vartheta}, \tilde{\kappa}, \tilde{\varphi}, \delta^G) = 0$ in (3.1c) takes the form

$$\mathbf{A}\tilde{\varphi}(\xi) = \tilde{\vartheta}(\xi) - \mathbf{B}\tilde{\kappa}(\xi) - \tilde{\delta}^G(\xi), \quad (3.18)$$

where the demand $\tilde{\delta}^G(\xi) = \delta^G + \xi$ is a random variable, modeling the random gas extraction rates from gas-fired power producers, such that parameter $\delta^G \in \mathbb{R}^M$ denotes the best-available gas extraction forecasts and $\xi \in \mathbb{R}^M$ is the random forecast error associated with them. The non-robust variant of problem (3.1) studying mitigation of uncertainty propagated to the gas system writes as

$$\min_{\tilde{\vartheta}, \tilde{\kappa}, \tilde{\varphi}, \tilde{\pi}} \mathbb{E}^{\mathbb{P}^\xi} [c_1^\top \tilde{\vartheta}(\xi) + \tilde{\vartheta}(\xi)^\top \text{diag}[c_2] \tilde{\vartheta}(\xi)] \quad (3.19a)$$

$$\text{s.t. } \mathbb{P}_\xi \left[\begin{array}{l} \mathbf{A}\tilde{\varphi}(\xi) = \tilde{\vartheta}(\xi) - \mathbf{B}\tilde{\kappa}(\xi) - \tilde{\delta}^G(\xi), \\ \tilde{\varphi}(\xi) = \mathbf{g}_1 + \mathbf{G}_2 \tilde{\pi}(\xi) + \mathbf{G}_3 \tilde{\kappa}(\xi), \\ \tilde{\pi}_r(\xi) = \dot{\pi}_r \end{array} \right] \stackrel{\text{a.s.}}{=} 1, \quad (3.19b)$$

$$\mathbb{P}_\xi \left[\begin{array}{l} \underline{\pi} \leq \tilde{\pi}(\xi) \leq \bar{\pi}, \underline{\vartheta} \leq \tilde{\vartheta}(\xi) \leq \bar{\vartheta}, \\ \underline{\kappa} \leq \tilde{\kappa}(\xi) \leq \bar{\kappa}, \tilde{\varphi}_e(\xi) \geq 0, \forall e \in \mathcal{E}_a \end{array} \right] \geq 1 - \varepsilon, \quad (3.19c)$$

where $c_1, c_2 \in \mathbb{R}_+^M$ represent the linear and quadratic cost components associated with the gas injections at the M nodes of the network. Appropriately-dimensioned parameter pairs $(\underline{\pi}, \bar{\pi})$, $(\underline{\vartheta}, \bar{\vartheta})$, and $(\underline{\kappa}, \bar{\kappa})$ denote the bounds on nodal pressures, gas injection, and pressure regulation rates, respectively. The constraints in problem (3.19) are linear equalities and inequalities, i.e., non-convexity of problem arises solely from the probabilistic constraints. Problem (3.19) remains infinite-dimensional, thereby requiring recourse actions to achieve tractability. However, since the feasible region defined by constraints (3.19b)-(3.19c) is polyhedral, affine control policies provide an exact analytical characterization of uncertainty response in contrast to the approximation they provide in problem (3.1), as remarked in Section 3.2.1.

Control policies and tractable reformulation

The analytical network response model of gas system towards uncertain gas extraction rates $\tilde{\delta}^G(\xi)$ consists of a functional dependency of the stochastic variables on the uncertainty. Relying on affine policies defined under a nodal characterization of uncertainty, the recourse actions by controllable stochastic variables, i.e., gas injection rates $\tilde{\vartheta}(\xi)$ and pressure regulation rates $\tilde{\kappa}(\xi)$ are given by

$$\tilde{\vartheta}(\xi) = \vartheta + \beta\xi \quad (3.20a)$$

$$\tilde{\kappa}(\xi) = \kappa + \gamma\xi. \quad (3.20b)$$

Here, the variables $\vartheta \in \mathbb{R}^M$ and $\kappa \in \mathbb{R}^E$ denote the nominal value, while $\beta \in \mathbb{R}^{M \times M}$ and $\gamma \in \mathbb{R}^{E \times M}$ represent the recourse actions by gas injections and pressure regulation provided by active pipelines during the real-time stage to mitigate the uncertainty. Observe that, contrary to the affine policies defined in (3.3), the policies in (3.20) provide a nodal response to uncertainty. Beyond the controllable actions by gas injections and pressure regulation rates defined in (3.20), Proposition 1 formalizes the analytical relationship between the state variables of the gas system and the uncertainty propagated to it.

Proposition 1 (Gas System Uncertainty Response Model). *Given the control policies (3.20), the response of the natural gas system to uncertain gas withdrawal rates $\tilde{\delta}^G(\xi) = \delta + \xi$, where $\xi \sim \mathbb{P}_\xi$, is analytically characterized by*

- (i) **State variables response:** The stochastic nodal gas pressures and the flow rates in pipelines are given by affine functions

$$\tilde{\pi}(\xi) = \pi + \check{\mathbf{G}}_2(\beta - \hat{\mathbf{G}}_3\gamma - \text{diag}[1])\xi \quad (3.21a)$$

$$\tilde{\varphi}(\xi) = \varphi + (\check{\mathbf{G}}_2(\beta - \text{diag}[1]) - \hat{\mathbf{G}}_3\gamma)\xi, \quad (3.21b)$$

where $\check{\mathbf{G}}_2, \hat{\mathbf{G}}_2, \hat{\mathbf{G}}_3, \check{\mathbf{G}}_3$ are constants obtained by linear transformations on \mathbf{G}_2 and \mathbf{G}_3 .

- (ii) **Network admissibility:** The gas network response model, comprised of (3.20) and (3.21a)-(3.21b), is network admissible if the nominal and recourse variables obey

$$\mathbf{A}\varphi = \vartheta - \mathbf{B}\kappa - \delta \quad (3.21c)$$

$$(\beta - \mathbf{B}\gamma)^\top \mathbb{1} = \mathbb{1}, \quad (3.21d)$$

$$\varphi = \mathbf{g}_1 + \mathbf{G}_2\pi + \mathbf{G}_3\kappa, \quad (3.21e)$$

$$\pi_r = \dot{\pi}_r, [\beta]_r^\top = \mathbb{0}, [\gamma]_r^\top = \mathbb{0}. \quad (3.21f)$$

The first part of Proposition 1 resolves the stochastic nodal pressures and flow rates into nominal and recourse components, wherein the recourse components involve the control policies allocated to gas injections and pressure regulation. This relationship is derived through substitutions, followed by rearrangement of terms. A crucial step underlying the derivation is obtaining a pseudo-inverse of the matrix \mathbf{AG}_2 , which is non-invertible due to the singularity of \mathbf{A} for all gas network topologies, except radial networks¹⁰. The second part of Proposition 1 ensures that the nominal and recourse actions satisfy the supply-demand balance and the gas flow constraints for all realizations of uncertainty. This is shown by a separation of coefficients in the almost-sure constraints (3.19b) that are zero- and first-order in the uncertain variable ξ , as in Section 3.2.1. Appendix A of [Paper D] elaborates the intermediate steps involved in deriving the gas system uncertainty response model.

Given the control policies, a tractable reformulation to the chance-constrained gas network optimization problem (3.19) is obtained by employing the Bonferroni approximation of the joint chance constraints in (3.19c) and a reformulation of the expected cost in the objective (3.19a). First, selecting a vector of constraint violation probabilities $\hat{\epsilon} \in \mathbb{R}_+^{N_{\leqslant}}$ such that $\hat{\epsilon}_k = \frac{\epsilon}{N_{\leqslant}+}$, $\forall n = 1, 2, \dots, N_{\leqslant}$, the joint chance constraint in (3.19c) is replaced by N_{\leqslant} individual scalar chance

¹⁰As elaborated in Appendix A of [Paper D], the pseudo-inverse is evaluated by inverting a matrix of lower dimensions than \mathbf{AG}_2 , where the dimension reduction is achieved by removing the row and column corresponding to the pressure reference node, r .

constraints [130]. Each individual scalar chance constraint involving an arbitrary recourse variable $\mathbf{a} \in \mathbb{R}^M$ of the form

$$\mathbb{P}_\xi[\xi^\top \mathbf{a} \leq b] \geq 1 - \hat{\varepsilon} \quad (3.22a)$$

is then replaced by its analytical reformulation as a SOC constraint

$$z_{\hat{\varepsilon}} \|\mathbf{X}\mathbf{a}\| \leq b - \mathbb{E}_\xi[\xi^\top \mathbf{a}], \quad (3.22b)$$

where $z_{\hat{\varepsilon}} \geq 0$ is a safety parameter as defined in [60] and \mathbf{X} is a factorization of the covariance matrix Σ such that $\Sigma = \mathbf{X}\mathbf{X}^\top$. The left-hand side of (3.22b) is the margin that ensures constraint feasibility given the parameters of the forecast errors distribution, i.e., a larger safety parameter $z_{\hat{\varepsilon}}$ improves system security. Typically, the system operator chooses $z_{\hat{\varepsilon}}$ based on the knowledge about distribution \mathbb{P}_ξ , yet it always increases as the risk tolerance $\hat{\varepsilon}$ reduces. As discussed in Section 3.1.2, this approach provides an inner convex approximation of the joint chance constraints.

Under control policies (3.20), the objective function (3.19a) modeling the quadratic cost of gas injections is rewritten as

$$\min_{\vartheta, \kappa, \varphi, \pi \atop \beta, \gamma} \mathbb{E}^{\mathbb{P}_\xi} [\mathbf{c}_1^\top (\vartheta + \beta \xi) + (\vartheta + \beta \xi)^\top \text{diag}[\mathbf{c}_2](\vartheta + \beta \xi)].$$

With the zero-mean assumption of ξ and using the property that expectation of the outer product of a zero-mean random variable results in its covariance, i.e., $\mathbb{E}^{\mathbb{P}_\xi}[\xi \xi^\top] = \Sigma$, the objective function adopts the following deterministic equivalent form

$$\min_{\vartheta, \kappa, \varphi, \pi \atop \beta, \gamma} \mathbf{c}_1^\top \vartheta + \vartheta^\top \text{diag}[\mathbf{c}_2] \vartheta + \text{Tr}[\beta^\top \text{diag}[\mathbf{c}_2] \beta \Sigma], \quad (3.23)$$

which is a convex quadratic function in the variables ϑ and β . As discussed in Chapter 2, it is of computational and analytical interest to reformulate the quadratic cost terms as rotated SOC constraints. The constraint reformulation of quadratic terms in (3.23) is covered in [Paper D].

Variance of state variables

While the control policies (3.20) are optimized such that uncertainty is mitigated at the minimum expected cost, it is likely that solutions that induce a high variance of the state variables are produced. For instance, in the electricity system, such optimal uncertainty mitigation solutions have been shown to increase the variance of flows in the power lines, thereby requiring a variance minimization strategy [67]. For effective mitigation of the uncertainty propagated, it is crucial to model the variance of state variables in the gas system. Equations (3.21a)-(3.21b) characterize the impacts of uncertainty on the state variables via functions that are affine in the control inputs β and γ . Therefore, an optimal selection of these control inputs is performed such that the variance of state variables during the real-time operation stage is minimized. As they admit conic reformulations, it is preferable to minimize the standard deviations of the state variables instead of their variance.

Let variables $s^\pi \in \mathbb{R}^M$ and $s^\varphi \in \mathbb{R}^E$ denote the standard deviations of nodal pressures and gas flows in pipelines, respectively. For given fixed values of β and γ , the variance of pressures and flows can be minimized by solving the following SOCP problem

$$\min_{s^\pi, s^\varphi} \mathbf{c}^\pi^\top s^\pi + \mathbf{c}^\varphi^\top s^\varphi \quad (3.24a)$$

$$\text{s.t. } \left\| \mathbf{X}[\check{\mathbf{G}}(\beta - \hat{\mathbf{G}}_3\gamma - \text{diag}[1])]_n^\top \right\| \leq s_m^\pi, \forall m \in \mathcal{M} \quad (3.24b)$$

$$\left\| \mathbf{X}[\check{\mathbf{G}}(\beta - \text{diag}[1]) - \hat{\mathbf{G}}_3\gamma]_e^\top \right\| \leq s_e^\varphi, \forall e \in \mathcal{E}, \quad (3.24c)$$

where $c^\pi \in \mathbb{R}^M$ and $c^\varphi \in \mathbb{R}^E$ are terms penalizing the variance of state variables. SOC constraints (3.24b)-(3.24c) are tight at optimality. The objective function in the final tractable SOCP form of problem (3.19) involves a co-optimization of the decision variables in (3.23) and the standard deviation of the state variables. The selection of penalty terms results in a trade-off between cost minimization and variance minimization, i.e., increasing variance penalty reduces the variance of corresponding state variable while increasing the cost of dispatch. Numerical results in Section 3.3.3 discuss the cost-variance trade-off in detail.

Approximation errors and real-time feasibility

While it enables a tractable chance-constrained problem formulation, the linearization strategy adopted for convexification of the non-convex gas flow constraints (3.15) introduces approximation errors. These errors stem from the first-order Taylor series expansion employed to approximate the non-convex relationship between pressures and flows under uncertain gas extraction rates. As discussed in Section 3.1.2, such approximation errors may lead to constraint violations in the gas network during real-time operation. To address this, [Paper D] provides *a priori* worst-case performance guarantees that these approximation errors do not exceed a certain threshold. Since gas networks in practice are typically limited by nodal pressures, these state variables are exclusively treated in [Paper D] to provide the feasibility guarantees.

Let $\tilde{\pi}^*(\xi)$ denote a vector of stochastic nodal pressures, retrieved from the optimal solution to the SOCP reformulation of problem (3.19), such that the affine function in (3.21a) rewrites as

$$\tilde{\pi}^*(\xi) = \pi^* + \check{\mathbf{G}}_2(\beta^* - \hat{\mathbf{G}}_3\gamma^* - \text{diag}[1])\xi, \quad (3.25)$$

where the superscript $*$ indicates optimal values. In contrast to the anticipated pressure changes characterized by (3.25), for a given forecast error realization $\hat{\xi}$ and given optimal control policies β^* and γ^* , the actual nodal pressures $\pi^*(\xi)$ can be retrieved by solving a projection problem given in (3.26). Problem (3.26) projects the optimal control inputs obtained from the SOCP problem to solve a deterministic non-convex gas network optimization problem, specific to the realization $\hat{\xi}$:

$$\pi^*(\hat{\xi}) \in \underset{\vartheta, \kappa, \varphi, \pi}{\text{argmin}} \quad \left\| \tilde{\vartheta}^*(\hat{\xi}) - \vartheta \right\| + \left\| \tilde{\kappa}^*(\hat{\xi}) - \kappa \right\| \quad (3.26a)$$

$$\text{s.t. } \mathbf{A}\varphi = \vartheta - \mathbf{B}\kappa - (\delta^G + \hat{\xi}), \quad (3.26b)$$

$$\varphi \circ |\varphi| = \text{diag}[\mathbf{k}^W](\mathbf{A}^\top \pi + \kappa), \quad (3.26c)$$

$$\underline{\pi} \leq \pi \leq \bar{\pi}, \quad \underline{\vartheta} \leq \vartheta \leq \bar{\vartheta}, \quad (3.26d)$$

$$\underline{\kappa} \leq \kappa \leq \bar{\kappa}, \quad \kappa_e \geq 0, \quad \forall e \in \mathcal{E}_a, \quad (3.26e)$$

where the optimal control actions are given by $\tilde{\vartheta}^*(\hat{\xi}) = \vartheta^* + \beta^*\hat{\xi}$ and $\tilde{\kappa}^*(\hat{\xi}) = \kappa^* + \gamma^*\hat{\xi}$. Using the stationary point from problem (3.26), the approximation errors induced in nodal pressures can be computed *a priori*. For a given realization $\hat{\xi}$, these approximation errors $\Delta\pi_m(\hat{\xi})$, $\forall m \in \mathcal{M}$ are the Euclidean distances between the actual non-convex solution $\pi^*(\hat{\xi})$ and the one obtained by deploying the optimal control policies, i.e.,

$$\Delta\pi_m(\hat{\xi}) = \left\| \tilde{\pi}_m^*(\hat{\xi}) - \pi_m^*(\hat{\xi}) \right\|, \quad \forall m \in \mathcal{M}. \quad (3.27)$$

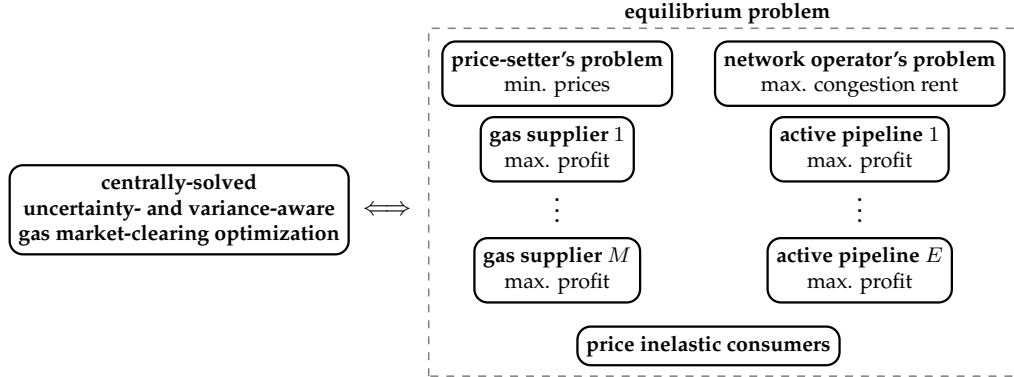


Figure 3.5: Equivalence between the uncertainty- and variance-aware gas market-clearing optimization problem and an equilibrium problem involving various market agents.

Theoretically, a worst-case bound on the pressure at node m can be computed by solving the following problem in auxiliary variable $y \in \mathbb{R}_+$

$$\min_y \quad y \tag{3.28a}$$

$$\text{s.t.} \quad \Delta\pi_m(\xi) - y \leq 0, \quad \forall \xi \in \mathbb{P}_\xi, \tag{3.28b}$$

such that a forecast error realization $\hat{\xi}$ corresponding to the largest Euclidean distance given by (3.27) is selected from the distribution \mathbb{P}_ξ . However, the infinite number of constraints in (3.28b) make the problem (3.28) computationally intractable. To resolve that, [Paper D] adopts a sample-based reformulation of problem (3.28) such that the constraint (3.28b) is enforced for a \hat{S} number of samples drawn from \mathbb{P}_ξ , i.e.,

$$\min_y \quad y \tag{3.29a}$$

$$\text{s.t.} \quad \Delta\pi_m(\hat{\xi}_s) - y \leq 0, \quad \forall s = 1, 2, \dots, \hat{S}. \tag{3.29b}$$

The expression in [152, Corollary 1] provides the minimum number of samples required to provide probabilistic guarantees that the pressure approximation error at a given node will remain under the optimal solution to problem (3.29), y^* . Here, y^* refers to the worst-case approximation error.

3.3.2 Towards pricing the mitigation of uncertainty propagation

The SOCP formulation of the gas system optimization under uncertainty enables an efficient pricing scheme for natural gas systems such that the prices reflect the mitigation of the uncertainty via adjustments by flexible agents. In addition, having closed-form expressions for the variance of state variables paves the path for developing an efficient pricing scheme to remunerate (or penalize) agents in the natural gas system based on their contribution towards mitigating (or aggravating) the variance. Using LP and SOCP duality, [Paper D] proposes an uncertainty- and variance-aware pricing scheme for natural gas systems, discussed in the following.

Interpretation as a competitive equilibrium

As illustrated in Figure 3.5, a stochastic gas pricing scheme is developed by leveraging the equivalence of the centrally-solved uncertainty- and variance-aware SOCP gas market clearing problem with an equilibrium problem involving various agents. These agents are: (i) a price-setter,

Nominal and recourse balance constraints for network admissibility:

$$\mathbf{A}\varphi = \vartheta - \mathbf{B}\kappa - \boldsymbol{\delta}^G : (\boldsymbol{\lambda}^c) \quad (3.30a)$$

$$(\beta - \mathbf{B}\gamma)^\top \mathbf{1} = \mathbf{1} : (\boldsymbol{\lambda}^r) \quad (3.30b)$$

$$\varphi = \mathbf{g}_1 + \mathbf{G}_2\pi + \mathbf{G}_3\kappa, \pi_r = \dot{\pi}_r : (\boldsymbol{\lambda}^w) \quad (3.30c)$$

Coupling constraints on nodal pressure variance and limits, $\forall m \in \mathcal{M}$:

$$\left\| \mathbf{X}[\check{\mathbf{G}}(\beta - \hat{\mathbf{G}}_3\gamma - \text{diag}[\mathbf{1}])]_n^\top \right\| \leq s_n^\pi : (\mathbf{u}_m^\pi, \lambda_m^\pi) \quad (3.30d)$$

$$z_\varepsilon \left\| \mathbf{X}[\check{\mathbf{G}}(\beta - \hat{\mathbf{G}}_3\gamma - \text{diag}[\mathbf{1}])]_m^\top \right\| \leq \bar{\pi}_m - \pi_m, \forall m \in \mathcal{M} : (\mathbf{u}_m^{\bar{\pi}}, \lambda_m^{\bar{\pi}}) \quad (3.30e)$$

$$z_\varepsilon \left\| \mathbf{X}[\check{\mathbf{G}}(\beta - \hat{\mathbf{G}}_3\gamma - \text{diag}[\mathbf{1}])]_m^\top \right\| \leq \pi_m - \underline{\pi}_m, \forall m \in \mathcal{M} : (\mathbf{u}_m^{\underline{\pi}}, \lambda_m^{\underline{\pi}}) \quad (3.30f)$$

Coupling constraints on flow variance and directionality:

$$\left\| \mathbf{X}[\check{\mathbf{G}}_2(\beta - \text{diag}[\mathbf{1}]) - \check{\mathbf{G}}_3\gamma]_e^\top \right\| \leq s_e^\varphi, \forall e \in \mathcal{E} : (\mathbf{u}_e^\varphi, \lambda_e^\varphi) \quad (3.30g)$$

$$z_\varepsilon \left\| \mathbf{X}[\check{\mathbf{G}}_2(\beta - \text{diag}[\mathbf{1}]) - \check{\mathbf{G}}_3\gamma]_e^\top \right\| \leq \varphi_e, \forall e \in \mathcal{E}_a : (\mathbf{u}_e^\varphi, \lambda_e^\varphi) \quad (3.30h)$$

responsible for seeking optimal prices for the coupling constraints involving the various agents, (ii) a network operator, maximizing the expected congestion rent in the gas network, (iii) a set of gas suppliers, maximizing their expected profits from selling gas and mitigating the uncertainty and variance, (iv) a set of active pipelines, maximizing their expected profits from pressure regulation and from mitigating the uncertainty and variance, and lastly, (v) a set of inflexible, inelastic consumers facing stochastic gas demand.

The coupling constraints in the centrally-solved uncertainty- and variance-aware gas market, which form the basis of the pricing scheme are given by (3.30). Lagrange multipliers associated with the constraints are denoted in parentheses next to them. The coupling constraints modeled as linear equalities comprised of: (i) nominal gas balance in (3.30a) and associated nodal price of gas $\boldsymbol{\lambda}^c \in \mathbb{R}^M$, (ii) balance of recourse actions to mitigate uncertainty in (3.30b) and associated price $\boldsymbol{\lambda}^r \in \mathbb{R}^M$, and (iii) linearized gas flow equation in (3.30c) and associated price $\boldsymbol{\lambda}^w \in \mathbb{R}^E$.

The SOC coupling constraints (3.30d)-(3.30h) admit tuples of dual variables associated with them. These SOC coupling constraints model the standard deviation of nodal pressures and flows in pipelines in (3.30d) and (3.30g), respectively, and network limits on the state variables, i.e., upper and lower bounds on nodal pressures given by (3.30e)-(3.30f), and lastly, the uni-directionality of flows in active pipelines in (3.30h). As discussed in Appendix C of [Paper D], for each of the SOC constraints in (3.30d)-(3.30h), a dual variable $\lambda \in \mathbb{R}_+$ and a vector $\mathbf{u} \in \mathbb{R}^M$ exist such that each element of \mathbf{u} corresponds component-wise to the uncertainty vector ξ . From SOCP dual feasibility condition, an optimal solution under strong duality is attained for $\|\mathbf{u}\| \leq \lambda$. Therefore, each SOC constraint is separable into a set of prices $\lambda, u_1, u_2, \dots, u_M$, thereby enabling the decomposition of revenues arising from them.

Expressions in (3.31) provide a functional representation of the various revenue streams for the agents in the gas system. Exact characterizations of these linear functions $r(\cdot)$ representing the revenue terms are in [Paper D]. Deterministic gas market proposals are limited in characterizing revenue terms corresponding to nominal balance and network congestion, thus resorting to externalized costs of recourse actions to mitigate uncertainty as well as the variance of state

variables resulting from it. In contrast to that, the uncertainty- and variance-aware pricing scheme internalizes these aspects by involving payments made to flexible gas suppliers and pressure regulation assets in the network for their contribution towards mitigating uncertainty, congestion, and variance in the natural gas network.

$$R_m^\vartheta = \underbrace{r_1^\vartheta(\vartheta_m, \lambda_m^c)}_{\text{nominal payment}} + \underbrace{r_2^\vartheta([\beta]_{(m,:)}, \lambda_m^r)}_{\text{recourse payment}} + \underbrace{z_\varepsilon r_3^\vartheta([\beta]_{(m,:)}, \bar{\mathbf{u}}, \mathbf{u}^\pi, \mathbf{u}^\varphi)}_{\text{congestion payment}} + \underbrace{r_4^\vartheta([\beta]_{(m,:)}, \mathbf{u}^\pi, \mathbf{u}^\varphi)}_{\text{variance payment}} \quad (3.31a)$$

$$R_e^\kappa = \underbrace{r_1^\kappa(\kappa_e, \boldsymbol{\lambda}^c, \boldsymbol{\lambda}^w)}_{\text{nominal payment}} + \underbrace{r_2^\kappa([\gamma]_{(e,:)}, \boldsymbol{\lambda}^r)}_{\text{recourse payment}} + \underbrace{z_\varepsilon r_3^\kappa([\gamma]_{(e,:)}, \bar{\mathbf{u}}, \mathbf{u}^\pi, \mathbf{u}^\varphi)}_{\text{congestion payment}} + \underbrace{r_4^\kappa([\gamma]_{(e,:)}, \mathbf{u}^\pi, \mathbf{u}^\varphi)}_{\text{variance payment}} \quad (3.31b)$$

$$R^{\text{rent}} = \underbrace{r_1^{\text{rent}}(\varphi, \boldsymbol{\lambda}^c, \boldsymbol{\lambda}^w, \boldsymbol{\lambda}^\varphi)}_{\text{flow congestion rent}} + \underbrace{r_2^{\text{rent}}(\pi, \boldsymbol{\lambda}^w, \boldsymbol{\lambda}^\pi, \boldsymbol{\lambda}^{\bar{\pi}})}_{\text{pressure congestion rent}} + \underbrace{r_3^{\text{rent}}(s^\pi, s^\varphi, \boldsymbol{\lambda}^\pi, \boldsymbol{\lambda}^\varphi)}_{\text{variance rent}} \quad (3.31c)$$

$$R_m^\delta = \underbrace{r_1^\delta(\delta_m^G, \lambda_m^c)}_{\text{nominal payment}} + \underbrace{r_2^\delta(\lambda_m^r)}_{\text{recourse payment}} + \underbrace{z_\varepsilon r_3^\delta(\bar{\mathbf{u}}, \mathbf{u}^\pi, \mathbf{u}^\varphi)}_{\text{congestion payment}} + \underbrace{r_4^\delta(\mathbf{u}^\pi, \mathbf{u}^\varphi)}_{\text{variance payment}} \quad (3.31d)$$

For the flexibility providers, i.e., gas suppliers in (3.31a) and active pipelines (3.31b), each agent receives payments towards providing nominal supply and pressure regulation services (nominal payment), mitigation of uncertainty (recourse payment), reducing congestion in the gas network (congestion payment), and minimizing the variance of state variables (variance payment). First, note that all revenue terms, except the nominal payments, depend on the control policies allocated to the agents. Second, observe that the congestion payments are a function of safety parameter z_ε selected by the system operator for the reformulation of the chance constraints, indicating that this revenue stream increases as the system operator's risk tolerance reduces. Third, the variance payment terms are proportional to the variance penalties c^π, c^φ set by the system operator. This proportionality results from the fact that at the optimal solution, the prices $\boldsymbol{\lambda}^\pi$ and $\boldsymbol{\lambda}^\varphi$ in (3.30d) and (3.30g) are attained such that $\boldsymbol{\lambda}^\pi = c^\pi$ and $\boldsymbol{\lambda}^\varphi = c^\varphi$. Next, the congestion rent in (3.31c) includes the deterministic components associated with the shadow prices of linearized gas flow equations, the unidirectionality of active pipelines, and the nodal pressure limits as well as stochastic components involving the variance of pressures and flows. Finally, the inflexible, inelastic consumers are charged in (3.31d) according to their consumption as well as contribution to uncertainty and variance in the gas system.

Economic properties of the competitive equilibrium

The payments described in (3.31) result in an uncertainty- and variance-aware competitive spatial price equilibrium in the gas system. In what follows, the market equilibrium is formalized and the satisfaction of desired economic properties are elaborated upon.

Theorem 4 (Gas system competitive equilibrium). *The centrally-solved uncertainty- and variance-aware gas market-clearing optimization problem is equivalent to a competitive spatial price equilibrium among the gas system agents, shown in Figure 3.5, such that*

- (i) *Each gas supplier at node $m \in \mathcal{M}$ maximizes expected profit when receiving payments as per (3.31a).*
- (ii) *Each active pipeline $e \in \mathcal{E}_a$ maximizes expected profit when receiving payments as per (3.31b).*

- (iii) *The network operator maximizes the expected congestion rent characterized by (3.31c).*
- (iv) *The expected payment by consumer located at node $m \in \mathcal{M}$ is minimized when they are charged as per (3.31d).*

Theorem 4 is proved in Appendix D of [Paper D] by the equivalence of the KKT optimality conditions of the optimization problem and the individual profit-maximization problems of the gas suppliers, active pipelines, the price setter, and the gas network operator. Being inflexible and inelastic, consumers demonstrate an infinite utility and therefore, do not employ individual utility maximization problems. The equivalence between optimization and market equilibrium established by Theorem 4 holds under certain common assumptions. First, the primal SOCP market-clearing optimization problem and its dual problems are essentially strictly feasible, i.e., they satisfy the constraint qualifications necessary for strong duality to hold. Second, the gas market is perfectly competitive, i.e., no market agent in Figure 3.5 exhibits strategic behavior and therefore, acts according to its true preferences. Lastly, the information on uncertainty distribution \mathbb{P}_ξ is consistent and symmetric for all the agents¹¹.

As discussed in Chapter 2.2.3, competitive market designs are evaluated for their satisfaction of economic properties that guarantee the efficiency of the market, cost recovery for the market participants, and revenue adequacy of the market. Under the uniform pricing scheme adopted in [Paper D], the following theorem formalizes the conditions under which these desired economic properties are satisfied.

Theorem 5 (Economic properties). *Given the equivalence between the centrally-solved optimization problem and the competitive market equilibrium established by Theorem 4, the following economic properties hold at optimality:*

- (i) **Market efficiency:** *Under the assumption of perfect competition, social welfare is maximized in expectation, i.e., no agent has incentives to unilaterally deviate from the market-clearing outcomes.*
- (ii) **Cost recovery:** *If the variable control actions in the gas system are bounded by zero, i.e., $\underline{\vartheta} = 0$, $\kappa_e = 0$, $\forall e \in \mathcal{E}_c$ and $\bar{\kappa}_e = 0$, $\forall e \in \mathcal{E}_v$, then the payments (3.31a) and (3.31b) are sufficient to recover expected costs for the gas suppliers and active pipelines, respectively.*
- (iii) **Revenue adequacy:** *If a gas network linearization following (3.17) is achieved such that $\mathbf{g}_1 = \mathbf{0}$ and the nodal pressures are bounded below by zero, i.e., $\underline{\pi} = \mathbf{0}$, then the payments described in (3.31) are revenue adequate in expectation, i.e., they satisfy*

$$\sum_{m \in \mathcal{M}} R_m^\delta \geq \sum_{m \in \mathcal{M}} R_m^\vartheta + \sum_{e \in \mathcal{E}} R_e^\kappa.$$

The property of market efficiency in Theorem 5 is proved under the conditions of perfect competition involving rational and self-interested agents in the gas network and is given by the equivalent KKT optimality conditions of the optimization and equilibrium problems. Cost recovery for the gas suppliers and active pipelines hosting compressors and valves is proved by showing that the

¹¹Here, information asymmetry refers to market agents solving their individual profit maximization problems with different probabilistic characterizations of the common forecast error uncertainty. Recent works, e.g., [153], have studied this in the context of electricity markets, wherein the equivalence of the centralized optimization and the equilibrium problem no longer holds, with the divergence depending on the degree of information asymmetry among agents.

dual problem to the individual profit maximization problems of these agents necessarily evaluates to non-negative values at optimality. This non-negative dual objective evaluation relies on the common assumption of a zero lower bounds on the non-negative variables (ϑ , κ_e , $\forall e \in \mathcal{E}_c$) and zero upper bounds on non-positive variables (κ_e , $\forall e \in \mathcal{E}_v$), similar to Chapter 2.2.3. Lastly, revenue adequacy is proved by rearranging terms in the KKT optimality conditions and is established under two conditions. The first condition arises from the linearization of the non-convex gas flow equations and is not expected to be satisfied in practice. However, a non-zero g_1 leads to an additional payment term, corresponding to the linearization operating point, charged to consumers¹² in (3.31d). Similar to cost recovery, the second condition relies on a gas network designed such that lower bounds of nodal pressures are 0. However, numerical results in [Paper D] demonstrate that revenue adequacy holds in practice even when this condition is not satisfied.

The desired economic properties in Theorem 5 are given for expected allocations, i.e, under the assumption that the nominal and recourse balance in the gas system, characterized by the equalities (3.21c)-(3.21d) in the network admissibility constraints, hold at the optimum. However, feasibility of the centrally-solved SOCP optimization problem ensures that these constraints are always met. Consequently, the expected optimal allocations are viable (in the sense of [31, 82]) for every realization $\hat{\xi}$ drawn from a probability distribution consistent with the distributional assumption levied on the uncertainty ξ . Thus, for a given choice of safety parameter $z_{\hat{\xi}}$, Theorem 5 holds for the expected value and every realization $\hat{\xi}$ drawn from the distribution \mathbb{P}_{ξ} characterized by a zero mean and covariance matrix Σ used in reformulation of the chance constraints, as shown in (3.22).

3.3.3 Numerical results

To evaluate the uncertainty mitigation, numerical experiments on a 48-node natural gas network with 22 stochastic gas extraction nodes were performed. For the stochastic gas extractions, the forecast error ξ was assumed to be drawn from a zero-mean multivariate Gaussian distribution with a standard deviation of 10%. Consequently, the safety parameter $z_{\hat{\xi}}$ is given by the inverse cumulative distribution function of the standard Gaussian distribution evaluated at $(1 - \hat{\varepsilon})$ -th quantile [60]. The joint constraint violation probability ε is set at 1%. Details on the gas network parameters as well as the costs and constraints of the market agents are in [Paper D].

The proposed chance-constrained gas system optimization is benchmarked against the prevalent deterministic gas system optimization using out-of-sample simulations. Without considering uncertainty, the deterministic approach leads to a least-cost dispatch, optimal w.r.t. the nominal gas extraction rates. However, the deterministic policies lead to real-time infeasibility for more than 50% of the out-of-sample forecast error realizations considered. On the other hand, the proposed approach leads to allocations of control policies that enable effective mitigation of uncertainty at an additional cost of 1.6% over the deterministic case. At the same time, the control inputs in the proposed methodology remain feasible during the real-time operation stage with a reliability level of $(1 - \varepsilon) = 99\%$, while requiring minimal effort to restore the feasibility of real-time gas flows. The worst-case approximation errors due to linearization, as discussed in Section 3.3.1, are observed to depend significantly on the amount of uncertainty. For the 10% standard deviation considered, the worst-case approximation errors across the 48 nodes of the network do not exceed 5.8% on average. Whereas for the deterministic approaches, these approximation errors are larger by at least an order of magnitude.

¹²While the inflexible and inelastic consumers modeled in [Paper D] can indeed be charged with this additional payment for linearization, its allocation among the consumers requires careful further analysis, specifically keeping fairness in mind.

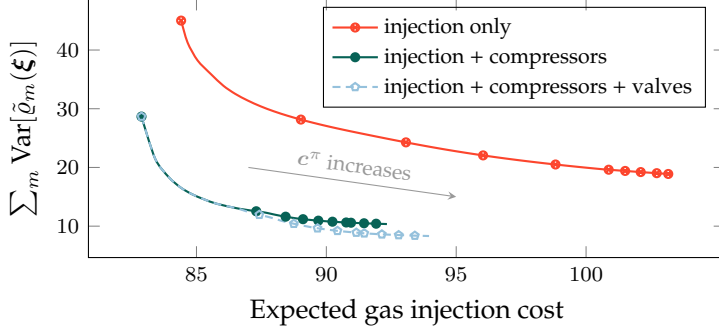


Figure 3.6: Expected gas injection cost (in \\$1000) versus pressure variance (in MPa²) for different assignments of control policies to flexible agents while pressure variance penalty $c^\pi \in [0.001, 0.1]$. Adapted from [Paper D].

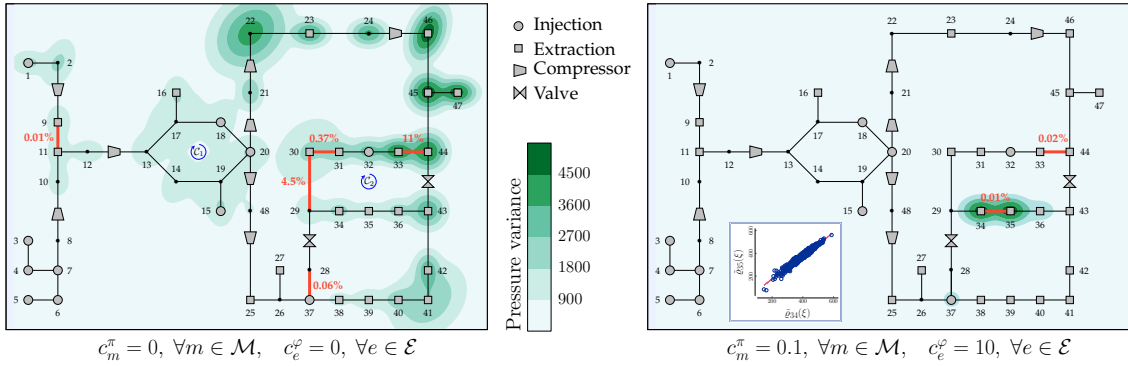


Figure 3.7: Comparison of the variance-agnostic (left) and variance-aware (right) chance-constrained control policies in terms of variance of the state variables for $\varepsilon = 0.1$. The red values show the probability of flow reversal in the pipelines. The inset plot shows the correlation between pressures at nodes 34 and 35. Adapted from [Paper D].

Cost-variance trade-off

The trade-off between expected cost and variance of state variables is studied by gradually increasing the penalties on the standard deviations, such that zero values of penalties in (3.24a) correspond to variance-agnostic chance-constrained gas system optimization. It was observed that without any substantial impact on expected cost, variance-aware control policies are able to reduce the variance of pressures and flows by 63.8% and 7.2%, respectively. These reductions in variance are attained by optimal pressure regulation provided by the active pipelines, with valves becoming more active as standard deviations of state variables are highly penalized while seeking further variance reduction. Figure 3.6 analyzes the contributions of various flexible agents in reducing the variance of nodal pressure in the natural gas system. The various line plots were obtained by selectively suppressing recourse actions. For instance, the ‘injection only’ case was obtained by enforcing active pipelines recourse actions $\gamma = 0$ while the case ‘injection + compressors’ was obtained by enforcing valve recourse actions to be zero, i.e., $[\gamma]_{(e,:)}^\top = 0$, $\forall e \in \mathcal{E}_v$. It is observed that as the pressure variance penalty increases, rapid reduction in variance is achieved at a lower cost as the gas system operator deploys pressure regulation to mitigate uncertainty and variance.

The density plots in Figure 3.7 show a comparison of variance-agnostic and variance-aware formulations of the proposed chance-constrained gas system optimization in terms of the variance of nodal pressures. The values in red show the probability of flow reversal in the gas pipelines, as compared to the nominal flow directions. It is observed that the variance-agnostic control

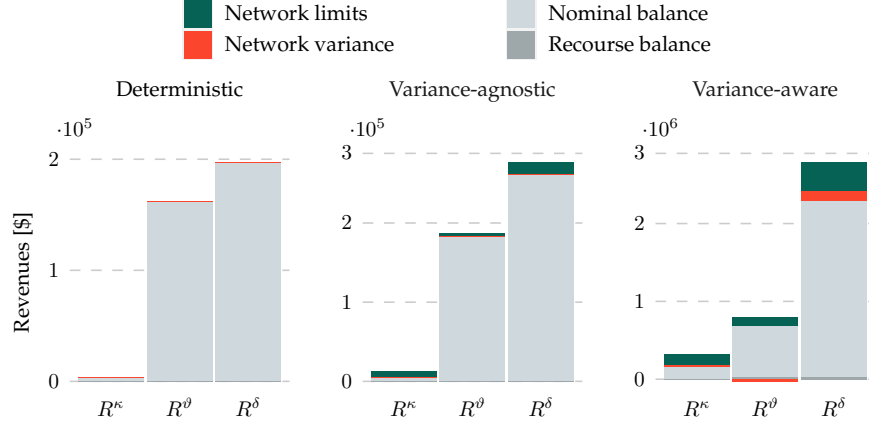


Figure 3.8: Comparison of total payments for the active pipelines R^κ , suppliers R^θ , and consumers R^δ under the deterministic, chance-constrained variance-agnostic and chance-constrained variance-aware ($c^\pi = 0.1$, $c^\varphi = 100$) gas market clearing. Adapted from [Paper D].

policies lead to large pressure variance in the eastern part of the network, having a concentration of stochastic gas extractions. Moreover, gas flows in certain pipelines are found highly susceptible to a reversal in direction (up to 11%) during real-time operation. With a suitable selection of standard deviation penalties, i.e., $c_m^\pi = 0.1$, $\forall m \in \mathcal{M}$, $c_e^\varphi = 10$, $\forall e \in \mathcal{E}$, variance-aware control policies (showed in right) achieve a drastic reduction in pressure and flow variance across the gas network. While the probability of flow reversals is significantly reduced, the pressure variance is localized across nodes 34 and 35. Incidentally, these nodes exhibit worse approximation errors due to the linearization compared to other nodes, and therefore, further minimization of pressure variance is not feasible. Nevertheless, the large pressure variance at these nodes does not lead to flow reversal in the edge (34,35) since these pressures are highly correlated, as shown in the inset plot.

Additionally, [Paper D] discusses the cost-variance trade-off w.r.t. the topology of the gas network, shown in Figure 3.7. In particular, breaking the cycles \mathcal{C}_1 and \mathcal{C}_2 by removing edges (13,14), (14,19), and (29,30) renders a radial network topology. As a result, the weakening of graph connectivity allows for more drastic pressure variance reduction at lower cost¹³.

Revenue analysis

Next, the revenues of the various gas market agents are compared in Figure 3.8 in the prevalent deterministic gas markets and the proposed chance-constrained gas market in both variance-agnostic and variance-aware implementations. Observe that the variance-agnostic markets lead to a substantial increase in payments compared to the deterministic markets, with variance-awareness coming with a further drastic increase. Apart from the expected additional components for uncertainty and variance mitigation, the payments for nominal balance also increase in the chance-constrained markets. This can be attributed to (i) increased marginal cost of gas injection since the gas consumption by active pipelines to provide pressure regulation increases demand, (ii) withholding of less expensive gas suppliers from supplying nominal gas injection such that the security margins of the chance constraints are respected, and (iii) the previously-discussed trade-off between choosing control policies that lead to a dispatch with minimum expected cost vs. those conducive for minimizing the variance of state variables.

¹³This observation agrees with the analytical expression defining the changes in pressure due to uncertainty propagation in (3.21a), since the linearization parameters $\tilde{\mathbf{G}}_2$ and $\tilde{\mathbf{G}}_3$ encode the graph connectivity.

3.4 Future perspectives

While the discussion on uncertainty-aware coordination among the energy systems in this chapter is limited to the integration of electricity and natural gas systems, similar issues with uncertainty propagation also arise at the interface of electricity and district heating, or water networks. In general, studying uncertainty propagation among energy systems poses significant analytical and computational challenges due to the nonlinearities and non-convexities inherent to the asset and network models. Nevertheless, the methodology developed in this thesis underscores crucial elements involved in modeling, analysis, and eventual market-based mitigation of uncertainty propagation among the energy systems while cross-carrier flexibility is harnessed. These elements include the need for (i) deploying physically-realistic yet computationally-tractable models of assets and networks in the energy systems, (ii) establishing a tight analytical dependency between the state variables of the energy systems and the uncertainty faced, and lastly, (iii) performing rigorous in-sample and out-of-sample simulations to validate and characterize the sub-optimality and approximation errors associated with the modeling choices. Together, these elements enable a reliable system operation in the integrated energy systems while harnessing cross-carrier flexibility during operational time scales.

Lastly, the proposed uncertainty propagation model could be extended to quantify and study systemic risk in integrated energy systems. Such a study would entail not only the consideration of resilience against extreme events triggered by potential faults but also the robustness against the propagation of shocks across the system boundaries. Future works could explore how the coupling and connectivity among the energy systems as well as their network topology impact systemic risk. New market products and flexibility services could be introduced to remunerate agents contributing towards mitigating such risks.

CHAPTER 4

Conclusions and Perspectives

This thesis provided scientific contributions to improve market-based coordination in integrated energy systems to incentivize, steer, and harness cross-carrier flexibility for the electricity system. The thesis contributed along two research directions. The first one rethought forward electricity markets, transforming them from energy-centric to flexibility-centric markets. The classical spatial price equilibrium problem was revisited in a conic optimization framework such that nonlinearities in cost and constraints of flexible assets and the networks comprising the integrated energy system were considered. The second direction focused on characterizing and mitigating the uncertainty propagation across energy system boundaries while harnessing cross-carrier flexibility in operational time scales. A general framework to study the propagation and market-based mitigation of uncertainty in integrated energy systems was developed and analyzed.

In what follows, the key findings of this thesis are reflected upon in Section 4.1, while future research directions are highlighted in Section 4.2.

4.1 Key findings

The research findings from this thesis are relevant for the integrated energy systems of the future from several perspectives.

From a market design perspective, this thesis proposed and analyzed a generic and efficient electricity market-clearing framework with flexibility procurement at the center. The proposed flexibility-centric market framework removes the market participation barriers for heterogeneous market participants across the integrated energy system by providing non-discriminatory market access to a variety of flexibility services. As a consequence, electricity markets are broadened to possibly include actors assuming new roles by leveraging innovative business models, which is beneficial from a regulatory standpoint. For instance, a novel variance minimization service facilitated the uncertainty-aware market-based coordination developed in this thesis. Flexible gas system agents such as gas suppliers and pressure regulation providers could subscribe to providing such services for additional revenue streams. Within the electricity system, similar roles can be envisioned for aggregators of flexible loads and electric vehicles, as well as other demand-side sources of flexibility. Furthermore, the proposed market frameworks were analytically proven to be efficient from an economic perspective. The satisfaction of the desired economic properties is crucial to market-based coordination in integrated energy systems so that cross-carrier flexibility is unraveled in a long-term and sustainable manner.

From a system operations perspective, these market frameworks enabled the introduction of new flexibility products and services, e.g., policy-based reserves, adjustment policies, variance minimization services, to accommodate the uncertainty in energy systems. Numerical results presented in this thesis highlighted that market-clearing algorithms based on chance-constrained

optimization exhibit computational tractability and desirable economic properties while endogenously characterizing the uncertainty faced by the energy systems. In addition to performance guarantees, the constraint violation probabilities inherent to chance constraints are aligned with the reliability metrics familiar to system operators, thereby making the chance-constrained market frameworks well-suited for a real-world implementation. From a modeling standpoint, a physically realistic representation of the steady-state dynamics of energy flows in the networks through the inclusion of SOC constraints allows system operators to optimally procure flexibility services from a variety of spatially-dispersed resources. Novel convexification strategies were developed to include the nonlinear and non-convex dynamics of flows in energy systems operating under uncertainty and its propagation across system boundaries. Numerical studies based on in-sample and out-of-sample simulations were performed to validate the convexification strategies and to benchmark the proposed market frameworks against available alternatives. When compared to prevalent deterministic and stochastic energy markets, the proposed market-clearing frameworks demonstrated improvement in social welfare arising from effective utilization of available cross-carrier flexibility.

For market participants in the integrated energy systems, the market frameworks developed in this thesis enable them to reflect the SOC-representable nonlinearities in their market participation strategies via the conic bids. Such nonlinearities could arise, for instance, from their cost functions or state equations, which are typically approximated by linear functions to fit the prevalent LP-based market-clearing problems. Moreover, the temporal coupling and multiple commodities involved in the proposed market frameworks enabled participants to represent their costs and constraints exactly, as opposed to the current practice of internalizing them through complex orders that link multiple price-quantity bids. Next, the inclusion of multiple flexibility services, e.g., uncertainty mitigation, variance minimization, and efficient prices associated with them opens avenues for flexibility-only market participants to recover their costs while providing these services in the market. For boundary agents operating at the interface of energy systems, nonlinearities aside, price competitiveness was improved as a result of the uncertainty-aware coordination developed in this thesis. Lastly, under the perfectly competitive setting assumed, the benefits for market participants are aligned with an improvement in the social welfare of energy markets.

4.2 Perspectives for future research

The insights gained in this thesis open up several future research paths. While suggestions for future research are provided throughout the main chapters of this thesis, in the following, three of the most promising research directions are highlighted.

First, the proposed generic, flexibility-centric market design for electricity markets and the uncertainty-aware coordination framework can be employed for various market-clearing use cases in future integrated energy systems. Leveraging the modeling examples and theoretical results in the thesis, such use cases may further unlock operational flexibility from heterogeneous market participants. An example within the electricity system is a market framework that entails an uncertainty- and network-aware coordination between the transmission and distribution system operators. This enables the flexibility available at the distribution level to be appropriately harnessed and priced within the market framework while considering physically-accurate network representation. Another example entails the development of new products and services, priced using the dual variables arising from the uncertainty-aware coordination among the energy systems.

While this thesis employed variance of state variables as a proxy for the uncertainty propagated across system boundaries, other uncertainty characterizations, e.g., intra- or inter-period variability, minimum or maximum bounds on variables, etc. could be used for new product definitions. Lastly, a further research aspect relates to the definition and analysis of new financial contracts in the form of options, physical or financial rights, etc., tailored for unconventional sources of cross-carrier flexibility, such as linepack flexibility. These financial instruments permit the gas network operator to efficiently allocate the surplus revenue generated from flexibility services.

The second research direction addresses further generalization of the LP-based energy markets. Within the realm of convex optimization, the SOCP framework featured prominently throughout this thesis as the backbone for market-clearing problems. A generalization of this framework can, for instance, be achieved by a semi-definite programming (SDP) based electricity market framework which admits broader feasibility regions shaped by cones of semidefinite matrices. In addition to SDP-based convexification approaches for the non-convex flows in the networks, such an extension allows further robustification of the uncertainty-aware coordination among energy systems [141]. As the theoretical results in this thesis rely on Lagrangian duality applied to generalized conic inequalities, it provides a foundation for studying an SDP-based spatial price equilibrium in the future. Generalization aside, moving towards SDP-based markets for electricity could bring further refinements to the procurement of operational flexibility. Considering the possible exactness of the SDP relaxation for the AC power flows in the electricity network [154], extending the proposed multi-commodity market with SDP constraints opens new avenues for market-based procurement of flexibility services related to the state variables in the electricity system, e.g., reactive power control, voltage regulation, phase regulation, etc. This opens avenues for further broadening of the electricity market access, providing novel revenue streams for new flexibility providers owning a variety of physical assets. Such flexibility providers could potentially trade energy and flexibility in a centralized (or decentralized, e.g., through peer-to-peer trades) manner to ensure both local and global balancing of supply-demand in the electricity system.

The third research direction relates to the central coordination framework employed by this thesis to study uncertainty propagation in the integrated energy system. While the centralized framework provides a relevant benchmark for the amount of cross-carrier flexibility harnessed and uncertainty propagation mitigated, it lacks appeal due to the existing and foreseen regulatory barriers to real-world implementation. System-level steering of flexibility aside, a large portion of the cross-carrier flexibility could potentially be harnessed through decentralized or local coordination among specific groups of agents in the integrated energy system while retaining the separate market structures. This local coordination improves the overall social welfare since it helps mitigate (to varying extents) the economic externalities associated with the multiple separate and asynchronous energy markets. Such local coordination could entail, for instance, sharing information in the form of signals, e.g., price forecasts, demand forecasts, cost uncertainty, etc. among these groups of agents. Further research is crucial in this direction to evaluate what types of signals are beneficial to be shared among which groups of agents to improve the amount of cross-carrier flexibility harnessed in the absence of a central coordinator. Studying such information sharing is not only interesting from a system point of view but also relevant from the perspective of the market participants. Since the flexibility providers are heterogeneous agents, often residing in different energy systems and are exposed to information barriers across the energy system boundaries, information sharing is appealing to them as it potentially improves their payoffs while making decisions under uncertainty.

Bibliography

- [1] International Energy Agency (IEA). World energy outlook 2021, 2021. <https://www.iea.org/reports/world-energy-outlook-2021> Last accessed: 31 March 2022.
- [2] Li Daqing, Jiang Yinan, Kang Rui, and Shlomo Havlin. Spatial correlation analysis of cascading failures: Congestions and blackouts. *Scientific Reports*, 4(1):5381, 2014.
- [3] Jinye Zhao, Tongxin Zheng, and Eugene Litvinov. A unified framework for defining and measuring flexibility in power system. *IEEE Transactions on Power Systems*, 31(1):339–347, 2016.
- [4] Mark J. O’Malley et al. Energy systems integration: Defining and describing the value proposition. Technical report, National Renewable Energy Laboratory, 2016.
- [5] Emiliano Dall’Anese, Pierluigi Mancarella, and Antonello Monti. Unlocking flexibility: Integrated optimization and control of multienergy systems. *IEEE Power and Energy Magazine*, 15(1):43–52, 2017.
- [6] Baraa Mohandes, Mohamed Shawky El Moursi, Nikos Hatziargyriou, and Sameh El Khatib. A review of power system flexibility with high penetration of renewables. *IEEE Transactions on Power Systems*, 34(4):3140–3155, 2019.
- [7] Mark J. O’Malley et al. Multicarrier energy systems: Shaping our energy future. *Proceedings of the IEEE*, 108(9):1437–1456, 2020.
- [8] Michael Chertkov and Göran Andersson. Multienergy systems. *Proceedings of the IEEE*, 108(9):1387–1391, 2020.
- [9] European Commission. Powering a climate-neutral economy: An EU strategy for energy system integration. July 2020.
- [10] Martin Geidl and Göran Andersson. Optimal power flow of multiple energy carriers. *IEEE Transactions on Power Systems*, 22(1):145–155, 2007.
- [11] Pierluigi Mancarella. MES (multi-energy systems): An overview of concepts and evaluation models. *Energy*, 65:1–17, 2014.
- [12] Gianfranco Chicco, Shariq Riaz, Andrea Mazza, and Pierluigi Mancarella. Flexibility from distributed multienergy systems. *Proceedings of the IEEE*, 108(9):1496–1517, 2020.
- [13] Daniel Kirschen and Goran Strbac. *Fundamentals of Power System Economics, 2nd Edition*. John Wiley & Sons, Ltd, US, 2018.
- [14] Juan M. Morales et al. *Integrating Renewables in Electricity Markets: Operational Problems*. Springer US, Boston, MA, 2014.

- [15] Jean-Michel Glachant, Michelle Hallack, and Miguel Vazquez. *Building Competitive Gas Markets in the EU*. Edward Elgar Publishing, Aug 2013.
- [16] Thorsten Koch, Marc E. Pfetsch, and Jessica Rövekamp. *Evaluating Gas Network Capacities*. Society for Industrial and Applied Mathematics (SIAM), 2013.
- [17] H. Lund, B. Möller, B.V. Mathiesen, and A. Dyrelund. The role of district heating in future renewable energy systems. *Energy*, 35(3):1381–1390, 2010.
- [18] Anna Schwele. Integration of electricity, natural gas and heat systems with market-based coordination. *Ph.D. Thesis*, 2020. Technical University of Denmark.
- [19] Antje Orths et al. Flexibility from energy systems integration: Supporting synergies among sectors. *IEEE Power and Energy Magazine*, 17(6):67–78, 2019.
- [20] Michael Chertkov, Scott Backhaus, and Vladimir Lebedev. Cascading of fluctuations in interdependent energy infrastructures: Gas-grid coupling. *Applied Energy*, 160:541–551, 2015.
- [21] Anna Schwele, Christos Ordoudis, Jalal Kazempour, and Pierre Pinson. Coordination of power and natural gas systems: Convexification approaches for linepack modeling. In *Proceedings of 13th IEEE PES PowerTech Conference*, Milan, 2019.
- [22] L. Mitridati and J. A. Taylor. Power systems flexibility from district heating networks. In *2018 Power Systems Computation Conference (PSCC)*, pages 1–7, June 2018.
- [23] W. W. Hogan. Market design practices: Which ones are best? [in my view]. *IEEE Power and Energy Magazine*, 17(1):100–104, 2019.
- [24] Benjamin F. Hobbs and Shmuel S. Oren. Three waves of U.S. reforms: Following the path of wholesale electricity market restructuring. *IEEE Power and Energy Magazine*, 17(1):73–81, 2019.
- [25] Anna Nagurney. Spatial price equilibrium. In *Encyclopedia of Optimization*, pages 3646–3652. Springer US, Boston, MA, 2009.
- [26] Roger E. Bohn, Michael C. Caramanis, and Fred C. Schweppe. Optimal pricing in electrical networks over space and time. *The RAND Journal of Economics*, 15(3):360–376, 1984.
- [27] Fred C. Schweppe, Michael C. Caramanis, Richard D. Tabors, and Roger E. Bohn. *Spot Pricing of Electricity*. Springer US, Boston, MA, 1988.
- [28] Erik Ela et al. Overview of wholesale electricity markets. In *Electricity Markets with Increasing Levels of Renewable Generation: Structure, Operation, Agent-based Simulation, and Emerging Designs*, pages 3–21. Springer International Publishing, Cham, 2018.
- [29] Xiaolong Kuang, Alberto J. Lamadrid, and Luis F. Zuluaga. Pricing in non-convex markets with quadratic deliverability costs. *Energy Economics*, 80:123–131, 2019.
- [30] A. Papavasiliou. Analysis of distribution locational marginal prices. *IEEE Transactions on Smart Grid*, 9(5):4872–4882, Sep. 2018.
- [31] Y. Dvorkin. A chance-constrained stochastic electricity market. *IEEE Transactions on Power Systems*, 35(4):2993–3003, 2020.

- [32] Robert Mieth, Jip Kim, and Yury Dvorkin. Risk- and variance-aware electricity pricing. *Electric Power Systems Research*, 189:106804, 2020.
- [33] Geoffrey Pritchard, Golbon Zakeri, and Andrew Philpott. A single-settlement, energy-only electric power market for unpredictable and intermittent participants. *Operations Research*, 58(4-part-2):1210–1219, 2010.
- [34] Victor M. Zavala, Kibaek Kim, Mihai Anitescu, and John Birge. A stochastic electricity market clearing formulation with consistent pricing properties. *Operations Research*, 65(3):557–576, 2017.
- [35] D. Bertsimas et al. Adaptive robust optimization for the security constrained unit commitment problem. *IEEE Transactions on Power Systems*, 28(1):52–63, Feb 2013.
- [36] Lina Silva-Rodriguez et al. Short term wholesale electricity market designs: A review of identified challenges and promising solutions. *Renewable and Sustainable Energy Reviews*, 160:112228, 2022.
- [37] Juan M. Morales, Antonio J. Conejo, and Juan Pérez-Ruiz. Simulating the impact of wind production on locational marginal prices. *IEEE Transactions on Power Systems*, 26(2):820–828, 2011.
- [38] Geunyeong Byeon and Pascal Van Hentenryck. Unit commitment with gas network awareness. *IEEE Transactions on Power Systems*, 35(2):1327–1339, 2020.
- [39] Lesia Mitridati, Jalal Kazempour, and Pierre Pinson. Heat and electricity market coordination: A scalable complementarity approach. *European Journal of Operational Research*, 283(3):1107–1123, 2020.
- [40] Pierre Pinson, Lesia Mitridati, Christos Ordoudis, and Jacob Østergaard. Towards fully renewable energy systems: Experience and trends in Denmark. *CSEE Journal of Power and Energy Systems*, 3(1):26–35, 2017.
- [41] Xinyu Chen et al. Increasing the flexibility of combined heat and power for wind power integration in china: Modeling and implications. *IEEE Transactions on Power Systems*, 30(4):1848–1857, 2015.
- [42] Tim McDonnell. Natural gas prices in europe hit the equivalent of \$600 oil, 2022. Quartz. <https://qz.com/2138680/natural-gas-prices-in-europe-hit-an-all-time-high/> Last accessed: 31 March 2022.
- [43] Richard Levitan, Sara Wilmer, and Richard Carlson. Pipeline to reliability: Unraveling gas and electric interdependencies across the eastern interconnection. *IEEE Power and Energy Magazine*, 12(6):78–88, 2014.
- [44] John E. Bistline. Electric sector capacity planning under uncertainty: Climate policy and natural gas in the US. *Energy Economics*, 51:236–251, 2015.
- [45] Ernest J. Moniz et al. The future of natural gas. Technical report, Massachusetts Institute of Technology, 2011.
- [46] PJM Interconnection. Analysis of operational events and market impacts during the January 2014 cold weather events, 2014.

- [47] Antonio J. Conejo, Miguel Carrión, and Juan M. Morales. Stochastic programming fundamentals. In *Decision Making Under Uncertainty in Electricity Markets*, pages 27–62. Springer US, Boston, MA, 2010.
- [48] Hong Chen, Bresler, et al. Toward bulk power system resilience: Approaches for regional transmission operators. *IEEE Power and Energy Magazine*, 18(4):20–30, 2020.
- [49] Carlos M Correa-Posada and Pedro Sánchez-Martín. Integrated power and natural gas model for energy adequacy in short-term operation. *IEEE Transactions on Power Systems*, 30(6):3347–3355, 2015.
- [50] Hossein Ameli, Meysam Qadrdan, and Goran Strbac. Coordinated operation strategies for natural gas and power systems in presence of gas-related flexibilities. *Energy Systems Integration*, 1(1):3–13, 2019.
- [51] Christos Ordoudis, Pierre Pinson, and Juan M Morales. An integrated market for electricity and natural gas systems with stochastic power producers. *European Journal of Operational Research*, 272(2):642–654, 2019.
- [52] Carleton Coffrin et al. The power grid library for benchmarking AC optimal power flow algorithms, 2021. arXiv preprint, <https://arxiv.org/abs/1908.02788>.
- [53] Alvin E. Roth and Robert B. Wilson. How market design emerged from game theory: A mutual interview. *Journal of Economic Perspectives*, 33(3):118–43, 2019.
- [54] Roger B. Myerson. Comments on “Games with incomplete information played by ‘Bayesian’ players, I–III Harsanyi’s games with incomplete information”. *Management Science*, 50(12_supplement):1818–1824, 2004.
- [55] Leonid Hurwicz. The design of mechanisms for resource allocation. *The American Economic Review*, 63(2):1–30, 1973.
- [56] Jerry Green and Jean-Jacques Laffont. Characterization of satisfactory mechanisms for the revelation of preferences for public goods. *Econometrica*, 45(2):427–438, 1977.
- [57] Pablo González, José Villar, Cristian A. Díaz, and Fco Alberto Campos. Joint energy and reserve markets: Current implementations and modeling trends. *Electric Power Systems Research*, 109:101–111, 2014.
- [58] Charles C. Holt, Franco Modigliani, and Herbert A. Simon. A linear decision rule for production and employment scheduling. *Management Science*, 2(1):1–30, 1955.
- [59] J. Warrington, P. Goulart, S. Mariéthoz, and M. Morari. Policy-based reserves for power systems. *IEEE Transactions on Power Systems*, 28(4):4427–4437, Nov. 2013.
- [60] Arkadi Nemirovski and Alexander Shapiro. Convex approximations of chance constrained programs. *SIAM Journal on Optimization*, 17(4):969–996, 2007.
- [61] Steven A. Gabriel et al. Optimality and complementarity. In *Complementarity Modeling in Energy Markets*, pages 31–69. Springer New York, New York, NY, 2013.
- [62] Francisco Facchinei and Jong-Shi Pang. *Finite-Dimensional Variational Inequalities and Complementarity Problems*, volume I. Springer New York, New York, NY, 2003.

- [63] Stephen Enke. Equilibrium among spatially separated markets: Solution by electric analogue. *Econometrica*, 19(1):40–47, 1951.
- [64] Paul A. Samuelson. Spatial price equilibrium and linear programming. *The American Economic Review*, 42(3):283–303, 1952.
- [65] L. V. Kantorovich. Mathematical methods of organizing and planning production. *Management Science*, 6(4):366–422, 1960.
- [66] Varmelast. What is load dispatching?, 2022. <https://www.varmelast.dk/lastfordeling/hvad-er-lastfordeling> Last accessed: 31 March 2022.
- [67] Daniel Bienstock and Apurv Shukla. Variance-aware optimal power flow: Addressing the tradeoff between cost, security, and variability. *IEEE Transactions on Control of Network Systems*, 6(3):1185–1196, 2019.
- [68] Stephen Boyd and Lieven Vandenberghe. *Convex Optimization*. Cambridge University Press, 2004.
- [69] Jacqueline Boucher and Yves Smeers. Alternative models of restructured electricity systems, part 1: No market power. *Operations Research*, 49(6):821–838, 2001.
- [70] CAISO. The role of the California ISO, 2020. <http://www.caiso.com/about/Pages/OurBusiness/The-role-of-the-California-ISO.aspx> Last accessed: 31 March 2022.
- [71] J. B. Rosen. Existence and uniqueness of equilibrium points for concave n-person games. *Econometrica*, 33(3):520–534, 1965.
- [72] Andreu Mas-Colell, Michael D. Whinston, Robert E. Bixby, and Jerry R. Green. *Microeconomic Theory*. Oxford University Press, Oxford, U.K., September 1995.
- [73] Benjamin F. Hobbs et al. Why this book? New capabilities and new needs for unit commitment modeling. In *The Next Generation of Electric Power Unit Commitment Models*, pages 1–14. Springer US, Boston, MA, 2001.
- [74] Richard P. O'Neill et al. Efficient market-clearing prices in markets with nonconvexities. *European Journal of Operational Research*, 164(1):269–285, 2005.
- [75] Steven H. Low. Convex relaxation of optimal power flow—Part I: Formulations and equivalence. *IEEE Transactions on Control of Network Systems*, 1(1):15–27, 2014.
- [76] Mary B. Cain, Richard P O'Neill, and Anya Castillo. *History of Optimal Power Flows and Formulations*. Federal Energy Regulatory Commission (FERC), Dec 2012.
- [77] Kyri Baker. Solutions of DC OPF are never AC feasible. In *The Twelfth ACM International Conference on Future Energy Systems (e-Energy '21)*, page 264–268, New York, USA, 2021.
- [78] Yael Parag and Benjamin K. Sovacool. Electricity market design for the prosumer era. *Nature Energy*, 1(4):16032, 2016.
- [79] Tiago Sousa et al. Peer-to-peer and community-based markets: A comprehensive review. *Renewable and Sustainable Energy Reviews*, 104:367–378, 2019.

- [80] F. Abbaspourtorbati and M. Zima. The Swiss reserve market: Stochastic programming in practice. *IEEE Transactions on Power Systems*, 31(2):1188–1194, 2016.
- [81] Wolfram Wiesemann, Daniel Kuhn, and Melvyn Sim. Distributionally robust convex optimization. *Operations Research*, 62(6):1358–1376, 2014.
- [82] D. Bienstock, M. Chertkov, and S. Harnett. Chance-constrained optimal power flow: Risk-aware network control under uncertainty. *SIAM Review*, 56(3):461–495, 2014.
- [83] Daniel Bienstock. Uncertainty-aware power systems operation. In *Advanced Data Analytics for Power Systems*, page 363–399. Cambridge University Press, 2021.
- [84] F. Alizadeh and D. Goldfarb. Second-order cone programming. *Mathematical Programming*, 95(1):3–51, 2003.
- [85] Mosek ApS. MOSEK Modeling Cookbook 3.2.3, 2021. <https://docs.mosek.com/modeling-cookbook/index.html> Last accessed: 31 March 2022.
- [86] Miguel Sousa Lobo, Lieven Vandenberghe, Stephen Boyd, and Hervé Lebret. Applications of second-order cone programming. *Linear Algebra and its Applications*, 284(1):193 – 228, 1998.
- [87] Aharon Ben-Tal and Arkadi Nemirovski. *Lectures on Modern Convex Optimization*, chapter 1. Society for Industrial and Applied Mathematics, Philadelphia, 2001.
- [88] R. A. Jabr. Radial distribution load flow using conic programming. *IEEE Transactions on Power Systems*, 21(3):1458–1459, 2006.
- [89] M Farivar and S. H. Low. Branch flow model: Relaxations and convexification-Part I. *IEEE Transactions on Power Systems*, 28(3):2554–2564, 2013.
- [90] Burak Kocuk, Santanu S. Dey, and X. Andy Sun. Strong SOCP relaxations for the optimal power flow problem. *Operations Research*, 64(6):1177–1196, 2016.
- [91] Federal Energy Regulatory Commission. Recent ISO software enhancements and future software and modelling plans, 2011. <https://cms.ferc.gov/sites/default/files/2020-05/rto-iso-soft-2011.pdf> Last accessed: 20 January 2022.
- [92] Maziar Raissi. *Conic Economics*. PhD thesis, University of Maryland, College Park, 2016. <https://search.proquest.com/docview/1861702044> Last accessed: 31 March 2022.
- [93] Daniel De Wolf and Yves Smeers. The gas transmission problem solved by an extension of the simplex algorithm. *Management Science*, 46(11):1454–1465, 2000.
- [94] Lesia Mitridati, Jalal Kazempour, and Pierre Pinson. Heat and electricity market coordination: A scalable complementarity approach. *European Journal of Operational Research*, 283(3):1107–1123, 2020.
- [95] Ximing Cai, Daene C. McKinney, Leon S. Lasdon, and David W. Watkins. Solving large nonconvex water resources management models using generalized benders decomposition. *Operations Research*, 49(2):235–245, 2001.
- [96] Costas Courcoubetis and Richard Weber. *Pricing Communication Networks*. John Wiley & Sons, Ltd, West Sussex, England, 2003.

- [97] Lawrence V. Snyder, Maria P. Scaparra, Mark S. Daskin, and Richard L. Church. Planning for disruptions in supply chain networks. In *Models, Methods, and Applications for Innovative Decision Making*, chapter 9, pages 234–257. INFORMS TutORials in Operations Research, 2014.
- [98] R. Mieth and Y. Dvorkin. Distribution electricity pricing under uncertainty. *IEEE Transactions on Power Systems*, 35(3):2325–2338, 2020.
- [99] George Liberopoulos and Panagiotis Andrianesis. Critical review of pricing schemes in markets with non-convex costs. *Operations Research*, 64(1):17–31, 2016.
- [100] Paul Gribik, William W. Hogan, and Susan Pope. Market-clearing electricity prices and energy uplift. Harvard Univ., Cambridge, MA, USA, working paper, 2007.
- [101] Congcong Wang, Peter B. Luh, Paul Gribik, Tengshun Peng, and Li Zhang. Commitment cost allocation of fast-start units for approximate extended locational marginal prices. *IEEE Transactions on Power Systems*, 31(6):4176–4184, 2016.
- [102] Bowen Hua and Ross Baldick. A convex primal formulation for convex hull pricing. *IEEE Transactions on Power Systems*, 32(5):3814–3823, 2017.
- [103] Manuel Garcia, Harsha Nagarajan, and Ross Baldick. Generalized convex hull pricing for the AC optimal power flow problem. *IEEE Transactions on Control of Network Systems*, 7(3):1500–1510, 2020.
- [104] Hande Y. Benson and Ümit Sağlam. Mixed-integer second-order cone programming: A survey. In *Theory Driven by Influential Applications*, chapter 2, pages 13–36. INFORMS TutORials in Operations Research, 2013.
- [105] Andy Philpott, Michael Ferris, and Roger Wets. Equilibrium, uncertainty and risk in hydro-thermal electricity systems. *Mathematical Programming*, 157(2):483–513, 2016.
- [106] Robert Mieth, Matt Roveto, and Yury Dvorkin. Risk trading in a chance-constrained stochastic electricity market. *IEEE Control Systems Letters*, 5(1):199–204, 2021.
- [107] Nord Pool. Nord Pool Day-ahead Trading, 2021. <https://www.nordpoolgroup.com/trading/Day-ahead-trading/> Last accessed: 31 March 2022.
- [108] José Fortuny-Amat and Bruce McCarl. A representation and economic interpretation of a two-level programming problem. *The Journal of the Operational Research Society*, 32(9):783–792, 1981.
- [109] Vanessa Krebs, Lars Schewe, and Martin Schmidt. Uniqueness and multiplicity of market equilibria on DC power flow networks. *European Journal of Operational Research*, 271(1):165–178, 2018.
- [110] Pär Holmberg and Ewa Lazarczyk. Congestion management in electricity networks: Nodal, zonal and discriminatory pricing, 2012. IFN Working Paper No. 915, 2012. <https://dx.doi.org/10.2139/ssrn.2055655>. Last accessed: 31 March 2022.
- [111] Kenneth J. Arrow and Gerard Debreu. Existence of an equilibrium for a competitive economy. *Econometrica*, 22(3):265–290, 1954.

- [112] Mingyu Guo et al. Budget-balanced and nearly efficient randomized mechanisms: Public goods and beyond. In *Internet and Network Economics*, pages 158–169. Springer Berlin Heidelberg, Berlin, Heidelberg, 2011.
- [113] Donald John Roberts and Andrew Postlewaite. The incentives for price-taking behavior in large exchange economies. *Econometrica*, 44(1):115–127, 1976.
- [114] J. Frédéric Bonnans and Alexander Shapiro. Additional material and applications. In *Perturbation Analysis of Optimization Problems*, pages 401–526. Springer New York, New York, NY, 2000.
- [115] R. Hettich and K. O. Kortanek. Semi-infinite programming: Theory, methods, and applications. *SIAM Review*, 35(3):380–429, 1993.
- [116] Aharon Ben-Tal, Laurent El Ghaoui, and Arkadi Nemirovski. *Robust optimization*. Princeton University Press, 2009.
- [117] Arkadi Nemirovski. On safe tractable approximations of chance constraints. *European Journal of Operational Research*, 219(3):707–718, 2012.
- [118] Angelos Georghiou, Wolfram Wiesemann, and Daniel Kuhn. Generalized decision rule approximations for stochastic programming via liftings. *Mathematical Programming*, 152(1):301–338, 2015.
- [119] Erick Delage and Dan A. Iancu. Robust multistage decision making. In *The Operations Research Revolution*, chapter 2, pages 20–46. INFORMS TutORials in Operations Research, 2015.
- [120] Angelos Georghiou, Daniel Kuhn, and Wolfram Wiesemann. The decision rule approach to optimization under uncertainty: Methodology and applications. *Computational Management Science*, 2018.
- [121] Teodoro Alamo, Roberto Tempo, Amalia Luque, and Daniel R. Ramirez. Randomized methods for design of uncertain systems: Sample complexity and sequential algorithms. *Automatica*, 52:160–172, 2015.
- [122] Hamed Rahimian and Sanjay Mehrotra. Distributionally robust optimization: A review, 2019. arXiv preprint, <https://arxiv.org/abs/1908.05659>.
- [123] Sidhant Misra, Michael W. Fisher, Scott Backhaus, Russell Bent, Michael Chertkov, and Feng Pan. Optimal compression in natural gas networks: A geometric programming approach. *IEEE Transactions on Control of Network Systems*, 2(1):47–56, 2015.
- [124] Manish Kumar Singh and Vassilis Kekatos. Natural gas flow solvers using convex relaxation. *IEEE Transactions on Control of Network Systems*, 7(3):1283–1295, 2020.
- [125] Conrado Borraz-Sánchez, Russell Bent, Scott Backhaus, Hassan Hijazi, and Pascal Van Hentenryck. Convex relaxations for gas expansion planning. *INFORMS Journal on Computing*, 28(4):645–656, 2016.
- [126] Frode Rømo et al. Optimizing the norwegian natural gas production and transport. *INFORMS Journal on Applied Analytics*, 39(1):46–56, 2009.

- [127] Andreas Wächter and Lorenz T Biegler. On the implementation of an interior-point filter line-search algorithm for large-scale nonlinear programming. *Mathematical Programming*, 106(1):25–57, 2006.
- [128] Felix Hennings. Large-scale empirical study on the momentum equation’s inertia term, 2021. arXiv preprint, <https://arxiv.org/abs/2106.05120>.
- [129] Daniel Kuhn, Wolfram Wiesemann, and Angelos Georghiou. Primal and dual linear decision rules in stochastic and robust optimization. *Mathematical Programming*, 130(1):177–209, 2011.
- [130] Weijun Xie, Shabbir Ahmed, and Ruiwei Jiang. Optimized bonferroni approximations of distributionally robust joint chance constraints. *Mathematical Programming*, 2019.
- [131] Grani A. Hanasusanto, Vladimir Roitch, Daniel Kuhn, and Wolfram Wiesemann. Ambiguous joint chance constraints under mean and dispersion information. *Operations Research*, 65(3):751–767, 2017.
- [132] Anatoly Zlotnik et al. Coordinated scheduling for interdependent electric power and natural gas infrastructures. *IEEE Transactions on Power Systems*, 32(1):600–610, 2017.
- [133] Dan Hu and Sarah M. Ryan. Stochastic vs. deterministic scheduling of a combined natural gas and power system with uncertain wind energy. *International Journal of Electrical Power & Energy Systems*, 108:303–313, 2019.
- [134] Chuan He, Lei Wu, Tianqi Liu, and Mohammad Shahidehpour. Robust co-optimization scheduling of electricity and natural gas systems via admm. *IEEE Transactions on Sustainable Energy*, 8(2):658–670, 2017.
- [135] Cheng Wang, Wei Wei, Jianhui Wang, and Tianshu Bi. Convex optimization based adjustable robust dispatch for integrated electric-gas systems considering gas delivery priority. *Applied Energy*, 239:70–82, 2019.
- [136] Line A. Roald, Kaarthik Sundar, Anatoly Zlotnik, Sidhant Misra, and Göran Andersson. An uncertainty management framework for integrated gas-electric energy systems. *Proceedings of the IEEE*, 108(9):1518–1540, 2020.
- [137] Babatunde Odetayo, John MacCormack, WD Rosehart, and Hamidreza Zareipour. A chance constrained programming approach to integrated planning of distributed power generation and natural gas network. *Electric Power Systems Research*, 151:197–207, 2017.
- [138] Christos Ordoudis, Viet Anh Nguyen, Daniel Kuhn, and Pierre Pinson. Energy and reserve dispatch with distributionally robust joint chance constraints. *Operations Research Letters*, 49(3):291–299, 2021.
- [139] Dimitris Bertsimas and Melvyn Sim. The price of robustness. *Operations Research*, 52(1):35–53, 2004.
- [140] Kazi Nazmul Hasan, Robin Preece, and Jovica V Milanović. Existing approaches and trends in uncertainty modelling and probabilistic stability analysis of power systems with renewable generation. *Renewable and Sustainable Energy Reviews*, 101:168–180, 2019.
- [141] Erick Delage and Yinyu Ye. Distributionally robust optimization under moment uncertainty with application to data-driven problems. *Operations Research*, 58(3):595–612, 2010.

- [142] Grani A. Hanasusanto, Vladimir Roitch, Daniel Kuhn, and Wolfram Wiesemann. A distributionally robust perspective on uncertainty quantification and chance constrained programming. *Mathematical Programming*, 151(1):35–62, Jun 2015.
- [143] Bowen Li, Ruiwei Jiang, and Johanna L. Mathieu. Distributionally robust chance-constrained optimal power flow assuming unimodal distributions with misspecified modes. *IEEE Transactions on Control of Network Systems*, 6(3):1223–1234, 2019.
- [144] Vladimir Dvorkin, Dharik Mallapragada, Audun Botterud, Jalal Kazempour, and Pierre Pinson. Multi-stage linear decision rules for stochastic control of natural gas networks with linepack, 2021. arXiv preprint, <https://arxiv.org/abs/2110.02824>.
- [145] Garth P. McCormick. Computability of global solutions to factorable nonconvex programs: Part I - Convex underestimating problems. *Mathematical Programming*, 10(1):147–175, 1976.
- [146] Michael R. Wagner. Stochastic 0-1 linear programming under limited distributional information. *Operations Research Letters*, 36(2):150 – 156, 2008.
- [147] W. Xie and S. Ahmed. Distributionally robust chance constrained optimal power flow with renewables: A conic reformulation. *IEEE Transactions on Power Systems*, 33(2):1860–1867, 2018.
- [148] Pierre Pinson. Wind energy: Forecasting challenges for its operational management. *Statistical Science*, 28(4):564–585, 11 2013.
- [149] C. Coffrin, H. L. Hijazi, and P. Van Hentenryck. Strengthening the SDP relaxation of AC power flows with convex envelopes, bound tightening, and valid inequalities. *IEEE Transactions on Power Systems*, 32(5):3549–3558, 2017.
- [150] S. Chen, A. J. Conejo, R. Sioshansi, and Z. Wei. Unit commitment with an enhanced natural gas-flow model. *IEEE Transactions on Power Systems*, 34(5):3729–3738, 2019.
- [151] John E. Mitchell, Jong-Shi Pang, and Bin Yu. Convex quadratic relaxations of nonconvex quadratically constrained quadratic programs. *Optimization Methods and Software*, 29(1):120–136, 2014.
- [152] Giuseppe Calafiore and Marco C Campi. Uncertain convex programs: randomized solutions and confidence levels. *Mathematical Programming*, 102(1):25–46, 2005.
- [153] Vladimir Dvorkin, Jalal Kazempour, and Pierre Pinson. Electricity market equilibrium under information asymmetry. *Operations Research Letters*, 47(6):521–526, 2019.
- [154] J. Lavaei and S. H. Low. Zero duality gap in optimal power flow problem. *IEEE Transactions on Power Systems*, 27(1):92–107, 2012.

Collection of relevant publications

- [**Paper A**] A. Ratha, P. Pinson, H. Le Cadre, A. Virag and J. Kazempour, "Moving from Linear to Conic Markets for Electricity," submitted to *European Journal of Operational Research*, (under review, first round), 2021.
- [**Paper B**] A. Ratha, J. Kazempour, A. Virag and P. Pinson, "Exploring Market Properties of Policy-based Reserve Procurement for Power Systems," in *2019 IEEE 58th Conference on Decision and Control (CDC)*, 2019, pp. 7498-7505, doi: 10.1109/CDC40024.2019.9029777.
- [**Paper C**] A. Ratha, A. Schwele, J. Kazempour, P. Pinson, S. Shariat Torbhagan and A. Virag, "Affine Policies for Flexibility Provision by Natural Gas Networks to Power Systems," in *Electric Power Systems Research*, Volume 189, 2020, doi: 10.1016/j.epsr.2020.106565.
- [**Paper D**] V. Dvorkin, A. Ratha, P. Pinson and J. Kazempour, "Stochastic Control and Pricing for Natural Gas Networks," in *IEEE Transactions on Control of Network Systems (Early Access)*, 2021, doi: 10.1109/TCNS.2021.3112764.

[Pub. A] Moving from Linear to Conic Markets for Electricity

Authors:

Anubhav Ratha, Pierre Pinson, Hélène Le Cadre, Ana Virág, and Jalal Kazempour

Submitted to:

European Journal of Operational Research (EJOR)

Moving from Linear to Conic Markets for Electricity

Anubhav Ratha^{a,b,*}, Pierre Pinson^a, Hélène Le Cadre^b, Ana Virag^b, Jalal Kazempour^a

^aTechnical University of Denmark, Kgs. Lyngby, Denmark

^bFlemish Institute for Technological Research (VITO), Mol, Belgium

Abstract

We propose a new forward electricity market framework that admits heterogeneous market participants with second-order cone strategy sets, who accurately express the nonlinearities in their costs and constraints through conic bids, and a network operator facing conic operational constraints. In contrast to the prevalent linear-programming-based electricity markets, we highlight how the inclusion of second-order cone constraints enables uncertainty-, asset- and network-awareness of the market, which is key to the successful transition towards an electricity system based on weather-dependent renewable energy sources. We analyze our general market-clearing proposal using conic duality theory to derive efficient spatially-differentiated prices for the multiple commodities, comprising of energy and flexibility services. Under the assumption of perfect competition, we prove the equivalence of the centrally-solved market-clearing optimization problem to a competitive spatial price equilibrium involving a set of rational and self-interested participants and a price setter. Finally, under common assumptions, we prove that moving towards conic markets does not incur the loss of desirable economic properties of markets, namely market efficiency, cost recovery and revenue adequacy. Our numerical studies focus on the specific use case of uncertainty-aware market design and demonstrate that the proposed conic market brings advantages over existing alternatives within the linear programming market framework.

Keywords: OR in energy, spatial equilibrium, mechanism design, electricity markets, conic economics

1. Introduction

The spatial price equilibrium problem, as first analyzed by [Enke \(1951\)](#) and [Samuelson \(1952\)](#), computes commodity prices and trade flows that satisfy partial equilibrium conditions over a network. In a two-sided auction framework, this problem involves price-quantity supply offers and demand bids matched by an auctioneer to maximize the social welfare, contingent on the spatial constraints. Historically, spatial price equilibrium problems rely on linear programming (LP) theory ([Kantorovich, 1960](#)) to derive the market equilibrium prices from *marginal equalities*. Despite the success of LP in achieving *optimal* market-clearing outcomes and *efficient* prices with satisfactory computational effort, it is potentially limiting in *physical systems* as it may fail to accurately represent the *nonlinear* operational characteristics of assets and the network. Examples of such physical systems include electricity ([Bohn et al., 1984](#)), natural gas ([De Wolf and Smeers, 2000](#)), water ([Cai et al., 2001](#)), heat ([Mitridati et al., 2020](#)), telecommunication networks ([Courcoubetis and Weber, 2003](#)) and supply chains ([Snyder et al., 2014](#)). Even in *non-physical* systems facing

*Corresponding author.

Email addresses: arath@dtu.dk (Anubhav Ratha), ppin@dtu.dk (Pierre Pinson), helene.lecadre@vito.be (Hélène Le Cadre), ana.virag@vito.be (Ana Virag), seykaz@dtu.dk (Jalal Kazempour)

uncertainty, the use of LP compels a linear modeling of uncertainty and potential risk preferences, which is limiting at times.

A natural question then arises, why should the market-clearing problem be confined to the LP framework? This question is pertinent since LP is the simplest mathematical framework in the convex optimization theory, while more general convex frameworks such as conic programming are available. If such frameworks enable a more accurate representation of physical assets and networks as well as uncertainty, while retaining the advantages of LP in terms of optimality, pricing, and computational ease, it is then, indeed, appealing to adopt them. Leveraging the recent mathematical and computational advances in conic programming ([Alizadeh and Goldfarb, 2003](#); [Mosek ApS, 2021](#)), in this work, we introduce and analyze spatial price equilibrium in a market-clearing context based on the second-order cone programming (SOCP) framework, and demonstrate how it outperforms the LP-based markets. Although our theoretical results are generalizable to any market-clearing context, we choose the domain of electricity markets for exposition as it is rich in examples that worsen the adverse impacts of the limitations imposed by LP-based markets.

1.1. Limitations of LP-based Electricity Markets

In electricity markets, the nonlinearities arise from the costs (utilities) and constraints of producers (consumers) and the physics of power flow in the network. Currently, real-world electricity markets follow the original proposal by [Bohn et al. \(1984\)](#) to solve the spatial price equilibrium problem as an LP to obtain optimal production and consumption quantities and the spatially-differentiated nodal electricity prices, commonly referred to as *locational marginal prices* (LMPs) in the industry ([Kirschen and Strbac, 2018](#)). To reach climate change mitigation goals, electricity systems are transitioning towards a more sustainable future ([Chu and Majumdar, 2012](#)), by integrating larger shares of weather-dependent renewable energy sources such as wind and solar¹. This trend challenges LP-based markets on three accounts.

First, with large shares of variable and unpredictable renewable energy, electricity markets are exposed to significant uncertainty, which needs to be accounted for. Classical methods within the LP framework, such as scenario-based stochastic programs ([Pritchard et al., 2010](#); [Zavala et al., 2017](#)) and robust optimization techniques ([Bertsimas et al., 2013](#)) are unsuitable in practical settings as they suffer from computational intractability and solution conservatism, respectively. Going beyond LP-based markets is beneficial from an uncertainty modeling perspective. For instance, chance-constrained programming ([Kuang et al., 2018](#)), which admits nonlinear yet convex computationally tractable and analytically expressible uncertainty models, paves the way for *uncertainty-aware* electricity markets in practice.

Second, accommodating the uncertainty requires resources that provide *flexibility services* by adapting their operational status. Such flexible resources include, among others, energy storage ([Kim and Powell, 2011](#)), flexible consumers ([Anjos and Gómez, 2017](#)), as well as the coordination with natural gas ([Thompson, 2013](#)) and district heating ([Mitridati et al., 2020](#)) sectors. LP-based markets impose limitations because operational characteristics of flexibility providers, which are typically nonlinear, when approximated by linear constraints shrinks their actual feasibility set, thereby undermining the amount of flexibility that can be harnessed. At times, ignoring the characteristics induces operational and reliability risks for the flexibility provider and the electricity system, as witnessed during the 2014 polar vortex event in Northeastern United States ([PJM Interconnection, 2014](#)) and more recently, during the cold weather event in Texas ([Bushnell, 2021](#)). The need for an *asset-aware* electricity market remains unfulfilled within the LP framework.

¹In Denmark, for instance, 50% of annual national electricity consumption in 2020 was supplied by such renewable energy sources, and by 2030, this share is envisioned to reach 100% ([The Danish Government's Climate Partnership, 2020](#)). Similar, if not as ambitious, targets have been adopted by countries across the world to reduce electricity-related CO₂ emissions ([IRENA, 2015](#)).

Third, accurate operational modeling of flexible resources is valuable only if the *network constraints* are represented in sufficient detail, which is crucial as flexible resources are dispersed across the electricity network. Conventionally, a linear approximation of electricity network constraints is adopted to retain an LP-based market-clearing problem. With this approximation, the market-clearing problem may result in procurement of flexibility services from resources in a way that the simplified network constraints do not allow the flexibility to be delivered when needed ([Papavasiliou, 2018](#)). This is critical in the case of electricity markets as the loss of *real-time balance* between the production and consumption of electricity in the system may lead to minor, localized supply disruptions at best and a large-scale cascading blackout at worst ([Daqing et al., 2014](#)). A *network-aware* procurement of flexibility services is vital for maintaining the real-time balance.

On the above three accounts, the LP framework falls short in meeting the challenges of electricity markets of the future, necessitating a more advanced yet practical alternative.

1.2. Towards Conic Economics

Augmenting LP-based market-clearing problem with conic constraints alleviates the previously-discussed limitations to a great extent. Specifically, in electricity markets, admitting conic constraints incorporates the nonlinearities arising from modeling uncertainty, operational constraints of flexible resources, and physically-accurate representation of power flows. For instance, conic constraints resulting from the convex reformulation of chance constraints not only enable a computationally tractable model of the uncertainty from renewable energy but also an analytical characterization of the risk faced by the electricity markets while mitigating it ([Mieth et al., 2020](#)). Towards an asset-aware market, conic constraints model the nonlinearities associated with the flow of natural gas in pipelines that are fuel conduits for gas-fired power producers, which are currently the primary flexibility providers in electricity markets. Lastly, in the context of network-awareness, the foreseen evolution of decentralized market structures closer to consumption ([Parag and Sovacool, 2016](#)), and the flexibility available therein, is unlocked through the adoption of conic constraints, which are necessary to accurately model the networks.

A market-clearing problem with conic constraints fosters the so-called *conic economics*. Coined by [Raissi \(2016\)](#), conic economics was introduced in the context of general equilibrium theory, focusing on mitigation of financial risk. In a broader sense, in this work, we argue that the inclusion of second-order cone (SOC) constraints based on the Lorentz cones into the spatial price equilibrium problem alleviates the limitations of the prevalent LP-based framework. Enabling convexity-preserving modeling of nonlinearities, the resulting SOCP-based market-clearing problems are efficiently solved in polynomial time using interior-point methods ([Alizadeh and Goldfarb, 2003](#)) by several off-the-shelf commercial solvers such as MOSEK, Gurobi, and CPLEX. Our proposed conic market is uncertainty-, asset- and network-aware, which is crucial for many physical and non-physical systems, apart from the electricity system. Indeed, advances towards including SOC constraints in electricity market-clearing problems have been recently made, in particular by [Kuang et al. \(2018\)](#), [Papavasiliou \(2018\)](#), [Dvorkin \(2020\)](#) and [Mieth et al. \(2020\)](#). However, these works address one of three challenges discussed, i.e., related to uncertainty-awareness, asset-awareness or network-awareness; thereby, lacking a general appeal, and are limited in their practical applicability. Moreover, the non-generality of the bids implies that flexible resources, which are critical in the future electricity markets, are excluded.

1.3. Contributions

As a broad contribution, our work generalizes the prevalent LP-based market-clearing problem to the SOCP framework and applies *conic duality* to analyze the market equilibrium prices and the

economic properties of the underlying market-clearing problem². In the following, we discuss the specific contributions of this work from three perspectives, i.e., from a market design perspective, theoretical perspective, and finally from a practitioner’s perspective.

From a market design perspective, our primary contribution is an original proposal for a *general* conic electricity market. By general, we imply a market framework that is uncertainty-, asset- and network-aware. Our proposed market framework is uncertainty-aware by design, as it admits a chance-constrained market-clearing formulation. Towards an asset-aware electricity market, we enable heterogeneous market participants to accurately express SOC-representable nonlinearities in their cost (or utility) functions and constraints. Nonlinear network flow models underlying the physical delivery associated with the trades are also included in our proposal, leading to network-aware electricity markets. With the needs of future electricity markets in view, flexibility providers take a central role in our market design.

From a theoretical perspective, we first formulate the market-clearing problem as a centrally-solved optimization problem and address the challenge of *robust solvability* of SOCP problems. Theorem 1 provides the necessary and sufficient conditions for optimality and robustness of the market-clearing outcomes, while Theorem 2 gives an analytical expression for conic spatial prices of the traded commodities. Connecting the centrally-solved optimization problem to a spatial equilibrium problem involving rational and self-interested actors, Theorem 3 leverages conic duality to prove the equivalence of the optimization to a competitive equilibrium. Under common assumptions, Theorem 4 proves the satisfaction of economic properties, namely efficiency, cost recovery and revenue adequacy (Schweppe et al., 1988), in the proposed market-clearing. This analytically supports that the move towards conic markets does not incur the loss of any economic properties compared to the prevalent LP-based markets.

From a practitioner’s perspective, we illustrate the generality of our proposed market-clearing framework by defining a bid format for conic markets, enabling heterogeneous market participants to express their preferences. Our numerical studies highlight how the conic market encompasses an uncertainty-aware electricity market that efficiently remunerates the mitigation of uncertainty by the market participants, such that the real-time balance in the electricity system is ensured. We compare the proposed SOCP-based market-clearing proposal with two LP-based uncertainty-aware benchmarks, highlighting the advantages of moving towards a conic market framework.

Paper organization: In §2 we introduce the market setting, illustrate the relevance of SOC constraints via examples, introduce the bidding format, and present the general conic market-clearing as an optimization problem. In §3, we analyze the spatial equilibrium underlying the optimization problem and discuss the economic properties constituting the market equilibrium. Next, §4 presents numerical results on one of the market-clearing use cases by comparing an uncertainty-aware conic market with the available alternatives within the LP domain. Finally, §5 concludes by highlighting the key findings of this work and discusses future perspectives. Appendix A provides a concise background on SOCP duality, while we prove our theoretical results in Appendix B. We provide modeling examples and present the market-clearing problems employed in numerical studies in the Supplementary Material which serves as an electronic companion to the paper.

Notation: The set of natural and real numbers is denoted by \mathbb{N} and \mathbb{R} , respectively, whereas \mathbb{R}_+ and \mathbb{R}_- , respectively, denote the sets of non-negative and non-positive real numbers. Upper case alphabets with a script typeface, such as \mathcal{A} , represent sets, while vectors are denoted by lower case

²Beyond the SOCP framework, semidefinite programming (SDP) which operates on the cone of semi-definite matrices instead of the Lorentz cone, allows for further broadening of the scope of the market-clearing, albeit at the cost of a higher computational burden. Our theoretical results and their proofs build on Lagrangian duality involving *generalized inequalities*, which lay the foundation for an SDP-based market framework in future.

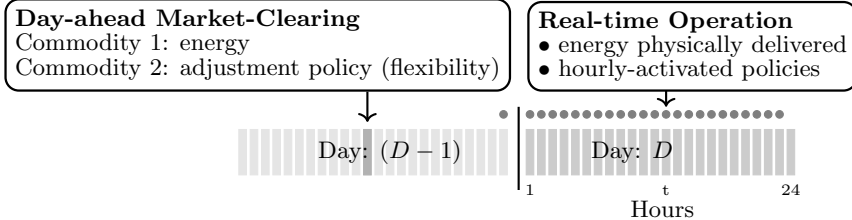


Figure 1: Illustration of commodities traded in an uncertainty-aware electricity market

boldface and matrices by upper case boldface alphabets. For a vector \mathbf{x} , the operator \mathbf{x}^\top denotes its transpose, $\|\mathbf{x}\|_2$ represents its Euclidean norm and $\text{diag}(\mathbf{x})$ returns a diagonal matrix with vector \mathbf{x} as the leading diagonal. We retrieve the k -th element of the vector \mathbf{x} as the scalar x_k and use the operator $[\cdot]_k$ to retrieve the k -th element of a general vector expression. $\mathbf{0}$ and $\mathbf{1}$ are vectors of zeros and ones; arithmetic operators \leq , $=$, and \geq on vectors are understood element-wise. For a matrix $\mathbf{M} \in \mathbb{R}^{p \times q}$, $[\mathbf{M}]_{(:,k)} \in \mathbb{R}^p$ retrieves its k -th column while $[\mathbf{M}]_{(k,:)} \in \mathbb{R}^{1 \times q}$ retrieves its k -th row. The operator $\text{tr}(\mathbf{M})$ returns the trace of the matrix \mathbf{M} , while the expression $\mathbf{M} \succcurlyeq 0$ indicates its positive-semidefiniteness. Lastly, the operator \otimes denotes the Kronecker product.

2. A General Conic Market for Electricity

We discuss the setting of our conic market-clearing problem in §2.1, followed by introducing SOC constraints in a market-clearing context in §2.2. In §2.3, we discuss the equality constraints and present the conic market bids in §2.4. Lastly, we formulate the general market-clearing problem in §2.5 as an SOCP problem.

2.1. Market Setting

We consider a forward electricity market involving multiple discrete clearing periods within the finite time horizon of a single day. We focus on *hourly* electricity markets prevalent across the world and collect the hours of the day in a set $\mathcal{T} = \{1, 2, \dots, T\}$, where $T = 24$.

Commodities: Without loss of generality, we assume that participants in the forward market compete at the *day-ahead* stage. The hourly clearing periods at the day-ahead stage, therefore, correspond to the hours of the next day, which we collectively refer to as the *real-time operation*. The two types of commodities to be traded are (i) energy and (ii) flexibility services. Both types of commodities are traded hourly in the day-ahead market, which is a purely financial market in the sense that the physical delivery of these commodities occurs during the real-time operation. The former commodity, i.e., energy, represents the quantity in MWh to be exchanged among the market participants during the real-time operation. The latter, i.e., flexibility services, refers to the exchanges that contribute to the supply-demand balance during the real-time operation. For instance, these exchanges could be a result of *adjustment policies* of flexible market participants in response to an operational need that may arise during the real-time operation. A potential occurrence of an imbalance between the total production and consumption of energy in the system during the real-time operation is such an operational need. Figure 1 illustrates a two-commodity market, highlighting the day-ahead clearing and the activities during the real-time operation, which we employ in our numerical studies in §4. As another example, flexibility services could also be traded for mitigation of a foreseeable congestion in parts of the electricity network. We define a set $\mathcal{P} = \{1, 2, \dots, P\}$ to denote the P commodities traded in the market.

Market participants: Our market framework admits heterogeneous competing participants buying or selling one or more commodities in the market. We introduce the notation and discuss properties applicable to all participants here, while delegating the elaboration on various kinds of participants

to §2.2. Let the set $\mathcal{I} = \{1, 2, \dots, I\}$ collect I participants, such that $I \geq 2$. For each participant $i \in \mathcal{I}$, let $\mathbf{q}_{it} \in \mathbb{R}^{K_i}$ denote the $K_i \geq P$ number of decision variables at hour t . We retrieve the k -th element of the decision variable at hour t as $q_{itk} \in \mathbb{R}$, $\forall k \in \{1, 2, \dots, K_i\}$. To facilitate a multi-period market-clearing, we stack \mathbf{q}_{it} for the $T = 24$ hours, extending each participant's decision vector to $\mathbf{q}_i \in \mathbb{R}^{K_i T}$. The first P elements of the vector \mathbf{q}_{it} represent contribution towards the P commodities in hour t . For notational compactness, we introduce $\mathbf{q}_{ip} \in \mathbb{R}^T$, $\forall p \in \mathcal{P}$ as a subvector of \mathbf{q}_i extracting the hourly contributions by participant i towards the trades of the p -th commodity over the T hours. Apart from the contributions towards the commodity trades, each participant may have $K_i - P$ state variables at each hour t , which are involved in the participant's operational constraints. Let $c_{it}(\mathbf{q}_{it}) : \mathbb{R}^{K_i} \mapsto \mathbb{R}$ denote the participant's cost function, such that each $c_{it}(\mathbf{q}_{it})$ is increasing, convex and twice-differentiable in \mathbf{q}_{it} and satisfies $c_{it}(\mathbf{0}) = 0$. We adopt a sign convention that $c_{it}(\mathbf{q}_{it}) > 0$ applies for injection into the network and $c_{it}(\mathbf{q}_{it}) < 0$ for withdrawal, thereby representing the convex cost of injection and concave benefit of withdrawal. The temporally-separable structure of the cost function ensures its convexity while accommodating participants such as firms owning energy storage units, who toggle between being producers (discharging) and consumers (charging).

Electricity network: We represent the electricity network as a directed graph $(\mathcal{N}, \mathcal{L})$ formed by a set of nodes $\mathcal{N} = \{1, 2, \dots, N\}$, each potentially hosting multiple market participants, and a set of lines \mathcal{L} comprised of pairs of nodes (n, n') that are connected. We define $\mathcal{I}_n \subseteq \mathcal{I}$, $\forall n \in \mathcal{N}$ as the set of market participants connected to node n . The quantity of power flowing over each line and the direction of the flow is governed by Kirchhoff's laws during the real-time operation. Moreover, the flow across the network is limited by a maximum flow quantity in each line, known as the thermal limit or rated capacity of a power line.

System operator: A system operator ensures that (i) optimal market-clearing outcomes and efficient prices are achieved, and (ii) a continuous balance between consumption and generation is maintained during the real-time operation, while satisfying the transport limits of the underlying electricity network. Evidently, these roles correspond to the tasks of operating the market and operating the network, respectively. In this paper, we assume that the system operator is responsible for both the day-ahead market-clearing and the real-time operation, which is consistent with the prevalent organization in the United States.

Competition and timeline: For the simplicity of exposition, this work assumes that no market participant acts strategically to exercise market power. Moreover, we overcome the non-convexity arising from integrality constraints by accepting offers (bids) from participants already committed to producing (consuming). In our market setting, the committed market participants submit their day-ahead supply offers and demand bids to the central system operator, before a predefined gate closure time, without any knowledge of the bids and offers from other participants. Thereafter, the market is cleared by the system operator matching the offers with the bids, while ensuring the feasibility of network constraints. Finally, cleared prices and quantities for all the commodities are publicly disclosed.

Payment mechanism: As in majority of electricity markets worldwide, we adopt a *uniform pricing* scheme for pricing of energy, implying that all accepted supply offers and demand bids are cleared with a common price at a given location and time. Alternative payment mechanisms, e.g., pay-as-bid and Vickrey-Clarke-Groves pricing in a single commodity setting (Vickrey, 1961) are other possibilities and our market-clearing problem is generalizable to admit them.

2.2. SOC Constraints in a Market-Clearing Problem

Our general market framework admits heterogeneous market participants of four kinds. First, we consider conventional power producers such as firms that own coal-fired, gas-fired, nuclear, and hydro power plants. These producers are *dispatchable* at the day-ahead stage, i.e., they are able to plan their production during real-time operation with a high degree of certainty. Some are flexible, e.g., gas-fired and hydro, meaning that their planned production quantities can be modified during the real-time operation, if needed. On the contrary, some producers are relatively less flexible, e.g., coal-fired and nuclear power producers. Second, we consider firms owning weather-dependent renewable power production sources such as wind and solar power plants. These producers are *non-dispatchable* and inflexible. Third, we consider energy consumers such as small-scale end-consumers or large industries. Some of these consumers may be flexible and can be counted as flexible resources. Last, we consider additional types of flexibility providers, which may not necessarily be conventional power producers or flexible consumers, for instance, firms owning energy storage units.

SOC constraints applicable to these market participants are derived from a second-order cone, which is a convex set and is alternatively referred to as Lorentz cone or ice-cream cone. For the variable \mathbf{q}_i of participant i , $\forall i \in \mathcal{I}$, a SOC constraint in its general form is given by

$$\|\mathbf{A}_i \mathbf{q}_i + \mathbf{b}_i\|_2 \leq \mathbf{d}_i^\top \mathbf{q}_i + e_i \Leftrightarrow \begin{bmatrix} \mathbf{A}_i \\ \mathbf{d}_i^\top \end{bmatrix} \mathbf{q}_i + \begin{bmatrix} \mathbf{b}_i \\ e_i \end{bmatrix} \in \mathcal{C}_i \subseteq \mathbb{R}^{m_i+1}, \quad (1)$$

where \mathcal{C}_i is a second-order cone of dimension $m_i + 1$, where $m_i \in \mathbb{N}$. The dimensions $m_i + 1$ of the cone reflect the relationship within the decision variables. Considering the heterogeneous mix of market participants involved, the dimensions of the cone in the SOC constraints are not necessarily identical among the various participants or even among the constraints of each participant. Parameters $\mathbf{A}_i \in \mathbb{R}^{m_i \times K_i T}$, $\mathbf{b}_i \in \mathbb{R}^{m_i}$, $\mathbf{d}_i \in \mathbb{R}^{K_i T}$ and $e_i \in \mathbb{R}$ embody the structural and geometrical information for each constraint. We use the two equivalent forms in (1) interchangeably, preferring the form with Euclidean norm while discussing the modeling of participant constraints and the conic form in the analytical proofs.

Linear constraints: Any single-period or multi-period linear constraint arising from the operation of physical assets owned by a participant i is represented by (1) with appropriate choice of parameters. Linear constraints are represented by the SOC constraint (1), provided that \mathbf{A}_i is a null matrix or the cone is dimensioned such that $m_i = 0$. In the former case, (1) reduces to the linear constraint $0 \leq \mathbf{d}_i^\top \mathbf{q}_i + e_i$, which denotes a halfspace. Whereas in the latter case, (1) reformulates into a linear constraint $0 \leq \mathbf{d}_i^\top \mathbf{q}_i + e'_i$, where $e'_i = e_i - \|\mathbf{b}_i\|_2$. For power producers, such constraints are, e.g., minimum or maximum production limits and ramping rate constraints that limit production change over subsequent hours.

Quadratic constraints: While linear constraints are admissible in LP-based electricity markets, convex quadratic constraints are not. However, any convex quadratic operational constraint related to the assets of participant i can be represented by (1) if $\mathbf{d}_i = \mathbf{0}$ and $e_i \geq 0$. Example EC.1 in the Supplementary Material illustrates the conic reformulation of such a quadratic constraint.

Other nonlinear constraints: In a more general sense, beyond linear and convex quadratic constraints, (1) captures the relationship among the $K_i T$ number of decision variables for each market participant, contributing towards asset-awareness of the market-clearing problem. For instance, such nonlinear constraints arise in the coordination between the electricity system and natural gas system, wherein the operational constraints of the natural gas system become relevant to the day-ahead electricity market-clearing problem. Example EC.2 in Supplementary Material provides further modeling details for these constraints.

Lastly, beyond asset-awareness, SOC constraints in their general form enable an uncertainty-aware market-clearing problem. Specifically, chance constraints enable endogenous modeling of uncertainty and risk faced by market participants and are analytically reformulated as SOC constraints under some mild conditions (Nemirovski and Shapiro, 2007), see Example 1 below.

Example 1 (Chance Constraints). Consider a market-clearing problem wherein, in addition to the nominal production quantities, a flexibility service is contracted from the flexibility providers in the market. A traded flexibility service is organized as an adjustment policy. As mentioned in §2.1, these adjustment policies allow mitigation of the uncertainty realized during the real-time operation, while look-ahead decisions are made by the system operator at the day-ahead market-clearing stage. Such uncertainty could, for example, arise from imperfect forecasts for the production from weather-dependent renewable energy sources or from imperfect load forecasts for consumers. Assuming a single-period market-clearing problem for notational simplicity, let the set $\mathcal{W} = \{1, 2, \dots, W\}$ collect the W independent sources of uncertainty in the electricity system and vector $\xi \in \mathbb{R}^W$ denote the random forecast errors representing this uncertainty. Assume that ξ follows a probability distribution \mathbb{P}_ξ , parameterized by the moments, mean $\mu \in \mathbb{R}^W$ and covariance $\Sigma \in \mathbb{R}^{W \times W}$, which are estimated by the system operator with access to a finite number of historical measurements. Under the chance-constrained optimization framework, the system operator allocates adjustment policies to flexible producers while allowing them to violate their operational constraints with a small probability $\hat{\varepsilon} \in [0, 1]$. Assume again that participant i has $K_i = 2$ decision variables such that $\mathbf{q}_{i1} = [\hat{q}_{i1} \ \alpha_{i1}]^\top \in \mathbb{R}^2$, where \hat{q}_{i1} and α_{i1} are, respectively, the nominal production quantity and the adjustment policy. A chance constraint limiting the total production, i.e., the sum of nominal and adjustment, of the participant to its upper limit \bar{Q}_i is written as

$$\mathbb{P}_\xi \left(\begin{bmatrix} 1 & \mathbf{1}^\top \xi \end{bmatrix} \begin{bmatrix} \hat{q}_{i1} \\ \alpha_{i1} \end{bmatrix} \leq \bar{Q}_i \right) \geq (1 - \hat{\varepsilon}), \quad (2a)$$

where the uncertainty is characterized by the total forecast error $\mathbf{1}^\top \xi \in \mathbb{R}$. This probabilistic constraint reformulates to its analytic equivalent, based on Nemirovski and Shapiro (2007), as

$$r_{\hat{\varepsilon}} \|\mathbf{X} \mathbf{1} \ \alpha_{i1}\|_2 \leq \bar{Q}_i - \hat{q}_{i1} - \mathbf{1}^\top \mu \ \alpha_{i1}, \quad (2b)$$

where all vectors of ones are $\mathbf{1} \in \mathbb{R}^W$, and $\mathbf{X} \in \mathbb{R}^{W \times W}$ denotes a factorization of the covariance matrix such that $\Sigma = \mathbf{X} \mathbf{X}^\top$. For instance, since $\Sigma \succcurlyeq 0$ from the definition of covariance matrices, such a factorization can be obtained in a computationally efficient manner using Cholesky decomposition, resulting in \mathbf{X} having a lower-triangular structure. This decomposition is uniquely determined for covariance matrices that are full rank, i.e., all uncertainty sources are linearly independent, as assumed. The parameter $r_{\hat{\varepsilon}} \in \mathbb{R}_+$ is a safety parameter chosen by the system operator relying on the knowledge of the distribution \mathbb{P}_ξ , such that $r_{\hat{\varepsilon}}$ increases as $\hat{\varepsilon}$ reduces³. Constraint (2b) is represented by the general SOC constraint (1) with parameters

$$\mathbf{A} = [\mathbf{0} \quad \mathbf{X} \mathbf{1}], \quad \mathbf{b} = \mathbf{0}, \quad \mathbf{d} = -1/r_{\hat{\varepsilon}} [1 \quad \mathbf{1}^\top \mu]^\top \text{ and } e = \bar{Q}_i/r_{\hat{\varepsilon}},$$

³When the random forecast errors ξ are assumed to be normally distributed, the safety parameter $r_{\hat{\varepsilon}}$ is given by the inverse cumulative distribution function of the standard Gaussian distribution evaluated at $(1 - \hat{\varepsilon})$ -quantile (Nemirovski and Shapiro, 2007). Dropping the assumption of normality, a more conservative choice of $r_{\hat{\varepsilon}}$ is obtained based on the so-called moment-based distributionally-robust chance constraints (Wagner, 2008), which considers the distribution \mathbb{P}_ξ to lie inside an ambiguity set of all probability distributions characterized by the empirically-estimated moments μ and Σ . In that case, the safety parameter $r_{\hat{\varepsilon}} = \sqrt{\frac{1-\hat{\varepsilon}}{\hat{\varepsilon}}}$. A further generalization that considers even the moments of distribution \mathbb{P}_ξ to lie in well-defined uncertainty sets such as ellipsoids (Delage and Ye, 2010), lead to a semidefinite constraint instead of the SOC constraint in (2b), leading to a SDP-based market-clearing problem.

thereby resulting in a SOC constraint of dimension $W+1$. Further modeling details showcasing the analytical reformulation of more complicated constraints, such as inter-temporal chance constraints of market participants, are covered in the Supplementary Material.

Finally, accounting for the potentially multiple SOC constraints faced by participant i , we introduce a set $\mathcal{J}_i = \{1, 2, \dots, J_i\}$ collecting the J_i constraints that extend (1) as

$$\|\mathbf{A}_{ij}\mathbf{q}_i + \mathbf{b}_{ij}\|_2 \leq \mathbf{d}_{ij}^\top \mathbf{q}_i + e_{ij}, \quad \forall j \in \mathcal{J}_i, \quad (3)$$

where each constraint with parameters $\mathbf{A}_{ij} \in \mathbb{R}^{m_{ij} \times K_i T}$, $\mathbf{b}_{ij} \in \mathbb{R}^{m_{ij}}$, $\mathbf{d}_{ij} \in \mathbb{R}^{K_i T}$ and $e_{ij} \in \mathbb{R}$ corresponds to a second-order cone $\mathcal{C} \subseteq \mathbb{R}^{m_{ij}+1}$. The feasibility region for (3) is formed by the Cartesian product of J_i second-order cones $\mathcal{C}_i = \prod_{j \in \mathcal{J}_i} \mathcal{C}_{ij} = \mathcal{C}_{i1} \times \dots \times \mathcal{C}_{iJ_i}$, which is convex.

2.3. Equality Constraints

Each participant may be involved in trades corresponding to the P commodities, subject to equality constraints that arise while considering temporal and spatial dynamics underlying their asset models. We model the equality constraints on the decision variable \mathbf{q}_i of participant i as $\mathbf{F}_i \mathbf{q}_i = \mathbf{h}_i$, where $\mathbf{F}_i \in \mathbb{R}^{R_i \times K_i T}$ and $\mathbf{h}_i \in \mathbb{R}^{R_i}$ are parameters encoding the R_i equality constraints on \mathbf{q}_i , such that $R_i \leq K_i T$ and \mathbf{F}_i has full row rank.

The market-clearing conditions are also modeled as marginal equalities coupling the decisions of the participants such that supply-demand balance is ensured for each of the P commodities traded in the market. Modeling these conditions, given the heterogeneous mix of market participants in our framework, requires the following definition.

Definition 1 (Physical Fulfillment of Commodity Trades). For participant $i \in \mathcal{I}$, the hourly injection or withdrawal towards commodity p is given by $\mathbf{G}_{ip} \mathbf{q}_{ip} \in \mathbb{R}^T$, where $\mathbf{G}_{ip} \in \mathbb{R}^{T \times T}$ is a *coupling matrix* formed by elements encoding the injection or withdrawal coefficients.

We now elaborate on this definition. The contribution by a dispatchable producer (either flexible or inflexible) towards the commodity representing energy is $\mathbf{q}_{ip} \in \mathbb{R}_+^T$, whereas for inflexible consumers, the contribution is $\mathbf{q}_{ip} \in \mathbb{R}_-^T$. For both kinds of market participants, the coupling matrices \mathbf{G}_{ip} are identity matrices, i.e., $\mathbf{G}_{ip} = \text{diag}(\mathbf{1})$. Meanwhile, the contribution from energy storage units \mathbf{q}_{ip} to the commodity corresponding to energy adopts different signs in the various hours depending on whether the storage unit is discharging (injection) or charging (withdrawal). Information on the conversion factors for participants from other sectors such as natural gas or district heating is also encoded within the entries of the matrix \mathbf{G}_{ip} . Finally, in addition to those traded system-wide, the market-clearing problem may entail commodities traded among a subset of all participants and thereby, reflect the agreements among that subset. \mathbf{G}_{ip} may thus be null matrices for some commodities and for some participants.

2.4. Bid Format in the Conic Electricity Market

For the sake of generality, we adopt a common bid format for the supply offers and demand bids, referring to them as supply and demand bids, respectively and define them in the following.

Definition 2 (Conic Market Bids). Let \mathcal{B}_i denote a bid submitted by the market participant i to the system operator. The bid \mathcal{B}_i is a tuple defined as

$$\mathcal{B}_i := \left(n_i, \{\mathbf{A}_{ij}, \mathbf{b}_{ij}, \mathbf{d}_{ij}, e_{ij}\}_{j \in \mathcal{J}_i}, \mathbf{F}_i, \mathbf{h}_i, \{\mathbf{G}_{ip}\}_{p \in \mathcal{P}}, \{\mathbf{c}_{it}^Q, \mathbf{c}_{it}^L\}_{t \in \mathcal{T}} \right),$$

where $n_i \in \mathcal{N}$ is the electricity network node at which the participant i is located. Parameters $\mathbf{A}_{ij}, \mathbf{b}_{ij}, \mathbf{d}_{ij}, e_{ij}, \forall j \in \mathcal{J}_i$ are linked to the J_i SOC constraints; $\mathbf{G}_{ip}, \forall p \in \mathcal{P}$ correspond to the coupling matrices for the P commodities; \mathbf{F}_i and \mathbf{h}_i correspond to the R_i equality constraints; and lastly, $\mathbf{c}_{it}^Q, \mathbf{c}_{it}^L, \forall t \in \mathcal{T}$ denote the temporally-separated quadratic and linear bid prices.

Remark 1 (Conic Market Bids vs. Price-Quantity Bids). The bids \mathcal{B}_i are a generalization of the so-called *price-quantity* bids that form the backbone of various orders placed in currently-operational LP-based electricity markets, see [Nord Pool \(2021\)](#) for example. As the name indicates, in addition to the participant's locational information, a price-quantity bid comprises a bid price representing the bidder's willingness-to-pay or willingness-to-receive for the associated quantity. In the proposed conic market bids, the quantities are formed by the parameters of the j -th SOC constraint $\{\mathbf{A}_{ij}, \mathbf{b}_{ij}, \mathbf{d}_{ij}, e_{ij}\}$ admitting the simple linear characterization of quantities \mathbf{q}_i when \mathbf{A}_{ij} is a null matrix or when $m_{ij} = 0$, while more intricate representations of the operational constraints are covered by a suitable choice of the SOC constraint parameters, as discussed in §2.2. In an attempt to accommodate the operational constraints of market participants, prevalent LP-based markets allow specialized order types, such as block orders ([Nord Pool, 2021](#)). These block orders are derived by logically-linking several price-quantity bids over multiple periods and to some extent, enable market participants to reflect their operational constraints on their market participation strategies. Besides the inability to model physically-realistic, nonlinear operational constraints of the participants, such complex orders mandate the use of integrality constraints which leads to the loss of guarantees on the satisfaction of the desired economic properties of the market.

2.5. Market-Clearing as an SOCP Problem

Network constraints: An accurate modeling of the physics of power flows in the electricity network introduces nonlinearities and non-convexities. Convexification of these power flow equations have utilized SOCP ([Kocuk et al., 2016](#)) and SDP ([Lavaei and Low, 2012](#)) relaxations to ensure optimality while solving electricity system-related optimization problems. However, electricity market-clearing problems across the world adopt a linearized approximation of the power flow equations, relying on a number of assumptions ([Cain et al., 2012](#)). Consistent with current practice and for simplicity of exposition, our formulation adopts a variation of linearized power flow equations that leverages the so-called Power Transfer Distribution Factor (PTDF) matrix. Nevertheless, Example EC.3 in Supplementary Material demonstrates the network-awareness of our market-clearing problem by showing how it can be extended to include the SOCP relaxation of power flow equations.

Definition 3 (Power flows using PTDF). With the set $\mathcal{I}_n \subseteq \mathcal{I}$ collecting market participants located at node n , the power flow s_ℓ^a along a line $\ell = (n, n')$ at hour t is given by

$$s_\ell^a = \sum_{n \in \mathcal{N}} [\Psi]_{(\ell, n)} \left(\sum_{i \in \mathcal{I}_n} \sum_{p \in \mathcal{P}} [\mathbf{G}_{ip} \mathbf{q}_{ip}]_t \right),$$

where $\Psi \in \mathbb{R}^{L \times N}$ denotes the PTDF matrix of the electricity network. Derived from the physical parameters of power lines comprising the network, entries of the PTDF matrix are the sensitivity of changes in the flow in any line to a unit injection at a given node. The expression $\sum_{i \in \mathcal{I}_n} \sum_{p \in \mathcal{P}} [\mathbf{G}_{ip} \mathbf{q}_{ip}]_t \in \mathbb{R}$ computes the algebraic sum of injections or withdrawals of all participants located at node n towards the P commodities at hour t .

Remark 2. All P commodities share the common physical network for fulfillment of the trades, as reflected by the summation in the expression for power flows in Definition 3.

Conic market-clearing problem, \mathcal{M}^c : Without loss of generality, we assume that the participants have quadratic cost functions which satisfy the conditions in §2.1. In the interest of computational

and analytical simplicity, we reformulate the quadratic costs as SOC constraints following the approach in Example EC.1. The market-clearing problem, hereafter referred to as \mathcal{M}^c , is formulated as

$$\min_{\mathbf{q}_i, \mathbf{z}_i} \sum_{i \in \mathcal{I}} \sum_{t \in \mathcal{T}} \left(z_{it} + \mathbf{c}_{it}^L \top \mathbf{q}_{it} \right) \quad (4a)$$

$$\text{s.t. } \left\| \mathbf{C}_{it}^Q \mathbf{q}_{it} \right\|_2^2 \leq z_{it}, \forall t, \forall i : (\boldsymbol{\mu}_{it}^Q, \kappa_{it}^Q, \nu_{it}^Q) \quad (4b)$$

$$\left\| \mathbf{A}_{ij} \mathbf{q}_i + \mathbf{b}_{ij} \right\|_2 \leq \mathbf{d}_{ij}^\top \mathbf{q}_i + e_{ij}, \forall j \in \mathcal{J}_i, \forall i : (\boldsymbol{\mu}_{ij}, \nu_{ij}) \quad (4c)$$

$$\mathbf{F}_i \mathbf{q}_i = \mathbf{h}_i, \forall i : (\boldsymbol{\gamma}_i) \quad (4d)$$

$$\sum_{i \in \mathcal{I}} \mathbf{G}_{ip} \mathbf{q}_{ip} = \mathbf{0}_T, \forall p, : (\boldsymbol{\lambda}_p) \quad (4e)$$

$$\left| \sum_{n \in \mathcal{N}} [\boldsymbol{\Psi}]_{(:,n)} \left(\sum_{i \in \mathcal{I}_n} \sum_{p \in \mathcal{P}} [\mathbf{G}_{ip} \mathbf{q}_{ip}]_t \right) \right| \leq \bar{s}, \forall t, : (\underline{\boldsymbol{\rho}}_t, \bar{\boldsymbol{\rho}}_t) \quad (4f)$$

where the objective (4a) minimizes social disutility (or maximizes social welfare) of the market-clearing problem over the time horizon, $t \in \mathcal{T}$. The optimization variables are the decision variables of the market participants $\mathbf{q}_i \in \mathbb{R}^{K_i T}, \forall i$ and $\mathbf{z}_i \in \mathbb{R}^T, \forall i$. Recall that $\mathbf{q}_{it} \in \mathbb{R}^{K_i}$ and $\mathbf{q}_{ip} \in \mathbb{R}^T$ are subsets of the i -th participant's decision vector \mathbf{q}_i . The Lagrange multipliers associated with the constraints are shown in parentheses next to them. The constraint parameters, in their order of appearance, are $\mathbf{A}_{ij} \in \mathbb{R}^{m_{ij} \times K_i T}$, $\mathbf{b}_{ij} \in \mathbb{R}^{m_{ij}}$, $\mathbf{d}_{ij} \in \mathbb{R}^{K_i T}$, $e_{ij} \in \mathbb{R}$, $\mathbf{F}_i \in \mathbb{R}^{R_i \times K_i T}$, $\mathbf{h}_i \in \mathbb{R}^{R_i}$, $\mathbf{G}_{ip} \in \mathbb{R}^{T \times T}$, $[\boldsymbol{\Psi}]_{(:,n)} \in \mathbb{R}^L$ and $\bar{s} \in \mathbb{R}^L$. The index $j \in \mathcal{J}_i$ refers to the J_i SOC constraints of participant i as discussed in §2.2, while the index $p \in \mathcal{P}$ refers to the P commodities traded among the participants. Constraints (4b)-(4d) are participant-specific, while (4e)-(4f) are related to the commodities exchanged in the market.

The temporally-separable quadratic and linear bid prices of participant i are given by $\mathbf{c}_{it}^Q, \mathbf{c}_{it}^L \in \mathbb{R}^{K_i}$ and $\mathbf{C}_{it}^Q \in \mathbb{R}^{K_i \times K_i}$ is a factorization of the quadratic cost matrix such that $\text{diag}(\mathbf{c}_{it}^Q) = \mathbf{C}_{it}^{Q \top} \mathbf{C}_{it}^Q$. Lagrange multipliers $\boldsymbol{\mu}_{it}^Q \in \mathbb{R}^{K_i}$, $\kappa_{it}^Q \in \mathbb{R}_+$ and $\nu_{it}^Q \in \mathbb{R}_+$, $\forall t, \forall i$, are participant-specific dual variables associated with the rotated SOC constraints. Constraints (4c) model the SOC constraints applicable to the market participants that enable asset- and uncertainty-awareness of the market-clearing problem. The tuple of dual variables associated with the SOC constraints (4c) are $(\boldsymbol{\mu}_{ij}, \nu_{ij})$, where $\boldsymbol{\mu}_{ij} \in \mathbb{R}^{m_{ij}}$ and $\nu_{ij} \in \mathbb{R}_+$. Likewise, the dual variable $\boldsymbol{\gamma}_i \in \mathbb{R}^{R_i}$ associates with the R_i equality constraints for the participant i , see §2.3.

Constraints (4e) are the system-wide balance constraints that couple the decisions of the market participants for each of the P commodities traded in the market, such that the Lagrange multipliers associated with these constraints $\boldsymbol{\lambda}_p \in \mathbb{R}^T$ are interpretable as commodity prices. For instance, the Lagrange multiplier associated with the balance between electricity production and consumption is the nodal price of electricity. Lastly, constraints (4f) limit the magnitude of power flow in the lines to their rated capacity, \bar{s} , as given by Definition 3. Given the element-wise absolute value operator in this constraint, we associate a pair of non-negative dual variables $\underline{\boldsymbol{\rho}}_t, \bar{\boldsymbol{\rho}}_t \in \mathbb{R}_+^L$ with it. Naturally, constraints (4f) can be altered to include asymmetric limits, i.e., the limits which depend on the direction of flow in the power lines, without significant change to the analytical results that follow. Further, note that instead of the chosen PTDF-based formulation, implementing an SOCP relaxation for the formulation of power flow equations affects the constraint (4f). However, the overall market-clearing problem \mathcal{M}^c remains within the SOCP framework.

Remark 3 (Strict Convexity). Observe that the optimization problem \mathcal{M}^c has a strictly convex objective function (4a) provided every market participant incurs a non-zero quadratic cost at all

hours for each of its K_i variables. To see that, we recall that every positive semidefinite matrix is the Gram matrix for some set of vectors. For the quadratic cost matrix $\text{diag}(\mathbf{c}_{it}^Q) \succcurlyeq 0$,

$$\mathbf{q}_{it}^\top \text{diag}(\mathbf{c}_{it}^Q) \mathbf{q}_{it} = \mathbf{q}_{it}^\top \mathbf{C}_{it}^Q \mathbf{C}_{it}^{Q\top} \mathbf{C}_{it}^Q \mathbf{q}_{it} = \left\| \mathbf{C}_{it}^Q \mathbf{q}_{it} \right\|_2^2, \quad \forall t, \forall i,$$

such that strict convexity is guaranteed only if the quadratic cost matrix is positive definite, i.e., $\text{diag}(\mathbf{c}_{it}^Q) \succ 0$, which requires $c_{itk}^Q \neq 0$, $\forall k = 1, 2, \dots, K_i$, $\forall t, \forall i$.

3. Economic Interpretation and Equilibrium Analysis

We discuss the price formation process for the P commodities traded in the market in §3.1, followed by the theoretical results that characterize the spatial price equilibrium underlying the centrally-solved market-clearing problem \mathcal{M}^c in §3.2.

3.1. Conic Spatial Prices for Commodities

Deriving optimal market-clearing prices for the problem \mathcal{M}^c is not straightforward, since strong duality is not trivial to establish for an SOCP problem (Ben-Tal and Nemirovski, 2001). Unlike their LP counterparts where strong duality is guaranteed merely by the feasibility of the primal and dual problems as formulated in Farkas' lemma, strong duality in SOCP problems derives from the existence of *strictly feasible*⁴ solutions to both the primal and dual problems (Alizadeh and Goldfarb, 2003, Theorem 13). Following Slater's constraint qualification for convex optimization problems, strict feasibility refers to the existence of points within the feasibility set of the primal problem where all inequalities - SOC and linear - are strictly satisfied. Additionally, a refinement to Slater's constraint qualification yields the so-called *essentially strict feasibility* of an SOCP problem.

Definition 4 (Essentially Strict Feasibility). The market-clearing problem \mathcal{M}^c is essentially strictly feasible, if there exists a feasible solution tuple denoted by $(\mathbf{q}_i, \mathbf{z}_i)$, $\forall i$ such that

$$\begin{aligned} \left\| \mathbf{C}_{it}^Q \mathbf{q}_{it} \right\|_2^2 &< z_{it}, \quad \forall t, \forall i, \\ \|\mathbf{A}_{ij} \mathbf{q}_i + \mathbf{b}_{ij}\|_2 &< \mathbf{d}_{ij}^\top \mathbf{q}_i + e_{ij}, \quad \forall j \in \mathcal{J}_i, \forall i. \end{aligned}$$

Observe that essentially strict feasibility is a weaker requirement as compared to strict feasibility. Nevertheless, it is necessary and sufficient for strong duality to hold for \mathcal{M}^c since other inequalities (4f) are linear in decision variables (Boyd and Vandenberghe, 2004, §5.2.3). We now provide the analytical results crucial to deriving optimal prices from the market-clearing problem \mathcal{M}^c .

Theorem 1 (Strong Duality). *Let \mathcal{D}^c denote the dual problem to the market-clearing problem \mathcal{M}^c . If the set of feasible solutions to the primal problem \mathcal{M}^c is non-empty, then both the primal problem \mathcal{M}^c and dual problem \mathcal{D}^c are essentially strictly feasible, and consequently, strong duality holds for the primal-dual pair of problems \mathcal{M}^c and \mathcal{D}^c .*

Conditioned on feasibility of the primal market-clearing problem \mathcal{M}^c , Theorem 1 enables economic interpretations of the market-clearing outcomes. Relying on classical Lagrangian duality theory, we provide an analytical expression for the optimal, spatially-differentiated nodal prices of the P commodities in the following theorem.

⁴Conventionally, in a market-clearing context, ensuring the strict feasibility or even merely the feasibility of market-clearing problem is considered at a market design stage and is not of high relevance for the market operator. Nevertheless, in the interest of generality and wider acceptance of our conic market-clearing proposal, we address this crucial issue in our analytical results.

Theorem 2 (Conic Spatial Prices). *The solution to the conic market-clearing problem \mathcal{M}^c results in optimal contributions \mathbf{q}_{ip}^* , $\forall i \in \mathcal{I}$ for the $p \in \mathcal{P}$ commodities and the market clears with optimal prices $\boldsymbol{\Pi}_p^* \in \mathbb{R}^{N \times T}$ for the p -th commodity given by*

$$\boldsymbol{\Pi}_p^* = \boldsymbol{\Lambda}_p^* - \boldsymbol{\Psi}^\top (\bar{\boldsymbol{\rho}}^* - \underline{\boldsymbol{\rho}}^*), \quad \forall p \in \mathcal{P}, \quad (5)$$

where $\underline{\boldsymbol{\rho}}^*, \bar{\boldsymbol{\rho}}^* \in \mathbb{R}^{L \times T}$ and $\boldsymbol{\Lambda}_p^* \in \mathbb{R}^{N \times T}$ are variables with stacked columns of optimal dual variables $\underline{\boldsymbol{\varrho}}_t^*, \bar{\boldsymbol{\varrho}}_t^*$, $\forall t$ and $\boldsymbol{\lambda}_p^*$, $\forall n$, respectively, over the T market-clearing hours, i.e.,

$$\bar{\boldsymbol{\rho}}^* = [\bar{\boldsymbol{\varrho}}_1^* \cdots \bar{\boldsymbol{\varrho}}_T^*], \quad \underline{\boldsymbol{\rho}}^* = [\underline{\boldsymbol{\varrho}}_1^* \cdots \underline{\boldsymbol{\varrho}}_T^*], \quad \text{and} \quad \boldsymbol{\Lambda}_p^* := \mathbb{1}_N^\top \otimes \boldsymbol{\lambda}_p^*.$$

The commodity prices given by Theorem 2 are analogous in structure to the LMPs resulting from the prevalent LP-based electricity market-clearing frameworks. Specifically, the optimal prices $\boldsymbol{\Pi}_p^*$ comprise of a nodal price component for each commodity $\boldsymbol{\Lambda}_p^*$ and a network price component which is non-zero only if congestion arises in the network as a consequence of the power flows along the lines to fulfill the trades.

3.2. \mathcal{M}^c as a Spatial Equilibrium Problem

First, we show the equivalence of the optimization problem \mathcal{M}^c to a spatial equilibrium problem. Referring to the two roles played by the system operator discussed in §1, consider a virtual separation of the system operator into a *market operator* and a *network operator*. First, the market operator, acting as a *price setter*, collects the conic market bids from market participants and is responsible for clearing the day-ahead market and for the real-time operation of the system. Second, the network operator, responsible for the physical fulfillment of the commodities, acts as a *spatial arbitrager* to collect a non-zero revenue, *congestion rent*, whenever the trades lead to congestion in the network.

Consider an equilibrium problem \mathcal{E}^c comprised of a set of individual optimization problems of the $i \in \mathcal{I}$ market participants, the network operator and the market-clearing conditions. For market participant i located at node $n_i \in \mathcal{N}$, let $\mathbf{W}_{ip} \in \mathbb{R}^{N \times T}$ denote the quantities of the commodity $p \in \mathcal{P}$ transacted (bought or sold) over the N nodes at the T hours. Under the perfect competition assumption, the commodity prices $\boldsymbol{\Pi}_p$, $\forall p$ are exogenous to the participants' optimization problem. Therefore, participant i maximizes her profit by deciding the optimal contributions \mathbf{q}_{ip} , $\forall p \in \mathcal{P}$ commodities traded in the market, subject to her operational constraints, by solving the problem

$$\begin{aligned} \max_{\mathbf{q}_i, \mathbf{z}_i, \mathbf{W}_{ip}} \quad & \sum_{p \in \mathcal{P}} \text{tr}(\boldsymbol{\Pi}_p^\top \mathbf{W}_{ip}) - \sum_{t \in \mathcal{T}} \left(z_{it} + \mathbf{c}_{it}^L{}^\top \mathbf{q}_{it} \right) \\ & - \sum_{t \in \mathcal{T}} \boldsymbol{\omega}_t^\top \left(\sum_{p \in \mathcal{P}} ([\mathbf{W}_{ip}]_{(:,t)} - \mathbb{1}_{n_i} [\mathbf{G}_{ip} \mathbf{q}_{ip}]_t) \right) \end{aligned} \quad (6a)$$

$$\text{s.t.} \quad \left\| \mathbf{C}_{it}^Q \mathbf{q}_{it} \right\|_2^2 \leq z_{it}, \quad \forall t \quad : (\boldsymbol{\mu}_{it}^Q, \kappa_{it}^Q, \nu_{it}^Q) \quad (6b)$$

$$\|\mathbf{A}_{ij} \mathbf{q}_i + \mathbf{b}_{ij}\|_2 \leq \mathbf{d}_{ij}^\top \mathbf{q}_i + e_{ij}, \quad \forall j \in \mathcal{J}_i \quad : (\boldsymbol{\mu}_{ij}, \nu_{ij}) \quad (6c)$$

$$\mathbf{F}_i \mathbf{q}_i = \mathbf{h}_i \quad : (\boldsymbol{\gamma}_i) \quad (6d)$$

$$\mathbf{W}_{ip}^\top \mathbb{1} = \mathbf{G}_{ip} \mathbf{q}_{ip}, \quad \forall p \in \mathcal{P}, \quad : (\hat{\boldsymbol{\lambda}}_{ip}) \quad (6e)$$

where the three terms comprising the objective function (6a) are the revenues generated by the transactions, the cost (utility) of production (consumption) and the third term is the transport cost for the physical fulfillment of the transactions at the nodes where they are delivered. Here, the indicator vector $\mathbb{1}_{n_i} \in \mathbb{R}^N$ contains the element corresponding to the location of participant i as 1, while all other elements are 0. Constraints (6e) ensure a balance of the commodity transactions

with the contributions towards the trades as given by Definition 1. Variables $\hat{\lambda}_{ip} \in \mathbb{R}^T$ are the Lagrange multipliers associated with these constraints. Note that the nodal commodity prices Π_p and the price of transmitting power $\omega_t \in \mathbb{R}^N$, $\forall t$ are set by the market operator and, as such, are considered as fixed by the participant.

Next, the network operator maximizes congestion rent, while fulfilling the trades of all the commodities in the market. Let $\mathbf{y}_t \in \mathbb{R}^N$, $\forall t$ denote the net power injection comprising of all commodities and all market participants at the N nodes at each hour. The network operator solves the following maximization problem subject to the network limits

$$\max_{\mathbf{y}_t} \quad \sum_{t \in \mathcal{T}} \boldsymbol{\omega}_t^\top \mathbf{y}_t \quad \text{s.t.} \quad -\bar{\mathbf{s}} \leq \boldsymbol{\Psi} \mathbf{y}_t \leq \bar{\mathbf{s}}, \quad : (\underline{\boldsymbol{\varrho}}_t, \bar{\boldsymbol{\varrho}}_t), \quad (7)$$

where $\boldsymbol{\omega}_t$ are variables exogenous to the network operator and the constraints limit the power flows along the lines to their rated capacity in both directions.

Lastly, the market operator clears the market based on the following equalities

$$\sum_{p \in \mathcal{P}} [\mathbf{Q}_p^{\text{inj}}]_{(:,t)} = \mathbf{y}_t, \quad \forall t \quad : (\boldsymbol{\omega}_t) \quad (8a)$$

$$\sum_{i \in \mathcal{I}} \mathbf{G}_{ip} \mathbf{q}_{ip} = \mathbf{0}, \quad \forall p \in \mathcal{P}, \quad : (\boldsymbol{\lambda}_p) \quad (8b)$$

where the auxiliary variable $\mathbf{Q}_p^{\text{inj}} \in \mathbb{R}^{N \times T}$ denotes the commodity-specific net nodal injections

$$\mathbf{Q}_p^{\text{inj}} := \left[\sum_{i \in \mathcal{I}_1} (\mathbf{G}_{ip} \mathbf{q}_{ip})^\top \quad \sum_{i \in \mathcal{I}_2} (\mathbf{G}_{ip} \mathbf{q}_{ip})^\top \quad \cdots \quad \sum_{i \in \mathcal{I}_N} (\mathbf{G}_{ip} \mathbf{q}_{ip})^\top \right]^\top. \quad (9)$$

The market-clearing equalities (8a) ensure the net injection at each of the nodes of the network is balanced by the transport service provided by the network operator. The shadow price of this constraint, $\boldsymbol{\omega}_t$, appears as a parameter in the network operator's maximization (7) and is interpreted as the price of transmitting power from an arbitrary hub to the each of the nodes. As discussed previously, (8b) ensure the system-wide balance of traded commodities.

Theorem 3 (Competitive Spatial Equilibrium). *The convex market-clearing problem \mathcal{M}^c solved centrally by the system operator is equivalent to a competitive spatial equilibrium \mathcal{E}^c comprised of market participants, $i \in \mathcal{I}$ each solving the profit maximization (6), the network operator solving the congestion rent maximization (7) and the market operator clearing the market by enforcing the equalities (8).*

The proof for Theorem 3 relies on the equivalence of the Karush-Kuhn-Tucker (KKT) optimality conditions of the two problems.

Corollary 1 (Existence and Uniqueness). *The solution to the competitive spatial price equilibrium problem \mathcal{E}^c exists and is unique in allocations \mathbf{q}_i^* , provided all market participants bid with non-zero quadratic price components, i.e., $c_{itk}^Q \neq 0$, $\forall k = 1, 2, \dots, K_i$, $\forall t$, $\forall i \in \mathcal{I}$.*

We next analyze the desirable economic properties underlying the equilibrium \mathcal{E}^c .

Theorem 4 (Economic Properties). *The market-clearing problem \mathcal{M}^c and its equivalent competitive spatial equilibrium \mathcal{E}^c result in optimal allocations \mathbf{q}_i^* , $\forall i \in \mathcal{I}$ and spatial commodity prices Π_p^* , $\forall p \in \mathcal{P}$ such that the following economic properties are attained at optimality:*

- (i) **Market efficiency:** Under the perfect competition assumption, social welfare is maximized, such that no participant desires to unilaterally deviate from the market-clearing outcomes.

- (ii) **Cost recovery:** Let the market bids \mathcal{B}_i for each market participant $i \in \mathcal{I}$ be such that $e_{ij} \geq \|\mathbf{b}_{ij}\|_2, \forall j \in \mathcal{J}_i$ and $\mathbf{h}_i = \mathbf{0}$. Then, the optimal allocations \mathbf{q}_i^* , $\forall i \in \mathcal{I}$ and optimal spatial commodity prices $\boldsymbol{\Pi}_p^*$, $\forall p \in \mathcal{P}$ ensure cost recovery for the market participants.
- (iii) **Revenue adequacy:** The market operator does not incur financial deficit at the end of the market-clearing horizon, i.e.,

$$\sum_{p \in \mathcal{P}} \sum_{i \in \mathcal{I}} \text{tr}(\boldsymbol{\Pi}_p^{*\top} \mathbf{W}_{ip}^*) - \sum_{t \in \mathcal{T}} \boldsymbol{\omega}_t^{*\top} \mathbf{y}_t^* \geq 0.$$

Theorem 4 characterizes the economic properties underlying the market-clearing outcomes from the conic market-clearing \mathcal{M}^c . While market efficiency is guaranteed under the perfect competition assumption, cost recovery is ensured for all participants under two conditions, which we elaborate in the following. First, as shown in the modeling examples in the Supplementary Material, the condition $e_{ij} \geq \|\mathbf{b}_{ij}\|_2$ holds true for all participants in most practical settings, with the notable exception of market participants having a non-zero lower bound on their decision variables. The practical issue of non-guarantee of cost recovery for such market participants also prevails in currently-operational LP-based electricity markets. The second condition relates to the homogeneity of the linear equality constraints (4d), i.e., $\mathbf{q}_i = \mathbf{0}$, $\forall i$ is a feasible solution to the market-clearing problem. Observe that, the feasibility of a zero-allocation solution, i.e., $\mathbf{q}_i = \mathbf{0}$, $\forall i$ also satisfies the first condition, thereby indicating that these two conditions are equivalent. Lastly, the condition for revenue adequacy for the market operator requires that the net payments received from the market participants $i \in \mathcal{I}$ less the payments made by the market operator to the network operator towards transmission service is non-negative.

Remark 4 (Incentive Compatibility). The incentive for actors to deviate from price-taking, perfectly-competitive behavior decreases to zero as the number of actors goes to infinity [Roberts and Postlewaite \(1976\)](#). Thus, assuming a very large number of market participants, the conic market-clearing proposal tends towards incentive compatibility, i.e., at the limit participants bid according to their *true* preferences. The conditions under which incentive compatibility is satisfied by \mathcal{M}^c is akin to the prevalent LP-based electricity markets, thereby preserving this desirable economic property in the move towards a SOCP-based market-clearing framework.

Beyond the desirable economic properties discussed so-far, we analyze the robustness of the market-clearing outcomes resulting from \mathcal{M}^c against small changes in parameters. Strong duality aside, in the context of a market-clearing problem, this property is crucial to be studied for SOCP problems. *Robust solvability* refers to the property of an SOCP problem such that it remains solvable and obtains the optimal solution even when the problem parameters are changed by arbitrary small perturbations. Proposition 1.4.6 in [Ben-Tal and Nemirovski \(2001\)](#) establishes that robust solvability is guaranteed by the strict feasibility of both primal and dual problems. The following corollary to Theorem 1 formalizes robust solvability of the conic market-clearing problem.

Corollary 2 (Robust Solvability of \mathcal{M}^c). *The market-clearing problem \mathcal{M}^c is robust solvable, i.e., for the $p \in \mathcal{P}$ commodities traded in the market, both the optimal contributions \mathbf{q}_{ip}^* , $\forall i$ and the optimal prices $\boldsymbol{\Pi}_p^*$ obtained, are robust against small perturbations in the parameters comprising the bids \mathcal{B}_i , $\forall i \in \mathcal{I}$.*

The proof to Corollary 2 is a direct consequence of Theorem 1. This result ensures robust outcomes from a large-scale market-clearing problem admitting hundreds (possibly thousands) of market participants and their SOC constraints. Robust solvability status of the market-clearing problem implies that numerical pathologies arising from approximations, e.g., rounding-off errors, estimation of uncertain parameters, etc. do not cause solvability-related issues.

4. Numerical Studies

We perform numerical experiments on a 24-node electricity system wherein the various market participants, comprising of 6 wind power producers, 9 flexible and 3 inflexible power producers (PPs), 3 identical energy storage units (ESUs) owners, and 17 inflexible consumers, are connected at the nodes as shown in Figure 2(a). The system data is adapted from Conejo et al. (2010) to include the wind farms and ESUs. We study the market-clearing outcomes under various renewable energy share (RES) paradigms⁵, ranging from 10% to 60% of the total energy demand from consumers met by the wind power producers. The wind power producers bid at zero prices to ensure acceptance of bids, and ESU owners bid at prices lower than the cheapest flexible PP. We assume that the inflexible loads exhibit perfect inelasticity of demand, rendering the social welfare maximization problem equivalent to finding cost-minimal dispatch, in expectation, for PPs and ESUs to provide energy and flexibility services needed to meet the net demand⁶. To highlight the impact of network congestion on spatial prices and quantities, we consider two network configurations: (i) without any network bottlenecks and (ii) with network bottlenecks induced by reducing capacities of three transmission lines of the network, shown in blue in Figure 2(a). Based on this setup, §4.1 demonstrates the uncertainty-awareness of our market-clearing proposal, followed by an analysis of the market-clearing outcomes and conic spatial equilibrium prices. In §4.2, we compare the proposed SOCP market-clearing problem with two uncertainty-aware alternatives within the LP domain. While we discuss our numerical results solely in the context of an uncertainty-aware market framework in this section, the examples provided in the Supplementary Material can be used to extend the market-clearing problem to include asset- and/or network-awareness.

4.1. SOCP-based Uncertainty-aware Energy and Flexibility Market

Recalling Example 1, we consider a chance-constrained electricity market-clearing problem wherein two commodities, energy and adjustment policies, are cleared by the system operator. The commodities are traded such that an uncertainty-aware spatial price equilibrium is achieved. Optimal adjustment policies allocated to flexibility providers enable the mitigation of uncertainty realized during the real-time operation, while look-ahead decisions are made by the system operator at the day-ahead market-clearing stage, see Figure 1. Activated during the real-time operation, these policies are in *per unit* and imply the contribution of each flexibility provider towards mitigating the potential real-time imbalance in the system. For example, a flexibility provider may, in the day-ahead market, be allocated a policy corresponding to 10% adjustment, implying that it contributes to mitigating 10% of any type of imbalance (either over- or under-supply) during the real-time operation. In addition to payments for energy, flexibility providers are paid for the flexibility service upfront, i.e., at the day-ahead stage. Considering the novelty of admitting adjustment policies as opposed to the conventional flexible capacity to meet the uncertain net demand, we provide insights into the endogenous consideration of uncertainty and quantify the flexibility payments in the following. The modeling of market participants, chance-constrained market-clearing problem and its SOCP reformulation (which we refer to hereafter as \mathcal{M}^{cc}) is provided in the Supplementary Material.

⁵These paradigms are derived by suitably varying the installed capacity of the wind farms while dimensioning the ESUs such that the total available charging/discharging capacity remains fixed at 12.5% of the total wind farm installed capacity. Such dynamic dimensioning of storage-related flexibility is crucial to ensure market-clearing feasibility for the high RES paradigms.

⁶Here, net demand refers to the energy demand from inelastic loads reduced by the production from wind farms during the real-time operation. There is no uncertainty in the inelastic demand. The expected net demand based on the day-ahead wind power production forecasts for the 50% RES paradigm is shown in Figure 2(b). Naturally, the market operator faces high uncertainty in the hours with smaller net demand due to the high share of weather-dependent renewable energy.

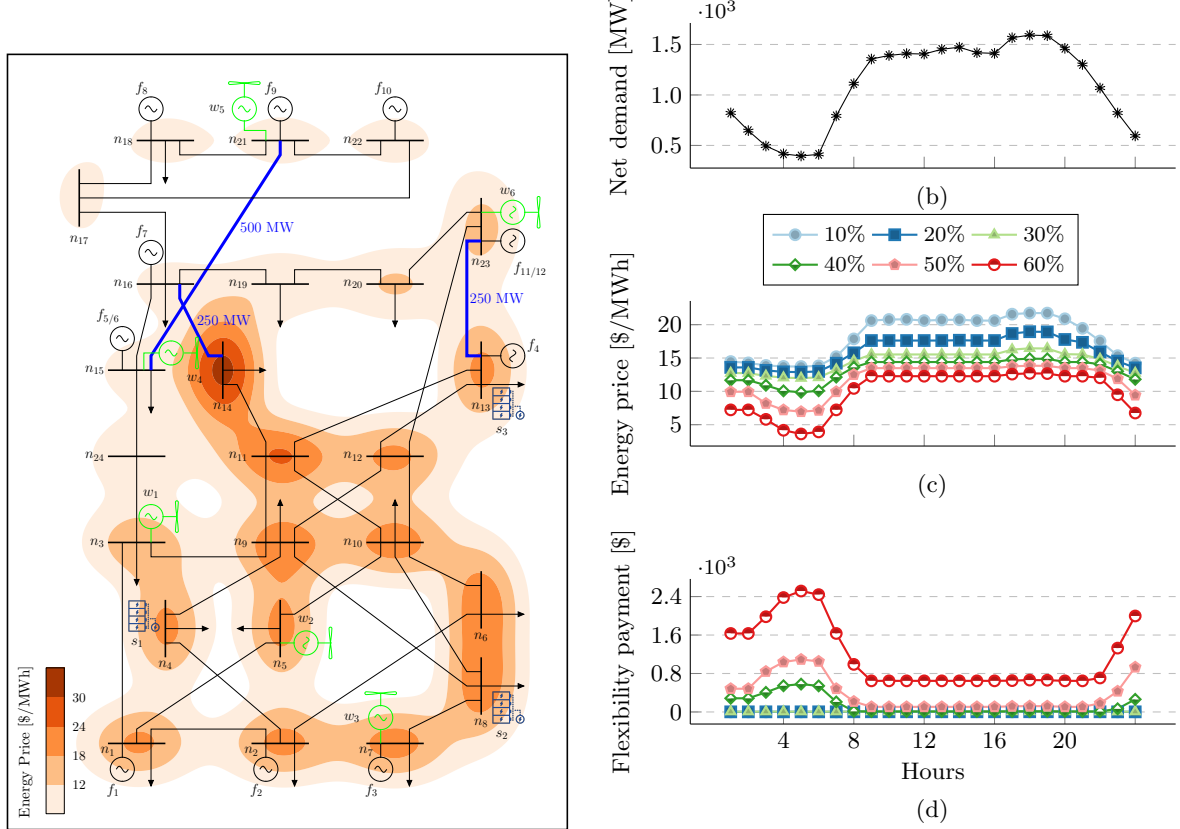


Figure 2: (a) 24-node electricity network showing a visualization of spatial prices of energy for the network configuration with bottlenecks, (b) expected net demand for the 50% RES paradigm, (c) system-wide prices for energy and (d) the total hourly flexibility payments for various RES paradigms

Impact of congestion and uncertainty on prices: The density plot in Figure 2(a) visualizes the impact of network bottlenecks on the day-ahead energy prices for hour 23 under the 50% renewable energy share paradigm. Figures 2(c) and 2(d) show the commodity prices for the network configuration without bottlenecks for the various RES paradigms. Observe that with higher shares of renewable energy, the payment made by the market operator towards flexibility increases, complementary to the gradual reduction in the energy price due to wind farms bidding with zero prices. Overall, increasing uncertainty faced at the day-ahead market-clearing stage leads to lower energy prices while the payments towards flexibility services increase, thereby resulting in the right market signals for investments in flexibility over the long run. Note that, since the adjustment policies are quantified in per unit, the hourly flexibility payments shown in Figure 2(d) correspond to total payments made by the market operator towards flexibility, adopting an allocation determined by the adjustment policies of individual flexibility providers and as such, following a *differentiated pricing* scheme. We now discuss the allocation of adjustment policies and provide further insights into the pricing of flexibility.

Flexibility allocation and payments: For the 50% RES paradigm, Figures 3(a)-3(f) show the optimal allocation of dispatch and adjustment policies to the PPs (f_1, f_2, \dots, f_{12}) and to the ESUs (s_1, s_2, s_3) for selected hours of the day for both network configurations. First, observe that non-zero adjustment policies are only allocated to flexibility providers that are also dispatched for the commodity energy, which is consistent with the requirement that both over- and under-supply imbalances during the real-time operation are mitigated by the flexibility delivered. Second, the network configuration with bottlenecks mandates the allocation of adjustment policies to more number of flexible power producers, as network congestion is expected to impact the flexibility

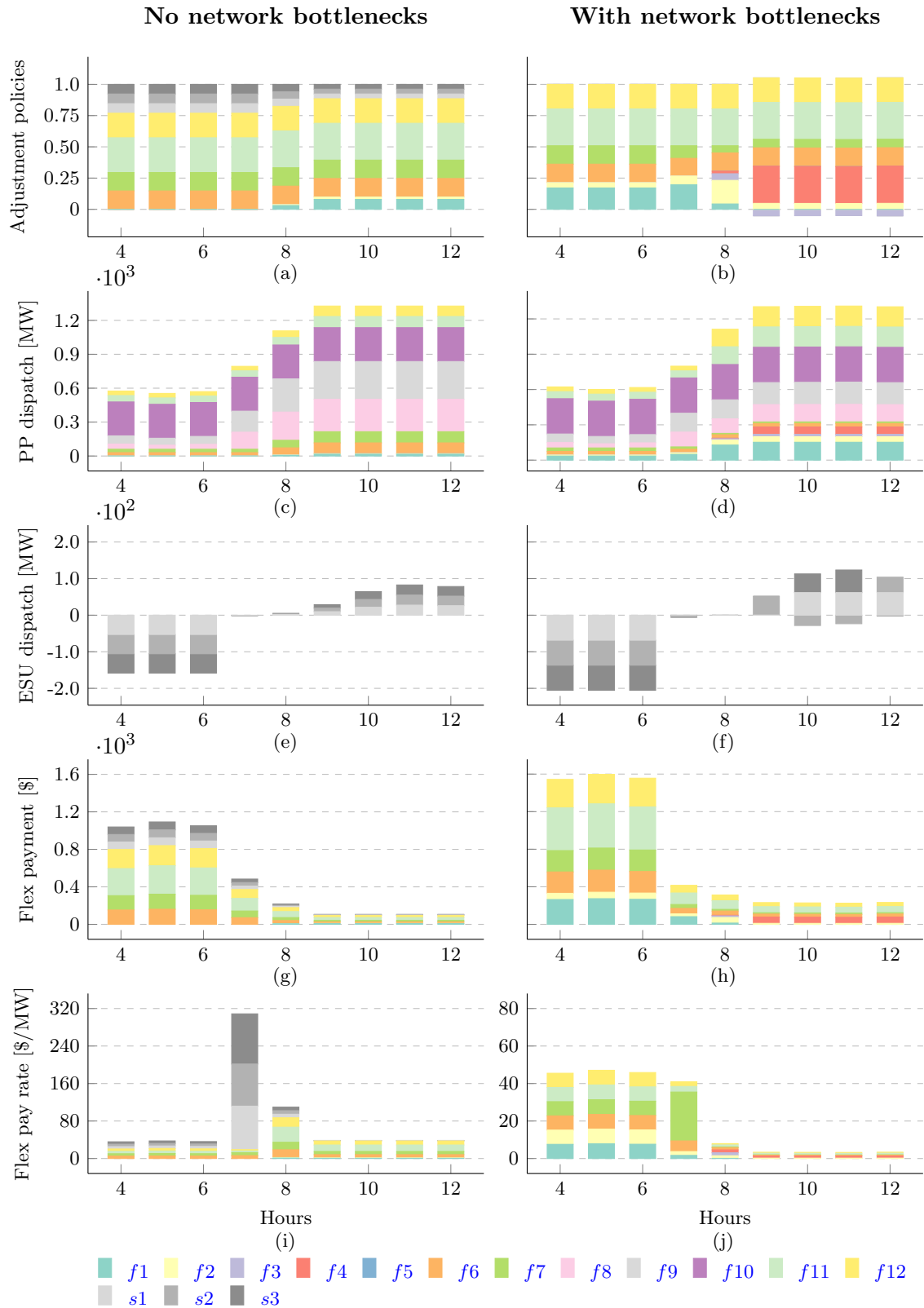


Figure 3: Market-clearing outcomes in hours 4-12: (a)-(b) show the adjustment policies, (c)-(f) show the nominal dispatch of power producers (PPs) and energy storage units (ESUs) for both the network configurations, and (g)-(h) show the flexibility payments and (i)-(j) show the flexibility payment rates (FPRs)

delivery during real-time operation. However, note that ESUs are not allocated adjustment policies in this configuration. This is explained by (i) the availability of flexible PPs in favorable locations of the network with respect to congested power lines, and (ii) the inter-temporal constraints and end-of-day energy balance requirement for ESUs (see Supplementary Material). Indeed, for the paradigm with 60% RES (not shown in the Figure), ESUs in the case with network bottlenecks are allocated non-zero adjustment policies to contribute towards flexibility provision, with the market-clearing problem choosing a more expensive flexibility allocation, offset by the reduced cost of energy provision. Finally, observe in Figure 3(b) that the adjustment policies may take negative values, implying that the action (increasing/decreasing) production by power producers may be in opposition to the system requirement (under-/over-supply), provided it leads to cost-optimal flexibility provision under congested network conditions.

Figures 3(g)-3(h) show the flexibility payments made to flexibility providers under the two network configurations. Flexibility payments are, in general, higher for the case with network bottlenecks as compared to the case without any bottlenecks. Moreover, as previously-discussed in reference to Figure 2(d), flexibility payments are higher for hours with high production from wind farms. In the short run, this incentivizes market participants to bid their flexibility in these hours. To further analyze how flexibility is valued and paid for by the market operator, we introduce an ex-post parameter called *flexibility payment rate* (FPR). Defined for each flexibility provider i , FPR is the rate in \$/MWh at which she is paid for the flexibility service:

$$FPR_{it} = \frac{[\Pi_p^*]_{(n_i,t)} \times \alpha_{it}^*}{|\hat{q}_{it}^* - \bar{q}_{it}|}, \quad (10)$$

where $[\Pi_p^*]_{(n_i,t)}$ retrieves the price of the commodity flexibility service at the node n_i where the participant i is located, \hat{q}_{it}^* and α_{it}^* denote the nominal dispatch and adjustment policy allocated to the participant i , respectively. The quantity \bar{q}_{it} is the dispatch under the perfect forecast case, i.e., when the day-ahead market-clearing is deterministic. We obtain \bar{q}_{it} by solving the market-clearing problem \mathcal{M}^{cc} assuming day-ahead forecasts are realized perfectly during the real-time operation, such that all adjustment policies are set to zero, i.e., $\alpha_{it} = 0, \forall t, \forall i \in \mathcal{I}$. Figures 3(i) - 3(j) show the FPRs for the various participants for the two network configurations. Observe that, equal segments within each bar indicate equal FPRs for all flexibility providers for a given hour. First, we note that, in general, more flexibility providers being allocated non-zero adjustment policies in the network configuration with bottlenecks leads to lower FPRs for the flexibility providers contrary to the one without bottlenecks. A notable exception is hour 7 in the case without bottlenecks, wherein ESUs are paid for the flexibility at very high rate. This is a consequence of two contributing factors: (i) ESUs are dispatched with small nominal quantities in the hours 7 and 8 (see Figure 3(e)) which implies that their ability to provide both charging and discharging flexibility is valued highly, and (ii) the net demand follows a steep rise in the hours 6-8 (see Figure 2(b)) and as a result the market-clearing problem faces a scarcity of not only flexible capacity, but also the ramping ability needed to meet this change in uncertainty. In contrast, in hour 8, while the ESUs are still nominally dispatched close to zero, the flexibility is no longer scarce in the system as the net demand rises sufficiently enough to lead to the nominal dispatch of power producer $f1$, thereby homogenizing the FPRs again. Overall, the FPR for a flexibility provider depends on a number of factors, including the level of uncertainty perceived by the system (quantified by the forecast error covariance matrix as well as the day-ahead forecasts), the location of the flexibility provider, congestion in the network and whether other flexibility providers are available.

4.2. Comparison with LP-based Uncertainty-aware Benchmarks

Next, using numerical simulations corresponding to realizations of the uncertain wind power production, we compare the market-clearing outcomes and performance of the proposed SOCP-based uncertainty-aware market-clearing problem \mathcal{M}^{cc} to alternatives within the LP-domain.

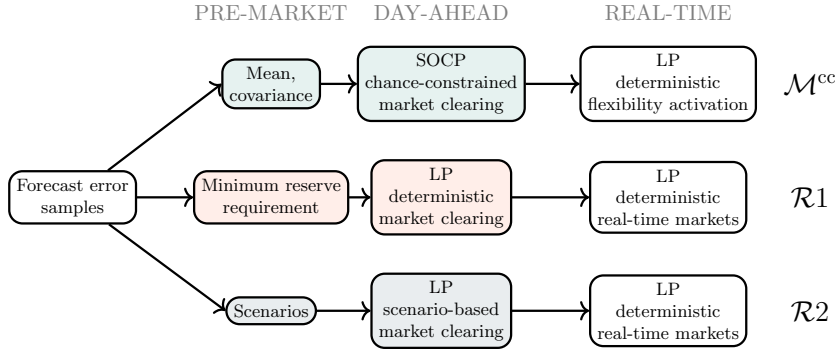


Figure 4: Illustration of the SOCP market-clearing and the LP-based reference problems

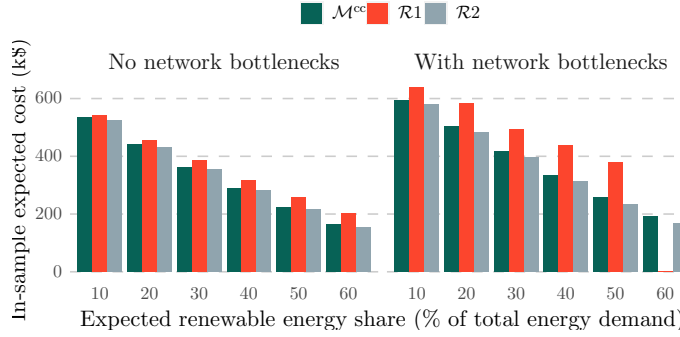


Figure 5: In-sample market-clearing cost in the various RES paradigms considered

We consider two LP-based market-clearing problems as benchmarks: $\mathcal{R}1$ and $\mathcal{R}2$. While it is most closely related to the currently-operational electricity markets, the deterministic market-clearing problem $\mathcal{R}1$ considers uncertainty during the day-ahead clearing stage by commissioning flexibility in the form of reserve capacity. The procured capacity is subsequently activated in real-time electricity markets, cleared closer to physical delivery. To ensure a cost-optimal allocation of the reserve capacity, the market operator enforces a *exogenously-determined* minimum reserve requirement to procure flexible capacity from flexibility providers. Market-clearing problem $\mathcal{R}2$ considers uncertainty based on day-ahead scenarios for realizations of uncertain renewable energy production. The market operator seeks to maximize the expected social welfare under uncertainty, resulting in a day-ahead schedule which is then adjusted during real-time operation for each of the foreseen scenarios. Similarly to \mathcal{M}^{cc} , this approach considers uncertainty endogenously as parameterized by the scenarios considered while solving the market-clearing problem. However, leaving aside the fundamental question of trusting the scenario-generating agent, this approach mandates a large number of scenarios to appropriately represent the uncertainty, thereby, limiting its practical adoption from a computational perspective. Figure 4 illustrates the market-clearing activities, starting with pre-market processing of forecast error samples to generate statistical moments (mean and covariance), to dimension the reserve requirement and to generate scenarios, for \mathcal{M}^{cc} , $\mathcal{R}1$ and $\mathcal{R}2$, respectively. In our numerical studies, we impose a minimum reserve requirement such that the probability of demand curtailment, due to unavailability of flexible capacity to be dispatched during the real-time operation, is less than 5% for the forecast error samples considered. Moreover, observe that the real-time operation in \mathcal{M}^{cc} does not involve pricing and can be done without re-optimization provided uncertainty bounds defined by statistical moments are reliable, whereas both $\mathcal{R}1$ and $\mathcal{R}2$ involve real-time markets, whose outcomes are used to price flexibility services. As with \mathcal{M}^{cc} , the market-clearing formulations and further details on the two reference problems $\mathcal{R}1$ and $\mathcal{R}2$ are provided in the Supplementary Material.

In-sample market-clearing results: First, we study the *in-sample* performance of the market-clearing problems. In-sample refers to the forecast samples used in the pre-market stage to obtain the parameters and scenarios for the market-clearing problems \mathcal{M}^{cc} and the benchmarks $\mathcal{R}1$ and $\mathcal{R}2$, see Figure 4. For the 6 wind farms in the network, we consider 100 forecast error samples drawn from a multivariate Gaussian distribution having zero mean and a standard deviation of 10% of the nominal day-ahead forecast values. Consequently, the safety parameter r_ε is the inverse cumulative distribution function of the standard Gaussian distribution evaluated at $(1 - \varepsilon)$ -quantile. For \mathcal{M}^{cc} , we fix the system operator's constraint violation probability at $\varepsilon = 0.05$. Figure 5 shows a comparison of the expected day-ahead market-clearing cost for the three market-clearing problems under the two network configurations in the various RES paradigms. Observe that, with increasing share of renewable energy, due to its exogenous consideration of uncertainty, market-clearing problem $\mathcal{R}1$ performs increasingly worse compared to the other problems for both the network configurations, leading to infeasibility of market-clearing problem at 60% renewable energy share for the case with network bottlenecks. Furthermore, market-clearing problems \mathcal{M}^{cc} and $\mathcal{R}2$ result in comparable in-sample expected cost. However, it is worth noting that, contrary to \mathcal{M}^{cc} , $\mathcal{R}2$ does not provide any guarantees on the feasibility of market-clearing problem when faced with scenarios beyond those considered as in-sample⁷. We discuss the out-of-sample performance further in the following. The first two rows in Table 1 provide a comparison for the cost and computation times of the various market-clearing problems in the 50% RES paradigm.

Out-of-sample performance: To examine the out-of-sample performance, we perform a deterministic real-time market clearing such that the day-ahead decisions made for each of the market-clearing problems are fixed while adjustments are made in real-time to meet the uncertainty realization. For the market-clearing problem \mathcal{M}^{cc} , this implies that the flexible market participants adjust their production in real-time strictly in accordance to the adjustment policies assigned at the day-ahead market-clearing stage. On the other hand, for the LP-based reference market-clearing problems $\mathcal{R}1$ and $\mathcal{R}2$, the adjustments in real-time are allowed up to the flexible capacity limits obtained at the day-ahead stage. Consistent with the prevalent practice on handling real-time adjustments in electricity markets, we introduce a 10% premium over the bid prices in the day-ahead market-clearing stage to incentivize the market participants to adjust their schedule during real-time operation. Since some wind forecast scenarios may lead to infeasibility of the market-clearing problem due to unavailability of flexibility during the real-time operation, we introduce contingency actions in the market-clearing that correspond to load shedding and wind curtailment respectively. Variables corresponding to these contingency actions are penalized in the market-clearing objective such that they are the last resort in ensuring supply-demand balance.

We prepare a test dataset comprised of 500 wind forecast scenarios, distinct from those used for in-sample simulations, drawn from the same multivariate Gaussian distribution. The box and whiskers plots in Figure 6 show the distribution of the resulting out-of-sample cost for the market-clearing problems under the 50% RES paradigm. For each box, the central line indicates the median, whereas the ends denote the 25th and 75th percentiles. The whiskers extend upto 1.5 times the inter-quartile range, while remaining values are shown as outliers in the form of rings. The second part of Table 1 provides the results from the out-of-sample simulations. First, referring to Figure 6, observe that the ordering in terms of expected cost is preserved from the in-sample simulations, i.e., $\mathcal{R}1$ leads to higher costs. We note that market-clearing problem $\mathcal{R}2$ results in

⁷Depending on the constraint violation probability ε and the number of decision variables, (Alamo et al., 2015, Theorem 4) provides an analytical expression for the number of scenarios that must be considered while solving $\mathcal{R}2$ to obtain the same probabilistic feasibility guarantee as \mathcal{M}^{cc} . For the network considered in this numerical study, this evaluates to $> 80,000$ scenarios, thereby rendering problem $\mathcal{R}2$ unable to provide such a guarantee while being cleared within the desired day-ahead market-clearing solve times (typically, about 1-2 hours).

Table 1: In-sample and out-of-sample performance of market-clearing problems for the 50% RES paradigm

Parameter	Unit	No network bottlenecks			With network bottlenecks		
		\mathcal{M}^{cc}	$\mathcal{R}1$	$\mathcal{R}2$	\mathcal{M}^{cc}	$\mathcal{R}1$	$\mathcal{R}2$
In-sample expected cost	\$1000	221.85	257.85	216.49	256.62	377.56	235.16
Market-clearing computation time	s	2.08	0.22	178.23	2.38	0.27	215.5
Out-of-sample expected cost	\$1000	221.76	259.57	224.29	256.51	396.86	244.28
Out-of-sample infeasibility	%	0.2	3.2	0	0.2	0.6	8.8
Load shedding probability	%	0	0	0	0	1.0	0.4
Wind curtailment probability	%	0	0	46.0	0	0	50.8

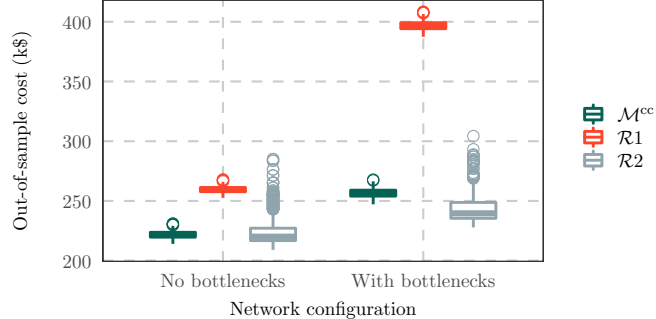


Figure 6: Out-of-sample market-clearing cost comparison in the 50% RES paradigm

highly variable out-of-sample costs compared to the SOCP market-clearing problem \mathcal{M}^{cc} . Second, the out-of-sample expected cost for \mathcal{M}^{cc} is close to the in-sample case, mentioned in Table 1. On the other hand, market-clearing problem $\mathcal{R}1$ exhibits an increase in cost of 0.75% and 5.34% over their in-sample values for the network configurations with and without bottlenecks, respectively. Similarly, problem $\mathcal{R}2$ results in out-of-sample expected cost which exceeds that in-sample expected cost by 3.54% and 4.1%, respectively for the network configurations with and without bottlenecks. Finally, both the LP-based market-clearing problems endure load shedding or wind curtailment when faced with unknown forecast samples. These results highlight how the proposed SOCP-based uncertainty-aware market-clearing problem outperforms the prevalent LP-based alternatives. Next, we provide comparative insights on the day-ahead market-clearing outcomes for the three problems.

Day ahead-market-clearing outcomes: For the 50% RES paradigm, Figure 7 compares the day-ahead market-clearing outcomes among the three problems for the network configuration without any bottlenecks. Observe that, as expected, the energy price in Figure 7(a) closely follows the swings in net demand, shown in Figure 2(b). Figure 7(b) compares the flexibility payment at the day-ahead market-clearing stage for the problems \mathcal{M}^{cc} and $\mathcal{R}1$. In contrast to \mathcal{M}^{cc} wherein flexibility payments are a result of the dual solution to the market-clearing problem, flexibility payments in $\mathcal{R}1$ correspond to the primal solution, i.e., the payments made towards the reserve capacity to meet the minimum reserve requirement. The difference in hourly flexibility payments illustrate the challenge in dimensioning the capacity-based reserves properly. Note that, in absence of any specific capacity reservation or a meaningful flexibility balance at the day-ahead clearing stage, $\mathcal{R}2$ mandates the real-time markets for pricing of flexibility services and is therefore omitted from the comparison⁸. Figures 7(c) and 7(d) show the scheduled dispatch of PPs and ESUs, respectively, for a selection of hours of the day. On account of the minimum reserve requirement associated with

⁸A real-time balance is indeed enforced in $\mathcal{R}2$, such that real-time adjustments in each scenario is aligned with the supply-demand balance. However, the price convergence between day-ahead energy prices and real-time prices is a desirable property to maximize welfare, as discussed in Zavala et al. (2017). This price convergence is in fact a characteristic of our implementation $\mathcal{R}2$, but it limits the ability to explicitly extract values corresponding to flexibility payment either from the primal or dual solutions to the market-clearing problem.

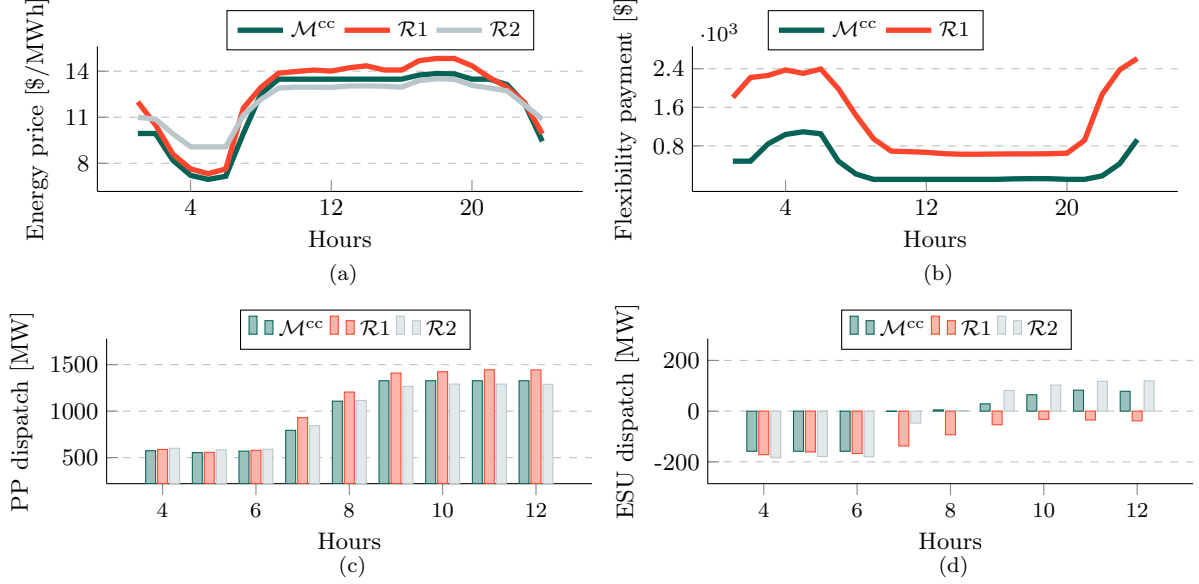


Figure 7: Day-ahead market-clearing outcome for various problems: (a) hourly system-level energy price, (b) hourly flexibility payment, (c) dispatch of power producers (PPs) and (d) dispatch of energy storage units (ESUs)

market-clearing problem $\mathcal{R}1$, in contrast with the other two problems which consider uncertainty endogenously, the dispatch involves higher generation in hours 7 through 12. The excess generation, which partly explains the higher market-clearing cost associated with $\mathcal{R}1$, is used to charge the ESUs in the network such that sufficient flexible capacity is available to meet the minimum reserve requirement. This effect further underscores the importance of endogenous consideration of uncertainty within the market-clearing framework.

5. Concluding Remarks

We proposed and analyzed a new conic formulation for forward markets, which we applied to the specific case of electricity markets. Our contribution is threefold. From a market design perspective, we revisited the spatial price equilibrium problem beyond the LP framework by formulating the market-clearing problem within an SOCP framework. From a theoretical perspective, we relied on Lagrangian duality theory for SOCP problems to characterize the solution to the spatial price equilibrium problem involving rational and self-interested market participants in terms of optimality and robustness to parameter perturbation. We derived analytical expressions for conic spatial prices of the traded commodities and provided analytical proofs to demonstrate that moving towards conic markets for electricity does not incur the loss of any desirable economic properties, i.e., the proposed conic market retains market efficiency, cost recovery and revenue adequacy, under common assumptions also applicable to LP-based markets. Finally, from a practitioner’s perspective, we illustrated the generality of our proposed market-clearing framework by defining a bid format for conic markets.

Our conic market proposal admits SOC-representable nonlinearities underlying the costs and constraints of market participants and the system operator to enable an uncertainty-, asset- and network-aware market-clearing problem. This step in the evolution of electricity markets is crucial for the successful transition of electricity systems worldwide from dispatchable, fossil fuel-based system towards a weather-dependent, renewable energy-based system, supported by a heterogeneous mix of energy and flexibility providers. Our numerical studies leverage in-sample and out-of-sample simulations to showcase the benefits of the proposed SOCP-based market-clearing problem over the LP-based benchmarks in terms of social welfare and its invariability, endogenous

representation of uncertainty, appropriate dimensioning of flexibility need, and guarantees on the feasibility of the market-clearing problem. We provide insights into payments associated with the flexibility procurement based on adjustment policies, which are central to our uncertainty-aware SOCP-based market-clearing proposal.

This paper opens up a variety of important directions for future work. First, considering the generality of the proposal, it is potentially interesting to model market-clearing use cases that involve one or more of the attributes related to uncertainty-, asset- and network-awareness. For instance, the modeling examples and the theoretical results developed in this work can be used to study the coordination between the transmission and distribution system operators in an uncertainty- and network-aware setting. This enables the flexibility available at the distribution level to be appropriately harnessed and priced within the market framework while considering a physically-accurate network constraint representation. Along similar lines is the use case studying the market-based coupling of the electricity and natural gas sectors. Here, the focus of the analysis potentially broadens from merely an optimal network- and asset-aware flexibility procurement to one that designs well-aligned incentives and risk measures to ensure a reliable and resilient system operation in both the interdependent sectors. Second, the conic market bids introduced in §2.4 merit further evaluation in terms of acceptance by market participants, alignment with market regulatory agencies as well as adaptations needed in the prevalent market-clearing algorithms to adopt them. Intended to accelerate their practical adoption, such evaluations could take shape as market simulations and participant-specific sensitivity studies to systematically quantify the costs and benefits of moving towards conic electricity markets. Third, the theoretical results discussed in the paper can be extended to include market participants that act strategically. One can then leverage conic complementarity programs to investigate how exercising market power influences the market-clearing outcomes, specifically in the context of the flexibility payments involved in uncertainty-aware use case analyzed in §4, and more generally regarding the satisfaction of desired economic properties. Another important direction to pursue is the extension of the analytical results we derived on the Lorentz cone to the cone of semidefinite matrices, which results in an SDP-based market-clearing framework. Further generalization over the LP framework aside, such an extension could potentially give rise to markets that consider uncertainty under the paradigm of distributionally-robust chance-constrained optimization and that admit an SDP-based convexification approach for non-convex power flows in the electricity network. Finally, beyond the electricity system, the theoretical results in this work are of potential interest in competitive settings involving physical or non-physical systems wherein cost- and constraint-based nonlinearities currently mandate the use of approximation techniques via linearization.

Appendix A. Lagrangian Duality for SOCP Problems

In Appendix A.1, we provide a concise theoretical background of SOCP duality, while directing interested readers to Lobo et al. (1998), Ben-Tal and Nemirovski (2001) and Alizadeh and Goldfarb (2003) for details. The dual problem to market-clearing problem \mathcal{M}^c is provided in Appendix A.2.

Appendix A.1. Preliminaries

Consider an arbitrary SOCP problem in variable $\mathbf{x} \in \mathbb{R}^N$ of the form

$$\min_{\mathbf{x}} \quad \mathbf{c}^\top \mathbf{x} \quad \text{s.t.} \quad \|\mathbf{A}_j \mathbf{x} + \mathbf{b}_j\|_2 \leq \mathbf{d}_j^\top \mathbf{x} + e_j, \quad \forall j = 1, 2, \dots, J, \quad (\text{A.1})$$

with parameters $\mathbf{c} \in \mathbb{R}^N$, $\mathbf{A}_j \in \mathbb{R}^{k_j \times N}$, $\mathbf{b}_j \in \mathbb{R}^{k_j}$, $\mathbf{d}_j \in \mathbb{R}^N$ and $e_j \in \mathbb{R}$. Based on (1), the SOC constraint in problem (A.1) may be expressed as

$$\begin{bmatrix} \mathbf{A}_j \\ \mathbf{d}_j^\top \end{bmatrix} \mathbf{x} + \begin{bmatrix} \mathbf{b}_j \\ e_j \end{bmatrix} \in \mathcal{C}_j \Leftrightarrow -\begin{bmatrix} \mathbf{A}_j \mathbf{x} + \mathbf{b}_j \\ \mathbf{d}_j^\top \mathbf{x} + e_j \end{bmatrix} \leq_{\mathcal{C}_j} 0,$$

where $\mathcal{C}_j \subseteq \mathbb{R}^{k_j+1}$ is the standard second-order cone and generalized inequality $\leq_{\mathcal{C}_j}$ denotes a partial ordering over the cone \mathcal{C}_j . The Lagrangian function for (A.1) writes as

$$\Theta(\mathbf{x}, \boldsymbol{\lambda}_1, \dots, \boldsymbol{\lambda}_J) = \mathbf{c}^\top \mathbf{x} - \sum_{j=1}^J \boldsymbol{\lambda}_j^\top \left(\begin{bmatrix} \mathbf{A}_j \\ \mathbf{d}_j^\top \end{bmatrix} \mathbf{x} + \begin{bmatrix} \mathbf{b}_j \\ e_j \end{bmatrix} \right),$$

where $\boldsymbol{\lambda}_j \in \mathbb{R}^{k_j+1}$ for $j = 1, 2, \dots, J$ are Lagrange multipliers. The dual function is given by

$$g(\boldsymbol{\lambda}_1, \dots, \boldsymbol{\lambda}_J) = \begin{cases} -\sum_{j=1}^J \boldsymbol{\lambda}_j^\top \begin{bmatrix} \mathbf{b}_j \\ e_j \end{bmatrix}, & \mathbf{c} = \sum_{j=1}^J \begin{bmatrix} \mathbf{A}_j \\ \mathbf{d}_j^\top \end{bmatrix}^\top \boldsymbol{\lambda}_j, \\ -\infty, & \text{otherwise.} \end{cases}$$

Lastly, the dual problem to (A.1) after substituting $\boldsymbol{\lambda}_j = [\boldsymbol{\mu}_j^\top \ \nu_j]^\top$, such that $\boldsymbol{\mu}_j \in \mathbb{R}^{k_j}$ and $\nu_j \in \mathbb{R}_+$ are auxiliary dual variables, can be written as

$$\max_{\boldsymbol{\mu}_j, \nu_j} -\sum_{j=1}^J (\mathbf{b}_j^\top \boldsymbol{\mu}_j + e_j \nu_j) \quad (\text{A.2a})$$

$$\text{s.t. } \sum_{j=1}^J (\mathbf{A}_j^\top \boldsymbol{\mu}_j + \mathbf{d}_j \nu_j) = \mathbf{c} \quad (\text{A.2b})$$

$$\|\boldsymbol{\mu}_j\|_2 \leq \nu_j, \quad \forall j = 1, 2, \dots, J. \quad (\text{A.2c})$$

Similarly, we write an arbitrary SOCP problem with rotated SOC constraints as

$$\min_{\mathbf{x}} \mathbf{c}^\top \mathbf{x} \quad \text{s.t. } \|\mathbf{A}_j \mathbf{x} + \mathbf{b}_j\|_2^2 \leq \mathbf{d}_j^\top \mathbf{x} + e_j, \quad \forall j = 1, 2, \dots, J. \quad (\text{A.3})$$

From the definition of a rotated second-order cone (Mosek ApS, 2021), we have the equivalence

$$\|\mathbf{A}_j \mathbf{x} + \mathbf{b}_j\|_2^2 \leq \mathbf{d}_j^\top \mathbf{x} + e_j \Leftrightarrow -\begin{bmatrix} \mathbf{A}_j \mathbf{x} + \mathbf{b}_j \\ \mathbf{d}_j^\top \mathbf{x} + e_j \\ \frac{1}{2} \end{bmatrix} \leq_{\mathcal{C}_j^R} 0,$$

where $\mathcal{C}_j^R \subseteq \mathbb{R}^{k_j+2}$ denotes the rotated second-order cone. As before, defining Lagrange multipliers $\boldsymbol{\lambda}_j = [\boldsymbol{\mu}_j^\top \ \nu_j \ \kappa_j]^\top \in \mathbb{R}^{k_j+2}$ for $j = 1, 2, \dots, J$, such that $\boldsymbol{\mu}_j \in \mathbb{R}^{k_j}$, $\nu_j \in \mathbb{R}_+$ and $\kappa_j \in \mathbb{R}_+$, the Lagrangian function for the problem (A.3) can be written as

$$\Theta(\mathbf{x}, \boldsymbol{\mu}_1, \dots, \boldsymbol{\mu}_J, \nu_1, \dots, \nu_J, \kappa_1, \dots, \kappa_J) = \mathbf{c}^\top \mathbf{x} - \sum_{j=1}^J (\boldsymbol{\mu}_j^\top \mathbf{A}_j \mathbf{x} + \boldsymbol{\mu}_j^\top \mathbf{b}_j + \frac{1}{2} \kappa_j + \nu_j \mathbf{d}_j^\top \mathbf{x} + \nu_j e_j),$$

from which the dual problem is derived as

$$\max_{\boldsymbol{\mu}_j, \nu_j, \kappa_j} -\sum_{j=1}^J (\mathbf{b}_j^\top \boldsymbol{\mu}_j + e_j \nu_j + \frac{1}{2} \kappa_j) \quad (\text{A.4a})$$

$$\text{s.t. } \sum_{j=1}^J (\mathbf{A}_j^\top \boldsymbol{\mu}_j + \mathbf{d}_j \nu_j) = \mathbf{c} \quad (\text{A.4b})$$

$$\|\boldsymbol{\mu}_j\|_2^2 \leq \kappa_j \nu_j, \quad \forall j = 1, 2, \dots, J. \quad (\text{A.4c})$$

Appendix A.2. Dual Problem to Problem \mathcal{M}^c

Let \mathcal{D}^c denote the dual problem to the market-clearing problem \mathcal{M}^c . We now derive \mathcal{D}^c relying on the dualization approach in [Appendix A.1](#). Let $\Theta(\mathbf{q}_i, \mathbf{z}_i, \boldsymbol{\mu}_{it}^Q, \kappa_{it}^Q, \nu_{it}^Q, \boldsymbol{\mu}_{ij}, \nu_{ij}, \boldsymbol{\gamma}_i, \boldsymbol{\lambda}_p, \underline{\boldsymbol{\rho}}_t, \bar{\boldsymbol{\rho}}_t)$ denote the Lagrangian function of \mathcal{M}^c given by

$$\begin{aligned}\Theta = & \sum_{i \in \mathcal{I}} \sum_{t \in \mathcal{T}} \left(z_{it} + \mathbf{c}_{it}^L \top \mathbf{q}_{it} \right) - \sum_{i \in \mathcal{I}} \sum_{t \in \mathcal{T}} \left(\boldsymbol{\mu}_{it}^Q \top \mathbf{C}_{it}^Q \mathbf{q}_{it} + \frac{1}{2} \kappa_{it}^Q + \nu_{it}^Q z_{it} \right) \\ & - \sum_{i \in \mathcal{I}} \sum_{j \in \mathcal{J}_i} \left(\boldsymbol{\mu}_{ij}^\top (\mathbf{A}_{ij} \mathbf{q}_i + \mathbf{b}_{ij}) + \nu_{ij} (\mathbf{d}_{ij}^\top \mathbf{q}_i + e_{ij}) \right) + \boldsymbol{\gamma}^\top (\mathbf{F}_i \mathbf{q}_i - \mathbf{h}_i) - \sum_{p \in \mathcal{P}} \boldsymbol{\lambda}_p^\top \sum_{i \in \mathcal{I}} \mathbf{G}_{ip} \mathbf{q}_{ip} \\ & + \sum_{t \in \mathcal{T}} \left(\bar{\boldsymbol{\rho}}_t^\top \left(\sum_{n \in \mathcal{N}} [\boldsymbol{\Psi}]_{(:,n)} \left(\sum_{i \in \mathcal{I}_n} \sum_{p \in \mathcal{P}} [\mathbf{G}_{ip} \mathbf{q}_{ip}]_t \right) - \bar{s} \right) - \underline{\boldsymbol{\rho}}_t^\top \left(\sum_{n \in \mathcal{N}} [\boldsymbol{\Psi}]_{(:,n)} \left(\sum_{i \in \mathcal{I}_n} \sum_{p \in \mathcal{P}} [\mathbf{G}_{ip} \mathbf{q}_{ip}]_t \right) + \bar{s} \right) \right).\end{aligned}$$

For notational convenience, let cost vectors for various hours be stacked to obtain $\mathbf{c}_i^L \in \mathbb{R}^{K_i T}$ and a block diagonal matrix $\mathbf{C}_i^Q = \mathbf{C}_{i1}^Q \oplus \dots \oplus \mathbf{C}_{iT}^Q \in \mathbb{R}^{K_i T \times K_i T}$. Let $\boldsymbol{\mu}_i^Q \in \mathbb{R}^{K_i T}$ and $\boldsymbol{\nu}_i^Q \in \mathbb{R}^T$ denote the stacked dual variables $\boldsymbol{\mu}_{it}^Q$ and ν_{it}^Q , respectively. Let $\hat{\boldsymbol{\lambda}}_i \in \mathbb{R}^{K_i T}$ denote the stacked version of an auxiliary dual variable $\hat{\boldsymbol{\lambda}}_{it} \in \mathbb{R}^{K_i}$ for each market participant i with its k -th element given by

$$\hat{\lambda}_{itk} = \begin{cases} [\mathbf{G}_{ip} \boldsymbol{\lambda}_p]_t, & \text{if } k = p, \\ 0, & \text{otherwise.} \end{cases} \quad (\text{A.5})$$

This auxiliary dual variable represents the contribution of each market participant towards the trades of the P commodities in the market. Finally, we define an auxiliary variable representing the i -th participant's contribution towards network congestion, denoted as $\hat{\boldsymbol{\rho}}_{it} \in \mathbb{R}^{K_i}$, given by

$$\hat{\rho}_{itk} = \begin{cases} \mathbb{1}^\top [\mathbf{G}_{ip}]_{(:,t)} \mathbb{1}_{n_i} \boldsymbol{\Psi}^\top (\bar{\boldsymbol{\rho}}_t - \underline{\boldsymbol{\rho}}_t), & \text{if } k = p, \\ 0, & \text{otherwise,} \end{cases} \quad (\text{A.6})$$

where $\mathbb{1} \in \mathbb{R}^T$ and $\mathbb{1}_{n_i} \in \mathbb{R}^N$ is an indicator vector having the element corresponding to the node $n_i \in \mathbb{N}$ where participant i is located as 1, while all other elements are zero. The variables $\hat{\boldsymbol{\rho}}_{it}$ are then stacked to obtain $\hat{\boldsymbol{\rho}}_i \in \mathbb{R}^{K_i T}$. With these substitutions, we write the dual problem \mathcal{D}^c as

$$\max_{\Xi} - \sum_{i \in \mathcal{I}} \sum_{j \in \mathcal{J}_i} (\mathbf{b}_{ij}^\top \boldsymbol{\mu}_{ij} + e_{ij} \nu_{ij}) - \sum_{i \in \mathcal{I}} \sum_{t \in \mathcal{T}} \frac{1}{2} \kappa_{it}^Q - \sum_{t \in \mathcal{T}} \bar{s}^\top (\underline{\boldsymbol{\rho}}_t + \bar{\boldsymbol{\rho}}_t) \quad (\text{A.7a})$$

$$\text{s.t. } \mathbb{1} - \boldsymbol{\nu}_i^Q = \mathbb{0}, \forall i \quad (\text{A.7b})$$

$$\mathbf{c}_i^L - \mathbf{C}_i^Q \boldsymbol{\mu}_i^Q - \sum_{j \in \mathcal{J}_i} (\mathbf{A}_{ij}^\top \boldsymbol{\mu}_{ij} + \mathbf{d}_{ij}^\top \nu_{ij}) + \mathbf{F}_i^\top \boldsymbol{\gamma}_i - \hat{\boldsymbol{\lambda}}_i + \hat{\boldsymbol{\rho}}_i = \mathbb{0}, \forall i \quad (\text{A.7c})$$

$$\left\| \boldsymbol{\mu}_{it}^Q \right\|_2^2 \leq \kappa_{it}^Q \nu_{it}^Q, \forall t, \forall i \quad (\text{A.7d})$$

$$\left\| \boldsymbol{\mu}_{ij} \right\|_2 \leq \nu_{ij}, \forall j \in \mathcal{J}_i, \forall i. \quad (\text{A.7e})$$

$$(\text{A.5}) - (\text{A.6}), \forall k = 1, 2, \dots, K_i, \forall t, \forall i, \quad (\text{A.7f})$$

which is an SOCP problem in variables $\Xi = \{\boldsymbol{\mu}_i^Q, \kappa_{it}^Q, \boldsymbol{\nu}_i^Q, \boldsymbol{\mu}_{ij}, \nu_{ij}, \boldsymbol{\gamma}_i, \boldsymbol{\lambda}_p, \hat{\boldsymbol{\lambda}}_i, \underline{\boldsymbol{\rho}}_t, \bar{\boldsymbol{\rho}}_t, \hat{\boldsymbol{\rho}}_i\}$.

Appendix B. Proofs

Proof of Theorem 1

First, we prove the existence of essentially strictly feasible solutions to the market-clearing problem \mathcal{M}^c and its dual \mathcal{D}^c , inspired by the theory in [Lobo et al. \(1998\)](#). From Definition 4,

finding strictly feasible solutions to the primal market-clearing problem \mathcal{M}^c reduces to finding tuples $(\mathbf{q}_i, \mathbf{z}_i)$, $\forall i$, which strictly satisfy the SOC constraints (4b)-(4c). Likewise, proving strict dual feasibility reduces to finding tuples $(\boldsymbol{\mu}_{it}^Q, \kappa_{it}^Q, \nu_{it}^Q)$, $\forall t, \forall i$ and $(\boldsymbol{\mu}_{ij}, \nu_{ij})$, $\forall j \in \mathcal{J}_i, \forall i$ that strictly satisfy the SOC constraints (A.7d)-(A.7e), respectively. Relying on a variant of the big-M method widely applied to LP problems (Fortuny-Amat and McCarl, 1981), we require the following auxiliary result to find strictly feasible solutions to \mathcal{D}^c .

Lemma 1. *Given the feasibility of the market-clearing problem \mathcal{M}^c , for each market participant $i \in \mathcal{I}$, there exists a large enough finite scalar bound $\bar{D}_i^Q \in \mathbb{R}$ on the Euclidean norm of \mathbf{q}_i given by $\|\mathbf{q}_i\|_2 \leq \bar{D}_i^Q$, such that the optimal solution to \mathcal{M}^c , denoted by $(\mathbf{q}_i^*, \mathbf{z}_i^*)$, is unchanged with addition of the norm bounds.*

Proof. For each participant $i \in \mathcal{I}$, the K_i number of decision variables at each hour t constituting \mathbf{q}_{it} are either the commodity contributions $[\mathbf{q}_{ip}]_t$ for the $p \in \mathcal{P}$ physical commodities discussed in §2.1 or any physical state variables pertaining to the participants. Hence, \mathbf{q}_{it} , $\forall t$ are finite and both bounded above and below. Observe that, a bounded \mathbf{q}_{it} results in a bounded z_{it} due to (4b). Given feasible points \mathbf{q}_i , $\forall i$, one could arbitrarily choose scalars \bar{D}_i^Q such that $\bar{D}_i^Q \geq \|\mathbf{q}_i\|_2$, $\forall i$ and iteratively solve \mathcal{M}^c for values of \bar{D}_i^Q large enough such that the optimal solution $(\mathbf{q}_i^*, \mathbf{z}_i^*)$, $\forall i$ no longer changes over the subsequent iterations. Such an iterative scheme would result in the norm bounds \bar{D}_i^Q , $\forall i$, thereby completing the proof. \square

Due to Definition 4 and Lemma 1, we write a reduced form of market-clearing problem \mathcal{M}^c while retaining only the SOC constraints with additional norm bound constraints

$$\min_{\mathbf{q}_i, \mathbf{z}_i} \sum_{i \in \mathcal{I}} \sum_{t \in \mathcal{T}} (z_{it} + \mathbf{c}_{it}^L \top \mathbf{q}_{it}) \quad (\text{B.1a})$$

$$\text{s.t. } \left\| \mathbf{C}_{it}^Q \mathbf{q}_{it} \right\|_2^2 \leq z_{it}, \forall t, \forall i : (\boldsymbol{\mu}_{it}^Q, \kappa_{it}^Q, \nu_{it}^Q) \quad (\text{B.1b})$$

$$\left\| \mathbf{A}_{ij} \mathbf{q}_i + \mathbf{b}_{ij} \right\|_2 \leq \mathbf{d}_{ij}^\top \mathbf{q}_i + e_{ij}, \forall j \in \mathcal{J}_i, \forall i : (\boldsymbol{\mu}_{ij}, \nu_{ij}) \quad (\text{B.1c})$$

$$\|\mathbf{q}_i\|_2 \leq \bar{D}_i^Q, \forall i, : (\bar{\boldsymbol{\mu}}_i, \bar{\nu}_i) \quad (\text{B.1d})$$

where Lagrangian multipliers $\bar{\boldsymbol{\mu}}_i \in \mathbb{R}^{K_i T}$ and $\bar{\nu}_i \in \mathbb{R}_+$ are associated with the norm bound constraints. Following the approach in Appendix A.1, the dual problem to (B.1) in variables $\Xi^R = \{\boldsymbol{\mu}_i^Q, \kappa_{it}^Q, \nu_i^Q, \boldsymbol{\mu}_{ij}, \nu_{ij}, \bar{\boldsymbol{\mu}}_i, \bar{\nu}_i\}$ writes as

$$\max_{\Xi^R} - \sum_{i \in \mathcal{I}} \sum_{j \in \mathcal{J}_i} (\mathbf{b}_{ij}^\top \boldsymbol{\mu}_{ij} + e_{ij} \nu_{ij}) - \sum_{i \in \mathcal{I}} \sum_{t \in \mathcal{T}} \frac{1}{2} \kappa_{it}^Q - \sum_{i \in \mathcal{I}} \bar{D}_i^Q \bar{\nu}_i \quad (\text{B.2a})$$

$$\text{s.t. } \mathbf{1} - \boldsymbol{\nu}_i^Q = \mathbf{0}, \forall i \quad (\text{B.2b})$$

$$\mathbf{c}_i^L - \mathbf{C}_i^Q \boldsymbol{\mu}_i^Q - \sum_{j=1}^{J_i} (\mathbf{A}_{ij}^\top \boldsymbol{\mu}_{ij} + \mathbf{d}_{ij} \nu_{ij}) + \bar{\boldsymbol{\mu}}_i = \mathbf{0}, \forall i \quad (\text{B.2c})$$

$$\left\| \boldsymbol{\mu}_{it}^Q \right\|_2^2 \leq \kappa_{it}^Q \nu_{it}^Q, \forall t, \forall i \quad (\text{B.2d})$$

$$\|\boldsymbol{\mu}_{ij}\|_2 \leq \nu_{ij}, \forall j \in \mathcal{J}_i, \forall i \quad (\text{B.2e})$$

$$\|\bar{\boldsymbol{\mu}}_i\|_2 \leq \bar{\nu}_i, \forall i. \quad (\text{B.2f})$$

Proving the existence of strictly feasible points for (B.2) is straightforward. Choosing any arbitrary vectors $\boldsymbol{\mu}_{ij}$, $\forall j \in \mathcal{J}_i$, $\forall i$ and $\boldsymbol{\mu}_{it}^Q$, $\forall t$, $\forall i$, we can compute the values of $\nu_{ij} > \|\boldsymbol{\mu}_{ij}\|_2$ and $\kappa_{it}^Q > \|\boldsymbol{\mu}_{it}^Q\|_2$, while $\nu_{it}^Q = 1$ from (B.2b). Now, the variable $\bar{\boldsymbol{\mu}}_i$ follows from the equality (B.2c) and

consequently, $\bar{\nu}_i$ can be any number larger than $\|\bar{\mu}_i\|_2$. Hence, we have found at least one strictly feasible solution to (B.2), which proves essentially strict feasibility of the dual problem \mathcal{D}^c , given that Lemma 1 holds.

Next, we prove essentially strict feasibility of the primal market-clearing problem \mathcal{M}^c employing the so-called Phase-I method, discussed in [Boyd and Vandenberghe \(2004, §11.4\)](#). Consider an SOCP problem in variables $(\mathbf{q}_i, \mathbf{z}_i, x_i, x_i^Q)$ where $x_i \in \mathbb{R}$ and $x_i^Q \in \mathbb{R}$ are arbitrary slack variables

$$\min_{\mathbf{q}_i, \mathbf{z}_i, x_i, x_i^Q} \sum_{i \in \mathcal{I}} \sum_{t \in \mathcal{T}} (z_{it} + \mathbf{c}_{it}^L \top \mathbf{q}_{it}) + \sum_{i \in \mathcal{I}} (x_i + x_i^Q) \quad (\text{B.3a})$$

$$\text{s.t. } \left\| \mathbf{C}_{it}^Q \mathbf{q}_{it} \right\|_2^2 \leq z_{it} + x_i^Q, \forall t, \forall i \quad (\text{B.3b})$$

$$\|\mathbf{A}_{ij} \mathbf{q}_i + \mathbf{b}_{ij}\|_2 \leq \mathbf{d}_{ij}^\top \mathbf{q}_i + e_{ij} + x_i, \forall j \in \mathcal{J}_i, \forall i. \quad (\text{B.3c})$$

Observe that, obtaining strictly solutions to the primal problem (B.3) and its dual problem is straightforward. For instance, choosing

$$\mathbf{q}_i = \emptyset, x_i > \max_{j \in \mathcal{J}_i} \|b_{ij}\|_2 - e_{ij}, \forall i, \quad (\text{B.4a})$$

$$\text{any } \mathbf{z}_i \in \mathbb{R}_+^T \text{ and } x_i^Q > \max_{t \in \mathcal{T}} -z_{it}, \forall i, \quad (\text{B.4b})$$

gives a strictly feasible primal solution to (B.3). Likewise, a strictly feasible solution for the dual problem to (B.3) can be found by an approach (omitted from presentation, for the sake of brevity) discussed above, i.e., by adding non-binding upper bound constraints on the primal variables (x_i, x_i^Q) , $\forall i$. Consequently, [Alizadeh and Goldfarb \(2003, Theorem 13\)](#) establishes strong duality for (B.3) due to strict primal and dual feasibility. We now provide an auxiliary result relating the augmented problem (B.3) to the primal market-clearing problem \mathcal{M}^c .

Lemma 2. *For the tuple $(\mathbf{q}_i^*, \mathbf{z}_i^*, x_i^*, x_i^{Q*})$, $\forall i$ denoting the optimal solution to problem (B.3), only one of the following conditions holds:*

- (i) if $x_i^* < 0$, $\forall i$ and $x_i^{Q*} < 0$, $\forall i$, then $(\mathbf{q}_i^*, \mathbf{z}_i^*)$, $\forall i$ is strictly feasible for the problem \mathcal{M}^c , or
- (ii) if for any participant i , $x_i^* = 0$ or $x_i^{Q*} = 0$, then for that participant $(\mathbf{q}_i^*, \mathbf{z}_i^*)$ is strictly feasible for problem \mathcal{M}^c , provided $e_{ij} > \|\mathbf{b}_{ij}\|_2$, $\forall j \in \mathcal{J}_i$ and the quadratic cost components $\mathbf{c}_{it}^Q \neq \emptyset$, $\forall t$.

Proof. First, observe that if the tuple of optimal solution solution $(\mathbf{q}_i^*, \mathbf{z}_i^*, x_i^*, x_i^{Q*})$, $\forall i$ to problem (B.3) is such that for any i , $x_i^* > 0$ or $x_i^{Q*} > 0$, then it implies that problem \mathcal{M}^c is infeasible, which contradicts our assumption in Theorem 1. Hence, for feasibility of the problem (B.3), we have $x_i \leq 0$, $\forall i$ and $x_i^Q \leq 0$, $\forall i$. Now, from (B.3b) and (B.3c), it is clear that if both $x_i^* < 0$, $\forall i$ and $x_i^{Q*} < 0$, $\forall i$ hold, we have found $(\mathbf{q}_i^*, \mathbf{z}_i^*)$, $\forall i$ which strictly satisfy the SOC inequalities in \mathcal{M}^c , i.e., (4b) and (4c). Conversely, if the optimal solution is obtained such that for any i , $x_i^* = 0$ or $x_i^{Q*} = 0$, then $(\mathbf{q}_i^*, \mathbf{z}_i^*)$ strictly satisfies the SOC inequalities corresponding to the i -th participant in \mathcal{M}^c under some mild conditions derived from (B.4). Note that $x_i^{Q*} = 0 > \max_t -z_{it}$ holds true only if $z_{it} > 0$, $\forall t$. This is ensured by non-zero quadratic cost components of the market participant i at all hours, i.e., $\mathbf{c}_{it}^Q \neq \emptyset$, $\forall t$. Moreover if any $\mathbf{c}_{it}^Q = \emptyset$, then the constraint (4b) corresponding to that hour is trivially satisfied and therefore, can be possibly eliminated. Lastly, from $x_i^* = 0 > \max_{j \in \mathcal{J}_i} \|b_{ij}\|_2 - e_{ij}$, we obtain $\|b_{ij}\|_2 - e_{ij} < 0$, $\forall j \in \mathcal{J}_i$, which is then a requirement for $\mathbf{q}_i^* = \emptyset$ from (B.4a) to be strictly feasible for (4c). This completes the proof. \square

From Lemma 2, solving problem (B.3) leads to $(\mathbf{q}_i, \mathbf{z}_i)$, $\forall i$ that are essentially strictly feasible for \mathcal{M}^c under some mild conditions. Evident from the Examples and formulations in the Supplementary Material, these conditions are met in the practical implementations of \mathcal{M}^c . We have now proved that an essentially strictly feasible solution to primal problem \mathcal{M}^c exists.

Essentially strict feasibility of the primal and dual problems is necessary and sufficient for strong duality to hold for the primal-dual pair of problems \mathcal{M}^c and \mathcal{D}^c (Ben-Tal and Nemirovski, 2001, Theorem 1.4.4), thereby completing the proof.

Proof of Theorem 2

The proof follows from the partial Lagrangian function of \mathcal{M}^c , obtained by keeping the constraints (4b)-(4d) and relaxing the others, which we write as

$$\begin{aligned}\hat{\Theta} = & - \sum_{p \in \mathcal{P}} \boldsymbol{\lambda}_p^\top \sum_{i \in \mathcal{I}} \mathbf{G}_{ip} \mathbf{q}_{ip} + \sum_{t \in \mathcal{T}} \bar{\boldsymbol{\varrho}}_t^\top \left(\sum_{n \in \mathcal{N}} [\boldsymbol{\Psi}]_{(:,n)} \left(\sum_{i \in \mathcal{I}_n} \sum_{p \in \mathcal{P}} [\mathbf{G}_{ip} \mathbf{q}_{ip}]_t \right) - \bar{\mathbf{s}} \right) \\ & - \sum_{t \in \mathcal{T}} \underline{\boldsymbol{\varrho}}_t^\top \left(\sum_{n \in \mathcal{N}} [\boldsymbol{\Psi}]_{(:,n)} \left(\sum_{i \in \mathcal{I}_n} \sum_{p \in \mathcal{P}} [\mathbf{G}_{ip} \mathbf{q}_{ip}]_t \right) + \bar{\mathbf{s}} \right).\end{aligned}$$

With the substitution of the auxiliary variable $\mathbf{Q}_p^{\text{inj}}$, $\forall p \in \mathcal{P}$ defined in (9) followed by a rearrangement of terms, the partial Lagrangian equivalently writes as follows

$$\hat{\Theta} = \underbrace{- \sum_{p \in \mathcal{P}} \boldsymbol{\lambda}_p^\top \mathbf{Q}_p^{\text{inj}} \mathbf{1}}_{\text{System-wide balance}} + \underbrace{\sum_{t \in \mathcal{T}} \bar{\boldsymbol{\varrho}}_t^\top \left(\sum_{p \in \mathcal{P}} \boldsymbol{\Psi} [\mathbf{Q}_p^{\text{inj}}]_{(:,t)} \right) - \sum_{t \in \mathcal{T}} \bar{\boldsymbol{\varrho}}_t^\top \bar{\mathbf{s}} - \sum_{t \in \mathcal{T}} \underline{\boldsymbol{\varrho}}_t^\top \left(\sum_{p \in \mathcal{P}} \boldsymbol{\Psi} [\mathbf{Q}_p^{\text{inj}}]_{(:,t)} \right) - \sum_{t \in \mathcal{T}} \underline{\boldsymbol{\varrho}}_t^\top \bar{\mathbf{s}}}_{\text{Line flow limits}} \quad (\text{B.5})$$

where the vector of ones $\mathbf{1} \in \mathbb{R}^N$. Here, the partial Lagrangian comprises of terms corresponding to the system-wide balance equalities and the line flow limit inequalities, as indicated. In the sense of Bohn et al. (1984), the spot price of electricity for consumers at a given hour is analytically expressed as the sum of shadow price of the system balance constraint and the sensitivity of changes in the demand to the flow in the capacity-constrained transmission lines. We denote these optimal prices $\boldsymbol{\Pi}_p \in \mathbb{R}^{N \times T}$ for the p -th commodity and provide an analytical expression in the following. We derive an expression for the spot price of commodities as the negative sensitivity of the partial Lagrangian (B.5) to the nodal injections as

$$\frac{\partial \hat{\Theta}}{\partial [\mathbf{Q}_p^{\text{inj}}]_{(:,t)}} = - \left(-\mathbf{1}[\boldsymbol{\lambda}_p]_t + \boldsymbol{\Psi}^\top (\bar{\boldsymbol{\varrho}}_t - \underline{\boldsymbol{\varrho}}_t) \right), \quad \forall p, \quad \forall t, \quad (\text{B.6})$$

where the negative sign originates from the sign convention adopted in this work, such that the consumption (withdrawals) are given by $\mathbf{q}_{ip} \in \mathbb{R}_-^T$. For compactness of expression, we extend (B.6) to all hours by defining auxiliary variables $\boldsymbol{\rho}$, $\bar{\boldsymbol{\rho}} \in \mathbb{R}^{L \times T}$ and $\boldsymbol{\Lambda}_p \in \mathbb{R}^{N \times T}$, such that $\bar{\boldsymbol{\rho}} = [\bar{\boldsymbol{\varrho}}_1 \cdots \bar{\boldsymbol{\varrho}}_T]$, $\underline{\boldsymbol{\rho}} = [\underline{\boldsymbol{\varrho}}_1 \cdots \underline{\boldsymbol{\varrho}}_T]$ and $\boldsymbol{\Lambda}_p = \mathbf{1}^\top \otimes \boldsymbol{\lambda}_p$. Lastly, we express the spatial prices as

$$\boldsymbol{\Pi}_p = \boldsymbol{\Lambda}_p - \boldsymbol{\Psi}^\top (\bar{\boldsymbol{\rho}} - \underline{\boldsymbol{\rho}}), \quad \forall p, \quad (\text{B.7})$$

which are analogous in structure to conventional LMPs prevalent in LP-based market-clearing problems. Theorem 1 proves strong duality for the market-clearing problem \mathcal{M}^c , thereby ensuring the optimality of the spatial prices when the dual variables in (B.7) are replaced by their values at the optimal solution.

Proof of Theorem 3.

To prove the equivalence of the optimization problem \mathcal{M}^c with the equilibrium \mathcal{E}^c , we show that the KKT conditions of the equilibrium problem are identical to those of the optimization. First, for the network operator's congestion rent maximization problem (7), let Θ_{NO} denote the Lagrangian function of the problem (7). We write the KKT conditions defining the optimal solution as

- *Stationarity condition:*

$$\frac{\partial \Theta_{\text{NO}}}{\partial \mathbf{y}_t} = \boldsymbol{\omega}_t + \boldsymbol{\Psi}^\top (\bar{\boldsymbol{\rho}}_t - \underline{\boldsymbol{\rho}}_t) = \mathbb{0}, \quad \forall t \quad (\text{B.8a})$$

- *Primal feasibility, dual feasibility and complementarity conditions:*

$$-\boldsymbol{\Psi} \mathbf{y}_t \leq \bar{\mathbf{s}}; \quad \underline{\boldsymbol{\rho}}_t \geq \mathbb{0}; \quad \underline{\boldsymbol{\rho}}_t \odot (\boldsymbol{\Psi} \mathbf{y}_t + \bar{\mathbf{s}}) = \mathbb{0} \quad (\text{B.8b})$$

$$\boldsymbol{\Psi} \mathbf{y}_t \leq \bar{\mathbf{s}}; \quad \bar{\boldsymbol{\rho}}_t \geq \mathbb{0}; \quad \bar{\boldsymbol{\rho}}_t \odot (\boldsymbol{\Psi} \mathbf{y}_t - \bar{\mathbf{s}}) = \mathbb{0}, \quad (\text{B.8c})$$

where \odot denotes the Hadamard (element-wise) product operator.

For each participant $i \in \mathcal{I}$, let $\Theta_i(\mathbf{q}_i, \mathbf{z}_i, \boldsymbol{\mu}_{it}^Q, \kappa_{it}^Q, \nu_{it}^Q, \boldsymbol{\mu}_{ij}, \nu_{ij}, \boldsymbol{\gamma}_i, \hat{\boldsymbol{\lambda}}_{ip})$ denote the Lagrangian function for problem (6) given by

$$\begin{aligned} \Theta_i = & \sum_{p \in \mathcal{P}} \text{tr}(\boldsymbol{\Pi}_p^\top \mathbf{W}_{ip}) - \sum_{t \in \mathcal{T}} \left(z_{it} + \mathbf{c}_{it}^L \mathbf{q}_{it} \right) - \sum_{t \in \mathcal{T}} \boldsymbol{\omega}_t^\top \left(\sum_{p \in \mathcal{P}} [\mathbf{W}_{ip}]_{(:,t)} \right) + \sum_{t \in \mathcal{T}} \boldsymbol{\omega}_t^\top \left(\sum_{p \in \mathcal{P}} \mathbb{1}_{n_i} [\mathbf{G}_{ip} \mathbf{q}_{ip}]_t \right) \\ & + \sum_{t \in \mathcal{T}} \left(\boldsymbol{\mu}_{it}^Q \mathbf{C}_{it}^Q \mathbf{q}_{it} + \frac{1}{2} \kappa_{it}^Q + \nu_{it}^Q z_{it} \right) + \sum_{j \in \mathcal{J}_i} \left(\boldsymbol{\mu}_{ij}^\top (\mathbf{A}_{ij} \mathbf{q}_i + \mathbf{b}_{ij}) + \nu_{ij} (\mathbf{d}_{ij}^\top \mathbf{q}_i + e_{ij}) \right) \\ & - \boldsymbol{\gamma}_i^\top (\mathbf{F}_i \mathbf{q}_i - \mathbf{h}_i) + \hat{\boldsymbol{\lambda}}_{ip}^\top (\mathbf{G}_{ip} \mathbf{q}_{ip} - \mathbf{W}_{ip}^\top \mathbb{1}) \end{aligned} \quad (\text{B.9})$$

Using the auxiliary dual variables $\boldsymbol{\mu}_i^Q$, $\boldsymbol{\nu}_i$ and parameters \mathbf{c}_i^L , \mathbf{C}_i^Q defined previously in [Appendix A.2](#), we write the KKT optimality conditions for a participant $i \in \mathcal{I}$ as

- *Stationarity conditions:*

$$\begin{aligned} \frac{\partial \Theta_i}{\partial \mathbf{q}_i} = & -\mathbf{c}_i^L + \mathbf{C}_i^Q \boldsymbol{\mu}_i^Q + \sum_{j \in \mathcal{J}_i} (\mathbf{A}_{ij}^\top \boldsymbol{\mu}_{ij} + \mathbf{d}_{ij} \nu_{ij}) - \mathbf{F}_i^\top \boldsymbol{\gamma}_i + \frac{\partial}{\partial \mathbf{q}_i} \left(\hat{\boldsymbol{\lambda}}_{ip}^\top (\mathbf{G}_{ip} \mathbf{q}_{ip}) \right) \\ & + \frac{\partial}{\partial \mathbf{q}_i} \left(\sum_{t \in \mathcal{T}} \boldsymbol{\omega}_t^\top \left(\mathbb{1}_{n_i} \sum_{p \in \mathcal{P}} [\mathbf{G}_{ip} \mathbf{q}_{ip}]_t \right) \right) = \mathbb{0} \quad (\text{B.10a}) \end{aligned}$$

$$\frac{\partial \Theta_i}{\partial \mathbf{W}_{ip}} = \boldsymbol{\Pi}_p - \hat{\boldsymbol{\lambda}}_{ip} \mathbb{1}^\top - \boldsymbol{\Omega} = \mathbb{0}, \quad \forall p \in \mathcal{P}, \quad (\text{B.10b})$$

$$\frac{\partial \Theta_i}{\partial \mathbf{z}_i} = \mathbb{1} - \boldsymbol{\nu}_i = \mathbb{0} \quad (\text{B.10c})$$

where $\boldsymbol{\Omega} \in \mathbb{R}^{N \times T} := [\boldsymbol{\omega}_1 \ \boldsymbol{\omega}_2 \ \cdots \ \boldsymbol{\omega}_T]$, such that the term $\sum_{t \in \mathcal{T}} \boldsymbol{\omega}_t^\top \left(\sum_{p \in \mathcal{P}} [\mathbf{W}_{ip}]_{(:,t)} \right)$ in the Lagrangian (B.9) reduces to $\text{tr}(\boldsymbol{\Omega}^\top \mathbf{W}_{ip})$. Furthermore, from (B.8a), we have $\boldsymbol{\omega}_t = -\boldsymbol{\Psi}^\top (\bar{\boldsymbol{\rho}}_t - \underline{\boldsymbol{\rho}}_t)$ at the optimal solution. With this and from the definitions of $\hat{\boldsymbol{\lambda}}_i$ and $\hat{\boldsymbol{\rho}}_i$ in (A.5) and (A.6), respectively, (B.10a) reduces to

$$\frac{\partial \Theta_i}{\partial \mathbf{q}_i} = -\mathbf{c}_i^L + \mathbf{C}_i^Q \boldsymbol{\mu}_i^Q + \sum_{j \in \mathcal{J}_i} (\mathbf{A}_{ij}^\top \boldsymbol{\mu}_{ij} + \mathbf{d}_{ij}) - \mathbf{F}_i^\top \boldsymbol{\gamma}_i + \hat{\boldsymbol{\lambda}}_i - \hat{\boldsymbol{\rho}}_i = \mathbb{0} \quad (\text{B.10d})$$

Similarly, the stationarity condition (B.10b) reduces to

$$\frac{\partial \Theta_i}{\partial \mathbf{W}_{ip}} = \boldsymbol{\Pi}_p - \hat{\boldsymbol{\lambda}}_{ip} \mathbf{1}^\top + \boldsymbol{\Psi}^\top (\bar{\boldsymbol{\rho}} - \underline{\boldsymbol{\rho}}) = \mathbf{0}, \quad \forall p \in \mathcal{P}, \quad (\text{B.10e})$$

following the definitions of auxiliary dual variables $\bar{\boldsymbol{\rho}}$ and $\underline{\boldsymbol{\rho}}$ in Theorem 2.

- Primal feasibility, dual feasibility and complementarity conditions:

$$\left\| \mathbf{C}_{it}^Q \mathbf{q}_{it} \right\|_2^2 \leq z_{it}; \quad \left\| \boldsymbol{\mu}_{it}^Q \right\|_2^2 \leq \kappa_{it}^Q \nu_{it}^Q, \quad \kappa_{it}^Q \geq 0, \nu_{it}^Q \geq 0; \quad \begin{bmatrix} \boldsymbol{\mu}_{it}^{Q^\top} & \nu_{it}^Q & \kappa_{it}^Q \end{bmatrix} \begin{bmatrix} \mathbf{C}_{it}^Q \mathbf{q}_{it} \\ z_{it} \\ \frac{1}{2} \end{bmatrix} = 0, \quad \forall t \quad (\text{B.10f})$$

$$\left\| \mathbf{A}_{ij} \mathbf{q}_i + \mathbf{b}_{ij} \right\|_2 \leq \mathbf{d}_{ij}^\top \mathbf{q}_i + e_{ij}; \quad \left\| \boldsymbol{\mu}_{ij} \right\|_2 \leq \nu_{ij}, \quad \nu_{ij} \geq 0; \quad \begin{bmatrix} \boldsymbol{\mu}_{ij}^\top & \nu_{ij} \end{bmatrix} \left(\begin{bmatrix} \mathbf{A}_{ij} \\ \mathbf{d}_{ij}^\top \end{bmatrix} \mathbf{q}_i + \begin{bmatrix} \mathbf{b}_{ij} \\ e_{ij} \end{bmatrix} \right) = 0, \quad \forall j \in \mathcal{J}_i \quad (\text{B.10g})$$

$$\mathbf{F}_i \mathbf{q}_i = \mathbf{h}_i; \quad \gamma_i \text{ free} \quad (\text{B.10h})$$

$$(\text{A.5}) - (\text{A.6}), \quad \forall k = 1, 2, \dots, K_i, \quad \forall t, \quad \forall i. \quad (\text{B.10i})$$

Equations (B.8), (B.10c)-(B.10i), $\forall i \in \mathcal{I}$ and (8) form the KKT optimality conditions for the equilibrium problem \mathcal{E}^c . Observe that, in addition to the primal and dual feasibility involving SOC constraints, (B.10f)-(B.10g) ensure the conic complementarity condition is met at the optimal solution (Alizadeh and Goldfarb, 2003, Theorem 16).

To see that the KKT optimality conditions for the optimization problem \mathcal{M}^c are identical to those of the equilibrium, observe that at the optimal solution:

- (i) $\hat{\boldsymbol{\lambda}}_{ip}^*$, $\forall i \in \mathcal{I}$ appearing in (B.10e) are attained such that $\hat{\boldsymbol{\lambda}}_{ip}^* = \boldsymbol{\lambda}_p^*$, $\forall p \in \mathcal{P}$, $\forall i \in \mathcal{I}$, where $\boldsymbol{\lambda}_p^*$, $\forall p \in \mathcal{P}$ corresponds to the system-wide price of the commodities. Therefore, (B.10e) provides the analytical expression for conic spatial prices as formulated in Theorem 2, and
- (ii) \mathbf{y}_t^* , $\forall t$ appearing in (B.8b)-(B.8c) are obtained such that $\mathbf{y}_t^* = \sum_{p \in \mathcal{P}} [\mathbf{Q}_p^{\text{inj}*}]_{(:,t)}$, $\forall t$. This follows from the market-clearing condition (8a). Note that the auxiliary variable $\mathbf{Q}_p^{\text{inj}}$ appears in the partial Lagrangian of problem \mathcal{M}^c , as shown (B.5).

This establishes the equivalence of the KKT optimality conditions for the centrally-solved optimization problem \mathcal{M}^c and the equilibrium problem \mathcal{E}^c , thereby completing the proof.

Proof of Corollary 1

To prove existence of solutions to the competitive spatial price equilibrium problem \mathcal{E}^c , we recall Rosen (1965, Theorem 1) which provides an existence result for solutions to equilibrium problems conditioned on the convexity and compactness of each participant's strategy sets and the continuity of their payoff functions. For the market participants $i \in \mathcal{I}$, while convexity and closure of the strategy sets are given by the feasibility region defined by equalities and non-strict inequalities (6b)-(6e), Lemma 1 proves that $(\mathbf{q}_i, \mathbf{z}_i)$, $\forall i$ are bounded. Note that the quantities bought or sold by the i -th participant \mathbf{W}_{ip} , $\forall p$ are bounded, conditioned on the boundedness of \mathbf{q}_i due to (6e). Consequently, the strategy sets of the participants are convex as well as closed and bounded, thereby satisfying the convexity and compactness conditions. Further, each participant's cost function (6a) is continuous in the decision variables. For the network operator, convexity and compactness of the strategy set is given due to the network limits and continuity of the payoff function is satisfied by the linear objective function in (7). Therefore, from Rosen (1965, Theorem 1), this proves that at least one solution exists for the spatial price equilibrium problem \mathcal{E}^c . To derive conditions under which at most one solution exists to problem \mathcal{E}^c , we refer to the equivalence

of equilibrium problem \mathcal{E}^c to the convex market-clearing optimization problem \mathcal{M}^c established by Theorem 3. From this equivalence, the uniqueness of allocations \mathbf{q}_i^* , $\forall i$ at the equilibrium relies on the strict convexity of the problem \mathcal{M}^c , which we characterize in Remark 3. However, observe that, the uniqueness of solutions to the dual market-clearing problem \mathcal{D}^c is not given due to lack of the strict convexity property of the dual objective (A.7a). Therefore, uniqueness of spatially-differentiated conic prices $\boldsymbol{\Pi}_p^*$, $\forall p$ given by (5) is not guaranteed. This completes the proof.

Proof of Theorem 4

- (i) **Market efficiency:** An efficient market maximizes social welfare, such that no participant unilaterally deviates from the market-clearing outcomes since each participant maximizes her profit at the optimal allocations \mathbf{q}_i^* and prices $\boldsymbol{\Pi}_p^*$, $\forall p$. Under the assumption of perfectly competitive market participants, this is given if the KKT optimality conditions of the centrally-solved optimization problem \mathcal{M}^c and equilibrium problem \mathcal{E}^c involving rational and self-interested actors are identical, which we have established in Proof of Theorem 3.
- (ii) **Cost recovery:** Mathematically, the non-negativity of payoff for the market participants holds true, if at the optimal solution

$$\sum_{p \in \mathcal{P}} \text{tr}(\boldsymbol{\Pi}_p^{*\top} \mathbf{W}_{ip}^*) - \sum_{t \in \mathcal{T}} \left(z_{it}^* + \mathbf{c}_{it}^L{}^\top \mathbf{q}_{it}^* \right) - \sum_{t \in \mathcal{T}} \boldsymbol{\omega}_t^{*\top} \left(\sum_{p \in \mathcal{P}} ([\mathbf{W}_{ip}^*]_{(:,t)} - \mathbb{I}_{n_i} [\mathbf{G}_{ip} \mathbf{q}_{ip}^*]_t) \right) \geq 0, \quad \forall i \in \mathcal{I}. \quad (\text{B.11})$$

To prove that (B.11) holds, we derive dual problems to each participant's profit maximization problem (6). The dual problem in variables $\Xi_i = \{\boldsymbol{\mu}_i^Q, \kappa_{it}^Q, \boldsymbol{\nu}_i^Q, \boldsymbol{\mu}_{ij}, \nu_{ij}, \boldsymbol{\gamma}_i\}$ writes as

$$\forall i \in \mathcal{I} \left\{ \begin{array}{ll} \min_{\Xi_i} & \sum_{j \in \mathcal{J}_i} (\mathbf{b}_{ij}^\top \boldsymbol{\mu}_{ij} + e_{ij} \nu_{ij}) + \sum_{t \in \mathcal{T}} \frac{1}{2} \kappa_{it}^Q + \boldsymbol{\gamma}_i^\top \mathbf{h}_i \\ \text{s.t.} & (\text{B.10c}) - (\text{B.10e}) \\ & \left\| \boldsymbol{\mu}_{it}^Q \right\|_2^2 \leq \kappa_{it}^Q \nu_{it}^Q, \quad \forall t \\ & \left\| \boldsymbol{\mu}_{ij} \right\|_2 \leq \nu_{ij}, \quad \forall j \in \mathcal{J}_i \\ & \kappa_{it}^Q \geq 0, \quad \nu_{it}^Q \geq 0, \end{array} \right. \quad (\text{B.12})$$

Using Lemmas 1 and 2 provided in the Proof of Theorem 1, existence of strictly feasible primal-dual solutions to the participant's profit maximization problem (6) and its dual (B.12) is established (omitted from presentation, for the sake of brevity). Consequently, from Theorem 1, strong duality holds for this primal-dual pair, thereby enforcing the primal problem (6) and its dual (B.12) to attain identical objective function values at the optimal solution. Condition (B.11) is equivalent to the non-negativity of the dual objective in (B.12) at the optimal solution, which we now analyze in the following.

Observe that, the second term of the objective function of the dual problem (B.12) is non-negative from the primal feasibility condition $\kappa_{it} \geq 0$, $\forall i$. The first term, enclosed in parenthesis, is non-negative if $e_{ij} \geq \|\mathbf{b}_{ij}\|_2$, $\forall j \in \mathcal{J}_i$. This stems from the Cauchy-Schwarz Inequality, i.e., we have

$$|\mathbf{b}_{ij}^\top \boldsymbol{\mu}_{ij}| \leq \|\mathbf{b}_{ij}\|_2 \|\boldsymbol{\mu}_{ij}\|_2 \leq \|\mathbf{b}_{ij}\|_2 \nu_{ij}, \quad \forall j \in \mathcal{J}_i,$$

where the last inequality is due to the primal feasibility condition $\|\boldsymbol{\mu}_{ij}\|_2 \leq \nu_{ij}$, $\forall j \in \mathcal{J}_i$. With the condition $e_{ij} \geq \|\mathbf{b}_{ij}\|_2$, $\forall j \in \mathcal{J}_i$, we have $|\mathbf{b}_{ij}^\top \boldsymbol{\mu}_{ij}| \leq e_{ij} \nu_{ij}$, $\forall j \in \mathcal{J}_i$. Under the condition $e_{ij} \geq \|\mathbf{b}_{ij}\|_2$, $e_{ij} \nu_{ij} \geq 0$ $\forall j \in \mathcal{J}_i$; therefore, the first term in the objective is bounded below by 0. The variable $\boldsymbol{\gamma}_i$ is free, therefore the third term in the objective is guaranteed to be non-negative if $\mathbf{h}_i = \mathbf{0}$. This completes the proof of cost recovery for the market participants $i \in \mathcal{I}$ under the conditions: (i) $e_{ij} \geq \|\mathbf{b}_{ij}\|_2$, $\forall j \in \mathcal{J}_i$, $\forall i$ and (ii) $\mathbf{h}_i = \mathbf{0}$, $\forall i$.

(iii) **Revenue adequacy:** Mathematically, the market operator is revenue adequate if

$$\underbrace{\sum_{p \in \mathcal{P}} \sum_{i \in \mathcal{I}} \text{tr}(\boldsymbol{\Pi}_p^* \top \mathbf{W}_{ip}^*)}_{\text{Term A}} - \underbrace{\sum_{t \in \mathcal{T}} \boldsymbol{\omega}_t^* \top \mathbf{y}_t^*}_{\text{Term B}} \geq 0, \quad (\text{B.13})$$

where Term A refers to the net payments received from the $i \in \mathcal{I}$ market participants for the $p \in \mathcal{P}$ commodities and Term B refers to the payments made to the network operator towards transmission service. To reduce notational complexity, we drop the superscript $*$ denoting optimal values in the proof that follows, yet they are always implied. Using (B.6), we expand Term A and rearrange the summation operators to reflect the dependence of variables

$$\begin{aligned} \sum_{p \in \mathcal{P}} \sum_{i \in \mathcal{I}} \text{tr}(\boldsymbol{\Pi}_p \top \mathbf{W}_{ip}) &= \sum_{p \in \mathcal{P}} \sum_{i \in \mathcal{I}} \sum_{t \in \mathcal{T}} \left((\mathbb{1}[\boldsymbol{\lambda}_p]_t - \boldsymbol{\Psi}^\top(\bar{\boldsymbol{\varrho}}_t - \underline{\boldsymbol{\varrho}}_t))^\top [\mathbf{W}_{ip}]_{(:,t)} \right) \\ &= \sum_{p \in \mathcal{P}} \sum_{i \in \mathcal{I}} \sum_{t \in \mathcal{T}} ([\boldsymbol{\lambda}_p]_t \mathbb{1}^\top [\mathbf{W}_{ip}]_{(:,t)}) - \sum_{t \in \mathcal{T}} \left((\boldsymbol{\Psi}^\top(\bar{\boldsymbol{\varrho}}_t - \underline{\boldsymbol{\varrho}}_t))^\top \sum_{p \in \mathcal{P}} \sum_{i \in \mathcal{I}} [\mathbf{W}_{ip}]_{(:,t)} \right). \end{aligned} \quad (\text{B.14})$$

Gathering the equalities (6e) representing the transaction quantities with the injections (or withdrawals) for the I participants, we have $\mathbf{W}_{ip}^\top \mathbb{1} = \mathbf{G}_{ip} \mathbf{q}_{ip}$, $\forall i$. Since this equality holds individually for each participant, we can add them for all participants to get $\sum_{i \in \mathcal{I}} \mathbb{1}^\top \mathbf{W}_{ip} = \sum_{i \in \mathcal{I}} (\mathbf{G}_{ip} \mathbf{q}_{ip})^\top$, such that

$$\sum_{i \in \mathcal{I}} \mathbb{1}^\top [\mathbf{W}_{ip}]_{(:,t)} = \sum_{i \in \mathcal{I}} [\mathbf{G}_{ip} \mathbf{q}_{ip}]_t = 0, \quad \forall t, \quad (\text{B.15})$$

where the second equality results from the market-clearing condition (8b) that holds at optimality. Hence, the first term in (B.14) vanishes. The second term in (B.14) is non-zero only if there is a congestion in the grid, i.e., any $\bar{\boldsymbol{\varrho}}_t \neq 0$ or $\underline{\boldsymbol{\varrho}}_t \neq 0$. Next, we expand Term B in (B.13), using the stationarity condition (B.8a) and the market-clearing condition (8a), as

$$-\sum_{t \in \mathcal{T}} \boldsymbol{\omega}_t^\top \mathbf{y}_t = \sum_{t \in \mathcal{T}} \left(\boldsymbol{\Psi}^\top(\bar{\boldsymbol{\varrho}}_t - \underline{\boldsymbol{\varrho}}_t) \right)^\top \sum_{p \in \mathcal{P}} [\mathbf{Q}_p^{\text{inj}}]_{(:,t)} \quad (\text{B.16})$$

which is non-zero only if there is congestion in the network, i.e., the network operator earns congestion rent. We remove the summation over the hours by using the expression for the conic spatial prices given by Theorem 2 and the auxiliary variables defined therein, to rewrite Term B of (B.13) as

$$\begin{aligned} -\sum_{t \in \mathcal{T}} \boldsymbol{\omega}_t^\top \mathbf{y}_t &= \sum_{t \in \mathcal{T}} \left(\boldsymbol{\Psi}^\top(\bar{\boldsymbol{\varrho}}_t - \underline{\boldsymbol{\varrho}}_t) \right)^\top \sum_{p \in \mathcal{P}} [\mathbf{Q}_p^{\text{inj}}]_{(:,t)} \\ &= \sum_{p \in \mathcal{P}} \text{tr} \left((\boldsymbol{\Psi}^\top(\bar{\boldsymbol{\varrho}} - \bar{\boldsymbol{\varrho}}))^\top \mathbf{Q}_p^{\text{inj}} \right) = \sum_{p \in \mathcal{P}} \text{tr} \left((\boldsymbol{\Lambda}_p - \boldsymbol{\Pi}_p)^\top \mathbf{Q}_p^{\text{inj}} \right). \end{aligned} \quad (\text{B.17})$$

Similarly, using (B.15), we rewrite Term A of (B.13) after rearrangement as

$$\begin{aligned} \sum_{p \in \mathcal{P}} \sum_{i \in \mathcal{I}} \text{tr}(\boldsymbol{\Pi}_p \top \mathbf{W}_{ip}) &= -\sum_{t \in \mathcal{T}} \left((\boldsymbol{\Psi}^\top(\bar{\boldsymbol{\varrho}}_t - \underline{\boldsymbol{\varrho}}_t))^\top \sum_{p \in \mathcal{P}} \sum_{i \in \mathcal{I}} [\mathbf{W}_{ip}]_{(:,t)} \right) \\ &= -\sum_{p \in \mathcal{P}} \text{tr} \left((\boldsymbol{\Lambda}_p - \boldsymbol{\Pi}_p)^\top \left(\sum_{i \in \mathcal{I}} \mathbf{W}_{ip} \right) \right). \end{aligned} \quad (\text{B.18})$$

Observe that $\sum_{i \in \mathcal{I}} \mathbf{W}_{ip}$ sums the transaction quantities over the nodes and periods for all participants for a given commodity p , which is indeed equal to the commodity-specific net nodal injections given by (9), i.e., $\mathbf{Q}_p^{\text{inj}} = \sum_{i \in \mathcal{I}} \mathbf{W}_{ip}$, $\forall p$. Therefore, the terms in (B.17) and (B.18) cancel each other out, thereby satisfying the revenue adequacy condition for the market operator at the optimal solution. As a result, we have shown that there exists a budget balance for the market operator under the proposed conic market framework, i.e., the market-operator does not accrue any surplus revenue.

References

- Alamo, T., Tempo, R., Luque, A., Ramirez, D.R., 2015. Randomized methods for design of uncertain systems: Sample complexity and sequential algorithms. *Automatica* 52, 160–172.
- Alizadeh, F., Goldfarb, D., 2003. Second-order cone programming. *Mathematical Programming* 95, 3–51.
- Anjos, M.F., Gómez, J.A., 2017. Operations Research Approaches for Building Demand Response in a Smart Grid. *INFORMS TutORials in Operations Research*. chapter 7. pp. 131–152.
- Ben-Tal, A., Nemirovski, A., 2001. *Lectures on Modern Convex Optimization*. Society for Industrial and Applied Mathematics, Philadelphia. chapter 1.
- Bertsimas, D., Litvinov, E., Sun, X.A., Zhao, J., Zheng, T., 2013. Adaptive robust optimization for the security constrained unit commitment problem. *IEEE Transactions on Power Systems* 28, 52–63.
- Bohn, R.E., Caramanis, M.C., Schweppe, F.C., 1984. Optimal pricing in electrical networks over space and time. *The RAND Journal of Economics* 15, 360–376.
- Boyd, S., Vandenberghe, L., 2004. *Convex Optimization*. Cambridge University Press.
- Bushnell, J., 2021. To fix the power market, first fix the natural gas market. Energy Institute Blog, UC Berkeley. Last accessed: 30 June 2021. <https://energyathaas.wordpress.com/2021/03/01/to-fix-the-power-market-first-fix-the-natural-gas-market/>.
- Cai, X., McKinney, D.C., Lasdon, L.S., Watkins, D.W., 2001. Solving large nonconvex water resources management models using generalized benders decomposition. *Operations Research* 49, 235–245.
- Cain, M.B., O'Neill, R.P., Castillo, A., 2012. History of Optimal Power Flows and Formulations. Federal Energy Regulatory Commission (FERC).
- Chu, S., Majumdar, A., 2012. Opportunities and challenges for a sustainable energy future. *Nature* 488, 294–303.
- Conejo, A.J., Carrión, M., Morales, J.M., 2010. Decision making under uncertainty in electricity markets. Springer US, New York. volume 153. chapter App. B.
- Courcoubetis, C., Weber, R., 2003. Pricing Communication Networks. John Wiley & Sons, Ltd, West Sussex, England. chapter 9. pp. 219–233.
- Daqing, L., Yinan, J., Rui, K., Havlin, S., 2014. Spatial correlation analysis of cascading failures: Congestions and blackouts. *Scientific Reports* 4, 5381.
- De Wolf, D., Smeers, Y., 2000. The gas transmission problem solved by an extension of the simplex algorithm. *Management Science* 46, 1454–1465.
- Delage, E., Ye, Y., 2010. Distributionally robust optimization under moment uncertainty with application to data-driven problems. *Operations Research* 58, 595–612.
- Dvorkin, Y., 2020. A chance-constrained stochastic electricity market. *IEEE Transactions on Power Systems* 35, 2993–3003.
- Enke, S., 1951. Equilibrium among spatially separated markets: Solution by electric analogue. *Econometrica* 19, 40–47.
- Fortuny-Amat, J., McCarl, B., 1981. A representation and economic interpretation of a two-level programming problem. *The Journal of the Operational Research Society* 32, 783–792.
- IRENA, 2015. Renewable energy target setting. Last accessed: 30 June 2021. <https://www.irena.org/publications/2015/Jun/Renewable-Energy-Target-Setting>.
- Kantorovich, L.V., 1960. Mathematical methods of organizing and planning production. *Management Science* 6, 366–422.
- Kim, J.H., Powell, W.B., 2011. Optimal energy commitments with storage and intermittent supply. *Operations Research* 59, 1347–1360.
- Kirschen, D., Strbac, G., 2018. *Fundamentals of Power System Economics*, 2nd Edition. John Wiley & Sons, Ltd, US. chapter 3. pp. 51–88.
- Kocuk, B., Dey, S.S., Sun, X.A., 2016. Strong SOCP relaxations for the optimal power flow problem. *Operations Research* 64, 1177–1196.
- Kuang, X., Dvorkin, Y., Lamadrid, A.J., Ortega-Vazquez, M.A., Zuluaga, L.F., 2018. Pricing chance constraints in electricity markets. *IEEE Transactions on Power Systems* 33, 4634–4636.

- Lavaei, J., Low, S.H., 2012. Zero duality gap in optimal power flow problem. *IEEE Transactions on Power Systems* 27, 92–107.
- Lobo, M.S., Vandenberghe, L., Boyd, S., Lebret, H., 1998. Applications of second-order cone programming. *Linear Algebra and its Applications* 284, 193 – 228.
- Mieth, R., Kim, J., Dvorkin, Y., 2020. Risk- and variance-aware electricity pricing. *Electric Power Systems Research* 189, 106804.
- Mitridati, L., Kazempour, J., Pinson, P., 2020. Heat and electricity market coordination: A scalable complementarity approach. *European Journal of Operational Research* 283, 1107–1123.
- Mosek ApS, 2021. MOSEK Modeling Cookbook 3.2.3. Last accessed: 30 June 2021. <https://docs.mosek.com/modeling-cookbook/index.html>.
- Nemirovski, A., Shapiro, A., 2007. Convex approximations of chance constrained programs. *SIAM Journal on Optimization* 17, 969–996.
- Nord Pool, 2021. Nord Pool Day-ahead Trading. Last accessed: 30 June 2021. <https://www.nordpoolgroup.com/trading/Day-ahead-trading/>.
- Papavasiliou, A., 2018. Analysis of distribution locational marginal prices. *IEEE Transactions on Smart Grid* 9, 4872–4882.
- Parag, Y., Sovacool, B.K., 2016. Electricity market design for the prosumer era. *Nature Energy* 1, 16032.
- PJM Interconnection, 2014. Analysis of operational events and market impacts during the January 2014 cold weather events.
- Pritchard, G., Zakeri, G., Philpott, A., 2010. A single-settlement, energy-only electric power market for unpredictable and intermittent participants. *Operations Research* 58, 1210–1219.
- Raissi, M., 2016. Conic Economics. Ph.D. thesis. University of Maryland, College Park. Last accessed: 30 June 2021 <https://search.proquest.com/docview/1861702044>.
- Roberts, D.J., Postlewaite, A., 1976. The incentives for price-taking behavior in large exchange economies. *Econometrica* 44, 115–127.
- Rosen, J.B., 1965. Existence and uniqueness of equilibrium points for concave n-person games. *Econometrica* 33, 520–534.
- Samuelson, P.A., 1952. Spatial price equilibrium and linear programming. *The American Economic Review* 42, 283–303.
- Schweppé, F.C., Caramanis, M.C., Tabors, R.D., Bohn, R.E., 1988. Spot Pricing of Electricity. Springer US, Boston, MA. chapter 1.
- Snyder, L.V., Scaparra, M.P., Daskin, M.S., Church, R.L., 2014. Planning for Disruptions in Supply Chain Networks. INFORMS TutORials in Operations Research. chapter 9. pp. 234–257.
- The Danish Government's Climate Partnership, 2020. Powering Denmark's Green Transition. Last accessed: 30 June 2021. <https://www.danskenergi.dk/the-climate-partnership-the-energy-and-utilities-sector>.
- Thompson, M., 2013. Optimal economic dispatch and risk management of thermal power plants in deregulated markets. *Operations Research* 61, 791–809.
- Vickrey, W., 1961. Counterspeculation, auctions, and competitive sealed tenders. *The Journal of Finance* 16, 8–37.
- Wagner, M.R., 2008. Stochastic 0–1 linear programming under limited distributional information. *Operations Research Letters* 36, 150 – 156.
- Zavala, V.M., Kim, K., Anitescu, M., Birge, J., 2017. A stochastic electricity market clearing formulation with consistent pricing properties. *Operations Research* 65, 557–576.

Moving from Linear to Conic Markets for Electricity

Anubhav Ratha, Pierre Pinson, Hélène Le Cadre, Ana Virag, Jalal Kazempour

This document serves as an electronic companion (EC) for the paper “Moving from Linear to Conic Markets for Electricity”. In §EC.1, we provide modeling examples that illustrate how second order cone (SOC) constraints enable future electricity markets to be uncertainty-, asset- and network-aware. In §EC.2, we present the market-clearing problems of the proposed SOCP-based uncertainty-aware electricity market as well as the linear programming (LP) based market-clearing benchmarks. Numbered sections and equations throughout the electronic companion correspond to those in the paper, while a prefix ‘EC.’ denotes these elements within this document.

EC.1. Modeling Examples

This section demonstrates the versatility of SOC constraints in modeling the various asset- and network-related nonlinearities faced by electricity markets. While Example EC.1 covers the general case of including participants with quadratic costs in electricity markets, Example EC.2 discusses the modeling of nonlinearities in the context of coordination between electricity and natural gas system for harnessing flexibility. Lastly, Example EC.3 demonstrates the network-awareness of the market framework proposed in the paper by showing how it can be extended to include the SOCP relaxation of nonlinear and non-convex power flow equations.

EXAMPLE EC.1 (QUADRATIC COST). Consider participant i having a quadratic cost (utility) of production (consumption), such that the cost function at each hour t is given by $c_{it}(\mathbf{q}_{it}) = \mathbf{q}_{it}^\top \text{diag}(\mathbf{c}_{it}^Q) \mathbf{q}_{it} + \mathbf{c}_{it}^{L\top} \mathbf{q}_{it}$, where $\mathbf{c}_{it}^Q \in \mathbb{R}^{K_i}$ and $\mathbf{c}_{it}^L \in \mathbb{R}^{K_i}$ denote the quadratic and linear cost coefficients, respectively. Let $\mathbf{C}_{it}^Q \in \mathbb{R}^{K_i \times K_i}$ be defined as a factorization of the quadratic cost matrix such that $\text{diag}(\mathbf{c}_{it}^Q) = \mathbf{C}_{it}^{Q\top} \mathbf{C}_{it}^Q$. The existence of such a factorization is given since $\text{diag}(\mathbf{c}_{it}^Q) \succcurlyeq 0$, $\forall t, \forall i \in \mathcal{I}$. The quadratic objective function of the participant i is equivalently written as

$$\min_{\mathbf{q}_{it}, z_{it}} \sum_{t \in \mathcal{T}} (z_{it} + \mathbf{c}_{it}^{L\top} \mathbf{q}_{it}) \quad (\text{EC.1a})$$

$$\text{s.t. } \|\mathbf{C}_{it}^Q \mathbf{q}_{it}\|_2^2 \leq z_{it}, \forall t, \quad (\text{EC.1b})$$

where $z_{it} \in \mathbb{R}_+$ is an auxiliary variable, resulting in the linear objective function (EC.1a). The rotated SOC constraint (EC.1b) is a special form of the general SOC constraint (1), see Mosek ApS (2021). We illustrate this for single-period market-clearing, i.e., $T = 1$, assuming that participant

i has $K_i = 2$ decisions variables, such that $\mathbf{q}_{i1} \in \mathbb{R}^2$. Extending the decision vector of participant i to $\mathbf{q}_i = [\mathbf{q}_{i1}^\top \ z_{i1}]^\top \in \mathbb{R}^3$, we have the parameters $\mathbf{A}_i = [\mathbf{C}_{it}^Q \ \mathbf{0}_2]$, $\mathbf{d}_i = [0 \ 0 \ 1]^\top$, while $\mathbf{b}_i = \mathbf{0}_2$ and $e_i = 0$, resulting in a three-dimensional rotated SOC constraint, i.e., $m_i = 2$.

EXAMPLE EC.2 (NATURAL GAS NETWORK). The interdependence between electricity and natural gas systems primarily arises due to the significant role played by gas-fired power plants in providing flexibility to the electricity system facing uncertainty. Congestion in the gas network during the real-time operation of the electricity system jeopardizes the fuel-availability for gas-fired power plants and therefore, adversely impacting the flexibility provision (Byeon and Van Hentenryck 2020). One of the crucial operational constraints of the gas system is the relation between gas flows and nodal pressures in the network. The steady-state flow of gas in the pipelines is represented by a non-convex quadratic equality constraint that relates the squared flow magnitude with the difference in squared pressures at the terminal nodes. A convex relaxation of this non-convex equality takes the form of SOC constraints, as illustrated in the following.

Let $\varphi \in \mathbb{R}_+$ denote the flow of gas along a gas pipeline connecting two terminal nodes, the sending node s and the receiving node r , each with nodal pressures denoted by $\pi_s \in \mathbb{R}_+$ and $\pi_r \in \mathbb{R}_+$, respectively. As proposed by Borraz-Sánchez et al. (2016), the convex relaxation for the non-convex equality between the flow along a pipeline and the pressures at the terminal nodes is expressed as

$$\varphi^2 \leq \beta^2 (\pi_s^2 - \pi_r^2), \quad (\text{EC.2})$$

where $\beta \in \mathbb{R}_+$ is a constant which encodes the friction coefficient and geometry of pipelines. Ignoring all other pipelines and considering the gas network operator as an electricity market participant, we can denote its decision vector as $\mathbf{q}_{\text{GN}} = [\varphi \ \pi_r \ \pi_s]^\top$ and can represent the constraint (EC.2) as a SOC constraint of the form (1) with parameters

$$\mathbf{A} = \begin{bmatrix} \frac{1}{\beta} & 0 & 0 \\ 0 & 1 & 0 \end{bmatrix}, \quad \mathbf{b} = \mathbf{0}_2, \quad \mathbf{d} = [0 \ 0 \ 1]^\top \text{ and } e = 0,$$

which is a three-dimensional SOC constraint, i.e., $m_i = 2$. Similar SOC constraints are included for other pipelines in the gas network and over various hours, therefore enabling the consideration of gas network operational constraints within the electricity market-clearing problem.

EXAMPLE EC.3 (ELECTRICITY NETWORK). Known as the branch flow model (Farivar and Low 2013), the SOCP relaxation of power flow equations is exact for the distribution networks that exhibit a radial graph structure under mild conditions. The power flow equations model the non-linear relation of active and reactive power transported along a line with the current and terminal node voltages. While active power is the actual quantity in MWh of power produced or consumed,

reactive power is a necessary component oscillating within the network and regulates voltage across the nodes. Consider a power line $\ell = (n, n') \in \mathcal{L}$ connecting adjacent nodes $n, n' \in \mathcal{N}$. Let $s_\ell^a \in \mathbb{R}$ and $s_\ell^r \in \mathbb{R}$ denote the active power and reactive power; $\theta_\ell \in \mathbb{R}_+$ and $v_n \in \mathbb{R}_+$ denote the squared magnitude of current flow in the line ℓ and the squared voltage magnitude at the node n , respectively. The SOC relaxation for the power flow equations $\forall \ell = (n, n') \in \mathcal{L}$ is

$$s_\ell^{a2} + s_\ell^{r2} \leq \theta_\ell v_n \quad (\text{EC.3a})$$

$$s_\ell^{a2} + s_\ell^{r2} \leq \bar{s}_\ell^2, \quad (\text{EC.3b})$$

where $\bar{s}_\ell \in \mathbb{R}_+$ is a parameter denoting the rated power transfer capacity of line ℓ . Constraints (EC.3) can be reformulated as SOC constraints admitting the variables $[s_\ell^a \ s_\ell^r \ \theta_\ell \ v_n]^\top$. For instance, (EC.3a) is equivalent to a SOC constraint of the general form (1) with the parameters

$$\mathbf{A} = \begin{bmatrix} 2 & 0 & 0 & 0 \\ 0 & 2 & 0 & 0 \\ 0 & 0 & 1 & -1 \end{bmatrix}, \quad \mathbf{b} = \mathbf{0}_3, \quad \mathbf{d} = [0 \ 0 \ 1 \ 1]^\top \text{ and } e = 0,$$

which is a four-dimensional SOC constraint. Similarly, (EC.3b) is a three-dimensional SOC constraint with a structure similar that in Example EC.2.

EC.2. Market-clearing Problems

For the uncertainty-aware conic market framework proposed in the paper, we first outline the participant models in §EC.2.1, followed by the chance-constrained market-clearing problem and its reformulation as the SOCP problem \mathcal{M}^{cc} in §EC.2.2. In §EC.2.3 we provide formulations for the two LP-based uncertainty-aware benchmark market-clearing problems, $\mathcal{R}1$ and $\mathcal{R}2$. Finally, §EC.2.4 formulates the real-time market-clearing problem entailed in the out-of-sample simulation studies discussed in §4.

EC.2.1. Modeling of Market Participants

To enhance the clarity of exposition, we define subsets of market participants \mathcal{I} comprised of flexible power producers $\mathcal{F} \subseteq \mathcal{I}$, energy storage owners $\mathcal{S} \subseteq \mathcal{I}$ and inflexible consumers $\mathcal{D} \subseteq \mathcal{I}$. Let the uncertainty faced by the market-clearing problem arise from a set of weather-dependent renewable power producers $\mathcal{W} \subseteq \mathcal{I}$, such that $\mathcal{F} \cup \mathcal{S} \cup \mathcal{D} \cup \mathcal{W} = \mathcal{I}$ and $\mathcal{F} \cap \mathcal{S} \cap \mathcal{D} \cap \mathcal{W} = \emptyset$. We consider consumers to be inflexible. However, the methodology adopted in this paper is extendable to include demand-side flexibility providers.

Weather-dependent power producers: At the day-ahead stage, the stochastic power production $\tilde{q}_{it} \in \mathbb{R}$ from weather-dependent power producers $i \in \mathcal{W} = \{1, 2, \dots, W\}$ are modeled as

$$\tilde{q}_{it}(\xi_t) = \hat{q}_{it} - \xi_{it}, \quad \forall i \in \mathcal{W}, \forall t, \quad (\text{EC.4})$$

where $\hat{q}_{it} \in \mathbb{R}$ is the nominal production, usually in the form of the best-available day-ahead forecast, while the random variable $\xi_{it} \in \mathbb{R}$ is the forecast error encountered by producer i at hour t . The stochastic power production \tilde{q}_{it} has an upper bound given by the rated power production capacity \bar{Q}_i , while being bounded below by $\underline{Q}_i = 0$. The vector $\boldsymbol{\xi} = [\xi_{11} \quad \xi_{21} \quad \dots \quad \xi_{Wt} \quad \dots \quad \xi_{WT}]^\top \in \mathbb{R}^{WT}$ denotes the overall uncertainty faced by the market-clearing problem, formed by extending $\boldsymbol{\xi}_t \in \mathbb{R}^W$, as defined in Example 1, to a multi-period setting. We assume that $\boldsymbol{\xi}$ follows an unknown multivariate probability distribution \mathbb{P}_ξ , characterized by mean $\boldsymbol{\mu} \in \mathbb{R}^{WT}$ and covariance $\boldsymbol{\Sigma} \in \mathbb{R}^{WT \times WT}$, which are estimated by the system operator having an access to a finite number of historical measurement samples. Without much loss of generality, we assume the distribution \mathbb{P}_ξ to have a mean $\boldsymbol{\mu} = \mathbf{0}$, as any non-zero elements of the sample mean are used to update the forecast \hat{q}_{it} in (EC.4). The structure of $\boldsymbol{\Sigma}$ is such that its diagonal blocks, comprised of sub-matrices, $\boldsymbol{\Sigma}_t \in \mathbb{R}^{W \times W}$, $\forall t$, capture the spatial correlation among the forecast errors at hour t , while the off-diagonal blocks contain information about spatio-temporal correlation of uncertainty. The net deviation from the day-ahead forecasts realized during real-time operation at hour t is thus given by $\mathbf{1}^\top \boldsymbol{\xi}_t \in \mathbb{R}$. As a sign convention, $\mathbf{1}^\top \boldsymbol{\xi}_t > 0$ implies a deficit of production from renewable energy sources during real-time operation stage as compared to the day-ahead forecast. Weather-dependent power producers are associated with a decision vector $\mathbf{q}_{it} = [\hat{q}_{it} \quad \xi_{it}]^\top$, $\forall t, \forall i \in \mathcal{W}$ such that participation in the two commodities traded in the market is determined as follows. For the commodity energy, i.e., $p = 1$, the contribution is given by

$$\mathbf{q}_{ip} = [\hat{q}_{i1} \quad \hat{q}_{i2} \quad \dots \quad \hat{q}_{i(T-1)} \quad \hat{q}_{iT}]^\top, \quad \mathbf{G}_{ip} = \text{diag}(\mathbf{1}), \quad \forall i \in \mathcal{W},$$

where $\mathbf{1} \in \mathbb{R}^T$. For $p = 2$, i.e., flexibility, the weather-dependent power producers are modeled as the uncertainty sources

$$\mathbf{q}_{ip} = \mathbf{1}, \quad \mathbf{G}_{ip} = - \begin{bmatrix} \mathbf{1}^\top \boldsymbol{\xi}_1 & \dots & 0 \\ \vdots & \ddots & \vdots \\ 0 & \dots & \mathbf{1}^\top \boldsymbol{\xi}_T \end{bmatrix}, \quad \forall i \in \mathcal{W},$$

where $\mathbf{1} \in \mathbb{R}^T$ and the negative sign arises from the convention adopted in (EC.4).

Flexible power producers: For each flexible power producer $i \in \mathcal{F}$, we model the stochastic power production during real-time operation at hour t as

$$\tilde{q}_{it}(\boldsymbol{\xi}_t) = \hat{q}_{it} + h_{it}(\boldsymbol{\xi}_t), \quad \forall i \in \mathcal{F}, \quad \forall t, \tag{EC.5}$$

where \hat{q}_{it} denotes the nominal production and the function $h_{it}(\boldsymbol{\xi}_t) : \mathbb{R}^W \mapsto \mathbb{R}$ is the adjustment policy allocated to the market participant i , encoding its share in the recourse actions needed to mitigate the net deviation in the electricity system arising from forecast errors realized at hour t .

Typically, these adjustment policies $h_{it}(\boldsymbol{\xi}_t)$ represent convex decision rules, which may be linear (Georghiou et al. 2019) or generalized (Georghiou et al. 2015). In this work, we adopt adjustment policies affinely dependent on the total uncertainty faced by the system operator, such that

$$h_{it}(\boldsymbol{\xi}_t) = \mathbb{1}^\top \boldsymbol{\xi}_t \alpha_{it}, \quad \forall i \in \mathcal{F}, \forall t,$$

where α_{it} is the adjustment policy allocated to participant i at hour t . The nominal production quantity \hat{q}_{it} and the policy α_{it} are optimally decided by the day-ahead market-clearing program. Recalling Example 1, we write chance constraints limiting the production from participants to their upper limit \bar{Q}_i as

$$\mathbb{P}_\xi \left(\hat{q}_{it} + \mathbb{1}^\top \boldsymbol{\xi}_t \alpha_{it} \leq \bar{Q}_i \right) \geq (1 - \hat{\varepsilon}), \quad \forall t, \forall i \in \mathcal{F}, \quad (\text{EC.6a})$$

which is reformulated as a $W + 1$ -dimensional SOC constraint

$$r_{\hat{\varepsilon}} \|\mathbf{X}_t \mathbb{1} \alpha_{it}\|_2 \leq \bar{Q}_i - \hat{q}_{it}, \quad \forall t, \forall i \in \mathcal{F}, \quad (\text{EC.6b})$$

where $\mathbf{X}_t \in \mathbb{R}^{W \times W}$ is obtained by Cholesky decomposition of the submatrix $\boldsymbol{\Sigma}_t$ of the covariance matrix $\boldsymbol{\Sigma}$ such that $\boldsymbol{\Sigma}_t = \mathbf{X}_t \mathbf{X}_t^\top$. Recall that the parameter $r_{\hat{\varepsilon}}$ is a safety parameter, related to constraint violations, chosen by the system operator based on the knowledge of distribution \mathbb{P}_ξ , such that $r_{\hat{\varepsilon}}$ increases as $\hat{\varepsilon}$ decreases. Similar reformulation is obtained for the lower bounds on the production, \underline{Q}_i . Apart from the production bounds, a flexible power producer may have capacity bounds on the flexibility provision, denoted by $\underline{Q}_i^R, \bar{Q}_i^R$, which are reformulated in a similar manner. Lastly, inter-temporal constraints such as the limits on the downward and upward ramping rates $\underline{\Delta}_i, \bar{\Delta}_i \in \mathbb{R}$ are modeled as

$$\mathbb{P}_\xi \left((\hat{q}_{it} + \mathbb{1}^\top \boldsymbol{\xi}_t \alpha_{it}) - (\hat{q}_{i(t-1)} + \mathbb{1}^\top \boldsymbol{\xi}_{t-1} \alpha_{i(t-1)}) \geq -\underline{\Delta}_i \right) \geq (1 - \hat{\varepsilon}), \quad \forall t > 2, \forall i \in \mathcal{F} \quad (\text{EC.7a})$$

$$\mathbb{P}_\xi \left((\hat{q}_{it} + \mathbb{1}^\top \boldsymbol{\xi}_t \alpha_{it}) - (\hat{q}_{i(t-1)} + \mathbb{1}^\top \boldsymbol{\xi}_{t-1} \alpha_{i(t-1)}) \leq \bar{\Delta}_i \right) \geq (1 - \hat{\varepsilon}), \quad \forall t > 2, \forall i \in \mathcal{F} \quad (\text{EC.7b})$$

and reformulated as $2W + 1$ -dimensional SOC constraints of the form

$$r_{\hat{\varepsilon}} \left\| \mathbf{X}_{t-1:t} \begin{bmatrix} \mathbb{1}^\top \alpha_{i(t-1)} & -\mathbb{1}^\top \alpha_{it} \end{bmatrix}^\top \right\|_2 \leq \underline{\Delta}_i - (\hat{q}_{it-1} - \hat{q}_{it}), \quad \forall t > 2, \forall i \in \mathcal{F} \quad (\text{EC.7c})$$

$$r_{\hat{\varepsilon}} \left\| \mathbf{X}_{t-1:t} \begin{bmatrix} -\mathbb{1}^\top \alpha_{i(t-1)} & \mathbb{1}^\top \alpha_{it} \end{bmatrix}^\top \right\|_2 \leq \bar{\Delta}_i + (\hat{q}_{it-1} - \hat{q}_{it}), \quad \forall t > 2, \forall i \in \mathcal{F}, \quad (\text{EC.7d})$$

where $\mathbf{X}_{t-1:t} \in \mathbb{R}^{2W \times 2W}$ denotes the factorization of the blocks of covariance matrix $\boldsymbol{\Sigma}$ corresponding to the spatio-temporal covariance of forecast errors in two consecutive hours. Flexible power producers participate in the conic market with decision vectors $\mathbf{q}_{it} = [\hat{q}_{it} \quad \alpha_{it}]^\top, \forall t, \forall i \in \mathcal{F}$. Towards the commodity energy, i.e., $p = 1$, flexible generators contribute as

$$\mathbf{q}_{ip} = [\hat{q}_{i1} \quad \hat{q}_{i2} \dots \hat{q}_{i(T-1)} \quad \hat{q}_{iT}]^\top, \quad \mathbf{G}_{ip} = \text{diag}(\mathbb{1}), \quad \forall i \in \mathcal{F},$$

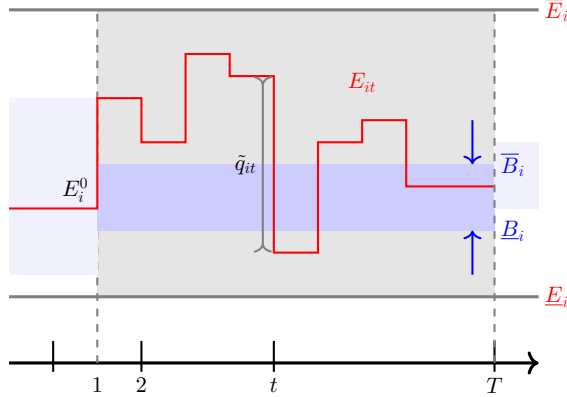


Figure EC.1 Illustration of the operation of an energy storage unit for flexibility provision.

with $\mathbb{1} \in \mathbb{R}^T$. For the commodity flexibility ($p = 2$), the contribution is given by

$$\mathbf{q}_{ip} = [\alpha_{i1} \quad \alpha_{i2} \dots \alpha_{i(T-1)} \quad \alpha_{iT}]^\top, \quad \mathbf{G}_{ip} = \begin{bmatrix} \mathbb{1}^\top \boldsymbol{\xi}_1 & \dots & 0 \\ \vdots & \ddots & \vdots \\ 0 & \dots & \mathbb{1}^\top \boldsymbol{\xi}_T \end{bmatrix}, \quad \forall i \in \mathcal{F}.$$

Energy storage operators: For each energy storage unit $s \in \mathcal{S}$, the power produced or consumed during real-time operation at hour t is given by

$$\tilde{q}_{it}(\boldsymbol{\xi}_t) = \hat{q}_{it} + \mathbb{1}^\top \boldsymbol{\xi}_t \gamma_{it}, \quad \forall i \in \mathcal{S}, \quad \forall t, \quad (\text{EC.8})$$

where \hat{q}_{it} is the nominal production/consumption and γ_{it} is the affine adjustment policy allocated. We adopt the sign convention $\tilde{q}_{it}(\boldsymbol{\xi}_t) > 0$ for hours when the storage is discharging (production), while $\tilde{q}_{it}(\boldsymbol{\xi}_t) < 0$ indicates charging (consumption). In practice, energy storage units are limited by their charging and discharging capacities which are modeled using chance constraints as

$$\mathbb{P}_\xi \left(\hat{q}_{it} + \mathbb{1}^\top \boldsymbol{\xi}_t \gamma_{it} \leq \eta_i^D \bar{Q}_i^D \right) \geq (1 - \hat{\varepsilon}), \quad \forall t, \quad \forall i \in \mathcal{S} \quad (\text{EC.9a})$$

$$\mathbb{P}_\xi \left(\hat{q}_{it} + \mathbb{1}^\top \boldsymbol{\xi}_t \gamma_{it} \geq -\frac{1}{\eta_i^C} \bar{Q}_i^C \right) \geq (1 - \hat{\varepsilon}), \quad \forall t, \quad \forall i \in \mathcal{S} \quad (\text{EC.9b})$$

and are reformulated as $W + 1$ -dimensional SOC constraints as

$$r_\varepsilon \|\mathbf{X}_t \mathbb{1} \gamma_{it}\|_2 \leq \eta_i^D \bar{Q}_i^D - \hat{q}_{it}, \quad \forall t, \quad \forall i \in \mathcal{S} \quad (\text{EC.9c})$$

$$r_\varepsilon \|\mathbf{X}_t \mathbb{1} \gamma_{it}\|_2 \leq \frac{1}{\eta_i^C} \bar{Q}_i^C + \hat{q}_{it}, \quad \forall t, \quad \forall i \in \mathcal{S}, \quad (\text{EC.9d})$$

where $\eta_i^D, \eta_i^C \in [0, 1]$ are energy conversion factors representing discharging and charging efficiencies, while $\bar{Q}_i^D, \bar{Q}_i^C \in \mathbb{R}$ are, respectively, the maximum discharging and charging capacities of the energy storage unit $i \in \mathcal{S}$. Inter-temporal constraints are critical for energy storage units to ensure that (i) the storage operation trajectory remains within the limits of state of charge, and (ii) the

storage unit is neither depleted nor over-charged at the end of market-clearing horizon. While the former ensures safe operation of the storage unit within its operational limits, the latter is relevant in a market-clearing setup where the storage unit is expected to provide flexibility to the grid on an ongoing basis. Figure EC.1 shows the trajectory (in red) of energy content of a storage unit. At each hour, the changes to energy content due to production (discharging) or consumption (charging) by the storage unit is given by $\tilde{q}_{it}(\xi_t)$, with the rate of change being limited by the charging and discharging power limits in (EC.9). The energy content of a storage unit evolves as

$$\mathbb{P}_\xi \left(E_i^0 - \sum_{t'=1}^t (\hat{q}_{it'} + \mathbf{1}^\top \boldsymbol{\xi}_t \gamma_{it'}) \leq \bar{E}_i \right) \geq (1 - \hat{\varepsilon}), \forall t, \forall i \in \mathcal{S} \quad (\text{EC.10a})$$

$$\mathbb{P}_\xi \left(E_i^0 - \sum_{t'=1}^t (\hat{q}_{it'} + \mathbf{1}^\top \boldsymbol{\xi}_t \gamma_{it'}) \geq \underline{E}_i \right) \geq (1 - \hat{\varepsilon}), \forall t, \forall i \in \mathcal{S}, \quad (\text{EC.10b})$$

which are reformulated as $W \times t + 1$, $\forall t$ -dimensional SOC constraints, expressed as

$$r_{\hat{\varepsilon}} \left\| \mathbf{X}_{1:t} [\mathbf{1}^\top \gamma_{i1} \quad \mathbf{1}^\top \gamma_{i2} \cdots \mathbf{1}^\top \gamma_{it}]^\top \right\|_2 \leq \bar{E}_i - E_i^0 + \sum_{t'=1}^t \hat{q}_{it'}, \forall t, \forall i \in \mathcal{S} \quad (\text{EC.10c})$$

$$r_{\hat{\varepsilon}} \left\| \mathbf{X}_{1:t} [\mathbf{1}^\top \gamma_{i1} \quad \mathbf{1}^\top \gamma_{i2} \cdots \mathbf{1}^\top \gamma_{it}]^\top \right\|_2 \leq E_i^0 - \underline{E}_i - \sum_{t'=1}^t \hat{q}_{it'}, \forall t, \forall i \in \mathcal{S}, \quad (\text{EC.10d})$$

where $E_i^0 \in \mathbb{R}$ is the energy content at $t = 0$ and $\underline{E}_i, \bar{E}_i \in \mathbb{R}$ are the minimum and maximum energy storage capacity of the storage unit, respectively, such that $E_i^0 \in [\underline{E}_i, \bar{E}_i]$. Furthermore, to ensure the ongoing market-participation of the storage unit, we utilize the concept of end-of-horizon energy neutrality. We define lower and upper bounds, $\underline{B}_i, \bar{B}_i \in \mathbb{R}$ respectively, around the initial energy stored E_i^0 to reflect the preference of the energy storage owner on the energy content at the end of market-clearing horizon, see Figure EC.1. This ensures the end-of-horizon energy content to be within $[E_i^0 - \underline{B}_i, E_i^0 + \bar{B}_i]$. These preferences are captured through chance constraints

$$\mathbb{P}_\xi \left(E_i^0 - \sum_{t'=1}^T (\hat{q}_{it'} + \mathbf{1}^\top \boldsymbol{\xi}_t \gamma_{it'}) \leq E_i^0 + \bar{B}_i \right) \geq (1 - \hat{\varepsilon}), \forall i \in \mathcal{S} \quad (\text{EC.11a})$$

$$\mathbb{P}_\xi \left(E_i^0 - \sum_{t'=1}^T (\hat{q}_{it'} + \mathbf{1}^\top \boldsymbol{\xi}_t \gamma_{it'}) \geq E_i^0 - \underline{B}_i \right) \geq (1 - \hat{\varepsilon}), \forall i \in \mathcal{S} \quad (\text{EC.11b})$$

which are reformulated as $W \times T + 1$ -dimensional SOC constraints, expressed as

$$r_{\hat{\varepsilon}} \left\| \mathbf{X}_{1:T} [\mathbf{1}^\top \gamma_{i1} \quad \mathbf{1}^\top \gamma_{i2} \cdots \mathbf{1}^\top \gamma_{iT}]^\top \right\|_2 \leq \bar{B}_i + \sum_{t'=1}^T \hat{q}_{it'}, \forall i \in \mathcal{S} \quad (\text{EC.11c})$$

$$r_{\hat{\varepsilon}} \left\| \mathbf{X}_{1:T} [\mathbf{1}^\top \gamma_{i1} \quad \mathbf{1}^\top \gamma_{i2} \cdots \mathbf{1}^\top \gamma_{iT}]^\top \right\|_2 \leq \underline{B}_i - \sum_{t'=1}^T \hat{q}_{it'}, \forall i \in \mathcal{S}. \quad (\text{EC.11d})$$

Each energy storage operators participates in the conic market with a decision vector $\mathbf{q}_{it} = [\hat{q}_{it} \quad \gamma_{it}]^\top, \forall t, \forall i \in \mathcal{S}$. Likewise, towards the commodity energy, i.e., $p = 1$, we have

$$\mathbf{q}_{ip} = [\hat{q}_{i1} \quad \hat{q}_{i2} \dots \hat{q}_{i(T-1)} \quad \hat{q}_{iT}]^\top, \mathbf{G}_{ip} = \text{diag}(\mathbb{1}), \forall i \in \mathcal{S},$$

with $\mathbb{1} \in \mathbb{R}^T$. For the commodity flexibility ($p = 2$), the storage unit contributes to the trades as

$$\mathbf{q}_{ip} = [\gamma_{i1} \quad \gamma_{i2} \dots \gamma_{i(T-1)} \quad \gamma_{iT}]^\top, \mathbf{G}_{ip} = \begin{bmatrix} \mathbb{1}^\top \boldsymbol{\xi}_1 & \dots & 0 \\ \vdots & \ddots & \vdots \\ 0 & \dots & \mathbb{1}^\top \boldsymbol{\xi}_T \end{bmatrix}, \forall i \in \mathcal{S}.$$

Inflexible consumers: For each inflexible consumer $d \in \mathcal{D}$, the power consumed during real-time operation at hour t is given by $\tilde{q}_{it}(\boldsymbol{\xi}_t) = \hat{q}_{it}, \forall i \in \mathcal{D}, \forall t$, where $\hat{q}_{it} \in \mathbb{R}_-$ is the power demand by consumer $d \in \mathcal{D}$. The above modeling can be extended to include flexible consumers that may respond to the uncertainty by reducing/increasing their consumption based on an affine adjustment policy, similar to flexible generators and energy storage units. However, for clarity of exposition, this paper is restricted to modeling inflexible and perfectly inelastic demand. Each consumer contributes towards the trades of commodity energy, i.e., for $p = 1$, as

$$\mathbf{q}_{ip} = [\hat{q}_{i1} \quad \hat{q}_{i2} \dots \hat{q}_{i(T-1)} \quad \hat{q}_{iT}]^\top, \mathbf{G}_{ip} = \text{diag}(\mathbb{1}), \forall i \in \mathcal{D},$$

where $\mathbb{1} \in \mathbb{R}^T$. Lastly, for $p = 2$, considering inflexible consumers, we have $\mathbf{q}_{ip} = \mathbf{0}, \mathbf{G}_{ip} = \mathbf{0}, \forall i \in \mathcal{D}$.

EC.2.2. Chance-constrained Market Clearing

In the following, we formulate the chance-constrained market-clearing problem in stochastic optimization variables $\tilde{q}_{it}(\boldsymbol{\xi}_t), \forall i \in \mathcal{I}$ which are functions of the random variable $\boldsymbol{\xi}_t$. We drop this dependency for notational convenience, yet it is always implied.

$$\min_{\tilde{q}_{it}} \mathbb{E}^{\mathbb{P}_{\boldsymbol{\xi}}} \left[\sum_{i \in \mathcal{I} \setminus \mathcal{D}} \sum_{t \in \mathcal{T}} \left(c_{it}^Q \tilde{q}_{it}^2 + c_{it}^L \tilde{q}_{it} \right) \right] \quad (\text{EC.12a})$$

$$\text{s.t. } \mathbb{P}_{\boldsymbol{\xi}} \left[\sum_{i \in \mathcal{I}} \mathbf{G}_{ip} \tilde{\mathbf{q}}_{ip} = \mathbf{0}_T, \forall p \in \mathcal{P}, \right] \stackrel{\text{a.s.}}{=} 1, \quad (\text{EC.12b})$$

$$\left. \begin{array}{l} \left[\begin{array}{l} \underline{Q}_i \leq \tilde{q}_{it} \leq \bar{Q}_i, \forall t, \forall i \in \mathcal{F} \cup \mathcal{W} \\ -\underline{Q}_i^R \leq h_{it}(\boldsymbol{\xi}_t) \leq \bar{Q}_i^R, \forall i \in \mathcal{F} \\ -\Delta_i \leq \tilde{q}_{it} - \tilde{q}_{i(t-1)} \leq \bar{\Delta}_i, \forall t > 2, \forall i \in \mathcal{F} \\ -\frac{1}{\eta_i^C} \bar{Q}_i^C \leq \tilde{q}_{it} \leq \eta_i^D \bar{Q}_i^D, \forall t, \forall i \in \mathcal{S} \end{array} \right] \\ \mathbb{P}_{\boldsymbol{\xi}} \left[\begin{array}{l} \underline{E}_i \leq E_i^0 - \sum_{t'=1}^t \tilde{q}_{it'} \leq \bar{E}_i, \forall t, \forall i \in \mathcal{S} \\ E_i^0 - \underline{B}_i \leq E_i^0 - \sum_{t'=1}^T \tilde{q}_{it'} \leq E_i^0 + \bar{B}_i, \forall i \in \mathcal{S} \\ -\bar{s}_{\ell} \leq \sum_{n \in \mathcal{N}} [\Psi]_{(\ell, n)} \left(\sum_{i \in \mathcal{I}_n} \sum_{p \in \mathcal{P}} [\mathbf{G}_{ip} \tilde{\mathbf{q}}_{ip}]_t \right) \leq \bar{s}_{\ell}, \forall t, \forall \ell \in \mathcal{L} \end{array} \right] \end{array} \right] \geq 1 - \varepsilon, \quad (\text{EC.12c})$$

where the objective function (EC.12a) minimizes the expected cost, which is equivalent to minimizing negative social welfare when facing an inflexible and perfectly inelastic demand. The almost sure (a. s.) constraint (EC.12b) ensures the satisfaction of the supply-demand balance constraint for both commodities with a probability of 1, whereas the chance constraint (EC.12c) ensures the inequalities are jointly met with a probability of $(1 - \varepsilon)$. The prescribed constraint violation probability $\varepsilon \in (0, 1)$ reflects risk tolerance of the system operator towards the violation of technical limits of the system and in our numerical studies discussed in §4, we set $\varepsilon = 0.05$. The chance-constrained market-clearing problem (EC.12) is computationally intractable since it involves infinitely many constraints arising from the uncertain production from weather-dependent power producers. We gain tractability by expressing the stochastic variables \tilde{q}_{it} , $\forall i, \forall t$ as affine, finite-dimensional functions of the random variable ξ as discussed in the previous section, resulting in an approximate solution to the infinite-dimensional problem. In the following, we discuss the reformulations to reach the final tractable SOCP-based chance-constrained market-clearing problem.

Reformulation of joint chance constraint: Observe that (EC.12c) models a joint violation of the constraints, in contrast to the individual chance constraints discussed so far. In this paper, following the Bonferroni approximation of joint chance constraints (Xie et al. 2019), we adopt a consideration of individual chance constraints with the analytical parameterization of risk. Let N^{ineq} denote the number of individual inequalities forming the joint chance constraint (EC.12c), such that $\hat{\varepsilon} \in \mathbb{R}_+^{N^{\text{ineq}}}$ collects all the individual violation probabilities for the inequality constraints. The Bonferroni reformulation of joint chance constraint mandates that the individual constraint violation probabilities be chosen such that $\mathbb{1}^\top \hat{\varepsilon} \leq \varepsilon$. Furthermore, this approach provides a joint constraint feasibility guarantee even if the choice of individual probabilities is done trivially, e.g., $\hat{\varepsilon}$ is chosen such that $\hat{\varepsilon}_k = \frac{\varepsilon}{N^{\text{ineq}}}$, $\forall k = 1, 2, \dots, N^{\text{ineq}}$. We compute the individual constraint violation probabilities in this manner and adopt the SOC reformulation techniques for individual chance constraints discussed so far.

Reformulation of almost sure constraint: The almost sure constraint (EC.12b) must be held at the optimal solution to (EC.12) with a probability of 1. Considering the affine dependency of the stochastic decision variables \tilde{q}_{it} , $\forall i, \forall t$ with respect to the random variables ξ_t , this amounts to a separation of (EC.12b) into nominal and recourse equalities. Corresponding to the two commodities energy and flexibility, these equalities are given by

$$\sum_{i \in \mathcal{I}} \mathbf{G}_{ip} \mathbf{q}_{ip} = \mathbf{0}, \quad p = 1 \tag{EC.13a}$$

$$\sum_{i \in \mathcal{I} \setminus (\mathcal{W} \cup \mathcal{D})} \text{diag}(\mathbb{1}) \mathbf{q}_{ip} = \mathbb{1}, \quad p = 2. \tag{EC.13b}$$

Power flow limits: Apart from the participant-specific chance constraints discussed so far, the constraints limiting the power flows in the network are

$$\mathbb{P}_\xi \left[\sum_{n \in \mathcal{N}} [\Psi]_{(\ell, n)} \left(\sum_{i \in \mathcal{I}_n} \sum_{p \in \mathcal{P}} [\mathbf{G}_{ip} \tilde{\mathbf{q}}_{ip}]_t \right) \leq \bar{s}_\ell \right] \geq 1 - \hat{\varepsilon}, \quad \forall t, \forall \ell \in \mathcal{L} \quad (\text{EC.14a})$$

$$\mathbb{P}_\xi \left[\sum_{n \in \mathcal{N}} [\Psi]_{(\ell, n)} \left(\sum_{i \in \mathcal{I}_n} \sum_{p \in \mathcal{P}} [\mathbf{G}_{ip} \tilde{\mathbf{q}}_{ip}]_t \right) \geq -\bar{s}_\ell \right] \geq 1 - \hat{\varepsilon}, \quad \forall t, \forall \ell \in \mathcal{L}, \quad (\text{EC.14b})$$

which require tractable reformulations. In the following, we illustrate the reformulation of (EC.14a) as an SOC constraint and adopt a similar approach for the other flow direction. First, we rewrite (EC.14a) such that nominal and uncertainty-dependent terms are separable. To that end, we define auxiliary network matrices $\Psi^F \in \mathbb{R}^{N \times |\mathcal{F}|}$, $\Psi^S \in \mathbb{R}^{N \times |\mathcal{S}|}$, $\Psi^W \in \mathbb{R}^{N \times W}$ and $\Psi^D \in \mathbb{R}^{N \times |\mathcal{D}|}$ which map the flexible power producers, energy storage units, weather-dependent power producers and consumers, respectively, to the electricity network nodes. We collect all commodity contributions by participant groups at a given hour by defining auxiliary variables $\tilde{\mathbf{q}}_t^F$, $\hat{\mathbf{q}}_t^F$, $\alpha_t \in \mathbb{R}^{|\mathcal{F}|}$ to denote the stochastic production, nominal production and the adjustment policies for the flexible power producers, $\tilde{\mathbf{q}}_t^S$, $\hat{\mathbf{q}}_t^S$, $\gamma_t \in \mathbb{R}^{|\mathcal{S}|}$ to denote stochastic production, nominal production and adjustment policies for the storage units, $\hat{\mathbf{q}}_t^W \in \mathbb{R}^W$ for the forecasted production from weather-dependent power producers and lastly, $\hat{\mathbf{q}}_t^D \in \mathbb{R}^{|\mathcal{D}|}$ for the inflexible demand from consumers. With that, we rewrite (EC.14a) as

$$\mathbb{P}_\xi \left[[\Psi(\Psi^F \tilde{\mathbf{q}}_t^F + \Psi^S \tilde{\mathbf{q}}_t^S + \Psi^W (\tilde{\mathbf{q}}_t^W - \xi_t) + \Psi^D \hat{\mathbf{q}}_t^D)]_\ell \leq \bar{s}_\ell \right] \geq 1 - \hat{\varepsilon}, \quad \forall t, \forall \ell \in \mathcal{L}, \quad (\text{EC.15})$$

which we then reformulate as an SOC constraint after separating the nominal and uncertainty-dependent terms. The final SOC reformulation for (EC.14a) results in $\forall t, \forall \ell \in \mathcal{L}$,

$$r_{\hat{\varepsilon}} \left\| \mathbf{X}_t [\Psi(\Psi^F \alpha_t \mathbf{1}^\top + \Psi^S \gamma_t \mathbf{1}^\top - \Psi^W)]_{(\ell, :)}^\top \right\|_2 \leq \bar{s}_\ell - [\Psi(\Psi^F \hat{\mathbf{q}}_t^F + \Psi^S \hat{\mathbf{q}}_t^S + \Psi^W \hat{\mathbf{q}}_t^W + \Psi^D \hat{\mathbf{q}}_t^D)]_\ell. \quad (\text{EC.16})$$

Objective function reformulation: We decompose the objective (EC.12a) among the various participants and expand the stochastic term to its nominal and recourse values to obtain

$$\begin{aligned} & \mathbb{E}^{\mathbb{P}_\xi} \left[\underbrace{\sum_{i \in \mathcal{F}} \sum_{t \in \mathcal{T}} \left(c_{it}^Q (\hat{q}_{it} + \mathbf{1}^\top \xi_t \alpha_{it})^2 + c_{it}^L (\hat{q}_{it} + \mathbf{1}^\top \xi_t \alpha_{it}) \right)}_{\text{Term A}} \right. \\ & \quad \left. + \underbrace{\sum_{i \in \mathcal{S}} \sum_{t \in \mathcal{T}} \left(c_{it}^Q (\hat{q}_{it} + \mathbf{1}^\top \xi_t \gamma_{it})^2 + c_{it}^L (\hat{q}_{it} + \mathbf{1}^\top \xi_t \gamma_{it}) \right)}_{\text{Term B}} + \underbrace{\sum_{i \in \mathcal{W}} \sum_{t \in \mathcal{T}} \left(c_{it}^Q (\hat{q}_{it} - \xi_{it})^2 + c_{it}^L (\hat{q}_{it} - \xi_{it}) \right)}_{\text{Term C}} \right]. \end{aligned}$$

Linearity of the expectation operator allows us to separate the cost terms and we rewrite the cost of flexible generators, i.e., Term A as

$$\sum_{i \in \mathcal{F}} \sum_{t \in \mathcal{T}} \left(c_{it}^Q \hat{q}_{it}^2 + c_{it}^Q \mathbb{E}^{\mathbb{P}_\xi}[(\mathbf{1}^\top \xi_t)^2] \alpha_{it}^2 + 2 \hat{q}_{it} c_{it}^Q \mathbb{E}^{\mathbb{P}_\xi}[\mathbf{1}^\top \xi_t] \alpha_{it} + c_{it}^L \hat{q}_{it} + c_{it}^L \mathbb{E}^{\mathbb{P}_\xi}[\mathbf{1}^\top \xi_t] \alpha_{it} \right).$$

The zero-mean assumption made on ξ_t factors out the terms last two terms under the expectation operator. As discussed in Bienstock et al. (2014), the first term under expectation operator can be reformulated as the variance of ξ_t , i.e., $\mathbb{E}^{\mathbb{P}^\xi}[(\mathbb{1}^\top \xi_t)^2] = \text{var}(\mathbb{1}^\top \xi_t) = \mathbb{1}^\top \Sigma_t \mathbb{1}$, where Σ_t is the covariance matrix as previously discussed. Therefore, the Term A reduces to

$$\sum_{i \in \mathcal{F}} \sum_{t \in \mathcal{T}} \left(c_{it}^Q \hat{q}_{it}^2 + c_{it}^Q \mathbb{1}^\top \Sigma_t \mathbb{1} \alpha_{it}^2 + c_{it}^L \hat{q}_{it} \right).$$

Lastly, following Example EC.1, we reformulate the quadratic cost terms as a rotated SOC constraint in the interest of analytical and computational appeal. Introducing variables $z_{it}^{\hat{q}} \in \mathbb{R}$ and $z_{it}^\alpha \in \mathbb{R}$, for any fixed values of \hat{q}_{it} and α_{it} , Term A of the objective function retrieves the expected cost by solving the following SOCP problem

$$\min_{z_{it}^{\hat{q}}, z_{it}^\alpha} \sum_{i \in \mathcal{F}} \sum_{t \in \mathcal{T}} \left(z_{it}^{\hat{q}} + z_{it}^\alpha + c_{it}^L \hat{q}_{it} \right) \quad (\text{EC.17a})$$

$$\text{s.t. } \left\| (c_{it}^Q)^{\frac{1}{2}} \hat{q}_{it} \right\|_2^2 \leq z_{it}^{\hat{q}}, \forall t, \forall i \in \mathcal{F} \quad (\text{EC.17b})$$

$$\left\| \mathbf{X}_t \mathbb{1} (c_{it}^Q)^{\frac{1}{2}} \alpha_{it} \right\|_2^2 \leq z_{it}^\alpha, \forall t, \forall i \in \mathcal{F}. \quad (\text{EC.17c})$$

Term B of the objective function characterizing the cost of operation of energy storage units follows a similar reformulation. For the set of wind power producers, i.e., the cost in Term C, we use the following equivalence to eliminate the expectation operator

$$\sum_{i \in \mathcal{W}} \sum_{t \in \mathcal{T}} \left(c_{it}^Q \hat{q}_{it}^2 + c_{it}^Q \mathbb{E}^{\mathbb{P}^\xi} [\xi_{it}^2] + c_{it}^L \hat{q}_{it} \right) \Leftrightarrow \sum_{i \in \mathcal{W}} \sum_{t \in \mathcal{T}} \left(c_{it}^Q \hat{q}_{it}^2 + c_{it}^Q \text{tr}[\Sigma_t] + c_{it}^L \hat{q}_{it} \right).$$

The quadratic term in the expression is then reformulated as a rotated SOC constraint as before. The term $c_{it}^Q \text{tr}[\Sigma_t]$ is a cost term that is constant, depending on the historical forecast error samples.

Adopting the reformulations of the objective function and the chance constraints, we obtain the final tractable chance-constrained market-clearing problem \mathcal{M}^{cc} . Solved centrally by the system operator, the problem \mathcal{M}^{cc} is an SOCP problem that results in optimal market-clearing quantities and prices for both the commodities traded in the market, i.e., energy and flexibility.

$$\min_{\nu^{\text{opt}}, \nu^{\text{aux}}} \sum_{i \in \mathcal{I} \setminus \mathcal{D}} \sum_{t \in \mathcal{T}} \left(z_{it}^{\hat{q}_{it}} + c_{it}^L \hat{q}_{it} \right) + \sum_{i \in \mathcal{F}} \sum_{t \in \mathcal{T}} z_{it}^\alpha + \sum_{i \in \mathcal{S}} \sum_{t \in \mathcal{T}} z_{it}^\gamma + \sum_{i \in \mathcal{W}} \sum_{t \in \mathcal{T}} c_{it}^Q \text{tr}[\Sigma_t] \quad (\text{EC.18a})$$

$$\text{s.t. } \left\| (c_{it}^Q)^{\frac{1}{2}} \hat{q}_{it} \right\|_2^2 \leq z_{it}^{\hat{q}}, \forall t, \forall i \in \mathcal{I} \setminus \mathcal{D} \quad (\text{EC.18b})$$

$$\left\| \mathbf{X}_t \mathbb{1} (c_{it}^Q)^{\frac{1}{2}} \alpha_{it} \right\|_2^2 \leq z_{it}^\alpha, \forall t, \forall i \in \mathcal{F} \quad (\text{EC.18c})$$

$$\left\| \mathbf{X}_t \mathbb{1} (c_{it}^Q)^{\frac{1}{2}} \gamma_{it} \right\|_2^2 \leq z_{it}^\gamma, \forall t, \forall i \in \mathcal{S} \quad (\text{EC.18d})$$

$$r_{\hat{\varepsilon}} \|\mathbf{X}_t \mathbb{1} \alpha_{it}\|_2 \leq \bar{Q}_i - \hat{q}_{it}, \forall t, \forall i \in \mathcal{F} \quad (\text{EC.18e})$$

$$r_{\hat{\varepsilon}} \|\mathbf{X}_t \mathbb{1} \alpha_{it}\|_2 \leq \hat{q}_{it} - \underline{Q}_i, \forall t, \forall i \in \mathcal{F} \quad (\text{EC.18f})$$

$$r_{\hat{\varepsilon}} \|\mathbf{X}_t \mathbb{1} \alpha_{it}\|_2 \leq \overline{Q}_i^R, \forall t, \forall i \in \mathcal{F} \quad (\text{EC.18g})$$

$$r_{\hat{\varepsilon}} \|\mathbf{X}_t \mathbb{1} \alpha_{it}\|_2 \leq \underline{Q}_i^R, \forall t, \forall i \in \mathcal{F} \quad (\text{EC.18h})$$

$$r_{\hat{\varepsilon}} \left\| \mathbf{X}_{t-1:t} \begin{bmatrix} -\mathbb{1}^\top \alpha_{i(t-1)} l & \mathbb{1}^\top \alpha_{it} \end{bmatrix}^\top \right\|_2 \leq \overline{\Delta}_i + (\hat{q}_{it-1} - \hat{q}_{it}), \forall t > 2, \forall i \in \mathcal{F} \quad (\text{EC.18i})$$

$$r_{\hat{\varepsilon}} \left\| \mathbf{X}_{t-1:t} \begin{bmatrix} \mathbb{1}^\top \alpha_{i(t-1)} & -\mathbb{1}^\top \alpha_{it} \end{bmatrix}^\top \right\|_2 \leq \underline{\Delta}_i - (\hat{q}_{it-1} - \hat{q}_{it}), \forall t > 2, \forall i \in \mathcal{F} \quad (\text{EC.18j})$$

$$r_{\hat{\varepsilon}} \|\mathbf{X}_t \mathbb{1} \gamma_{it}\|_2 \leq \eta_i^D \overline{Q}_i^D - \hat{q}_{it}, \forall t, \forall i \in \mathcal{S} \quad (\text{EC.18k})$$

$$r_{\hat{\varepsilon}} \|\mathbf{X}_t \mathbb{1} \gamma_{it}\|_2 \leq \frac{1}{\eta_i^C} \overline{Q}_i^C + \hat{q}_{it}, \forall t, \forall i \in \mathcal{S} \quad (\text{EC.18l})$$

$$r_{\hat{\varepsilon}} \left\| \mathbf{X}_{1:t} \begin{bmatrix} \mathbb{1}^\top \gamma_{i1} & \mathbb{1}^\top \gamma_{i2} & \cdots & \mathbb{1}^\top \gamma_{it} \end{bmatrix}^\top \right\|_2 \leq \overline{E}_i - E_i^0 + \sum_{t'=1}^t \hat{q}_{it'}, \forall t, \forall i \in \mathcal{S} \quad (\text{EC.18m})$$

$$r_{\hat{\varepsilon}} \left\| \mathbf{X}_{1:t} \begin{bmatrix} \mathbb{1}^\top \gamma_{i1} & \mathbb{1}^\top \gamma_{i2} & \cdots & \mathbb{1}^\top \gamma_{it} \end{bmatrix}^\top \right\|_2 \leq E_i^0 - \underline{E}_i - \sum_{t'=1}^t \hat{q}_{it'}, \forall t, \forall i \in \mathcal{S} \quad (\text{EC.18n})$$

$$r_{\hat{\varepsilon}} \left\| \mathbf{X}_{1:T} \begin{bmatrix} \mathbb{1}^\top \gamma_{i1} & \mathbb{1}^\top \gamma_{i2} & \cdots & \mathbb{1}^\top \gamma_{iT} \end{bmatrix}^\top \right\|_2 \leq \overline{B}_i + \sum_{t'=1}^T \hat{q}_{it'}, \forall i \in \mathcal{S} \quad (\text{EC.18o})$$

$$r_{\hat{\varepsilon}} \left\| \mathbf{X}_{1:T} \begin{bmatrix} \mathbb{1}^\top \gamma_{i1} & \mathbb{1}^\top \gamma_{i2} & \cdots & \mathbb{1}^\top \gamma_{iT} \end{bmatrix}^\top \right\|_2 \leq \underline{B}_i - \sum_{t'=1}^T \hat{q}_{it'}, \forall i \in \mathcal{S} \quad (\text{EC.18p})$$

$$\sum_{i \in \mathcal{I}} \mathbf{G}_{ip} \mathbf{q}_{ip} = \mathbb{0}, p = 1 \quad (\text{EC.18q})$$

$$\sum_{i \in \mathcal{I} \setminus (\mathcal{W} \cup \mathcal{D})} \text{diag}(\mathbb{1}) \mathbf{q}_{ip} = \mathbb{1}, p = 2 \quad (\text{EC.18r})$$

$$r_{\hat{\varepsilon}} \left\| \mathbf{X}_t [\Psi(\Psi^F \alpha_t \mathbb{1}^\top + \Psi^S \gamma_t \mathbb{1}^\top - \Psi^W)]_{(\ell,:)}^\top \right\|_2 \leq \bar{s}_\ell \\ - [\Psi(\Psi^F \hat{\mathbf{q}}_t^F + \Psi^S \hat{\mathbf{q}}_t^S + \Psi^W \hat{\mathbf{q}}_t^W + \Psi^D \hat{\mathbf{q}}_t^D)]_\ell, \forall t, \forall \ell \in \mathcal{L} \quad (\text{EC.18s})$$

$$r_{\hat{\varepsilon}} \left\| \mathbf{X}_t [\Psi(\Psi^F \alpha_t \mathbb{1}^\top + \Psi^S \gamma_t \mathbb{1}^\top - \Psi^W)]_{(\ell,:)}^\top \right\|_2 \leq \bar{s}_\ell \\ + [\Psi(\Psi^F \hat{\mathbf{q}}_t^F + \Psi^S \hat{\mathbf{q}}_t^S + \Psi^W \hat{\mathbf{q}}_t^W + \Psi^D \hat{\mathbf{q}}_t^D)]_\ell, \forall t, \forall \ell \in \mathcal{L}, \quad (\text{EC.18t})$$

where the set of optimization variables is $\mathcal{V}^{\text{opt}} = \{\hat{q}_{it}, z_{it}^{\hat{q}_{it}}, \alpha_{it}, z_{it}^{\hat{\alpha}_{it}}, \gamma_{it}, z_{it}^{\hat{\gamma}_{it}}\}$ and the set of auxiliary variables is $\mathcal{V}^{\text{aux}} = \{\mathbf{q}_{ip}, \hat{\mathbf{q}}_t^F, \alpha_t, \hat{\mathbf{q}}_t^S, \gamma_t, \hat{\mathbf{q}}_t^W, \hat{\mathbf{q}}_t^D\}$, formed as previously discussed.

EC.2.3. LP-based market-clearing benchmarks

In the following, we concisely formulate the two reference uncertainty-aware benchmarks within the LP framework. To account for the quadratic costs of market participants in an LP problem, we perform a piecewise linear approximation of the cost by discretizing the production quantities into a set of bins given by $\mathcal{Y} = \{1, 2, \dots, Y\}$.

Deterministic two-stage market framework: In the deterministic market-clearing problem $\mathcal{R}1$, the system operator procures energy and flexibility (in the form of reserve capacity) in the day-ahead market. Thereafter, during real-time operation stage, via another market-clearing mechanism, the reserves are activated based on the allocation capacity bounds cleared during the

day-ahead market. This two-stage deterministic market-clearing problem is a natural uncertainty-aware extension of currently-operational electricity markets.

Day-ahead market-clearing problem $\mathcal{R}1_a$:

$$\min_{q_{ity}^{\text{DA}}, q_{it}^{\text{R}}} \sum_{i \in \mathcal{I} \setminus \mathcal{D}} \sum_{t \in \mathcal{T}} \sum_{y \in \mathcal{Y}} \left(c_{ity}^{\text{Y}} q_{ity}^{\text{DA}} \right) + \sum_{i \in \mathcal{F} \cup \mathcal{S}} \sum_{t \in \mathcal{T}} c_{it}^{\text{R}} q_{it}^{\text{R}} \quad (\text{EC.19a})$$

$$\text{s.t. } 0 \leq q_{ity}^{\text{DA}} \leq \frac{1}{Y} (\bar{Q}_i - \underline{Q}_i), \forall y, \forall t, \forall i \in \mathcal{I} \setminus \mathcal{D} \quad (\text{EC.19b})$$

$$\underline{Q}_i \leq \sum_{y \in \mathcal{Y}} q_{ity}^{\text{DA}} \leq \bar{Q}_i, \forall t, \forall i \in \mathcal{F} \cup \mathcal{W} \quad (\text{EC.19c})$$

$$\underline{Q}_i \leq \sum_{y \in \mathcal{Y}} q_{ity}^{\text{DA}} + q_{it}^{\text{R}} \leq \bar{Q}_i, \forall t, \forall i \in \mathcal{F} \quad (\text{EC.19d})$$

$$-\Delta_i \leq \sum_{y \in \mathcal{Y}} (q_{ity}^{\text{DA}} - q_{i(t-1)y}^{\text{DA}}) \leq \bar{\Delta}_i, \forall t > 2, \forall i \in \mathcal{F} \quad (\text{EC.19e})$$

$$-\frac{1}{\eta_i^{\text{C}}} \bar{Q}_i^{\text{C}} \leq \sum_{y \in \mathcal{Y}} q_{ity}^{\text{DA}} \leq \eta_i^{\text{D}} \bar{Q}_i^{\text{D}}, \forall t, \forall i \in \mathcal{S} \quad (\text{EC.19f})$$

$$-\frac{1}{\eta_i^{\text{C}}} \bar{Q}_i^{\text{C}} \leq \sum_{y \in \mathcal{Y}} q_{ity}^{\text{DA}} + q_{it}^{\text{R}} \leq \eta_i^{\text{D}} \bar{Q}_i^{\text{D}}, \forall t, \forall i \in \mathcal{S} \quad (\text{EC.19g})$$

$$\underline{E}_i \leq E_i^0 - \sum_{t'=1}^t (\sum_{y \in \mathcal{Y}} q_{it'y}^{\text{DA}} + q_{it}^{\text{R}}) \leq \bar{E}_i, \forall t, \forall i \in \mathcal{S} \quad (\text{EC.19h})$$

$$E_i^0 - \underline{B}_i \leq E_i^0 - \sum_{t'=1}^t (\sum_{y \in \mathcal{Y}} q_{it'y}^{\text{DA}} + q_{it}^{\text{R}}) \leq E_i^0 + \bar{B}_i, \forall i \in \mathcal{S} \quad (\text{EC.19i})$$

$$0 \leq q_{it}^{\text{R}} \leq \bar{Q}_i^{\text{R}}, \forall t, \forall i \in \mathcal{F} \cup \mathcal{S} \quad (\text{EC.19j})$$

$$\sum_{i \in \mathcal{I}} \sum_{y \in \mathcal{Y}} q_{ity}^{\text{DA}} = 0, \forall t \quad (\text{EC.19k})$$

$$\sum_{i \in \mathcal{F} \cup \mathcal{S}} q_{it}^{\text{R}} \geq M_{\text{R}}, \forall t \quad (\text{EC.19l})$$

$$-\bar{s}_{\ell} \leq \sum_{n \in \mathcal{N}} [\Psi]_{(\ell, n)} \left(\sum_{i \in \mathcal{I}_n} \sum_{y \in \mathcal{Y}} q_{ity}^{\text{DA}} \right) \leq \bar{s}_{\ell}, \forall t, \forall \ell \in \mathcal{L}, \quad (\text{EC.19m})$$

where the parameter M_{R} is the exogenously-determined minimum reserve requirement set by the system operator. Next, closer to real-time the following flexibility activation problem is solved for each uncertainty realization, denoted by $\hat{\xi}$.

Real-time flexibility activation problem, $\mathcal{R}1_b, \forall \hat{\xi}$:

$$\min_{q_{ity}^{\text{RT}}} \sum_{i \in \mathcal{I} \setminus \mathcal{D}} \sum_{t \in \mathcal{T}} \sum_{y \in \mathcal{Y}} c_{ity}^{\text{Y}} q_{ity}^{\text{RT}} + \sum_{i \in \mathcal{W}} c^{\text{spill}} q_{it}^{\text{RT}} - \sum_{i \in \mathcal{D}} c^{\text{shed}} q_{it}^{\text{RT}} \quad (\text{EC.20a})$$

$$\text{s.t. } -\frac{q_{it}^{\text{R}^*}}{Y} \leq q_{ity}^{\text{RT}} \leq \frac{q_{it}^{\text{R}^*}}{Y}, \forall y, \forall t, \forall i \in \mathcal{F} \cup \mathcal{S} \quad (\text{EC.20b})$$

$$-q_{it}^{\text{R}^*} \leq \sum_{y \in \mathcal{Y}} q_{ity}^{\text{RT}} \leq q_{it}^{\text{R}^*}, \forall t, \forall i \in \mathcal{F} \cup \mathcal{S} \quad (\text{EC.20c})$$

$$0 \leq q_{ity}^{\text{RT}} \leq \frac{\hat{q}_{it} - \hat{\xi}_{it}}{Y}, \forall t, \forall i \in \mathcal{W} \quad (\text{EC.20d})$$

$$-\frac{\hat{q}_{it}}{Y} \leq q_{ity}^{\text{RT}} \leq 0, \forall t, \forall i \in \mathcal{D} \quad (\text{EC.20e})$$

$$\sum_{i \in \mathcal{I} \setminus \mathcal{W}} \sum_{y \in \mathcal{Y}} q_{ity}^{\text{RT}} = \mathbf{1}^\top \hat{\boldsymbol{\xi}}_t + \sum_{i \in \mathcal{W}} q_{it}^{\text{RT}}, \forall t \quad (\text{EC.20f})$$

$$-\bar{s}_\ell \leq \sum_{n \in \mathcal{N}} [\Psi]_{(\ell, n)} \left(\sum_{i \in \mathcal{I}_n} \sum_{y \in \mathcal{Y}} (q_{ity}^{\text{DA}*} + q_{ity}^{\text{RT}}) \right) \leq \bar{s}_\ell, \forall t, \forall \ell \in \mathcal{L}, \quad (\text{EC.20g})$$

where $(q_{ity}^{\text{DA}*}, q_{it}^{\text{R}*}) = \text{argmin } \mathcal{R}1_a$ are day-ahead dispatch and reserve capacity, respectively.

Scenario-based market framework: The scenario-based stochastic market-clearing problem $\mathcal{R}2$ is a two-stage problem. The first stage involves the day-ahead schedules as a result of the so-called *here-and-now* decisions, whereas the second stage adjusts the day-ahead schedules with real-time adjustments to mitigate the uncertainty from weather-dependent power producers (*wait-and-see*). The adjustment decisions for real-time stage are already included in the day-ahead market-clearing problem by considering a finite number of uncertainty realization scenarios, anticipating that the actual power production is captured in the scenarios considered. Like with $\mathcal{R}1$, we adopt a linear approximation of the quadratic costs to remain within the LP framework. In the following, we provide a concise formulation for this benchmark.

$$\min_{q_{ity}^{\text{DA}}, q_{ityk}^{\text{RT}}} \sum_{i \in \mathcal{I} \setminus \mathcal{D}} \sum_{t \in \mathcal{T}} \sum_{y \in \mathcal{Y}} (c_{ity}^{\text{Y}} q_{ity}^{\text{DA}}) + \sum_{k=1}^K \phi_k \left[\sum_{i \in \mathcal{I} \setminus \mathcal{D}} \sum_{t \in \mathcal{T}} \sum_{y \in \mathcal{Y}} (c_{ity}^{\text{Y}} q_{ity}^{\text{RT}}) \right] \quad (\text{EC.21a})$$

$$\text{s.t. } 0 \leq q_{ity}^{\text{DA}} \leq \frac{1}{Y} (\bar{Q}_i - \underline{Q}_i), \forall y, \forall t, \forall i \in \mathcal{I} \setminus \mathcal{D} \quad (\text{EC.21b})$$

$$\underline{Q}_i \leq \sum_{y \in \mathcal{Y}} q_{ity}^{\text{DA}} \leq \bar{Q}_i, \forall t, \forall i \in \mathcal{F} \cup \mathcal{W} \quad (\text{EC.21c})$$

$$-\Delta_i \leq \sum_{y \in \mathcal{Y}} (q_{ity}^{\text{DA}} - q_{i(t-1)y}^{\text{DA}}) \leq \bar{\Delta}_i, \forall t > 2, \forall i \in \mathcal{F} \quad (\text{EC.21d})$$

$$-\frac{1}{\eta_i^C} \bar{Q}_i^C \leq \sum_{y \in \mathcal{Y}} q_{ity}^{\text{DA}} \leq \eta_i^D \bar{Q}_i^D, \forall t, \forall i \in \mathcal{S} \quad (\text{EC.21e})$$

$$\underline{E}_i \leq E_i^0 - \sum_{t'=1}^t \sum_{y \in \mathcal{Y}} q_{it'y}^{\text{DA}} \leq \bar{E}_i, \forall t, \forall i \in \mathcal{S} \quad (\text{EC.21f})$$

$$E_i^0 - \underline{B}_i \leq E_i^0 - \sum_{t'=1}^T \sum_{y \in \mathcal{Y}} q_{it'y}^{\text{DA}} \leq E_i^0 + \bar{B}_i, \forall i \in \mathcal{S} \quad (\text{EC.21g})$$

$$\sum_{i \in \mathcal{I}} \sum_{y \in \mathcal{Y}} q_{ity}^{\text{DA}} = 0, \forall t \quad (\text{EC.21h})$$

$$-\bar{s}_\ell \leq \sum_{n \in \mathcal{N}} [\Psi]_{(\ell, n)} \left(\sum_{i \in \mathcal{I}_n} \sum_{y \in \mathcal{Y}} q_{ity}^{\text{DA}} \right) \leq \bar{s}_\ell, \forall t, \forall \ell \in \mathcal{L} \quad (\text{EC.21i})$$

$$-\frac{Q_i^R}{Y} \leq p_{ity}^{\text{RT}} \leq \frac{\bar{Q}_i^R}{Y} \forall y, \forall k, \forall t, \forall i \in \mathcal{F} \cup \mathcal{S} \quad (\text{EC.21j})$$

$$-\underline{Q}_i^R \leq \sum_{y \in \mathcal{Y}} p_{itky}^{\text{RT}} \leq \bar{Q}_i^R, \forall k, \forall t, \forall i \in \mathcal{F} \cup \mathcal{S} \quad (\text{EC.21k})$$

$$-\underline{Q}_i \leq \sum_{y \in \mathcal{Y}} (p_{ity}^{\text{DA}} + p_{itky}^{\text{RT}}) \leq \bar{Q}_i, \forall k, \forall t, \forall i \in \mathcal{F} \cup \mathcal{W} \quad (\text{EC.21l})$$

$$-\frac{1}{\eta_i^C} \bar{Q}_i^C \leq \sum_{y \in \mathcal{Y}} (q_{ity}^{\text{DA}} + q_{itky}^{\text{RT}}) \leq \eta_i^D \bar{Q}_i^D, \forall k, \forall t, \forall i \in \mathcal{S} \quad (\text{EC.21m})$$

$$\underline{E}_i \leq E_i^0 - \left(\sum_{t'=1}^t \sum_{y \in \mathcal{Y}} (q_{it'y}^{\text{DA}} + q_{it'ky}^{\text{RT}}) \right) \leq \bar{E}_i, \forall t, \forall i \in \mathcal{S} \quad (\text{EC.21n})$$

$$E_i^0 - \underline{B}_i \leq E_i^0 - \left(\sum_{t'=1}^t \sum_{y \in \mathcal{Y}} (q_{it'y}^{\text{DA}} + q_{it'ky}^{\text{RT}}) \right) \leq E_i^0 + \bar{B}_i, \forall k, \forall i \in \mathcal{S} \quad (\text{EC.21o})$$

$$\sum_{i \in \mathcal{I}} \sum_{y \in \mathcal{Y}} q_{itky}^{\text{RT}} = 0, \forall k, \forall t \quad (\text{EC.21p})$$

$$-\bar{s}_\ell \leq \sum_{n \in \mathcal{N}} [\Psi]_{(\ell, n)} \left(\sum_{i \in \mathcal{I}_n} \sum_{y \in \mathcal{Y}} (q_{ity}^{\text{DA}} + q_{itky}^{\text{RT}}) \right) \leq \bar{s}_\ell, \forall k, \forall t, \forall \ell \in \mathcal{L} \quad (\text{EC.21q})$$

EC.2.4. Out-of-sample simulations

Out-of-sample simulations are performed to evaluate the quality of the day-ahead market-clearing outcomes by fixing the decisions obtained at the day-ahead stage to their optimal values and solving a real-time flexibility activation problem. For the proposed conic market framework, the out-of-sample problem (EC.22) formulated in the following admits fixed day-ahead decisions $(q_{it}^*, \alpha_{it}^*, \gamma_{it}^*)$ obtained from the solution to \mathcal{M}^{cc} . For the LP-based benchmark problems, we use $q_{it}^* = \sum_{y \in \mathcal{Y}} q_{ity}^{\text{DA}*}$ from the solution to $\mathcal{R}1_a$ for the deterministic benchmark problem and $q_{it}^* = \sum_{y \in \mathcal{Y}} q_{ity}^{\text{DA}*}$ from the solution to $\mathcal{R}2$ for the scenario-based stochastic benchmark problem. We have, $\forall \hat{\xi}$:

$$\min_{q_{it}^{\text{RT}}} \sum_{i \in \mathcal{I} \setminus (\mathcal{D} \cup \mathcal{W})} \sum_{t \in \mathcal{T}} \left(c_{it}^{\text{Q}} (q_{it}^* + q_{it}^{\text{RT}})^2 + c_{it}^{\text{L}} (q_{it}^* + q_{it}^{\text{RT}}) \right) + \sum_{i \in \mathcal{W}} c^{\text{spill}} q_{it}^{\text{RT}} + \sum_{i \in \mathcal{D}} c^{\text{shed}} q_{it}^{\text{RT}} \quad (\text{EC.22a})$$

$$\text{s.t. } \underline{Q}_i \leq q_{it}^* + q_{it}^{\text{RT}} \leq \bar{Q}_i, \forall t, \forall i \in \mathcal{F} \quad (\text{EC.22b})$$

$$-\Delta_i \leq q_{it}^* + q_{it}^{\text{RT}} \leq \bar{\Delta}_i, \forall t > 1, \forall i \in \mathcal{F} \quad (\text{EC.22c})$$

$$-\frac{1}{\eta_i^C} \bar{Q}_i^C \leq q_{it}^* + q_{it}^{\text{RT}} \leq \eta_i^D \bar{Q}_i^D, \forall t, \forall i \in \mathcal{S} \quad (\text{EC.22d})$$

$$\underline{E}_i \leq E_i^0 - \left(\sum_{t'=1}^t q_{it'}^* + q_{it'}^{\text{RT}} \right) \leq \bar{E}_i, \forall t, \forall i \in \mathcal{S} \quad (\text{EC.22e})$$

$$E_i^0 - \underline{B}_i \leq E_i^0 - \left(\sum_{t'=1}^t q_{it'}^* + q_{it'}^{\text{RT}} \right) \leq E_i^0 + \bar{B}_i, \forall i \in \mathcal{S} \quad (\text{EC.22f})$$

$$0 \leq q_{it}^{\text{RT}} \leq \hat{q}_{it} - \hat{\xi}_{it}, \forall t, \forall i \in \mathcal{W} \quad (\text{EC.22g})$$

$$-\hat{q}_{it} \leq q_{it}^{\text{RT}} \leq 0, \forall t, \forall i \in \mathcal{D} \quad (\text{EC.22h})$$

$$-\underline{Q}_i^R \leq q_{it}^{\text{RT}} \leq \bar{Q}_i^R, \forall t, \forall i \in \mathcal{F} \cup \mathcal{S} \quad (\text{EC.22i})$$

$$\sum_{i \in \mathcal{I} \setminus \mathcal{W}} q_{it}^{\text{RT}} = \mathbb{1}^\top \hat{\boldsymbol{\xi}}_t + \sum_{i \in \mathcal{W}} q_{it}^{\text{RT}}, \forall t \quad (\text{EC.22j})$$

$$-\bar{s}_\ell \leq \sum_{n \in \mathcal{N}} [\boldsymbol{\Psi}]_{(\ell, n)} \left(\sum_{i \in \mathcal{I}_n} {q_{it}}^* + q_{it}^{\text{RT}} \right) \leq \bar{s}_\ell, \forall t, \forall \ell \in \mathcal{L} \quad (\text{EC.22k})$$

For \mathcal{M}^{cc} , these additional constraints restrict the real-time adjustments:

$$q_{it}^{\text{RT}} = \mathbb{1}^\top \hat{\boldsymbol{\xi}}_t \alpha_{it}^*, \forall t, \forall i \in \mathcal{F} \quad ; \quad q_{it}^{\text{RT}} = \mathbb{1}^\top \hat{\boldsymbol{\xi}}_t \gamma_{it}^*, \forall t, \forall i \in \mathcal{S}. \quad (\text{EC.22l})$$

References

- Bienstock D, Chertkov M, Harnett S (2014) Chance-constrained optimal power flow: Risk-aware network control under uncertainty. *SIAM Review* 56(3):461–495.
- Borraz-Sánchez C, Bent R, Backhaus S, Hijazi H, Hentenryck PV (2016) Convex relaxations for gas expansion planning. *INFORMS Journal on Computing* 28(4):645–656.
- Byeon G, Van Hentenryck P (2020) Unit commitment with gas network awareness. *IEEE Transactions on Power Systems* 35(2):1327–1339.
- Farivar M, Low SH (2013) Branch flow model: Relaxations and convexification-Part I. *IEEE Transactions on Power Systems* 28(3):2554–2564.
- Georghiou A, Kuhn D, Wiesemann W (2019) The decision rule approach to optimization under uncertainty: methodology and applications. *Computational Management Science* 16(4):545–576.
- Georghiou A, Wiesemann W, Kuhn D (2015) Generalized decision rule approximations for stochastic programming via liftings. *Mathematical Programming* 152(1):301–338.
- Xie W, Ahmed S, Jiang R (2019) Optimized bonferroni approximations of distributionally robust joint chance constraints. *Mathematical Programming* 1–34. URL <https://doi.org/10.1007/s10107-019-01442-8>

[Pub. B] Exploring Market Properties of Policy-based Reserve Procurement for Power Systems

Authors:

Anubhav Ratha, Jalal Kazempour, Ana Virag, and Pierre Pinson

Published in:

Proceedings of 2019 IEEE 58th Conference on Decision and Control (CDC)

DOI:

10.1109/CDC40024.2019.9029777

Exploring Market Properties of Policy-based Reserve Procurement for Power Systems

Anubhav Ratha, Jalal Kazempour, Ana Virag and Pierre Pinson

Abstract—This paper proposes a market mechanism for co-optimization of energy and reserve procurement in day-ahead electricity markets with high shares of renewable energy. The single-stage chance-constrained day-ahead market clearing problem takes uncertain wind in-feed into account, resulting in optimal day-ahead dispatch schedule and an affine participation policy for generators for the real-time reserve provision. Under certain assumptions, the chance-constrained market clearing is reformulated as a convex quadratic program. Using tools from equilibrium modeling and variational inequalities, we explore the existence and uniqueness of a Nash equilibrium. Under the assumption of perfect competition in the market, we evaluate the satisfaction of desirable market properties, namely cost recovery, revenue adequacy, market efficiency, and incentive compatibility. To illustrate the effectiveness of the proposed market clearing, it is benchmarked against a deterministic co-optimization of energy and reserve procurement. Biased and unbiased out-of-sample simulation results for a power systems test case highlight that the proposed market clearing results in lower expected system operations cost than the deterministic benchmark, without the loss of any desirable market properties.

I. INTRODUCTION

Real-time balancing between supply and demand of electricity is challenging for the operation of power systems with high shares of intermittent renewable energy sources such as wind energy. Operational reserves for power systems are services traded in the market, in addition to energy, which ensure that deviations of actual wind power production from its day-ahead forecasts can be mitigated during real-time operation. Technical challenges aside, electricity markets also need to evolve such that cost-efficient market-based procurement and activation of reserves can be achieved.

Market-based procurement of reserves has been a topic of great interest in recent years, see [1], [2]. In current practice, illustrated in Figure 1a, the Market Operator (MO) estimates a system-wide parameter, Minimum Reserve Requirement (MRR) which is the minimum reserve capacity that must be procured to ensure a secure and efficient real-time balancing. Derived either from empirical studies or through probabilistic analysis of uncertainty [3], the MRR is then allocated among available flexible generators in a reserve capacity scheduling

The work of A. Ratha was supported by a Ph.D. grant provided by the Flemish Institute for Technological Research (VITO) and scholarship from Technical University of Denmark (DTU).

A. Ratha, J. Kazempour and P. Pinson are with the Department of Electrical Engineering, Technical University of Denmark, Lyngby, Denmark. {arath, seykaz, ppin}@elektro.dtu.dk

A. Ratha and A. Virag are with the Flemish Institute of Technological Research (VITO), Boeretang 200, 2400 Mol, Belgium and with EnergyVille, ThorPark 8310, 3600 Genk, Belgium. {anubhav.ratha, ana.virag}@vito.be

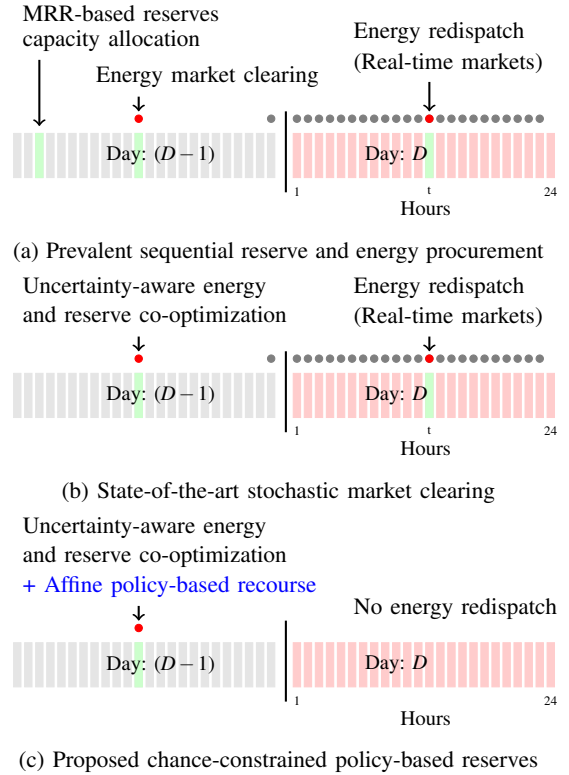


Fig. 1: Comparison of market clearing mechanisms for energy and reserve. Each (•) represents a market clearing.

market prior to the day-ahead market clearing¹. Finally, energy redispatch cost arises due to real-time markets that are necessary to activate the reserve energy from flexible generators to exactly meet the deviations. Faced with the situation to integrate an increasing amount of intermittent generation, over-estimation of MRR and thereby over-dimensioning of reserves has become a practice that increases the cost of operating power systems.

With the strong coupling that exists between the supply of energy and provision of reserves, recent studies have argued for co-optimization of energy and reserves in day-ahead markets [5], shown in Figure 1b. Primarily, two research streams have shaped this discussion. The first adopts scenario-based stochastic programming methods, for example in [6] and [7], to select reserves in the day-ahead stage such that the cost of activated reserves during real-time is optimal for the

¹This practice is followed by several European electricity markets (except a few markets such as the Italian electricity market) [4]. Markets in the US follow a deterministic co-optimization to procure energy and reserves, similar to the benchmark discussed in Case Study (Section IV).

expected realization of uncertainty and feasible for all the scenarios in the sample set considered. A very large number of scenarios is required to represent the uncertainty well and to ensure good out-of-sample performance, at the cost of higher computational need. The other research stream uses robust optimization techniques, such as in [8], [9] and [10], to allocate and operate reserves such that the cost of system operation is optimal with respect to the *worst-case* outcome and is feasible for any outcome of uncertainty within a parameterized uncertainty set. A market for reserves based on *control policies* was first proposed in [8], built upon a robust optimization model. While introducing computational ease, this approach by design results in a conservative solution and relies on meticulous study of uncertainty sets. Despite the new market direction introduced by [8], the market properties and pricing scheme were not elaborated upon.

In this paper, inspired by the control policy-based reserves discussed in [8], we propose a market clearing mechanism based on chance-constrained programming that co-optimizes energy and reserves at the day-ahead stage, as shown in Figure 1c. Chance-constrained programming, as highlighted in [11], provides a practical approach addressing drawbacks of the aforementioned techniques. Although it necessitates an additional step of convexification of chance constraints (see [12], [13]), it exhibits good out-of-sample performance and adjustable conservativeness at low computational cost. Based on the effectiveness of linear decision rules in decision-making under uncertainty, as examined in [14], we select an affine reserve policy such that participation in reserve activation during real-time operation stage is a linear function of the total balancing need. In addition to the optimal dimensioning of reserves, policy-based procurement of reserves has the advantage of resulting in efficient pricing for the reserve services while removing the requirement of real-time markets for reserve activation and associated energy redispatch cost. Under the assumption of perfect competition, aided by a study of Nash equilibria using tools from variational inequalities [15] in our proposed market clearing, we explore the existence and uniqueness of market equilibrium and the satisfaction of desirable market properties, namely cost recovery for agents, revenue adequacy for the MO, market efficiency and incentive compatibility [16].

We follow the analytical convexification of probabilistic chance constraints, introduced in [11], which results in a conic programming problem. Further, we use the direction suggested in [17] to simplify the conic constraints to linear formulations. In a case study built around a power system with a high share of installed wind power capacity and using biased and unbiased out-of-sample simulations, we benchmark the proposed market clearing method against a deterministic power and reserve co-optimization. This enables us to quantify the reduction in expected total system operations cost by the adoption of our proposed market clearing, under adverse realizations of uncertainty.

The paper is organized as follows: section II presents the proposed co-optimization of energy and reserves, stating the underlying assumptions and discussing its mathemati-

cal interpretations as an equilibrium problem and a non-cooperative game. Section III evaluates the satisfaction of market properties, while results of the numerical case study are presented and discussed in section IV. Finally, conclusions and future work are discussed in section V.

II. PROBLEM FORMULATION

The following considers a single-node power system comprising of a set of flexible generators, $g \in \mathcal{G}$, a set of wind farms, $k \in \mathcal{K}$, and an inflexible aggregated load, D .

A. Preliminaries

It is assumed that perfect competition exists in the market, such that no market participant exhibits strategic behavior. The wind farms are assumed to have zero marginal cost of production and excess wind spillage is considered free. Further, uncertainty in the form of wind forecast errors is considered to be the only source of uncertainty in the system. To avoid non-convexities introduced by the commitment status of generators, it is assumed that only scheduled generators participate in the day-ahead market clearing. The value of lost load as well as the price caps for the day-ahead market prices is considered to be €500/MWh.

B. Modeling of Uncertainty

In the day-ahead market clearing stage, forecast errors in power production from the wind farm k are modeled to follow a zero-mean Normal distribution, $\mathcal{N}(0, \sigma_k)$ centered around the best available point forecast, \hat{W}_k . The value of σ_k should be estimated from historical forecast errors for each wind farm location and time of the day.

Assumption 1: The standard deviations of the zero-mean normally distributed random forecast errors of wind farms, $\sigma_k, \forall k \in \mathcal{K}$, are temporally and spatially uncorrelated with respect to hours of the day and among wind farm sites, respectively.

Remark 1: The assumption of spatial independence of forecast errors is realistic for markets operating over a large geographical area, as discussed in [11]. The absence of temporal correlation is an assumption adopted in this paper to allow for hourly decoupling of the problem.

Under Assumption 1, the total error or deviation during real-time is defined as

$$\Delta = \sum_{k \in \mathcal{K}} \delta_k, \quad (1)$$

where δ_k refers to the error in forecast for the wind farm k . As a result, the uncertain parameter Δ is assumed to be drawn from a multivariate Normal distribution, $\mathcal{N}(\mathbf{0}_{N_k}, \Sigma)$, where $\Sigma = \text{diag}(\sigma_1^2, \sigma_2^2, \dots, \sigma_{N_k}^2)$.

C. Chance-constrained Policy-based Reserves

Considering α_g as a participation factor in the provision of reserves by generator g , we define an affine reserve policy such that when activated in real-time, the total generation from g is given by $\tilde{p}_g = p_g - \Delta\alpha_g$.

In the proposed day-ahead market clearing mechanism, optimal hourly reserve policies characterized by α_g , in

addition to the nominal hourly energy dispatch, p_g for each flexible generator are decided by the centralized MO. The reserve policies, which are then activated during real-time operation, define each generator's participation in the imbalance mitigation. Facing the uncertainty in wind power forecast errors Δ , MO's objective is to minimize the *expected cost* of operating the power system. We consider quadratic costs of generation and simplify the probabilistic expectation term in the objective function, using the zero-mean property of forecast errors, as discussed in [11]. Further, we consider a single-node model of the transmission grid. The chance-constrained optimization problem solved by the MO for joint clearing of energy and reserves is formulated as

$$\min_{p_g, \alpha_g} \sum_{g \in \mathcal{G}} \left[C_g^Q [p_g^2 + (\mathbf{e}^\top \Sigma \mathbf{e}) \alpha_g^2] + C_g^L p_g \right] \quad (2a)$$

$$\text{s.t.} \quad \sum_{g \in \mathcal{G}} p_g + \sum_{k \in \mathcal{K}} \hat{W}_k = D \quad (2b)$$

$$\sum_{g \in \mathcal{G}} \alpha_g = 1 \quad (2c)$$

$$\mathbb{P}[p_g - \Delta \alpha_g \geq 0] \geq (1 - \varepsilon_g), \quad \forall g \in \mathcal{G} \quad (2d)$$

$$\mathbb{P}[p_g - \Delta \alpha_g \leq p_g^{\max}] \geq (1 - \varepsilon_g), \quad \forall g \in \mathcal{G} \quad (2e)$$

$$\mathbb{P}[\Delta \alpha_g \leq R_g^{\text{DN,max}}] \geq (1 - \varepsilon_g), \quad \forall g \in \mathcal{G} \quad (2f)$$

$$\mathbb{P}[-\Delta \alpha_g \leq R_g^{\text{UP,max}}] \geq (1 - \varepsilon_g), \quad \forall g \in \mathcal{G} \quad (2g)$$

$$0 \leq \alpha_g \leq 1, \quad \forall g \in \mathcal{G}, \quad (2h)$$

where C_g^Q and C_g^L are the quadratic and linear production costs of generator g and $\mathbf{e} \in \mathbb{R}^{N_k}$ is a vector of all ones. Further, p_g^{\max} , $R_g^{\text{DN,max}}$ and $R_g^{\text{UP,max}}$ are the maximum production capacity, maximum downward reserve capacity and maximum upward reserve capacity available with generator g , respectively. $\mathbb{P}[\cdot]$ denotes probability and ε_g is the probability of the output from generator g to exceed the maximum and minimum limits of production and reserve capacity.

Constraint (2b) ensures the supply-demand balance for available point forecasts of wind power production, whereas (2c) ensures that the total deviation from point forecasts is exactly mitigated in real-time. These two constraints are deterministic and independent of wind power production realizations, thus ensuring security of supply for the inflexible demand for all realizations of the uncertainty.

Chance constraints (2d)-(2g) limit the probability of violation of bounds on net generation and activated reserves for all realizations of the uncertain parameter Δ to at most ε_g . The choice of risk parameter ε_g influences the conservativeness of the market clearing solution, with smaller values leading to a higher cost of operation. To study properties of the market clearing mechanism (2), we now introduce a linearized reformulation of the chance constraints inspired by [18], by adopting the following assumption.

Assumption 2: The participation factors, $\alpha_g, \forall g \in \mathcal{G}$, characterizing the affine reserve policy are non-negative, as enforced by (2h).

Remark 2: While it is intuitive to assume that α_g should be considered non-negative, it may be beneficial to drop this assumption when working with a more realistic power

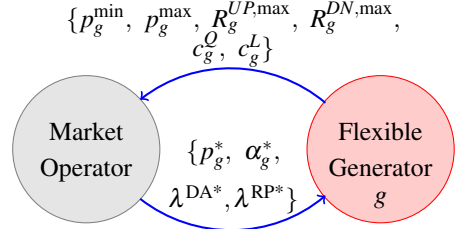


Fig. 2: Interaction between a flexible generator g and the market operator. Superscript * denotes optimal values.

system model that considers the transmission network or has elements such as energy storage. In that case, the resulting problem is a second-order cone program, evaluating the market properties of which is left for future work.

Under Assumptions 1 and 2, using [19, Theorem 10.4.1], the problem (2) can be exactly reformulated as a convex quadratic program in (p_g, α_g) , denoted by \mathcal{P}_{cc} , i.e.,

$$\min_{p_g, \alpha_g} \sum_{g \in \mathcal{G}} \left[C_g^Q [p_g^2 + (\mathbf{e}^\top \Sigma \mathbf{e}) \alpha_g^2] + C_g^L p_g \right] \quad (3a)$$

$$\text{s.t.} \quad \sum_{g \in \mathcal{G}} p_g + \sum_{k \in \mathcal{K}} \hat{W}_k = D : \lambda^{\text{DA}} \quad (3b)$$

$$\sum_{g \in \mathcal{G}} \alpha_g = 1 : \lambda^{\text{RP}} \quad (3c)$$

$$p_g - \Phi_{(1-\varepsilon_g)}^{-1} \alpha_g \sqrt{(\mathbf{e}^\top \Sigma \mathbf{e})} \geq 0, \quad \forall g \in \mathcal{G} \quad (3d)$$

$$p_g + \Phi_{(1-\varepsilon_g)}^{-1} \alpha_g \sqrt{(\mathbf{e}^\top \Sigma \mathbf{e})} \leq p_g^{\max}, \quad \forall g \in \mathcal{G} \quad (3e)$$

$$-\Phi_{(1-\varepsilon_g)}^{-1} \alpha_g \sqrt{(\mathbf{e}^\top \Sigma \mathbf{e})} \leq R_g^{\text{DN,max}}, \quad \forall g \in \mathcal{G} \quad (3f)$$

$$\Phi_{(1-\varepsilon_g)}^{-1} \alpha_g \sqrt{(\mathbf{e}^\top \Sigma \mathbf{e})} \leq R_g^{\text{UP,max}}, \quad \forall g \in \mathcal{G} \quad (3g)$$

$$0 \leq \alpha_g \leq 1, \quad \forall g \in \mathcal{G}, \quad (3h)$$

where $\Phi_{(\cdot)}^{-1}$ is the inverse cumulative distribution function or the quantile function of the standard Normal distribution $\mathcal{N}(0, 1)$. The risk parameter ε_g is chosen from the domain $[0, 0.5]$, such that $\Phi_{(1-\varepsilon_g)}^{-1}$ is always positive [18]. Note that all constraints are linear.

In problem \mathcal{P}_{cc} , the dual variables of constraints (3b) and (3c), provide the market clearing price for energy, λ^{DA} and reserve policies, λ^{RP} , which are then used for remuneration of the generators for energy p_g and reserve participation α_g , respectively. The interaction between a flexible generator, g and the market operator is illustrated in Figure 2.

In practice, it can be expected that hour-ahead of real-time operation, when the uncertainty in forecast is considerably reduced compared to the day-ahead stage, the market operator broadcasts the *best estimate* of “realized forecast errors” Δ which is used by flexible generators with non-zero α_g to adjust their real-time production for the next hour. Any remaining instantaneous errors are considered to be handled by primary frequency control or spinning reserves. This eliminates the need for an additional real-time balancing market, prevalent in current practice, in the proposed policy-based market clearing mechanism.

D. Mathematical Interpretations of Problem \mathcal{P}_{cc}

1) *As an equilibrium problem:* In alignment with the discussions in [20] and [21], problem \mathcal{P}_{cc} can be expressed as an equilibrium problem, wherein each market player solves a profit maximization problem while being connected through market clearing conditions (supply-demand balance). For the flexible generators, the profit maximization problem is

$$\forall g \in \mathcal{G} \begin{cases} \max_{p_g, \alpha_g} & (\lambda^{DA} p_g + \lambda^{RP} \alpha_g) \\ & - [C_g^Q (p_g^2 + (\mathbf{e}^\top \Sigma \mathbf{e}) \alpha_g^2) + C_g^L p_g] \\ \text{s.t.} & (3d) - (3h). \end{cases} \quad (4)$$

Unlike the flexible generators, the wind farms have no profit maximization strategy considering they have a zero cost of production and no cost associated with spillage of excess wind. Similarly, inflexible demand is considered to have no profit maximization role in problem \mathcal{P}_{cc} . However, the MO enforces the constraints (3b) and (3c), which are the coupling constraints that connect the flexible generators, wind farms and the inflexible demand.

2) *As a non-cooperative game:* The optimization problem \mathcal{P}_{cc} can be interpreted as a non-cooperative game among two sets of players. First, the flexible generators $g \in \mathcal{G}$, while operating within constraints of their production and reserve capacities, try to maximize their profits (or minimize their costs) from participation in the market for energy and reserves. Second, the MO who acts as a “price setter” to ensure that the market price for energy and reserves are set at as low values as possible, so that the inflexible demand D can be met at the lowest cost possible.

We define $x_g = [p_g \ \alpha_g]^\top$ as the decision vector for the flexible generator g , such that $x_g \in K_g$ where $K_g \subset \mathbb{R}_+^2$ is its strategy set, from which its choices for the bid quantity p_g and participation factor α_g are drawn. Similarly, we define $\Lambda = [\lambda^{DA} \ \lambda^{RP}]^\top$ as the decision vector for the MO, such that $\Lambda \in K_{MO}$ where $K_{MO} \subset \mathbb{R}_+^2$. The cost function for the flexible generator g can thus be expressed as

$$J_g(x_g, \Lambda) = (x_g^\top Q_g x_g + L_g^\top x_g) - \Lambda^\top x_g, \quad \forall x_g \in K_g, \quad (5)$$

where Λ denotes cleared market prices and represents decisions made by all other participants of the game i.e. the MO and flexible generators other than g , in the cost function for g .

The costs $Q_g = \begin{bmatrix} C_g^Q & 0 \\ 0 & C_g^Q (\mathbf{e}^\top \Sigma \mathbf{e}) \end{bmatrix}$ and $L_g = \begin{bmatrix} C_g^L \\ 0 \end{bmatrix}$ represent the quadratic and linear costs for g .

Similarly, the MO is subject to a cost function which can be expressed as

$$J_{MO}(\Lambda, x_g) = S^\top \Lambda, \quad \forall \Lambda \in K_{MO}, \quad (6)$$

where $S = \begin{bmatrix} -\sum_{g \in \mathcal{G}} p_g - \sum_{k \in \mathcal{K}} \hat{W}_k + D \\ -\sum_{g \in \mathcal{G}} \alpha_g + 1 \end{bmatrix}$ represents the decisions made by other players, i.e. all flexible generators $g \in \mathcal{G}$.

III. EVALUATION OF MARKET PROPERTIES

In this section, the problem definition and interpretations presented in section II are used to evaluate market properties of problem \mathcal{P}_{cc} .

A. Existence and Uniqueness of Nash equilibrium (NE)

Let $\Gamma(\mathcal{Z}, K, \{J_i\}_{i \in \mathcal{Z}})$ denote the non-cooperative game among the flexible generators and the market operator, where $\mathcal{Z} = (\mathcal{G} \cup \{MO\})$ denotes the set of all players and $K = \prod_i K_i = (K_1 \times K_2 \times \dots \times K_{N_g} \times K_{MO})$ denotes the strategy set for the game. Further, the decision variables of all players can be stacked to define a simultaneous strategy vector $z = [x_1^\top \dots x_{N_g}^\top \ \Lambda^\top]^\top$, such that $z \in \mathbb{R}^{2(N_g+1)}$ contains the strategy decisions of each of the players as a response to other players’ actions.

Proposition 1: For the non-cooperative game among flexible generators and the market operator, $\Gamma(\mathcal{Z}, K, \{J_i\}_{i \in \mathcal{Z}})$, a Nash equilibrium exists.

Proof: A simultaneous strategy vector $z^* \in K$ is a Nash equilibrium if and only if

$$J_i(z_i^*, z_{-i}^*) \leq J_i(z_i, z_{-i}^*), \quad \forall z_i \in K_i, \quad \forall i \in \mathcal{Z}. \quad (7)$$

To prove that Nash equilibria exist for the game Γ , we employ a theorem presented in [22, Theorem 1]. In the game Γ , each flexible generator g has a strategy set K_g formed by the upper and lower bounds of production and reserve capacities, while the market operator has a strategy set K_{MO} which is formed by the non-negativity bounds as well as price caps set for the market clearing. This satisfies the condition of compactness and convexity for K_i . Further, the cost function J_g in equation (5) is quadratic and thus, continuous over z and convex over x_g for fixed values of $x_{g'} = \bar{x}_{g'}$, $\forall g' \in (\mathcal{G} - \{g\})$ and $\Lambda = \bar{\Lambda}$. Likewise, the market operator’s cost function J_{MO} , given by equation (6) is linear and continuous in z and convex over Λ for fixed values of $x_g = \bar{x}_g$, $\forall g \in \mathcal{G}$. From [22, Theorem 1], this proves that at least one Nash equilibrium exists for the game Γ . ■

The vector(s) z^* are a set of strategies for the i players of the game Γ in which each player chooses the *best response* to other players’ decisions, implying that no player can lower their cost by unilaterally deviating their action from z_i^* to any other feasible point, \tilde{z}_i .

Proposition 2: For the non-cooperative game among flexible generators and market operator, $\Gamma(\mathcal{Z}, K, \{J_i\}_{i \in \mathcal{Z}})$ a unique Nash equilibrium exists.

Proof: This is proven by employing tools from Variational Inequalities (VIs) and their equivalence with Nash equilibria. For the game Γ , under the assumption that the game is played only by market players who have been dispatched or committed, the strategy sets K_i for flexible generators are compact, convex and nonempty. Further, as discussed in Proposition 1, the cost functions $J_i(z_i, z_{-i})$ for every fixed $z_{-i} \in K_{-i}$ are differentiable. Upon satisfaction of the above conditions, [15, Proposition 1.4.2] allows us to express the problem of finding Nash equilibria for Γ as a VI(F, K) problem with

$$F(z) = \begin{bmatrix} \nabla_1 J_1(z_1, z_{-1}) \\ \vdots \\ \nabla_{N_g} J_{N_g}(z_{N_g}, z_{-N_g}) \\ \nabla_{MO} J_{MO}(z_{MO}, z_{-MO}) \end{bmatrix} \quad (8)$$

and $K = \prod_i K_i = (K_1 \times K_2 \times \cdots \times K_{N_g} \times K_{MO})$, as defined before. The vector $F(z) \in \mathbb{R}^{2(N_g+1)}$ is also referred to as the “game map” for Γ . To prove the singleton nature of the solution set $SOL(F, K)$ to the $VI(F, K)$ (and by equivalence, as per [15, Proposition 1.4.2], uniqueness of Nash equilibria for Γ), we compute the Jacobian, $JF(z) \in \mathbb{R}^{2(N_g+1) \times 2(N_g+1)}$ of the game map, presented in Appendix A. As it can be observed, $JF(z)$ is symmetric which implies that there exists an equivalent optimization problem solving $VI(K, F)$, whose first-order optimality conditions are given by $JF(z)$. This optimization problem is identical to \mathcal{P}_{cc} which has a convex quadratic objective function and thus, has a unique minima. Thus, by equivalence of the optimization problem \mathcal{P}_{cc} with the $VI(K, F)$ and game Γ (per [15, Proposition 1.4.2]), we show that Γ has a unique Nash equilibrium. ■

B. Desirable Market Properties

Building further on the discussion regarding existence and uniqueness of Nash equilibria, the following evaluates the satisfaction of the desirable market properties [16] by the solution to problem \mathcal{P}_{cc} .

Proposition 3 (Cost recovery for flexible generators): An optimal solution to \mathcal{P}_{cc} ensures a non-negative payoff for the flexible generators under all possible market clearing outcomes and uncertainty realizations.

Proof: Mathematically, the non-negativity of payoff for flexible generators holds true if, at the optimal solution

$$(\lambda^{DA*} p_g^* + \lambda^{RP*} \alpha_g^*) - [C_g^Q (p_g^{*2} + (\mathbf{e}^\top \Sigma \mathbf{e}) \alpha_g^{*2}) + C_g^L p_g^*] \geq 0, \forall g, \quad (9)$$

where the superscript * indicates the optimal values for p_g , α_g , λ^{DA} and λ^{RP} . To prove the satisfaction of condition (9), we first formulate the dual problem for each flexible generator’s profit maximization problem, discussed in (4). Defining a set of Lagrangian multipliers, $\Xi = \{\underline{\mu}_g, \bar{\mu}_g, \rho_g^{DN}, \rho_g^{UP}, \chi_g, \bar{\chi}_g\}$ for the constraints (3d)-(3h), the dual problem can be formulated as

$$\forall g \in \mathcal{G} \left\{ \begin{array}{ll} \min_{\Xi} & \bar{\mu}_g p_g^{\max} + \rho_g^{DN} R_g^{DN,\max} + \rho_g^{UP} R_g^{UP,\max} + \bar{\chi}_g \\ \text{s.t.} & -\lambda^{DA} + 2C_g^Q p_g + C_g^L - \underline{\mu}_g + \bar{\mu}_g = 0 : p_g \\ & -\lambda^{RP} + 2C_g^Q \alpha_g - \underline{\chi}_g + \bar{\chi}_g \\ & + \Phi_{(1-\epsilon_g)}^{-1} \sqrt{\mathbf{e}^\top \Sigma \mathbf{e}} (\underline{\mu}_g - \bar{\mu}_g) \\ & - \rho_g^{DN} + \rho_g^{UP} = 0 : \alpha_g \\ & \underline{\mu}_g, \bar{\mu}_g, \rho_g^{DN}, \rho_g^{UP}, \chi_g, \bar{\chi}_g \geq 0. \end{array} \right. \quad (10)$$

It should be noted that the dual problem (10) has an objective that is a sum of products of non-negative parameters and variables and thus, is always non-negative. Strong duality theory enforces primal (4) and dual (10) problems to have identical objective functions at optimal solution. Thus, (9) holds true for all market price and uncertainty outcomes. ■

Proposition 4 (Revenue adequacy for the MO): An optimal solution to \mathcal{P}_{cc} ensures that the market operator never incurs a financial deficit for all possible market clearing outcomes and uncertainty realizations.

Proof: At the optimal solution to problem \mathcal{P}_{cc} , we multiply the equality constraints (3b) and (3c) with the optimal market clearing prices ($\lambda^{DA*}, \lambda^{RP*}$) and subtract (3c) from (3b) to obtain the following

$$(\lambda^{DA*} D - \lambda^{RP*}) = \sum_{g \in \mathcal{G}} \lambda^{DA*} p_g^* + \sum_{k \in \mathcal{K}} \lambda^{DA*} \hat{W}_k - \sum_{g \in \mathcal{G}} \lambda^{RP*} \alpha_g^*. \quad (11)$$

The left-hand side of (11) is the total payment from loads less the reserve policy payments made to flexible generators by the market operator. Under any realization of wind forecast errors Δ in real-time, the right-hand side of (11) equals to the left-hand side considering that constraints (3b) and (3c) are strict equalities that are satisfied at the optimal solution. The MO, therefore, never incurs a financial deficit. ■

Proposition 5 (Market efficiency): Under the assumption of perfect competition, the market clearing problem \mathcal{P}_{cc} ensures maximization of social welfare, such that no market participant desires to deviate from the market outcomes.

Proof: In an efficient market, social welfare is maximized and no market participant desires to deviate from the market outcomes, meaning that each market player maximizes their profit at the optimal solution of \mathcal{P}_{cc} . This is proven, under the assumption of perfect competition among flexible generators, by the identical Karush-Kuhn-Tucker (KKT) optimality conditions of \mathcal{P}_{cc} and the equilibrium problem interpretation discussed in section II-D.1. The identical KKT conditions are presented in Appendix B. ■

Proposition 6 (Incentive compatibility): Under the assumption of perfect competition, the market clearing problem \mathcal{P}_{cc} is such that each player can maximize its objective just by acting according to its “true” preferences.

Proof: Incentive compatibility implies that it is optimal for each participant to offer their production and reserves at a price equal to their “true” production cost. We define a bid made by a flexible generator g to MO prior to market clearing \mathcal{P}_{cc} , $B_g = [(C_g^Q, C_g^L), x_g]$ as a true-cost bid if the tuple (C_g^Q, C_g^L) represents its true production cost. From the game interpretation of \mathcal{P}_{cc} discussed in section II-D.2, the cost function for generator g at optimal solution (x_g^*, Λ^*) is

$$J_g(x_g^*, \Lambda^*) = (x_g^{*\top} Q_g x_g^* + L_g^\top x_g^*) - \Lambda^{*\top} x_g^*, \forall x_g \in K_g. \quad (12)$$

If a generator were to bid, $\tilde{B}_g = [(\tilde{C}_g^Q, \tilde{C}_g^L), x_g]$ with a cost tuple $(\tilde{C}_g^Q, \tilde{C}_g^L)$ higher than its true-cost tuple, which is the only rational deviation from a true-cost bid, the resulting cost function at the solution is given by (13) below. Note that, under the assumption of perfect competition, the optimal market clearing prices Λ^* are independent of a single generator’s bid.

$$J_g(\tilde{x}_g^*, \Lambda^*) = (\tilde{x}_g^{*\top} Q_g \tilde{x}_g^* + L_g^\top \tilde{x}_g^*) - \Lambda^{*\top} \tilde{x}_g^*, \forall x_g \in K_g. \quad (13)$$

Comparing (13) with (12), we point out that $J_g(\tilde{x}_g^*, \Lambda^*) \geq J_g(x_g^*, \Lambda^*)$ because from the proof of Proposition 1, \tilde{x}_g^* is a feasible suboptimal value for x_g . Thus, true-cost bidding is the dominant strategy for flexible generators. ■

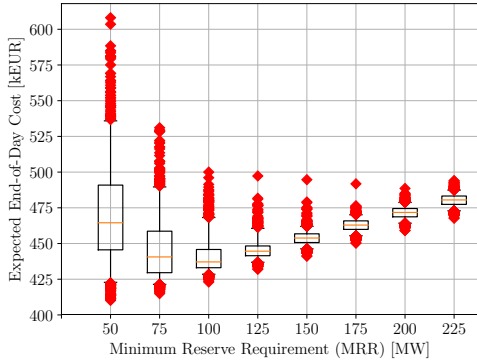


Fig. 3: Market clearing problem \mathcal{P}_{det} : Average expected end-of-day operations cost and its variability, considering different values of MRR.

IV. CASE STUDY

Data from a 24-bus system outlined in [23] is adapted to form a single-node electricity supply system with 6 wind farms. Each wind farm has an installed capacity of 200 MW and the power production from it has a zero-mean normally distributed forecast error with standard deviation, σ_k equal to 7.5% of installed capacity, as in [24]. Thus, problem \mathcal{P}_{cc} is solved considering the standard deviation of total forecast error as $\Sigma = \sum_k \sigma_k$. The value of risk parameter, ε_g for all generators is fixed as 0.05. The peak demand in the simulation time horizon of 24 hours is 2,650 MW. The cost and capacity data of the flexible generators as well as the demand data is available as an online appendix in [25].

To highlight benefits of the proposed policy-based reserve procurement and operation, a deterministic benchmark (\mathcal{P}_{det}) with energy and reserve co-optimization is set up. As formulated in Appendix C, the MO solves a day-ahead market clearing problem with an exogenous MRR, obtaining the optimal power dispatch as well as procuring the reserves needed. During real-time operation, through another market-based mechanism, reserves are activated based on the bounds defined by day-ahead reserve allocation. In the absence of currently operational joint clearing of energy and reserves in the European electricity markets, this benchmark reflects a natural extension to the sequential market clearing approach.

The parameter MRR for the problem \mathcal{P}_{det} is obtained by performing Out-of-Sample (OOS) simulations for 1000 scenarios of wind forecast errors to evaluate the expected end-of-day system operations cost while gradually increasing MRR, as shown in Figure 3. The orange line denotes the average value, boxes represent 25th and 75th percentiles and the whiskers extend to 5th and 95th percentiles. Red diamonds show the outliers. At low values of MRR, the expected cost of operation is observed to be high and has high variability due to load shedding in several scenarios of uncertainty realization, while at high values the cost increases due to the higher cost associated with over-dimensioning of reserve requirements. For comparison with results from the market clearing proposed in this paper, we fix the value of MRR at 200 MW.

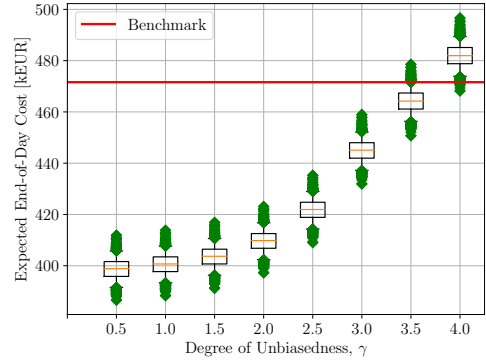


Fig. 4: Market clearing problem \mathcal{P}_{cc} : Average expected end-of-day operations cost and its variability, considering different values of γ .

First, biased OOS simulations² are performed wherein the 1000 scenarios for wind forecast errors are drawn from a Normal distribution identical to that assumed by the chance constraints in problem \mathcal{P}_{cc} for reformulation of the objective (3a) and chance constraints (3d)-(3g). It is expected that market clearing problem \mathcal{P}_{cc} should outperform \mathcal{P}_{det} , resulting in lower system operations cost. This stems from the fact that problem \mathcal{P}_{cc} provides an optimal solution with respect to this uncertainty distribution.

To study unbiased OOS simulations, considering the same set of scenarios, we replace the standard deviation, Σ in problem \mathcal{P}_{cc} with $(\gamma * \Sigma)$, such the parameter γ represents the degree of unbiasedness of the probability distribution assumed in \mathcal{P}_{cc} . Figure 4 shows the variation in expected end-of-day system operations cost with γ (green diamonds show the outliers). The red horizontal line indicates the average expected end-of-day cost for the benchmark market clearing \mathcal{P}_{det} , operating with an MRR, $M_R = 200$ MW. The case of $\gamma = 1$ is equivalent to the previously discussed biased OOS, considering that the probability distribution assumed in problem \mathcal{P}_{cc} is identical to actual wind forecast errors. For $\gamma < 1$, the problem \mathcal{P}_{cc} underestimates the actual wind forecast errors, resulting in lower costs of day-ahead reserve procurement. However, with the reserve control policy in place, the MO is able to successfully mitigate the imbalances in real-time at a low cost. For values of γ larger than 1, the problem \mathcal{P}_{cc} overestimates the actual wind forecast errors, thus resulting in higher costs of reserve procurement to ensure mitigation of imbalances in real-time. For $\gamma > 4$, we observed infeasibility of the market clearing problem \mathcal{P}_{cc} as we reach the limits of available reserve capacity from the generators to successfully mitigate the imbalance. Table I presents a comparison of average expected system operations cost for market clearing using problem \mathcal{P}_{det} with that using \mathcal{P}_{cc} for a selection of values of γ . As it can be observed, market clearing problem \mathcal{P}_{cc} leads to a reduction of 5.4% in the average expected end-of-day system operations cost

²Here, the notion of OOS simulations refers to the different second moments, Σ of the Normal distribution from which scenarios of actual wind forecast errors are drawn. In contrast, stochastic programming literature typically considers random scenarios drawn from other distributions as OOS.

TABLE I: Comparison between average expected costs obtained from \mathcal{P}_{det} and \mathcal{P}_{cc}

Costs [k€]	\mathcal{P}_{det} $M_R = 200 \text{ MW}$	\mathcal{P}_{cc} $\gamma = 0.5$	\mathcal{P}_{cc} $\gamma = 1.0$	\mathcal{P}_{cc} $\gamma = 3.0$
Operations	401.4	398.2	400.9	408.0
Reserves	70.2	0.6	2	38.1
Total	471.6	398.6	402.9	446.1
Change [%]	-	-15.5%	-14.6%	-5.4%

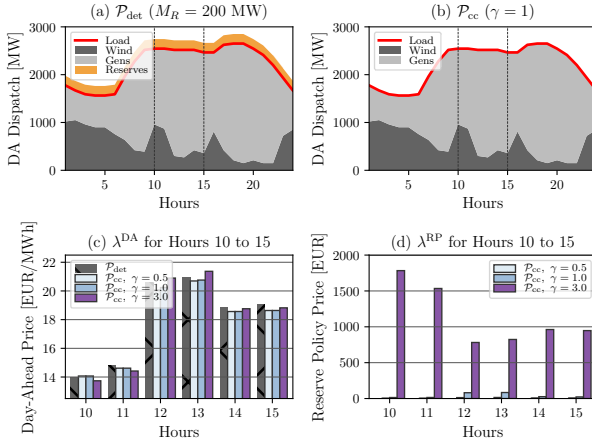


Fig. 5: \mathcal{P}_{det} , \mathcal{P}_{cc} : Day-ahead (DA) dispatch and market prices

compared to \mathcal{P}_{det} , even if the actual wind forecast errors are over-estimated by a factor of 3 ($\gamma = 3$). Results of the case study demonstrate the resilience of proposed market clearing problem \mathcal{P}_{cc} to large forecast errors within the normally distributed forecast error assumption.

A short discussion on the day-ahead market clearing outcomes of \mathcal{P}_{det} and \mathcal{P}_{cc} follows. Figures 5a and 5b show a comparison of the optimal dispatch of the flexible generators and wind farms to meet the inflexible load for \mathcal{P}_{det} and \mathcal{P}_{cc} . While reserve capacity is scheduled in the \mathcal{P}_{det} case, in \mathcal{P}_{cc} explicit capacity reserve procurement is replaced by control policies, characterized by α_g . Optimal day-ahead price for energy, λ^{DA} and for the reserve policies, λ^{RP} (in \mathcal{P}_{cc}) for Hours 10 through 15 are shown in Figures 5c and 5d. Hours with higher wind power forecast, $\sum_{k \in \mathcal{K}} \hat{W}_k$, result in lower prices, λ^{DA} for both P_{det} and P_{cc} , owing to the zero marginal cost of wind farms. Moreover, as observed in Figure 5d, higher values of the γ result in a higher price of reserve policies, λ^{RP} signifying the overestimation of actual wind forecast errors by the market clearing problem, \mathcal{P}_{cc} . Figure 6 shows the allocation of the participation factors, α_g for the same hours among the generators having available reserve capacity. It is observed that the more expensive generator G4 is allocated non-zero α_g in the hours with high share of wind and with higher values of γ .

V. CONCLUSION

We proposed a market clearing mechanism for day-ahead electricity markets that co-optimizes energy and control policy-based reserves using chance-constrained optimization techniques. Using tools from equilibrium modeling and VIs, we proved the existence and uniqueness of Nash equilibria for this market clearing. No desirable properties inherent

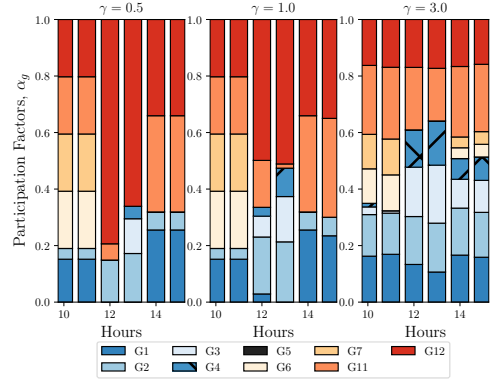


Fig. 6: Allocation of participation factors, α_g with γ

to the prevalent deterministic market clearing are lost in the proposed chance-constrained policy-based market clearing. Under assumptions of proper uncertainty modeling, we demonstrated the reduction in average expected system operations cost over a deterministic benchmark.

In future, the suggested non-requirement of energy redispatch should be further studied to determine its impact on system reliability and primary frequency control, considering that the estimation of the *true* moments of uncertainty is challenging. Evaluation of the properties of proposed policy-based reserve procurement considering the temporal and spatial correlation of uncertainty, a power system with congested line capacity limits and generic control policies defined to include other flexibility sources (e.g. demand response, energy storage) also remain topics for future work.

APPENDIX

A. Game Map for Γ

The Jacobian matrix, $JF(z)$, of the game map $F(z)$ for the non-cooperative game Γ , discussed in section III-A is

$$\begin{bmatrix} 2C_1^Q & 0 & \dots & 0 & 0 & -1 & 0 \\ 0 & 2C_1^Q(\mathbf{e}^\top \Sigma \mathbf{e}) & \dots & 0 & 0 & 0 & -1 \\ \vdots & \ddots & \ddots & \ddots & \ddots & \vdots & \vdots \\ 0 & 0 & \dots & 2C_{N_g}^Q & 0 & -1 & 0 \\ 0 & 0 & \dots & 0 & 2C_{N_g}^Q(\mathbf{e}^\top \Sigma \mathbf{e}) & 0 & -1 \\ -1 & 0 & \dots & -1 & 0 & 0 & 0 \\ 0 & -1 & \dots & 0 & -1 & 0 & 0 \end{bmatrix}.$$

B. KKTs of Optimization Problem \mathcal{P}_{cc}

Considering \mathcal{L} as the Lagrangian function for the optimization problem \mathcal{P}_{cc} , its KKT optimality conditions are given by (14). Its equivalent equilibrium problem (discussed in section II-D.1) has an identical set of KKT conditions.

$$(3b) - (3c) \quad (14a)$$

$$\frac{\partial \mathcal{L}}{\partial p_g} = 2C_g^Q p_g + C_g^L - \lambda^{\text{DA}} - \underline{\mu}_g + \bar{\mu}_g = 0, \quad \forall g \quad (14b)$$

$$\begin{aligned} \frac{\partial \mathcal{L}}{\partial \alpha_g} &= 2C_g^Q \alpha_g - \lambda^{\text{RP}} - \underline{\chi}_g + \bar{\chi}_g + \Phi_{(1-\varepsilon_g)}^{-1} \sqrt{\mathbf{e}^\top \Sigma \mathbf{e}} (\underline{\mu}_g \\ &\quad - \bar{\mu}_g - \rho_g^{\text{DN}} + \rho_g^{\text{UP}}) = 0, \quad \forall g \end{aligned} \quad (14c)$$

$$0 \leq (p_g - \Phi_{(1-\varepsilon_g)}^{-1} \alpha_g \sqrt{(\mathbf{e}^\top \Sigma \mathbf{e})}) \perp \underline{\mu}_g \geq 0, \forall g \quad (14d)$$

$$0 \leq (p_g^{\max} - p_g - \Phi_{(1-\varepsilon_g)}^{-1} \alpha_g \sqrt{(\mathbf{e}^\top \Sigma \mathbf{e})}) \perp \bar{\mu}_g \geq 0, \forall g \quad (14e)$$

$$0 \leq (R_g^{\text{DN},\max} + \Phi_{(1-\varepsilon_g)}^{-1} \alpha_g \sqrt{(\mathbf{e}^\top \Sigma \mathbf{e})}) \perp \rho_g^{\text{DN}} \geq 0, \forall g \quad (14f)$$

$$0 \leq (R_g^{\text{UP},\max} - \Phi_{(1-\varepsilon_g)}^{-1} \alpha_g \sqrt{(\mathbf{e}^\top \Sigma \mathbf{e})}) \perp \rho_g^{\text{UP}} \geq 0, \forall g \quad (14g)$$

$$0 \leq \alpha_g \perp \underline{\chi}_g \geq 0, \forall g \quad (14h)$$

$$0 \leq (1 - \alpha_g) \perp \bar{\chi}_g \geq 0, \forall g. \quad (14i)$$

C. Deterministic Benchmark, \mathcal{P}_{det}

The day-ahead deterministic co-optimization of energy and reserves solved by the MO is given in problem (15).

$$\min_{p_g, R_g} \sum_{g \in \mathcal{G}} [C_g^Q p_g^2 + C_g^L p_g + C_g^R R_g] \quad (15a)$$

$$\text{s.t.} \quad \sum_{g \in \mathcal{G}} p_g + \sum_{k \in \mathcal{K}} \hat{W}_k = D, \quad : \lambda^{\text{DA}} \quad (15b)$$

$$\sum_{g \in \mathcal{G}} R_g \geq M_R \quad (15c)$$

$$0 \leq p_g \leq p_g^{\max}, \forall g \in \mathcal{G} \quad (15d)$$

$$0 \leq R_g \leq R_g^{\max}, \forall g \in \mathcal{G} \quad (15e)$$

$$p_g + R_g \leq p_g^{\max}, \forall g \in \mathcal{G} \quad (15f)$$

$$p_g - R_g \geq 0, \forall g \in \mathcal{G}, \quad (15g)$$

where the MRR, M_R is an exogenous parameter, C_g^R denotes the cost of reserve procurement and (p_g, R_g) represents the set of power dispatch and reserve allocation for generator g . The real-time balancing market clearing, formulated in problem (16), activates the reserve energy from flexible generators, r_g , limited to the optimal reserve capacities R_g^* allocated day ahead (constraint (16c)). Further, considering that the actual forecast error Δ could take extreme values in some cases, real-time balancing allows for wind spillage, W_k^{sp} at zero cost and load shedding, D^{sh} at $C^{\text{VoLL}} = €500/\text{MWh}$.

$$\min_{r_g, D^{\text{sh}}, W_k^{\text{sp}}} \sum_{g \in \mathcal{G}} [C_g^Q (P_g^* + r_g)^2 + C_g^L (P_g^* + r_g)] + C^{\text{VoLL}} D^{\text{sh}} \quad (16a)$$

$$\text{s.t.} \quad \sum_{g \in \mathcal{G}} r_g = \Delta \quad (16b)$$

$$-R_g^* \leq r_g \leq R_g^*, \forall g \in \mathcal{G} \quad (16c)$$

$$0 \leq D^{\text{sh}} \leq D \quad (16d)$$

$$0 \leq W_k^{\text{sp}} \leq (\hat{W}_k + \delta_k), \forall k \in \mathcal{K}. \quad (16e)$$

REFERENCES

- [1] P. González, J. Villar, C. A. Díaz, and F. A. Campos, "Joint energy and reserve markets: Current implementations and modeling trends," *Electric Power Systems Research*, vol. 109, pp. 101–111, Apr. 2014.
- [2] J. Morales, M. Zugno, S. Pineda, and P. Pinson, "Electricity market clearing with improved scheduling of stochastic production," *European Journal of Operational Research*, vol. 235, pp. 765–774, Jun. 2014.
- [3] A. Papavasiliou, S. S. Oren, and R. P. O'Neill, "Reserve requirements for wind power integration: A scenario-based stochastic programming framework," *IEEE Transactions on Power Systems*, vol. 26, pp. 2197–2206, Nov. 2011.
- [4] R. Domínguez, G. Oggioni, and Y. Smeers, "Reserve procurement and flexibility services in power systems with high renewable capacity: Effects of integration on different market designs," *International Journal of Electrical Power & Energy Systems*, vol. 113, pp. 1014–1034, 2019.
- [5] A. Virág, A. Jokić, R. M. Hermans, and P. P. J. van den Bosch, "Combined bidding at power and ancillary service markets," in *8th International Conference on the European Energy Market (EEM)*, pp. 568–573, May 2011.
- [6] J. M. Morales, A. J. Conejo, and J. Perez-Ruiz, "Economic valuation of reserves in power systems with high penetration of wind power," *IEEE Transactions on Power Systems*, vol. 24, pp. 900–910, May 2009.
- [7] F. Abbaspourtorbati and M. Zima, "The Swiss reserve market: Stochastic programming in practice," *IEEE Transactions on Power Systems*, vol. 31, pp. 1188–1194, Mar. 2016.
- [8] J. Warrington, P. Goulart, S. Marithoz, and M. Morari, "Policy-based reserves for power systems," *IEEE Transactions on Power Systems*, vol. 28, pp. 4427–4437, Nov. 2013.
- [9] J. Warrington, C. Hohl, P. J. Goulart, and M. Morari, "Optimal unit commitment accounting for robust affine reserve policies," in *2014 American Control Conference*, pp. 5049–5055, Jun. 2014.
- [10] D. Bertsimas, E. Litvinov, X. A. Sun, J. Zhao, and T. Zheng, "Adaptive robust optimization for the security constrained unit commitment problem," *IEEE Transactions on Power Systems*, vol. 28, pp. 52–63, Feb. 2013.
- [11] D. Bienstock, M. Chertkov, and S. Harnett, "Chance-constrained optimal power flow: Risk-aware network control under uncertainty," *SIAM Review*, vol. 56, no. 3, pp. 461–495, 2014.
- [12] K. Margellos, P. Goulart, and J. Lygeros, "On the road between robust optimization and the scenario approach for chance constrained optimization problems," *IEEE Transactions on Automatic Control*, vol. 59, pp. 2258–2263, Aug. 2014.
- [13] A. Nemirovski, "On safe tractable approximations of chance constraints," *European Journal of Operational Research*, vol. 219, no. 3, pp. 707 – 718, 2012. Feature Clusters.
- [14] A. Georghiou, D. Kuhn, and W. Wiesemann, "The decision rule approach to optimization under uncertainty: Methodology and applications," *Computational Management Science*, Nov. 2018.
- [15] F. Facchinei and J.-S. Pang, *Finite-Dimensional Variational Inequalities and Complementarity Problems*. New York, NY: Springer New York, 2003.
- [16] F. C. Schweppe, M. C. Caramanis, R. D. Tabors, and R. E. Bohn, *Spot Pricing of Electricity*. Boston, MA: Springer US, 1988.
- [17] X. Kuang, Y. Dvorkin, A. J. Lamadrid, M. A. Ortega-Vazquez, and L. F. Zuluaga, "Pricing chance constraints in electricity markets," *IEEE Transactions on Power Systems*, vol. 33, pp. 4634–4636, Jul. 2018.
- [18] M. Lubin, Y. Dvorkin, and S. Backhaus, "A robust approach to chance constrained optimal power flow with renewable generation," *IEEE Transactions on Power Systems*, vol. 31, pp. 3840–3849, Sep. 2016.
- [19] A. Prékopa, *Convexity Theory of Probabilistic Constrained Problems*, vol. 324, pp. 301–317. Dordrecht, The Netherlands: Springer, 1995.
- [20] B. F. Hobbs, "Linear complementarity models of Nash-Cournot competition in bilateral and POOLCO power markets," *IEEE Transactions on Power Systems*, vol. 16, pp. 194–202, May 2001.
- [21] J. Kazempour, P. Pinson, and B. F. Hobbs, "A stochastic market design with revenue adequacy and cost recovery by scenario: Benefits and costs," *IEEE Transactions on Power Systems*, vol. 33, pp. 3531–3545, Jul. 2018.
- [22] J. B. Rosen, "Existence and uniqueness of equilibrium points for concave N-person games," *Econometrica*, vol. 33, pp. 520–534, 1965.
- [23] C. Ordoudis, P. Pinson, J. Morales González, and M. Zugno, *An Updated Version of the IEEE RTS 24-Bus System for Electricity Market and Power System Operation Studies*. Technical University of Denmark (DTU), 2016.
- [24] U. Focken, M. Lange, K. Monnich, H. Waldl, H. Beyer, and A. Luig, "Short-term prediction of the aggregated power output of wind farms - A statistical analysis of the reduction of the prediction error by spatial smoothing effects," *Journal of Wind Engineering and Industrial Aerodynamics*, vol. 90, pp. 231–246, Mar. 2002.
- [25] A. Ratha, J. Kazempour, A. Virág, and P. Pinson, "Online appendix for paper: Exploring market properties of policy-based reserve procurement for power systems," 2019. [Online]. Available: <https://doi.org/10.5281/zenodo.2595186>.

[Pub. C] Affine Policies for Flexibility Provision by Natural Gas Networks to Power Systems

Authors:

Anubhav Ratha, Anna Schwele, Jalal Kazempour, Pierre Pinson, Shahab Shariat Torbaghan, and Ana Virág

Published in:

Electric Power Systems Research (EPSR)

DOI:

10.1016/j.epsr.2020.106565

Affine Policies for Flexibility Provision by Natural Gas Networks to Power Systems

Anubhav Ratha^{*†}, Anna Schwele*, Jalal Kazempour*, Pierre Pinson*, Shahab Shariat Torbaghan[†] and Ana Virág[†]

* Center for Electric Power and Energy, Technical University of Denmark, Kgs. Lyngby, Denmark

{arath, schwele, seykaz, ppin}@elektro.dtu.dk

† Flemish Institute of Technological Research (VITO), Boeretang 200, 2400 Mol, Belgium

{anubhav.ratha, shahab.shariattorbaghan, ana.virag}@vito.be

Abstract—Using flexibility from the coordination of power and natural gas systems helps with the integration of variable renewable energy in power systems. To include this flexibility into the operational decision-making problem, we propose a distributionally robust chance-constrained co-optimization of power and natural gas systems considering flexibility from short-term gas storage in pipelines, i.e., linepack. Recourse actions in both systems, based on linear decision rules, allow adjustments to the dispatch and operating set-points during real-time operation when the uncertainty in wind power production is revealed. We convexify the non-linear and non-convex power and gas flow equations using DC power flow approximation and second-order cone relaxation, respectively. Our coordination approach enables a study of the mitigation of short-term uncertainty propagated from the power system to the gas side. We analyze the results of the proposed approach on a case study and evaluate the solution quality via out-of-sample simulations performed *ex-ante*.

Index Terms—Linear decision rules, Distributionally robust chance constraints, Linepack flexibility, Power and natural gas coordination, Second-order cone program.

I. INTRODUCTION

Natural gas-fired power plants (NGFPPs) typically provide operational flexibility to power systems with a high share of intermittent renewable energy. Short-term gas storage in natural gas pipelines, known as linepack, provides an additional source of flexibility [1] at no extra investment cost. Efficient procurement of flexibility from the natural gas system during day-ahead scheduling of power systems requires consideration of the operational constraints of the natural gas system. Further, with the increasing share of intermittent renewable energy sources in the power system, the need for flexibility and thereby, the interdependence between power and natural gas systems is becoming stronger [2]. As a result, the coordination between power and natural gas systems during the day-ahead dispatch has been a topic of research interest in recent years. For example, various levels of coordination and information exchange between the systems are discussed in [3], [4], while

The work of A. Ratha was supported by a Ph.D. grant provided by the Flemish Institute for Technological Research (VITO) and scholarship from Technical University of Denmark (DTU). The work of A. Schwele and J. Kazempour was supported by the Danish EUD Programme through the Coordinated Operation of Integrated Energy Systems (CORE) project under the grant 64017-0005.

[5], [6], [7], [8], [9] model full integration of the power with the natural gas system. The value of gas system related flexibility for the power system is quantified in [6] and [7] in a deterministic manner.

Increasing interactions between power and natural gas systems, however, result in the propagation of short-term uncertainty faced by power systems to the gas side. Prior works on the coordinated operation of power and natural gas systems have largely ignored this short-term uncertainty. This may result in additional recourse actions necessary during the real-time operation stage when the flexibility from the natural gas system is not correctly anticipated. Affine policies, built on the theory of linear decision rules, have been a preferred choice for day-ahead decision making, wherein nominal dispatch schedules along with the recourse actions for real-time operation are optimally decided [10]. In this paper, we introduce a unified framework to elicit flexibility based on affine policies from agents, e.g., power producers, natural gas suppliers as well as the network assets, i.e., linepack. Our affine policies are decided based on the features of uncertainty drawn from the historical measurements, with no distributional restriction imposed on the random variables.

Previous works discussing uncertainty-aware coordination between power and natural gas systems use stochastic programming approaches such as scenario-based [5], robust [8], and chance-constrained optimization [9]. Reference [5] proposes a two-stage stochastic program for the day-ahead and real-time operations of integrated power and natural gas system under uncertainty from renewable generation. In a similar direction, a robust dispatch framework is proposed in [8] which models uncertainty through intervals and extreme scenario approximation. Chance-constraints are introduced into the planning problem of the integrated power and natural gas system [9]. While scenario-based approaches [5] incur a high computational expense due to a large number of scenarios needed to characterize the uncertainty properly, robust approaches [8] often suffer from over-conservativeness of the solution due to the design objective to minimize worst-case cost. Distributionally robust chance-constrained formulation of the problem [11] allows for a tunable probabilistic violation of operational limits when facing extreme realizations of uncertainty which is characterized by an ambiguity set.

In this work, we adopt a distributionally robust chance-constrained optimization technique, considering its advantages over other stochastic programming approaches [11], to introduce a coordinated day-ahead dispatch of power and natural gas systems taking the flexibility provided by linepack into account. To the best of our knowledge, this is the first paper to bring linepack flexibility to the day-ahead dispatch problem, while modeling and mitigating the short-term uncertainty propagated from the power system to the natural gas system. Studying this uncertainty propagation opens new pathways for the endogenous valuation of the natural gas network as a provider of short-term flexibility to power systems. This could potentially result in the design of new market-based coordination mechanisms and market products enabling gas system agents and the network to play an active role in providing flexibility to the power system. From a methodological perspective, our main contribution is a tractable reformulation of distributionally robust chance constraints for the combined power and gas dispatch problem considering linepack.

The rest of this paper is organized as follows: Section II presents the distributionally robust chance-constrained power and natural gas dispatch problem. Section III discusses the solution methodology, which is then applied to a case study in Section IV. Finally, conclusions are drawn and the avenues for future work are discussed in Section V.

II. PROBLEM FORMULATION

A. Preliminaries

In the following, we introduce the operation of a coupled power and natural gas system, wherein power generated from dispatchable power plants $i \in \mathcal{I}$ and wind farms $j \in \mathcal{J}$ is used to meet the inelastic electricity demand from a set of loads $d \in \mathcal{D}$. The dispatchable generators comprise of NGFPPs $i \in \mathcal{G}$ and non-NGFPPs $i \in \mathcal{C}$, such that $\mathcal{G} \cap \mathcal{C} = \emptyset$ and $\mathcal{G} \cup \mathcal{C} = \mathcal{I}$. On the gas side, natural gas suppliers $k \in \mathcal{K}$, together with available linepack in the gas network, are dispatched to meet the natural gas demand from inelastic gas loads and the fuel needed by NGFPPs. The non-linear and non-convex power and gas flow equations are convexified using DC power flow approximation and second-order cone relaxation, respectively. We assume that wind power is available at zero marginal cost of production. Power produced by wind farms during real-time operation is the sole uncertainty source considered.

B. Uncertainty Model

For wind farm j , the day-ahead point forecast for time period $t \in \mathcal{T}$ is given by $W_{j,t}^{\text{PF}}$. The forecast error observed in real-time is assumed to be a random variable $\delta_{j,t}$, such that the overall system uncertainty can be characterized by $\Omega = [\delta_{11} \ \delta_{21} \ \dots \ \delta_{|\mathcal{J}|t} \ \dots \ \delta_{|\mathcal{J}||\mathcal{T}|}]^\top \in \mathbb{R}^{|\mathcal{J}||\mathcal{T}|}$, where \mathbb{R} is the set of real numbers and $|\cdot|$ is the cardinality operator over a set. We consider that Ω follows an unknown multivariate probability distribution $\mathbb{P} \in \Pi$, where Π is an ambiguity set defined as

$$\Pi = \{\mathbb{P} \in \Pi_0(\mathbb{R}^{|\mathcal{J}|}) : \mathbb{E}_{\mathbb{P}}[\Omega] = \mu^\Pi, \mathbb{E}_{\mathbb{P}}[\Omega\Omega^\top] = \Sigma^\Pi\}, \quad (1)$$

such that the family of distributions, $\Pi_0(\mathbb{R}^{|\mathcal{J}|})$ contains all probability distributions whose first and second-order moments are given by known parameters $\mu^\Pi \in \mathbb{R}^{|\mathcal{J}||\mathcal{T}|}$ and $\Sigma^\Pi \in \mathbb{R}^{|\mathcal{J}||\mathcal{T}| \times |\mathcal{J}||\mathcal{T}|}$, respectively. Further, $\mathbb{E}_{\mathbb{P}}[\cdot]$ denotes expectation with respect to the distribution \mathbb{P} and $(\cdot)^\top$ is the transpose operator. Without any loss of generality, we assume that the mean $\mu^\Pi = 0$ and that the covariance matrix Σ^Π can be empirically estimated from historical record of wind forecast errors. The structure of the positive semi-definite covariance matrix, Σ^Π is such that its diagonal blocks, comprised of sub-matrices, $\Sigma_t^\Pi \in \mathbb{R}^{|\mathcal{J}| \times |\mathcal{J}|}, \forall t \in \mathcal{T}$, capture the spatial correlation among the wind forecast errors in period t , while the off-diagonal blocks contain information about spatio-temporal correlation of the uncertain parameters.

With this description of uncertain wind forecast errors, the net deviation from the point forecasts of all wind farms in the time period t is $\mathbf{e}^\top \Omega_t$ where $\mathbf{e} \in \mathbb{R}^{|\mathcal{J}|}$ is a vector of all ones. The temporally collapsed random vector is formed as: $\Omega_t = F_t \Omega$, where $F_t \in \mathbb{R}^{|\mathcal{J}| \times |\mathcal{J}||\mathcal{T}|}$ is a *selector matrix* formed by blocks of null matrices $\mathbf{0} \in \mathbb{R}^{|\mathcal{J}| \times |\mathcal{J}|}$ and a single block of identity matrix $\mathbf{1} \in \mathbb{R}^{|\mathcal{J}| \times |\mathcal{J}|}$, starting at column $(|\mathcal{J}|(t-1) + 1), \forall t \in \mathcal{T}$. As a sign convention, $\mathbf{e}^\top \Omega_t > 0$ implies deficit of wind power available in the system during real-time operation stage as compared to the day-ahead forecast.

C. Uncertainty-Aware Power and Natural Gas Coordination

The proposed day-ahead coordinated electricity and natural gas model is a stochastic program, presented in (2) in the following. The objective function has a min-max structure such that the total *expected* system dispatch cost is minimized while the uncertain variable Ω draws from a probability distribution $\mathbb{P} \in \Pi$ that results in maximizing the expected cost of dispatch, i.e., the *worst-case* probability distribution.

$$\min_{\Theta_1} \max_{\mathbb{P} \in \Pi} \mathbb{E}_{\mathbb{P}} \left[\sum_{t \in \mathcal{T}} \left(\sum_{i \in \mathcal{C}} C_i^E \tilde{p}_{i,t} + \sum_{k \in \mathcal{K}} C_k^G \tilde{g}_{k,t} \right) \right] \quad (2a)$$

subject to

$$\mathbf{e}^\top \tilde{\mathbf{p}}_t + \mathbf{e}^\top (\mathbf{W}_t^{\text{PF}} - \Omega_t) = \mathbf{e}^\top \mathbf{D}_t^E, \quad \forall t, \quad (2b)$$

$$\tilde{\mathbf{P}}_t^{\text{inj}} = \Psi_{\mathbf{I}} \tilde{\mathbf{p}}_t + \Psi_{\mathbf{J}} (\mathbf{W}_t^{\text{PF}} - \Omega_t) - \Psi_{\mathbf{D}} \mathbf{D}_t^E, \quad \forall t, \quad (2c)$$

$$\begin{aligned} \min_{\mathbb{P} \in \Pi} \mathbb{P}[\{\Psi \tilde{\mathbf{P}}_t^{\text{inj}}\}_{(n,r)} \geq -\{\bar{\mathbf{F}}\}_{(n,r)}] \\ \geq (1 - \epsilon_{nr}), \quad \forall (n,r) \in \mathcal{L}, \quad \forall t, \end{aligned} \quad (2d)$$

$$\begin{aligned} \min_{\mathbb{P} \in \Pi} \mathbb{P}[\{\Psi \tilde{\mathbf{P}}_t^{\text{inj}}\}_{(n,r)} \leq \{\bar{\mathbf{F}}\}_{(n,r)}] \\ \geq (1 - \epsilon_{nr}), \quad \forall (n,r) \in \mathcal{L}, \quad \forall t, \end{aligned} \quad (2e)$$

$$\min_{\mathbb{P} \in \Pi} \mathbb{P}[\tilde{p}_{i,t} \geq \underline{P}_i] \geq (1 - \epsilon_i), \quad \forall i, \quad \forall t, \quad (2f)$$

$$\min_{\mathbb{P} \in \Pi} \mathbb{P}[\tilde{p}_{i,t} \leq \bar{P}_i] \geq (1 - \epsilon_i), \quad \forall i, \quad \forall t, \quad (2g)$$

$$\min_{\mathbb{P} \in \Pi} \mathbb{P}[\tilde{g}_{k,t} \geq \underline{G}_k] \geq (1 - \epsilon_k), \quad \forall k, \quad \forall t, \quad (2h)$$

$$\min_{\mathbb{P} \in \Pi} \mathbb{P}[\tilde{g}_{k,t} \leq \bar{G}_k] \geq (1 - \epsilon_k), \quad \forall k, \quad \forall t, \quad (2i)$$

$$\min_{\mathbb{P} \in \Pi} \mathbb{P}[\tilde{p}_{r_m,t} \geq \underline{PR}_m] \geq (1 - \epsilon_m), \quad \forall m, \quad \forall t, \quad (2j)$$

$$\min_{\mathbb{P} \in \Pi} \mathbb{P}[\tilde{p}_{r_m,t} \leq \bar{PR}_m] \geq (1 - \epsilon_m), \quad \forall m, \quad \forall t, \quad (2k)$$

$$\min_{\mathbb{P} \in \Pi} \mathbb{P}[\tilde{p}_r_{u,t} \leq \Gamma_{m,u} \tilde{p}_r_{m,t}] \geq (1 - \epsilon_{mu}), \quad \forall (m, u) \in \mathcal{Z}_c, \quad \forall t, \quad (2l)$$

$$\min_{\mathbb{P} \in \Pi} \mathbb{P}[\tilde{q}_{m,u,t} \geq 0] \geq (1 - \epsilon_{mu}), \quad \forall (m, u) \in \mathcal{Z}, \quad \forall t, \quad (2m)$$

$$\min_{\mathbb{P} \in \Pi} \mathbb{P}[\tilde{q}_{m,u,t}^{\text{in}} \geq 0] \geq (1 - \epsilon_{mu}), \quad \forall (m, u) \in \mathcal{Z}, \quad \forall t, \quad (2n)$$

$$\min_{\mathbb{P} \in \Pi} \mathbb{P}[\tilde{q}_{m,u,t}^{\text{out}} \geq 0] \geq (1 - \epsilon_{mu}), \quad \forall (m, u) \in \mathcal{Z}, \quad \forall t, \quad (2o)$$

$$\tilde{q}_{m,u,t}^2 = K_{m,u}^2 (\tilde{p}_r_{m,t}^2 - \tilde{p}_r_{u,t}^2), \quad \forall (m, u) \in \mathcal{Z}, \quad \forall t, \quad (2p)$$

$$\tilde{q}_{m,u,t} = \frac{\tilde{q}_{m,u,t}^{\text{in}} + \tilde{q}_{m,u,t}^{\text{out}}}{2}, \quad \forall (m, u) \in \mathcal{Z}, \quad \forall t, \quad (2q)$$

$$\tilde{h}_{m,u,t} = S_{m,u} \frac{\tilde{p}_r_{m,t} + \tilde{p}_r_{u,t}}{2}, \quad \forall (m, u) \in \mathcal{Z}, \quad \forall t, \quad (2r)$$

$$\tilde{h}_{m,u,t} = H_{m,u}^0 + \tilde{q}_{m,u,t}^{\text{in}} - \tilde{q}_{m,u,t}^{\text{out}}, \quad \forall (m, u) \in \mathcal{Z}, \quad t = 1, \quad (2s)$$

$$\tilde{h}_{m,u,t} = \tilde{h}_{m,u,(t-1)} + \tilde{q}_{m,u,t}^{\text{in}} - \tilde{q}_{m,u,t}^{\text{out}}, \quad \forall (m, u) \in \mathcal{Z}, \quad t > 1, \quad (2t)$$

$$\min_{\mathbb{P} \in \Pi} \mathbb{P}[\tilde{h}_{m,u,t} \geq H_{m,u}^0] \geq (1 - \epsilon_{mu}), \quad \forall (m, u) \in \mathcal{Z}, \quad t = |\mathcal{T}|, \quad (2u)$$

$$\sum_{k \in \mathcal{A}_m^K} \tilde{g}_{k,t} - \sum_{i \in \mathcal{A}_m^G} \phi_i \tilde{p}_{i,t} - \sum_{u:(m,u) \in \mathcal{Z}} (\tilde{q}_{m,u,t}^{\text{in}} - \tilde{q}_{u,m,t}^{\text{out}}) = D_{m,t}^G, \quad \forall m, \quad \forall t, \quad (2v)$$

where the set of stochastic variables is $\Theta_1 = \{\tilde{p}_{i,t}, \tilde{g}_{k,t}, \tilde{p}_r_{m,t}, \tilde{q}_{m,u,t}, \tilde{q}_{m,u,t}^{\text{in}}, \tilde{q}_{m,u,t}^{\text{out}}, \tilde{h}_{m,u,t}\}$. The terms in objective (2a) are the expected cost of power generation by non-NGFPPs and the cost of natural gas supply by gas suppliers derived from marginal production cost C_i^E and C_k^G , respectively.

The inequalities (2d)-(2o) and (2u) are modeled as distributionally robust chance constraints. This means that at the optimal solution to problem (2), the probability of meeting each individual constraint inside the square brackets $\mathbb{P}[\cdot]$ is modeled to have a confidence level of at least $(1 - \epsilon_{(\cdot)})$, where each $\epsilon_{(\cdot)}$ lies within 0 and 1, i.e., $\epsilon_{(\cdot)} \in [0, 1]$. Subscripts (\cdot) take the appropriate indices from the set $\{i, (n, r), k, m, (m, u)\}$ depending on the individual constraint.

Constraints (2b)-(2g) pertain to the power system. These constraints include the power balance (2b), limits on the stochastic power flows in the transmission lines (2c)-(2e) and the upper (\underline{P}_i) and lower bounds (\overline{P}_i) on the stochastic power production of generators (2f) and (2g). Vectors $\tilde{\mathbf{p}}_t \in \mathbb{R}^{|\mathcal{I}|}$, $\mathbf{W}_t^{\text{PF}} \in \mathbb{R}^{|\mathcal{J}|}$ and $\mathbf{D}_t^E \in \mathbb{R}^{|\mathcal{D}|}$ represent the power produced by generators, wind forecasts for wind farms and electricity demand from loads in period t , while Ω_t is the random vector of forecast errors, as previously defined. Vector coefficients, \mathbf{e} in (2b) are of appropriate dimensions such that the total supply and demand are balanced in each period t . The matrix $\Psi \in \mathbb{R}^{|\mathcal{L}| \times |\mathcal{N}|}$ represents the Power Transfer Distribution Factor (PTDF) matrix, derived from the reactances of power transmission lines [12], which maps the injections $\tilde{\mathbf{P}}_t^{\text{inj}} \in \mathbb{R}^{|\mathcal{N}|}$ at the electricity nodes to the power flows in each of the power lines $(n, r) \in \mathcal{L}$ respecting capacity limits $\overline{\mathbf{F}}$ in the network. Similarly, matrices $\Psi_I \in \mathbb{R}^{|\mathcal{N}| \times |\mathcal{I}|}$, $\Psi_J \in \mathbb{R}^{|\mathcal{N}| \times |\mathcal{J}|}$,

and $\Psi_D \in \mathbb{R}^{|\mathcal{N}| \times |\mathcal{D}|}$ map generators, wind farms and loads to the electricity nodes, such that (2c) gives the nodal power injections for all electricity nodes in the system.

Natural gas system constraints are given in (2h)-(2u). While constraints (2h) and (2i) limit the stochastic gas supply $\tilde{q}_{k,t}$ by supplier k in time period t to \underline{G}_k and \overline{G}_k , (2j) and (2k) limit the nodal gas pressure $\tilde{p}_r_{m,t}$ at each gas node $m \in \mathcal{M}$ to be within the physical limits $\underline{P}R_m$ and $\overline{P}R_m$. For the natural gas pipelines with compressors, $\mathcal{Z}_c \subset \mathcal{Z}$, compression is modeled linearly in (2l), which relate the inlet and outlet pressures of two adjacent nodes through compression factor $\Gamma_{m,u}$. We consider that the direction of gas flow in each pipeline $(m, u) \in \mathcal{Z}$ is predetermined and (2m)-(2o) enforce this flow direction in real-time. As remarked in [1], this assumption is non-limiting for the high-pressure, gas transmission networks when considering day-ahead operational problems. On the contrary, it can be a limiting assumption while considering a network expansion planning problem or a gas distribution system wherein injections from distributed gas producers (e.g., biogas plants) cannot be neglected¹. Equality constraints (2p), known as Weymouth equation, describe the flow $\tilde{q}_{m,u,t}$ (given by (2q) as the average of inflow, $\tilde{q}_{m,u,t}^{\text{in}}$ and outflow, $\tilde{q}_{m,u,t}^{\text{out}}$) along pipeline (m, u) as a quadratic non-convex function of the pressures $\tilde{p}_r_{m,t}$ and $\tilde{p}_r_{u,t}$ at the inlet (m) and outlet (u) nodes of the pipeline scaled by the pipeline resistance constant $K_{m,u}$. Constraints (2r) define the amount of linepack in the pipelines as the average of inlet and outlet pressures, scaled by the pipeline parameter $S_{m,u}$. Following the modeling approach in [7], (2s)-(2u) describe the evolution of the amount of linepack $\tilde{h}_{m,u,t}$ in a pipeline over time, with (2u) ensuring that the linepack is not depleted at the end of the simulation horizon beyond initial linepack amount $H_{m,u}^0$. Supply-demand balance of natural gas at each node is ensured in real-time by equality constraints (2v) which also couple the power and natural gas systems through the fuel consumed by the NGFPPs scaled by a fuel conversion factor ϕ_i . The sets $\mathcal{A}_m^K \subset \mathcal{K}$ and $\mathcal{A}_m^G \subset \mathcal{G}$ collect gas suppliers and NGFPPs that are located at node m , respectively, while $D_{m,t}^G$ is the nodal gas demand.

The requirement to solve the stochastic program (2) during the day-ahead stage renders the problem infinite dimensional, as the optimization variables are a function of uncertain parameters that are only revealed during real-time operation on the next day. To enable solvability of the problem, we adopt recourse actions based on linear decision rules [13] for the sources of flexibility in the coupled system, i.e., flexible power generation and natural gas supply and linepack. The assumption of affine response to uncertainty by flexible agents, although somewhat limiting in light of the non-linear dynamics of natural gas flow in the network, provides an intuitive understanding of the methodology behind uncertainty propagation from power system to natural gas system at a lower complexity of exposition. Generalized decision rules, for instance as discussed in [14], are left for future work.

¹The assumptions on fixed gas flow directions may be violated in extreme uncertainty realizations.

D. Affine Policies

When solving the day-ahead dispatch problem, flexible and adjustable agents in the coupled system, i.e., power producers and gas suppliers, are assigned optimal affine policies in addition to the nominal schedule. These affine policies govern their response to the realizations of uncertainty in wind forecast errors during the real-time operation.

a) *Power producers*: The affine response from dispatchable power plants (NGFPPs and non-NGFPPs) is given by

$$\tilde{p}_{i,t} = p_{i,t} + (\mathbf{e}^\top \Omega_t) \alpha_{i,t}, \quad \forall i \in \mathcal{I}, \quad \forall t \quad (3)$$

where $\tilde{p}_{i,t}$ is the stochastic power production of unit i in real-time, $p_{i,t}$ is the nominal power production schedule if the uncertainty were absent (perfect forecasts) and $\alpha_{i,t} \in [-1, 1]$ denotes the *participation factor* of the unit towards mitigation of the deviation.

b) *Gas suppliers*: The stochastic natural gas supply by supplier k is given by

$$\tilde{g}_{k,t} = g_{k,t} + (\mathbf{e}^\top \Omega_t) \beta_{k,t}, \quad \forall k \in \mathcal{K}, \quad \forall t \quad (4)$$

where $g_{k,t}$ is the nominal gas supply and $\beta_{k,t}$ is the participation factor of the supplier towards uncertainty mitigation.

The response to uncertainty by flexible network asset, i.e., linepack, is not directly adjustable as it depends on the allocation of the above affine policies, subject to the topology of the gas network and the physical gas flow constraints.

E. Uncertainty Response by Power and Gas Networks

Here, we discuss how uncertainty affects the flows in the power and gas networks. We consider the case of imperfect forecasts, i.e., $\mathbf{e}^\top \Omega_t \neq 0$.

During the real-time operation, power flows in the transmission lines, modeled by (2c)-(2e) change depending on the realized uncertainty Ω_t , the affine responses of power producers $\alpha_{i,t}$, and the spatial configuration of wind farms and power producers. Moreover, given the response from dispatchable power plants $\alpha_{i,t}$, the power balance constraint (2b) holds true for any realization of uncertainty Ω_t iff

$$\mathbf{e}^\top \mathbf{p}_t + \mathbf{e}^\top \mathbf{W}_t^{\text{PF}} = \mathbf{e}^\top \mathbf{D}_t^E, \quad \forall t, \quad (5a)$$

$$\mathbf{e}^\top \boldsymbol{\alpha}_t = 1, \quad \forall t. \quad (5b)$$

Constraints (5) are derived from (2b) by separating the nominal and uncertainty-dependent terms.

On the gas side, the uncertainty in gas flows, in response to changes in gas supply $\beta_{k,t}$ and in fuel demand from NGFPPs $\phi_i \alpha_{i,t}$, $\forall i \in \mathcal{G}$, is mitigated by the flexibility provided by linepack. It is vital to note that the real-time natural gas flows and nodal pressures are functions of $\beta_{k,t}$ and $\alpha_{i,t}$, $\forall i \in \mathcal{G}$. However, the analytical derivation of this relationship is not straightforward, given the non-linear gas flow dynamics and the inter-temporal linkages associated with the linepack model. As a simplification, we model the flow and pressure changes

as affine functions of uncertainty². We model the real-time natural gas flows in the pipelines as

$$\tilde{q}_{m,u,t} = q_{m,u,t} + (\mathbf{e}^\top \Omega_t) \gamma_{m,u,t}, \quad \forall (m, u) \in \mathcal{Z}, \quad \forall t, \quad (6a)$$

$$\tilde{q}_{m,u,t}^{\text{in}} = q_{m,u,t}^{\text{in}} + (\mathbf{e}^\top \Omega_t) \gamma_{m,u,t}^{\text{in}}, \quad \forall (m, u) \in \mathcal{Z}, \quad \forall t, \quad (6b)$$

$$\tilde{q}_{m,u,t}^{\text{out}} = q_{m,u,t}^{\text{out}} + (\mathbf{e}^\top \Omega_t) \gamma_{m,u,t}^{\text{out}}, \quad \forall (m, u) \in \mathcal{Z}, \quad \forall t, \quad (6c)$$

where $q_{m,u,t}$, $q_{m,u,t}^{\text{in}}$, $q_{m,u,t}^{\text{out}}$ denote the average flow rate, inflow and outflow rate of natural gas in the pipeline connecting nodes m and u , in absence of forecast errors and the variables $\gamma_{m,u,t}$, $\gamma_{m,u,t}^{\text{in}}$, $\gamma_{m,u,t}^{\text{out}}$ represent the auxiliary variables which model changes in these flow rates during real-time.

Consequently, the nodal balance constraint for natural gas (2v) holds true for any realization of uncertainty Ω_t iff

$$\begin{aligned} \sum_{k \in \mathcal{A}_m^K} g_{k,t} - \sum_{i \in \mathcal{A}_m^G} \phi_i p_{i,t} \\ - \sum_{u:(m,u) \in \mathcal{Z}} (q_{m,u,t}^{\text{in}} - q_{u,m,t}^{\text{out}}) = D_{m,t}^G, \quad \forall m, \quad \forall t, \end{aligned} \quad (7a)$$

$$\begin{aligned} \sum_{k \in \mathcal{A}_m^K} \beta_{k,t} - \sum_{i \in \mathcal{A}_m^G} \phi_i \alpha_{i,t} \\ - \sum_{u:(m,u) \in \mathcal{Z}} (\gamma_{m,u,t}^{\text{in}} - \gamma_{u,m,t}^{\text{out}}) = 0 \quad \forall m, \quad \forall t. \end{aligned} \quad (7b)$$

Constraints (7) are derived by separating the nominal and uncertainty-dependent terms in (2v). Following a similar approach, (2q), $\forall (m, u) \in \mathcal{Z}, \forall t$, decomposes into

$$q_{m,u,t}^{\text{in}} + q_{m,u,t}^{\text{out}}; \quad \gamma_{m,u,t} = \frac{\gamma_{m,u,t}^{\text{in}} + \gamma_{m,u,t}^{\text{out}}}{2}. \quad (8)$$

We model real-time pressures at gas nodes as

$$\tilde{p}_{m,t} = p_{m,t} + (\mathbf{e}^\top \Omega_t) \rho_{m,t}, \quad \forall m, \quad \forall t, \quad (9)$$

where $p_{m,t}$ and $\rho_{m,t}$ denote the nominal pressure and the auxiliary variable that models the change in pressure at node m in real-time, respectively. This allows us to expand the Weymouth equation in (2p) as, $\forall (m, u) \in \mathcal{Z}, \forall t$,

$$\begin{aligned} (q_{m,u,t}^2 + (\mathbf{e}^\top \Omega_t)^2 \gamma_{m,u,t}^2 + 2(\mathbf{e}^\top \Omega_t) \gamma_{m,u,t} q_{m,u,t}) = \\ K_{m,u}^2 (p_{m,t}^2 - p_{u,t}^2) + (\mathbf{e}^\top \Omega_t)^2 K_{m,u}^2 (\rho_{m,t}^2 - \rho_{u,t}^2) \\ + 2(\mathbf{e}^\top \Omega_t) K_{m,u}^2 (\rho_{m,t} p_{m,t} - \rho_{u,t} p_{u,t}). \end{aligned} \quad (10)$$

Separating terms that are independent of, quadratically- and linearly-dependent on uncertainty in (10), it can be replaced by the equalities (11) that must hold true for any realization of the uncertainty³. For pipelines $\forall (m, u) \in \mathcal{Z}, \forall t$,

$$q_{m,u,t}^2 = K_{m,u}^2 (p_{m,t}^2 - p_{u,t}^2), \quad (11a)$$

$$\gamma_{m,u,t}^2 = K_{m,u}^2 (\rho_{m,t}^2 - \rho_{u,t}^2), \quad (11b)$$

$$\gamma_{m,u,t} q_{m,u,t} = K_{m,u}^2 (\rho_{m,t} p_{m,t} - \rho_{u,t} p_{u,t}). \quad (11c)$$

²In future works, the simplified approach adopted in this paper must be enhanced by considering the true, non-linear analytical relationship of changes in real-time flows and nodal pressures to the affine policies.

³Modeling of uncertainty propagation to physical variables such as $\tilde{q}_{m,u,t}$ and $\tilde{p}_{m,t}$ by estimating sensitivities using Taylor series expansion around the forecast has recently been applied to AC optimal power flow (see, e.g., [15]). Since we solve the dispatch problem in day-ahead, wherein uncertainty around the forecast point is non-negligible, we cannot justify such a sensitivity-based approach.

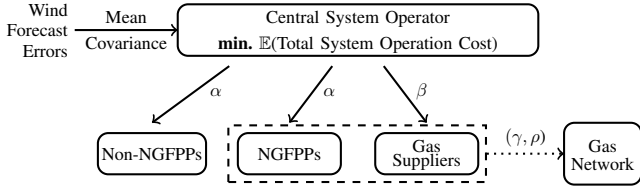


Fig. 1. Coordinated power and natural gas day-ahead dispatch

In addition to the Weymouth equations, the auxiliary variables for flow changes ($\gamma_{m,u,t}$, $\gamma_{m,u,t}^{\text{in}}$, $\gamma_{m,u,t}^{\text{out}}$) and pressure changes ($\rho_{m,t}$) are coupled by the equality constraints (2r)-(2t) that govern the amount of linepack and evolution of linepack in the pipelines. On separating nominal and uncertainty-dependent terms, these constraints should hold true for any realization of Ω_t iff the equalities (12) hold. For pipelines $\forall(m, u) \in \mathcal{Z}$,

$$h_{m,u,t} = H_{m,u}^0 + q_{m,u,t}^{\text{in}} - q_{m,u,t}^{\text{out}}, \quad t = 1, \quad (12a)$$

$$h_{m,u,t} = h_{m,u,(t-1)} + (q_{m,u,t}^{\text{in}} - q_{m,u,t}^{\text{out}}), \quad t > 1, \quad (12b)$$

$$\frac{S_{m,u}}{2} (\rho_{m,t} + \rho_{u,t} - \rho_{m,(t-1)} - \rho_{u,(t-1)}) \\ = (\gamma_{m,u,t}^{\text{in}} - \gamma_{m,u,t}^{\text{out}}), \quad t > 1, \quad (12c)$$

where $h_{m,u,t}$ is the nominal linepack in the pipeline in case perfect forecasts of wind power production were to be realized. It is worth noting that, considering the initial linepack amount $H_{m,u}^0$ is uncertainty-independent, constraint (2s) decomposes solely as (12a). Whereas the linepack amount in hours $t > 1$, given by (2t), decomposes as nominal (12b) and uncertainty-dependent (12c) equalities, which govern the change in nominal linepack amount and the response to uncertainty during real-time operation, respectively.

F. Power and Natural Gas Coordination with Affine Policies

In the following we present a finite-dimensional solvable approximation of the stochastic program (2), under the strategy of affine response to uncertainty. As shown in Fig. 1, this day-ahead problem is solved by a central system operator.

$$\min_{\Theta_2} \sum_{t \in \mathcal{T}} \left(\sum_{i \in \mathcal{C}} C_i^E p_{i,t} + \sum_{k \in \mathcal{K}} C_k^G g_{k,t} \right) \quad (13a)$$

subject to

$$\min_{\mathbb{P} \in \Pi} \mathbb{P}[p_{i,t} + (\mathbf{e}^\top \Omega_t) \alpha_{i,t} \geq \underline{P}_i] \geq (1 - \epsilon_i), \quad \forall i, \quad \forall t, \quad (13b)$$

$$\min_{\mathbb{P} \in \Pi} \mathbb{P}[p_{i,t} + (\mathbf{e}^\top \Omega_t) \alpha_{i,t} \leq \bar{P}_i] \geq (1 - \epsilon_i), \quad \forall i, \quad \forall t, \quad (13c)$$

$$\min_{\mathbb{P} \in \Pi} \mathbb{P}[g_{k,t} + (\mathbf{e}^\top \Omega_t) \beta_{k,t} \geq \underline{G}_k] \geq (1 - \epsilon_k), \quad \forall k, \quad \forall t, \quad (13d)$$

$$\min_{\mathbb{P} \in \Pi} \mathbb{P}[g_{k,t} + (\mathbf{e}^\top \Omega_t) \beta_{k,t} \leq \bar{G}_k] \geq (1 - \epsilon_k), \quad \forall k, \quad \forall t, \quad (13e)$$

$$\min_{\mathbb{P} \in \Pi} \mathbb{P}[pr_{m,t} + (\mathbf{e}^\top \Omega_t) \rho_{m,t} \geq \underline{PR}_m] \geq (1 - \epsilon_m), \quad \forall m, \quad \forall t, \quad (13f)$$

$$\min_{\mathbb{P} \in \Pi} \mathbb{P}[pr_{m,t} + (\mathbf{e}^\top \Omega_t) \rho_{m,t} \leq \bar{PR}_m] \\ \geq (1 - \epsilon_m), \quad \forall m, \quad \forall t, \quad (13g)$$

$$\min_{\mathbb{P} \in \Pi} \mathbb{P}[(pr_{u,t} - \Gamma_{m,u} pr_{m,t}) + (\mathbf{e}^\top \Omega_t)(\rho_{u,t} \\ - \Gamma_{m,u} \rho_{m,t}) \leq 0] \geq (1 - \epsilon_{mu}), \quad \forall (m, u) \in \mathcal{Z}_c, \quad \forall t, \quad (13i)$$

$$\begin{aligned} \min_{\mathbb{P} \in \Pi} \mathbb{P}[q_{m,u,t} + (\mathbf{e}^\top \Omega_t) \gamma_{m,u,t} \geq 0] \\ \geq (1 - \epsilon_{mu}), \quad \forall (m, u) \in \mathcal{Z}, \quad \forall t, \end{aligned} \quad (13j)$$

$$\begin{aligned} \min_{\mathbb{P} \in \Pi} \mathbb{P}[q_{m,u,t}^{\text{in}} + (\mathbf{e}^\top \Omega_t) \gamma_{m,u,t}^{\text{in}} \geq 0] \\ \geq (1 - \epsilon_{mu}), \quad \forall (m, u) \in \mathcal{Z}, \quad \forall t, \end{aligned} \quad (13k)$$

$$\begin{aligned} \min_{\mathbb{P} \in \Pi} \mathbb{P}[q_{m,u,t}^{\text{out}} + (\mathbf{e}^\top \Omega_t) \gamma_{m,u,t}^{\text{out}} \geq 0] \\ \geq (1 - \epsilon_{mu}), \quad \forall (m, u) \in \mathcal{Z}, \quad \forall t, \end{aligned} \quad (13l)$$

$$\begin{aligned} \min_{\mathbb{P} \in \Pi} \mathbb{P}[h_{m,u,t} + S_{m,u}(\mathbf{e}^\top \Omega_t) \frac{\rho_{m,t} + \rho_{u,t}}{2} \geq H_{m,u}^0] \\ \geq (1 - \epsilon_{mu}), \quad \forall (m, u) \in \mathcal{Z}, \quad t = |\mathcal{T}|, \end{aligned} \quad (13m)$$

$$(2c) - (2e), (5), (7), (8), (11), (12), \quad (13n)$$

where the optimization variables are $\Theta_2 = \{ p_{i,t}, \alpha_{i,t}, g_{k,t}, \beta_{k,t}, pr_{m,t}, \rho_{m,t}, q_{m,u,t}, \gamma_{m,u,t}, q_{m,u,t}^{\text{in}}, \gamma_{m,u,t}^{\text{out}}, h_{m,u,t} \}$. The expectation term in objective (2a) reduces to (13a) on account of the zero-mean assumption of Ω_t . As discussed in [16] for programs with a similar structure, the stochastic program (13) is computationally intractable due to the probabilistic distributionally robust chance constraints. To achieve tractability, a convex second-order cone (SOC) approximation of the non-convex individual distributionally robust chance constraints is adopted. Furthermore, the non-convex quadratic equality constraints (11) representing the Weymouth equation for the uncertainty-aware gas flows require convexification. The approach towards solving (13) along with its final tractable form is discussed in the next section.

III. SOLUTION APPROACH

A. SOC Reformulation of Probabilistic Constraints

For distributionally robust individual chance constraints under the assumption of known first and second-order moments of the underlying probability distribution, [17, Theorem 2.2] provides a SOC approximation based on a variant of Chebyshev's Inequality. While interested readers are directed to [17] for a proof, convex reformulation of constraint (13c) is presented below as an illustration.

With $\Sigma_t^\Pi \in \mathbb{R}^{|\mathcal{T}| \times |\mathcal{T}|}$ as the t -th diagonal sub-matrix of the covariance matrix Σ^Π in time period t and $\mathbf{e} \in \mathbb{R}^{|\mathcal{T}|}$ denoting a vector of all ones, the probabilistic chance constraints (13c) can be approximated by the following SOC constraints:

$$\sqrt{\frac{1 - \epsilon_i}{\epsilon_i}} \left\| \alpha_{i,t} \mathbf{e}^\top (\Sigma_t^\Pi)^{1/2} \right\|_2 \leq -p_{i,t} + \bar{P}_i, \quad \forall i, \quad \forall t. \quad (14)$$

Similar reformulation is performed for the other distributionally robust chance constraints in (13). References [18] and [19] remark that such conic reformulation based on Chebyshev's Inequality results in over-conservative solutions as $\epsilon_i \rightarrow 0$ while approaching infeasibility for $\epsilon_i \approx 0$. Exact reformulation of such chance constraints improving on this issue has been recently proposed in [18]. However, since the focus of this work is on uncertainty-aware coordination between electricity and natural gas systems, our formulation is limited to the conic approximation. We ensure that large enough risk measures $\epsilon_{(.)}$ are considered in the case study (Section IV) such that infeasibility is avoided.

TABLE I
VARIABLE BOUNDS FOR MCCORMICK RELAXATION.

Variable	Lower bound	Upper bound
$pr_{m,t}$	$\underline{P}R_m$	$\overline{P}R_m$
$\rho_{m,t}$	$-(\overline{P}R_m - \underline{P}R_m)/\widehat{W}$	$(\overline{P}R_m - \underline{P}R_m)/\widehat{W}$
$q_{m,u,t}$	0	\overline{Q}
$\gamma_{m,u,t}$	$-\overline{Q}/\widehat{W}$	\overline{Q}/\widehat{W}

B. Convex Relaxation of Weymouth Equation

The non-convex quadratic equality constraints in (11a) can be equivalently written as

$$q_{m,u,t}^2 \leq K_{m,u}^2(pr_{m,t}^2 - pr_{u,t}^2), \quad \forall(m,u) \in \mathcal{Z}, \quad \forall t, \quad (15a)$$

$$q_{m,u,t}^2 \geq K_{m,u}^2(pr_{m,t}^2 - pr_{u,t}^2), \quad \forall(m,u) \in \mathcal{Z}, \quad \forall t. \quad (15b)$$

To relax (11a), we adopt the convex SOC constraints (15a) and drop the non-convex constraints (15b)⁴. The tightness of this relaxation is analyzed in [20] and will be further examined in Section IV. Note that (11b) can be convexified in the same manner. However, this convexification strategy cannot be applied to (11c). We adopt McCormick relaxation [21], defining rectangular envelopes around the bi-linear terms in (11c) based on the known and estimated bounds on variables. We first define auxiliary variables $\nu_{m,t}$ for gas nodes $m \in \mathcal{M}$ and $\lambda_{m,u,t}$ for the pipelines $(m,u) \in \mathcal{Z}, \forall t$ and then replace (11c) by the following set of constraints:

$$\lambda_{m,u,t} - K_{m,u}^2\nu_{m,t} + K_{m,u}^2\nu_{u,t} = 0, \quad \forall(m,u) \in \mathcal{Z}, \quad \forall t, \quad (16a)$$

$$\lambda_{m,u,t} = q_{m,u,t}\gamma_{m,u,t}, \quad \forall(m,u) \in \mathcal{Z}, \quad \forall t, \quad (16b)$$

$$\nu_{m,t} = pr_{m,t}\rho_{m,t}, \quad \forall m, \quad \forall t, \quad (16c)$$

$$\nu_{u,t} = pr_{u,t}\rho_{u,t}, \quad \forall u : (m,u) \in \mathcal{Z}, \quad \forall t. \quad (16d)$$

To illustrate the McCormick relaxation, the inequalities that replace the non-convex constraints (16c) are

$$\forall m, t \begin{cases} \rho_{m,t}^L pr_{m,t} + pr_{m,t}^L \rho_{m,t} \leq \nu_{m,t} + pr_{m,t}^L \rho_{m,t}^L \\ \rho_{m,t}^U pr_{m,t} + pr_{m,t}^U \rho_{m,t} \leq \nu_{m,t} + pr_{m,t}^U \rho_{m,t}^U \\ \rho_{m,t}^L pr_{m,t} + pr_{m,t}^U \rho_{m,t} \geq \nu_{m,t} + pr_{m,t}^U \rho_{m,t}^L \\ \rho_{m,t}^U pr_{m,t} + pr_{m,t}^L \rho_{m,t} \geq \nu_{m,t} + pr_{m,t}^L \rho_{m,t}^U, \end{cases} \quad (17)$$

where superscripts L and U indicate lower and upper bounds of the variables, respectively. Constraints (16b) and (16d) are treated similarly. The variable bounds used to construct the McCormick envelopes are listed in Table I. Parameter \widehat{W} is the total installed wind capacity in the system and parameter \overline{Q} denotes the upper bound on gas flow in the pipelines, which we obtain by solving a deterministic version of problem (2) with $e^\top \Omega_t = 0$. The bounds for network response variables, $\gamma_{m,u,t}$ and $\rho_{m,u,t}$, are trivially deduced from equations (6a) and (9), respectively.

Following the convex approximation of probabilistic constraints and relaxation of Weymouth equations, the tractable

⁴Linear approximations of the dropped non-convex constraints, as proposed by [1] in a deterministic setting, may also be included to the problem.

form of the distributionally robust chance-constrained day-ahead coordinated power and natural gas dispatch is presented in Appendix A. Problem (20) is a convex second-order cone program (SOCP) and is solvable using off-the-shelf convex optimization solvers.

IV. CASE STUDY

A. Input Data

A coupled power and natural gas system consisting of a 12-node gas network connected to the IEEE 24-bus reliability test system [5] is used to evaluate our proposed coordinated dispatch. The installed wind capacity reaches one-thirds of the peak demand in the simulation horizon of 24 hours. Data for the parameters of the power and natural gas networks and for the operational characteristics of all assets in the system are provided in online appendix [22]. A dataset of 1,000 zero-mean wind forecast error scenarios based on actual measurements recorded in Western Denmark [23] is used to empirically estimate the covariance matrix Σ^{Π} . The parameters $\epsilon(\cdot)$ for all distributionally robust chance constraints in (20) are set to identical values.

The problem is implemented in Julia v1.1.1 modeled with JuMP v0.2 and solved to optimality by Mosek v9.0 with an average CPU time of 1.67 seconds on a personal computer with 8GB memory running on Intel Core i5 clocked at 2.3 GHz. The optimal solution provides nominal dispatch schedule as well as affine policies that quantify the response to uncertain wind realizations during real-time.

B. Optimal Affine Policies

In Fig. 2, we show the optimal allocations from the distributionally robust chance-constrained day-ahead coordinated power and natural gas model (20) for violation probabilities $\epsilon(\cdot)$ set to 0.05. Fig. 2(a) shows the nominal dispatch of NGFPPs and non-NGFPPs to meet the forecasted net electricity demand, i.e., load minus wind production forecast, while Fig. 2(b) shows their affine responses to uncertainty. Similarly, Figs. 2(c)-(d) present the nominal schedule and the response policies for the three gas suppliers. We highlight our main observations in the following.

First, when power producers and gas suppliers are either dispatched not at all or at full capacity, they are not eligible to adjust their output to mitigate uncertainty. Thus, the response policies for these units are zero. As a result, expensive generators, which are not dispatched in hours with low net demand, are assigned zero α_i in these hours. Similarly, the most expensive gas supplier ($k3$) is not expected to respond to uncertainty in hours 1-13, while not dispatched. On the other hand, the least expensive gas supplier ($k1$) cannot provide a response to uncertainty in hours 1-10, because her nominal dispatch is already at maximum capacity.

Second, NGFPPs are the main providers of flexibility in response to wind uncertainty during hours 8-24, see Fig. 2(b). Although the volatility of gas demand from NGFPPs can be mitigated by linepack, gas suppliers are also required to respond to uncertainty, especially in hours 14-24, see Fig. 2(d).

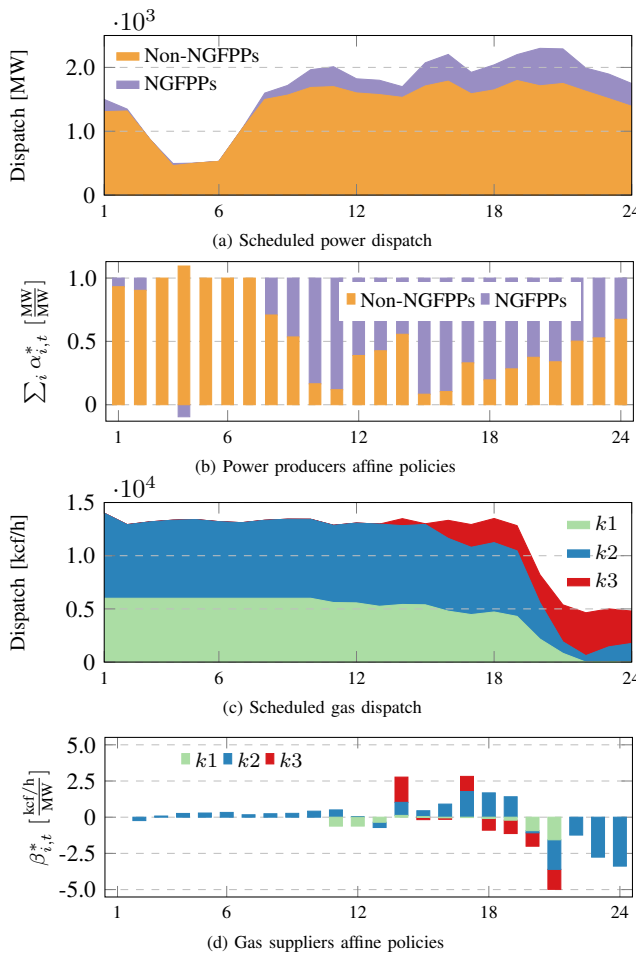


Fig. 2. Optimal dispatch and affine policies for $\epsilon_{(\cdot)} = 0.05$ for the simulation horizon of 24 hours.

Not only the availability and cost structure of power and gas supply, but also network effects impact the optimal response. The spatial correlations of uncertain wind forecasts and location of flexibility providers in both power and gas networks affect the response policies. An example of network effects is the allocation of affine policies in hour 4 in Fig. 2(b). Here, flexibility is provided not only with respect to cost efficiency, but also considering locational benefits and preferable energy flow effects.

C. Choice of Violation Probabilities $\epsilon_{(\cdot)}$

To evaluate the quality of the solution obtained and to make an informed choice for $\epsilon_{(\cdot)}$, we perform *ex-ante* simulations using a test dataset of wind realization scenarios, distinct from those used to estimate the covariance matrix. With fixed day-ahead decisions, i.e., nominal production schedules and affine policies, we compute the violation probability of the distributionally robust chance constraints (13b)-(13m) and (2d)-(2e) for a choice of $\epsilon_{(\cdot)}$ as

$$\eta_\epsilon = \frac{1}{N_s} \sum_{s=1}^{N_s} \mathbb{I}_s. \quad (18)$$

The indicator function \mathbb{I}_s takes a value 1 if at least one of these

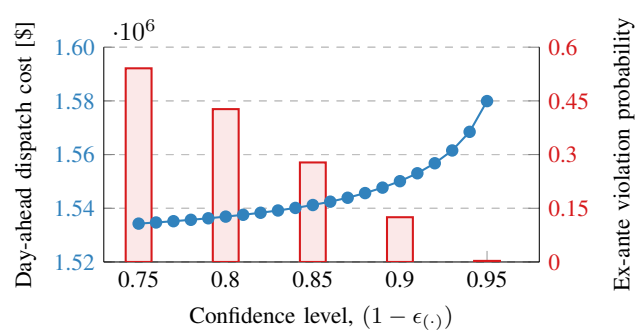


Fig. 3. Day-ahead dispatch cost (left y-axis) with values of $\epsilon_{(\cdot)}$ chosen for the distributionally robust chance constraints is shown by line with markers ●. The ex-ante violation probability (right y-axis) of these constraints, evaluated for 1,000 test samples, is shown in bars.

constraints is violated for the wind realization that corresponds to scenario s . Referring to the left-hand y-axis, the lineplot in Fig. 3 shows the expected cost of day-ahead dispatch at various values of confidence levels $(1 - \epsilon_{(\cdot)})$ imposed on the probabilistic constraints. With a higher confidence of meeting the constraints, the expected cost of day-ahead dispatch increases. The bars, which refer to the right-hand y-axis, show the ex-ante violation probability computed at selected confidence level values. For $\epsilon_{(\cdot)} = 0.05$, an ex-ante violation probability of 0.003 is expected at a day-ahead expected dispatch cost of \$1,580,000.

D. Ex-Ante Violation Probabilities

Next, we analyse the violation probabilities (18) for each of the following chance-constraints: I. generator bounds (13b) and (13c), II. line flow limits (2d) and (2e), III. non-depletion of linepack in pipelines requirement (13m), IV. natural gas flow direction constraints (13j)-(13l), V. nodal gas pressure bounds (13f) and (13g), and VI. gas supplier bounds (13d) and (13e). Fig. 4 shows the probability of violation of these individual constraints for different choices of $\epsilon_{(\cdot)}$.

Power generation limits (13b) and (13c) are most susceptible to violation at all values of $\epsilon_{(\cdot)}$. Power transmission lines are not prone to reaching their operational limits. We do not observe any violation probability of power flow limits until decreasing the confidence level to 0.75. On the gas side, the constraints of gas flow directions (13j)-(13l) are susceptible to violations, causing the dependent nodal pressure limits (13f) and (13g) to be violated as well. On the one hand, this can be explained by the relaxation gap for the gas flow equations, which is discussed in detail in the following. On the other hand, this motivates future work to consider bi-directional gas flows, specially in the context of flexibility provision by linepack, albeit at the cost of losing convexity due to introduction of integer variables. The non-depletion of linepack constraints are, however, satisfied even at $\epsilon_{(\cdot)} = 0.25$. This indicates that there is enough short-term gas storage available in the gas pipelines such that they are not depleted at the end of the day while providing flexibility to the power system. Notably, these outcomes and resulting inferences are system-specific.

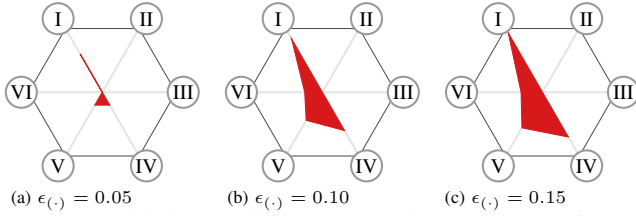


Fig. 4. Ex-ante violation probabilities by constraint type. Corners of the hexagons represent a violation probability of 0.005, 0.15 and 0.3 for (a), (b) and (c), respectively.

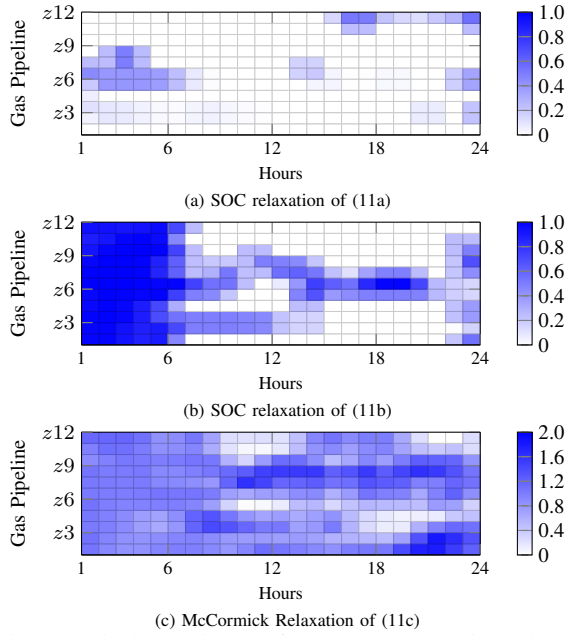


Fig. 5. Normalized relaxation gap for the convex relaxations adopted for Weymouth equation in (11) for $\epsilon(\cdot) = 0.05$.

E. Tightness of Convex Relaxations

We examine the tightness of the relaxation for the non-convex Weymouth equation (11) by comparing the left-hand and right-hand sides of each of these equality constraints. We define the normalized root mean square relaxation gap Ξ for the original equality constraint $X_{m,u,t} = Y_{m,u,t}, \forall (m,u) \in \mathcal{Z}, \forall t$ relaxed to $X_{m,u,t} \leq Y_{m,u,t}, \forall (m,u) \in \mathcal{Z}, \forall t$ as

$$\Xi = \left[\frac{1}{|\mathcal{Z}| |\mathcal{T}|} \sum_{t \in \mathcal{T}} \sum_{z \in \mathcal{Z}} \left(\frac{Y_{m,u,t}^* - X_{m,u,t}^*}{Y_{m,u,t}^*} \right)^2 \right]^{\frac{1}{2}}, \quad (19)$$

where superscript * indicates values obtained at optimality. For $\epsilon(\cdot) = 0.05$, we observe a Ξ -value of 0.78, 1.67 and 2.87 for (11a), (11b) and (11c), respectively.

Fig. 5 presents heatmaps of the normalized root mean square relaxation gap Ξ for each gas pipeline in each hour of the simulation horizon for $\epsilon(\cdot) = 0.05$. The occurrence of relaxation gap is lower for constraint (11a) than for (11b). While the relaxation of constraint (11a) seems to be sufficiently tight in Fig. 5(a), the relaxation of (11b) is not always exact, see Fig. 5(b). The relaxation gap is particularly extant in hours 1-6. The structure of the gas network, which is non-radial and cyclical, and the inter-temporal dynamics of linepack contribute to the

lack of tightness of the relaxations. Conditions for exactness of the relaxation of the Weymouth equation can be found in [20] and [24], while approaches for tightening these SOC relaxations are proposed in [1] and [25]. For the McCormick relaxation of constraint (11c) the relaxation gap occurs very frequently and with high severity, see Fig. 5(c). Adversely negative values of γ and/or ρ in the bilinear terms lead to normalized relaxation gaps even larger than 1. Improvements on this approach, such as iterative tightening of the bounds or by convex quadratic enhancement of McCormick relaxation as proposed in [26], will be considered in future works. However, in the context of the proposed coordinated day-ahead dispatch, the tightness of the relaxation is of limited importance, since an additional gas flow feasibility problem [24] is expected to be solved closer to real-time by the gas network operator.

V. CONCLUSION AND FUTURE PERSPECTIVES

A. Conclusion

We proposed a distributionally robust chance-constrained coordination of power and natural gas systems to study the propagation of uncertainty from the power to the gas side. Our tractable reformulation of the stochastic program, using recourse actions from the flexible agents in the coupled system and adopting a simplified model for real-time gas flows and nodal pressures, results in a convex SOCP. Ex-ante out-of-sample evaluations are used to demonstrate the quality of the solution while highlighting a trade-off between dispatch cost and violation probability, which influences the choice of allowable violation probabilities. The proposed coordination model enables efficient harnessing of short-term flexibility from the assets in natural gas networks for power systems facing uncertainty. Analysis of the optimal affine policies highlights that our proposed approach enables cost-efficient dispatch and allocation of flexibility across energy sectors facing spatio-temporal effects of uncertainty.

B. Future Perspectives

For future works, detailed out-of-sample simulation studies should be undertaken to better understand the quality of optimal affine responses. Studying the impact of the response policies on the feasibility of the physical constraints of power and natural gas networks in real-time operation and testing the severity of allowed constraint violations are of interest. Convexity-preserving algorithms that tighten the relaxation of gas flow equations can be employed in future works. Further, power-to-gas units that provide additional inter-sectoral flexibility could be included in the model.

Analyzing the proposed coordination in a market context wherein payments for the provision of flexibility-as-a-service are considered, is an interesting topic to investigate in future. Moreover, the impact of limited information sharing among sectors as opposed to the central dispatch considered in this work would be highly insightful. Finally, a market clearing mechanism involving auctions that elicit flexibility from the natural gas sector is a viable pathway towards real-world implementation that is opened up by this paper.

APPENDIX A

The final tractable form of the proposed distributionally robust chance-constrained coordination of power and natural gas systems is the SOCP presented below:

$$\min_{\Theta_2 \cup \{\lambda_{m,u,t}, \nu_{m,t}\}} \sum_{t \in \mathcal{T}} \left(\sum_{i \in \mathcal{C}} C_i^E p_{i,t} + \sum_{k \in \mathcal{K}} C_k^G g_{k,t} \right) \quad (20a)$$

subject to

$$\xi_i \left\| -\alpha_{i,t} \mathbf{e}^\top (\Sigma_t^\Pi)^{1/2} \right\|_2 \leq p_{i,t} - \underline{P}_i, \quad \forall i, \forall t, \quad (20b)$$

$$\xi_i \left\| \alpha_{i,t} \mathbf{e}^\top (\Sigma_t^\Pi)^{1/2} \right\|_2 \leq -p_{i,t} + \bar{P}_i, \quad \forall i, \forall t, \quad (20c)$$

$$\begin{aligned} \xi_{nr} \left\| \{ \Psi(\Psi_1 \alpha_t \mathbf{e}^\top - \Psi_J) \}_{(n,r)} (\Sigma_t^\Pi)^{1/2} \right\|_2 &\leq \{\bar{\mathbf{F}} \\ &+ \Psi(\Psi_D \mathbf{D}_t^E - \Psi_I \mathbf{p}_t - \Psi_J \mathbf{W}_t^{PF})\}_{(n,r)}, \quad \forall (n,r) \in \mathcal{L}, \forall t, \end{aligned} \quad (20d)$$

$$\begin{aligned} \xi_{nr} \left\| -\{\Psi(\Psi_1 \alpha_t \mathbf{e}^\top - \Psi_J)\}_{(n,r)} (\Sigma_t^\Pi)^{1/2} \right\|_2 &\leq \{\bar{\mathbf{F}} \\ &- \Psi(\Psi_D \mathbf{D}_t^E - \Psi_I \mathbf{p}_t - \Psi_J \mathbf{W}_t^{PF})\}_{(n,r)}, \quad \forall (n,r) \in \mathcal{L}, \forall t, \end{aligned} \quad (20e)$$

$$\xi_k \left\| -\beta_{k,t} \mathbf{e}^\top (\Sigma_t^\Pi)^{1/2} \right\|_2 \leq g_{k,t} - \underline{G}_i, \quad \forall k, \forall t, \quad (20f)$$

$$\xi_k \left\| \beta_{k,t} \mathbf{e}^\top (\Sigma_t^\Pi)^{1/2} \right\|_2 \leq -g_{k,t} + \bar{G}_i, \quad \forall k, \forall t, \quad (20g)$$

$$\xi_m \left\| -\rho_{m,t} \mathbf{e}^\top (\Sigma_t^\Pi)^{1/2} \right\|_2 \leq pr_{m,t} - \underline{PR}_m, \quad \forall m, \forall t, \quad (20h)$$

$$\xi_m \left\| \rho_{m,t} \mathbf{e}^\top (\Sigma_t^\Pi)^{1/2} \right\|_2 \leq -pr_{m,t} + \bar{PR}_m, \quad \forall m, \forall t, \quad (20i)$$

$$\begin{aligned} \xi_{mu} \left\| (\rho_{u,t} - \Gamma_{m,u} \rho_{m,t}) \mathbf{e}^\top (\Sigma_t^\Pi)^{1/2} \right\|_2 &\leq \Gamma_{m,u} pr_{m,t} - pr_{u,t}, \quad \forall (m,u) \in \mathcal{Z}_c, \forall t, \end{aligned} \quad (20j)$$

$$\xi_{mu} \left\| -\gamma_{m,u,t} \mathbf{e}^\top (\Sigma_t^\Pi)^{1/2} \right\|_2 \leq q_{m,u,t}, \quad \forall (m,u) \in \mathcal{Z}, \forall t, \quad (20k)$$

$$\xi_{mu} \left\| -\gamma_{m,u,t}^{\text{in}} \mathbf{e}^\top (\Sigma_t^\Pi)^{1/2} \right\|_2 \leq q_{m,u,t}^{\text{in}}, \quad \forall (m,u) \in \mathcal{Z}, \forall t, \quad (20l)$$

$$\xi_{mu} \left\| -\gamma_{m,u,t}^{\text{out}} \mathbf{e}^\top (\Sigma_t^\Pi)^{1/2} \right\|_2 \leq q_{m,u,t}^{\text{out}}, \quad \forall (m,u) \in \mathcal{Z}, \forall t, \quad (20m)$$

$$\gamma_{m,u,t}^2 \leq K_{m,u}^2 (\rho_{m,t}^2 - \rho_{u,t}^2), \quad \forall (m,u) \in \mathcal{Z}, \forall t, \quad (20n)$$

$$\begin{aligned} \xi_{mu} \left\| -(\rho_{m,t} + \rho_{u,t}) \left(\frac{S_{m,u}}{2} \right)^{\frac{1}{2}} \mathbf{e}^\top (\Sigma_t^\Pi)^{1/2} \right\|_2 &\leq h_{m,u,t} - H_{m,u}^0, \quad \forall (m,u) \in \mathcal{Z}, \quad t = |\mathcal{T}|, \end{aligned} \quad (20o)$$

McCormick envelopes of (16b) and (16d), $(20p)$

(12), (7), (5), (15a), (16a), (17), $(20q)$

where $\xi_i = \sqrt{\frac{1-\epsilon_i}{\epsilon_i}}$, $\xi_{nr} = \sqrt{\frac{1-\epsilon_{nr}}{\epsilon_{nr}}}$, $\xi_k = \sqrt{\frac{1-\epsilon_k}{\epsilon_k}}$, $\xi_m = \sqrt{\frac{1-\epsilon_m}{\epsilon_m}}$, $\xi_{mu} = \sqrt{\frac{1-\epsilon_{mu}}{\epsilon_{mu}}}$ are parameters.

REFERENCES

- [1] S. Chen, A. J. Conejo, R. Sioshansi, and Z. Wei, "Unit commitment with an enhanced natural gas-flow model," *IEEE Transactions on Power Systems*, vol. 34, no. 5, pp. 3729–3738, 2019.
- [2] P. Pinson, L. Mitridati, C. Ordoudis, and J. Østergaard, "Towards fully renewable energy systems: Experience and trends in Denmark," *CSEE Journal of Power and Energy Systems*, vol. 3, no. 1, pp. 26–35, 2017.
- [3] G. Byeon and P. Van Hentenryck, "Unit commitment with gas network awareness," *IEEE Transactions on Power Systems*, vol. 35, no. 2, pp. 1327–1339, 2020.
- [4] A. Zlotnik, L. Roald, S. Backhaus, M. Chertkov, and G. Andersson, "Coordinated scheduling for interdependent electric power and natural gas infrastructures," *IEEE Transactions on Power Systems*, vol. 32, no. 1, pp. 600–610, 2017.
- [5] C. Ordoudis, P. Pinson, and J. M. Morales, "An integrated market for electricity and natural gas systems with stochastic power producers," *European Journal of Operational Research*, vol. 272, no. 2, pp. 642–654, 2019.
- [6] H. Ameli, M. Qadrdaan, and G. Strbac, "Coordinated operation strategies for natural gas and power systems in presence of gas-related flexibilities," *Energy Systems Integration*, vol. 1, no. 1, pp. 3–13, 2019.
- [7] A. Schewe, C. Ordoudis, J. Kazempour, and P. Pinson, "Coordination of power and natural gas systems: Convexification approaches for linepack modeling," in *Proc. 13th IEEE PES PowerTech Conference*, Milan, 2019.
- [8] C. Wang, W. Wei, J. Wang, and T. Bi, "Convex optimization based adjustable robust dispatch for integrated electric-gas systems considering gas delivery priority," *Applied Energy*, vol. 239, pp. 70–82, 2019.
- [9] B. Odetayo, J. MacCormack, W. Rosehart, and H. Zareipour, "A chance constrained programming approach to integrated planning of distributed power generation and natural gas network," *Electric Power Systems Research*, vol. 151, pp. 197–207, 2017.
- [10] A. Ratha, J. Kazempour, A. Virag, and P. Pinson, "Exploring market properties of policy-based reserve procurement for power systems," in *2019 IEEE 58th Conference on Decision and Control (CDC)*, 2019, pp. 7498–7505.
- [11] W. Wiesemann, D. Kuhn, and M. Sim, "Distributionally robust convex optimization," *Operations Research*, vol. 62, no. 6, pp. 1358–1376, 2014.
- [12] R. D. Christie, B. F. Wollenberg, and I. Wangensteen, "Transmission management in the deregulated environment," *Proceedings of the IEEE*, vol. 88, no. 2, pp. 170–195, 2000.
- [13] A. Georghiou, D. Kuhn, and W. Wiesemann, "The decision rule approach to optimization under uncertainty: Methodology and applications," *Computational Management Science*, vol. 16, no. 4, pp. 545–576, 2019.
- [14] A. Georghiou, W. Wiesemann, and D. Kuhn, "Generalized decision rule approximations for stochastic programming via liftings," *Mathematical Programming*, vol. 152, no. 1, pp. 301–338, 2015.
- [15] L. Roald and G. Andersson, "Chance-constrained AC optimal power flow: Reformulations and efficient algorithms," *IEEE Transactions on Power Systems*, vol. 33, no. 3, pp. 2906–2918, 2018.
- [16] S. Zymler, D. Kuhn, and B. Rustem, "Distributionally robust joint chance constraints with second-order moment information," *Mathematical Programming*, vol. 137, no. 1, pp. 167–198, 2013.
- [17] M. R. Wagner, "Stochastic 0-1 linear programming under limited distributional information," *Operations Research Letters*, vol. 36, no. 2, pp. 150 – 156, 2008.
- [18] W. Xie and S. Ahmed, "Distributionally robust chance constrained optimal power flow with renewables: A conic reformulation," *IEEE Transactions on Power Systems*, vol. 33, no. 2, pp. 1860–1867, 2018.
- [19] Y. Dvorkin, "A chance-constrained stochastic electricity market," *IEEE Transactions on Power Systems (Early Access)*, 2019.
- [20] C. Borraz-Sánchez, R. Bent, S. Backhaus, H. Hijazi, and P. Van Hentenryck, "Convex relaxations for gas expansion planning," *INFORMS Journal on Computing*, vol. 28, no. 4, pp. 645–656, 2016.
- [21] G. P. McCormick, "Computability of global solutions to factorable nonconvex programs: Part I - Convex underestimating problems," *Mathematical Programming*, vol. 10, no. 1, pp. 147–175, 1976.
- [22] A. Ratha, A. Schewe, J. Kazempour, P. Pinson, S. S. Torbaghan, and A. Virag, "Online appendix for paper: Affine policies for flexibility provision by natural gas networks to power systems," 2020. [Online]. Available: <https://doi.org/10.5281/zenodo.3755120>
- [23] P. Pinson, "Wind energy: Forecasting challenges for its operational management," *Statistical Science*, vol. 28, no. 4, pp. 564–585, 11 2013.
- [24] M. K. Singh and V. Kekatos, "Natural gas flow equations: Uniqueness and an MI-SOCP solver," in *2019 American Control Conference (ACC)*, 2019, pp. 2114–2120.
- [25] C. Coffrin, H. L. Hijazi, and P. Van Hentenryck, "Strengthening the SDP relaxation of AC power flows with convex envelopes, bound tightening, and valid inequalities," *IEEE Transactions on Power Systems*, vol. 32, no. 5, pp. 3549–3558, 2017.
- [26] J. E. Mitchell, J.-S. Pang, and B. Yu, "Convex quadratic relaxations of nonconvex quadratically constrained quadratic programs," *Optimization Methods and Software*, vol. 29, no. 1, pp. 120–136, 2014.

[Pub. D] Stochastic Control and Pricing for Natural Gas Networks

Authors:

Vladimir Dvorkin, Anubhav Ratha, Pierre Pinson, and Jalal Kazempour

Published in:

IEEE Transactions on Control of Network Systems (Early Access)

DOI:

10.1109/TCNS.2021.3112764

Stochastic Control and Pricing for Natural Gas Networks

Vladimir Dvorkin, Anubhav Ratha, Pierre Pinson and Jalal Kazempour

Abstract—We propose stochastic control policies to cope with uncertain and variable gas extractions in natural gas networks. Given historical gas extraction data, these policies are optimized to produce the real-time control inputs for nodal gas injections and for pressure regulation rates by compressors and valves. We describe the random network state as a function of control inputs, which enables a chance-constrained optimization of these policies for arbitrary network topologies. This optimization ensures the real-time gas flow feasibility and a minimal variation in the network state up to specified feasibility and variance criteria. Furthermore, the chance-constrained optimization provides the foundation of a stochastic pricing scheme for natural gas networks, which improves on a deterministic market settlement by offering the compensations to network assets for their contribution to uncertainty and variance control. We analyze the economic properties, including efficiency, revenue adequacy and cost recovery, of the proposed pricing scheme and make them conditioned on the network design.

Index Terms—Chance-constrained programming, conic duality, gas pricing, natural gas network, uncertainty, variance.

I. INTRODUCTION

Deterministic operational and market-clearing practices of the natural gas network operators struggle with the growing uncertainty and variability of natural gas extractions [1]. Ignorance of the uncertain and variable extractions results in technical and economical failures, as demonstrated by the congested network during the 2014 polar vortex event in the United States [2]. The recent study [3] shows that expanding the network to avoid the congestion is financially prohibitive, which encourages us to develop stochastic control policies to gain gas network reliability and efficiency in a short run.

Since the prediction of gas extractions involves errors, a gas network optimization problem has been addressed using the methods from robust optimization [4], scenario-based and chance-constrained stochastic programming [5]. Besides forecasts, they require a network response model to uncertainty, i.e., the mapping from random forecast errors to the network state. The robust solutions [6] optimize the network response to ensure the feasibility within robust uncertainty sets, but result in overly conservative operational costs. To alleviate the conservatism, scenario-based stochastic programs [7] optimize the network response to provide the minimum

The authors would like to thank Ana Virág and Hélène Le Cadre for their helpful comments, Jochen Stiasny and Tue Jensen for the advice on visualizations, Robert Mieth and Yury Dvorkin for discussions.

V. Dvorkin is with MIT Energy Initiative and Laboratory for Information and Decision Systems, Cambridge, MA, USA. Email: dvorkin@mit.edu

A. Ratha and J. Kazempour are with the Department of Electrical Engineering, Technical University of Denmark, Lyngby, Denmark. Email: {arath, seykaz}@elektro.dtu.dk

P. Pinson is with the Department of Technology, Management and Economics, Technical University of Denmark, Lyngby, Denmark. Email: ppin@dtu.dk

A. Ratha is also with the Flemish Institute of Technological Research (VITO), Boeretang 200, 2400 Mol, Belgium and with EnergyVille, ThorPark 8310, 3600 Genk, Belgium. {anubhav.ratha}@vito.be

expected cost and ensure feasibility within a finite number of discrete scenarios. The major drawback of robust and scenario-based programs is their ignorance of the network state within the prescribed uncertainty set or outside the chosen scenarios. The chance-constrained programs [8], [9], in turn, yield an optimized network response across the entire forecast error distribution (or a family of those [10]), thus resulting in more advanced prediction and control of uncertain network state.

This work advocates the application of chance-constrained programming to the optimal natural gas network control under uncertainty. By optimal control, we imply the optimization of gas injection and pressure regulation policies that ensure gas flow feasibility and market efficiency for a given forecast error distribution. Towards this goal, we require a network response model with a strong analytic dependency between the network state and random forecast errors. Since natural gas flows are governed by non-convex equations, the design of network response models reduces to finding convex approximations. The work in [8, Chapter 6] enjoys the so-called controllable flow model [11], which balances gas injection and uncertain extractions but disregards pressure variables. It thus does not permit policies for pressure control and corresponding financial remunerations. The work in [9] preserves the integrity of system state variables and relies on the relaxation of non-convex equations. Although the relaxations are known to be tight [12], [13], the results of [9] show that even a marginal relaxation gap yields a poor out-of-sample performance of the chance-constrained solution. Furthermore, the relaxations involve the integrality constraints to model bidirectional gas flows, which prevents extracting the dual solution and thus designing an optimal pricing scheme. One needs to introduce the unidirectional flow assumption to avoid integrality constraints, which is restrictive for gas networks under uncertainty [9].

This work bypasses the simplifying assumptions on network operations through the linearization of the non-convex natural gas equations, and provides a convex stochastic network optimization problem with performance guarantees. The problem ensures the real-time gas flow feasibility, enables the control of network state variability, and provides an efficient pricing scheme. Specifically, we make the following contributions:

- 1) We propose stochastic control policies for gas injections and pressure regulation rates that provide real-time control inputs for network operators. Through linearization, we describe the uncertain state variables, such as nodal pressures and flow rates as affine functions of control inputs; thus capturing the dependency of the uncertain network state on operator's decisions. To establish performance guarantees, we provide a sample-based method to bound approximation errors induced due to linearization.
- 2) We introduce a chance-constrained program to optimize the control policies and provide its computationally efficient second-order cone programming (SOCP) reformu-

lation. The policy optimization ensures that the network state remains within network limits with a high probability and utilizes the statistical moments of the state variables to trade-off between the expected cost and the variance of the state variables.

- 3) We propose a conic pricing scheme that remunerates network assets, i.e., gas suppliers, compressors and valves, for their contribution to uncertainty and variance control. Unlike the standard linear programming duality, the conic duality enables the decomposition of revenue streams associated with the coupling chance-constraints. We analyze the economic properties of the conic pricing scheme, e.g. revenue adequacy and cost recovery, and make them conditioned on the network design.

At the operational planning stage, the optimized policies provide the best approximation (up to forecast quality) of the real-time control actions. They can be augmented into preoperational routines of network operators within the deterministic steady-state [13] or transient [14], [15] gas models in the form of gas injection and pressure regulation set-points, while providing the strong foundation for necessary financial remunerations. We corroborate the effectiveness of the proposed policies using a 48-node natural gas network.

Outline: Section II explains the gas network modeling, while Section III describes the stochastic network optimization, control policies and tractable reformulations. Section IV introduces the pricing scheme and its theoretical properties. Section V provides numerical experiments, and Section VI concludes. All proofs are relegated to Appendix.

Notation: Operation \circ is the element-wise vector (matrix) product. Operator $\text{diag}[x]$ returns an $n \times n$ diagonal matrix with elements of vector $x \in \mathbb{R}^n$. For a $n \times n$ matrix A , $[A]_i$ returns an i^{th} row ($1 \times n$) of matrix A , $\langle A \rangle_i$ returns an i^{th} column ($n \times 1$) of matrix A , and $\text{Tr}[A]$ returns the trace of matrix A . Symbol $^\top$ stands for transposition, vector $\mathbf{1}$ ($\mathbf{0}$) is a vector of ones (zeros), and $\|\cdot\|$ denotes the Euclidean norm.

II. PRELIMINARIES

A. Gas Network Equations

A natural gas network is modeled as a directed graph comprising a set of nodes $\mathcal{N} = \{1, \dots, N\}$ and a set of edges $\mathcal{E} = \{1, \dots, E\}$. Nodes represent the points of gas injection, extraction or network junction, while edges represent pipelines. Each edge is assigned a direction from sending node n to receiving node n' , i.e., if $(n, n') \in \mathcal{E}$, then $(n', n) \notin \mathcal{E}$. The graph may contain cycles, while parallel edges and self-loops should not exist. The graph topology is described by a node-edge incidence matrix $A \in \mathbb{R}^{N \times E}$, such that

$$A_{k\ell} = \begin{cases} +1, & \text{if } k = n \\ -1, & \text{if } k = n' \\ 0, & \text{otherwise} \end{cases} \quad \forall \ell = (n, n') \in \mathcal{E}.$$

Let $\varphi \in \mathbb{R}^E$ be a vector of gas flow rates and let $\delta \in \mathbb{R}_+^N$ be a vector of gas extractions, which must be satisfied by the gas injections $\vartheta \in \mathbb{R}^N$ across the network given their injection limits $\underline{\vartheta}, \bar{\vartheta} \in \mathbb{R}_+^N$. The gas conservation law is thus

$$A\varphi = \vartheta - \delta.$$

The gas flow rates in network edges relate to the nodal pressures through non-linear, partial differential equations [16]. Under steady-state assumptions [13], however, the flows are related to pressures through the Weymouth equation:

$$\varphi_\ell |\varphi_\ell| = w_\ell (\varrho_n^2 - \varrho_{n'}^2), \quad \forall \ell = (n, n') \in \mathcal{E},$$

where $\varrho \in \mathbb{R}^N$ is a vector of pressures contained within technical limits $\underline{\varrho}, \bar{\varrho} \in \mathbb{R}_+^N$, and $w \in \mathbb{R}_+^E$ are constants that encode the friction coefficient and geometry of pipelines. To avoid non-linear pressure drops, let $\pi_n = \varrho_n^2$ be the squared pressure at node n with limits $\underline{\pi}_n = \underline{\varrho}_n^2$ and $\bar{\pi}_n = \bar{\varrho}_n^2$.

To support the desired nodal pressures, the gas network operator regulates the pressure using active pipelines $\mathcal{E}_a \subset \mathcal{E}$, which host either compressors $\mathcal{E}_c \subset \mathcal{E}_a$ or valves $\mathcal{E}_v \subset \mathcal{E}_a$, assuming $\mathcal{E}_c \cap \mathcal{E}_v = \emptyset$. These network assets respectively increase and decrease the gas pressure along their corresponding edges. To rewrite the gas conservation law and Weymouth equation accounting for these components, let $\kappa \in \mathbb{R}^E$ be a vector of pressure regulation variables. Pressure regulation is non-negative $\kappa_\ell \geq 0$ for every compressor edge $\ell \in \mathcal{E}_c$ and it is non-positive $\kappa_\ell \leq 0$ for every valve edge $\ell \in \mathcal{E}_v$. This information is encoded in the pressure regulation limits $\underline{\kappa}, \bar{\kappa} \in \mathbb{R}^E$. Pressure regulation involves an additional extraction of the gas mass to fuel active pipelines. Let matrix $B \in \mathbb{R}^{N \times E}$ relate the active pipelines to their sending nodes accounting for conversion factors, i.e.,

$$B_{k\ell} = \begin{cases} b_\ell, & \text{if } k = n, k \in \mathcal{E}_c \\ -b_\ell, & \text{if } k = n, k \in \mathcal{E}_v \\ 0, & \text{otherwise} \end{cases} \quad \forall \ell = (n, n') \in \mathcal{E},$$

where b_ℓ is a conversion factor from the gas mass to the pressure regulation rate. The network equations become

$$A\varphi = \vartheta - B\kappa - \delta, \quad (1a)$$

$$\varphi \circ |\varphi| = \text{diag}[w](A^\top \pi + \kappa), \quad (1b)$$

$$\varphi_\ell \geq 0, \quad \forall \ell \in \mathcal{E}_a. \quad (1c)$$

Here, the gas extraction $B\kappa$ by compressor and valve edges in (1a) is always non-negative. Equation (1b) is the Weymouth equation in a vector form that accounts for both pressure loss and pressure regulation. The absolute value operator in (1b) is understood element-wise. Finally, equality (1c) enforces the unidirectional condition for the gas flow in active pipelines, because they permit the gas flow only in one direction.

B. Deterministic Gas Network Optimization

The gas network optimization seeks the minimum of gas injection costs while satisfying gas flow equations and network limits. Let $c_1 \in \mathbb{R}_+^N$ and $c_2 \in \mathbb{R}_+^N$ be the coefficients of a quadratic gas injection cost function. With a perfect extraction forecast, the deterministic gas network optimization is

$$\min_{\vartheta, \kappa, \varphi, \pi} c_1^\top \vartheta + \vartheta^\top \text{diag}[c_2] \vartheta \quad (2a)$$

$$\text{s.t. } A\varphi = \vartheta - B\kappa - \delta, \quad (2b)$$

$$\varphi \circ |\varphi| = \text{diag}[w](A^\top \pi + \kappa), \quad (2c)$$

$$\underline{\pi} \leq \pi \leq \bar{\pi}, \quad \underline{\vartheta} \leq \vartheta \leq \bar{\vartheta}, \quad (2d)$$

$$\underline{\kappa} \leq \kappa \leq \bar{\kappa}, \quad \varphi_\ell \geq 0, \quad \forall \ell \in \mathcal{E}_a. \quad (2e)$$

Despite the non-convexity of (2), it has been solved successfully using algorithmic solvers [13], [17] or general-purpose solvers [18] when all optimization parameters are known. These solvers no longer apply when the parameters are uncertain, because one needs to establish a convex dependency of optimization variables on uncertain parameters [19]. This convex dependency is established in this work by means of the linearization of the Weymouth equation (2c).

C. Linearization of the Weymouth Equation

Let $\mathcal{W}(\varphi, \pi, \kappa) = \emptyset$ denote the non-convex constraint (2c), and let $\mathcal{J}(x) \in \mathbb{R}^{E \times n}$ denote the Jacobian of (2c) w.r.t. an arbitrary vector $x \in \mathbb{R}^n$. The relation between the gas flow rates, nodal pressures, and pressure regulation rates can thus be approximated by the first-order Taylor series expansion:

$$\begin{aligned} \mathcal{W}(\varphi, \pi, \kappa) &\approx \mathcal{W}(\dot{\varphi}, \dot{\pi}, \dot{\kappa}) + \mathcal{J}(\dot{\varphi})(\varphi - \dot{\varphi}) \\ &+ \mathcal{J}(\dot{\pi})(\pi - \dot{\pi}) + \mathcal{J}(\dot{\kappa})(\kappa - \dot{\kappa}) = \emptyset, \end{aligned} \quad (3)$$

where $(\dot{\varphi}, \dot{\pi}, \dot{\kappa})$ is a stationary point retrieved by solving non-convex problem (2). As $\mathcal{W}(\dot{\varphi}, \dot{\pi}, \dot{\kappa}) = \emptyset$ at a stationary point, equation (3) implies the affine relation:

$$\begin{aligned} \varphi - \dot{\varphi} &= \mathcal{J}(\dot{\varphi})^{-1} \mathcal{J}(\dot{\pi})(\dot{\pi} - \pi) + \mathcal{J}(\dot{\varphi})^{-1} \mathcal{J}(\dot{\kappa})(\dot{\kappa} - \kappa) \\ \Leftrightarrow \varphi &= \underbrace{\mathcal{J}(\dot{\varphi})^{-1} (\mathcal{J}(\dot{\pi})\dot{\pi} + \mathcal{J}(\dot{\kappa})\dot{\kappa})}_{\gamma_1(\dot{\varphi}, \dot{\pi}, \dot{\kappa})} + \underbrace{\mathcal{J}(\dot{\varphi})^{-1} \mathcal{J}(\dot{\pi})\pi}_{\gamma_2(\dot{\varphi}, \dot{\pi})} + \underbrace{\mathcal{J}(\dot{\varphi})^{-1} \mathcal{J}(\dot{\kappa})\kappa}_{\gamma_3(\dot{\varphi}, \dot{\kappa})} \\ \Leftrightarrow \varphi &= \gamma_1(\dot{\varphi}, \dot{\pi}, \dot{\kappa}) + \gamma_2(\dot{\varphi}, \dot{\pi})\pi + \gamma_3(\dot{\varphi}, \dot{\kappa})\kappa, \end{aligned} \quad (4)$$

where $\gamma_1 \in \mathbb{R}^E$, $\gamma_2 \in \mathbb{R}^{E \times N}$ and $\gamma_3 \in \mathbb{R}^{E \times E}$ are coefficients encoding the sensitivity of gas flow rates to pressures and pressure regulation rates. These coefficients depend on the stationary point. For notational convenience, this dependency is dropped but always implied. In what follows, the Greek letter γ denotes sensitivity coefficients and their transformations.

Remark 1 (Reference node): Since $\text{rank}(\gamma_2) = N - 1$, system (4) is rank-deficient. Since the graph is connected, we have $E > N - 1$, thus resulting in infinitely many solutions to system (4). A unique solution is obtained by choosing a reference node (r) and fixing the reference pressure $\pi_r = \dot{\pi}_r$. The reference node does not host a variable injection or extraction, nor should be a terminal node of active pipelines. In practice, this is a node with a large and constant gas injection.

III. GAS NETWORK OPTIMIZATION UNDER UNCERTAINTY

A. Chance-Constrained Formulation

At the operational planning stage, well ahead of the real-time operations, the unknown gas extractions are modeled as

$$\tilde{\delta}(\xi) = \delta + \xi, \quad (5)$$

where $\delta \in \mathbb{R}^N$ is the mean value of the gas withdrawal rates and $\xi \in \mathbb{R}^N$ is a vector of zero-mean random forecast errors. Equation (5) suffices to model disturbances in gas extractions without an explicit modeling of gas consumption by gas-fired power plants in adjacent electrical power grids. We assume

that the forecast error distribution \mathbb{P}_ξ of ξ and covariance $\Sigma = \mathbb{E}[\xi\xi^\top]$ can be estimated from the historical observations of electrical loads and renewable power generation, that are known to obey Normal, Log-Normal and Weibull distributions [20]. Though, more complex distributions may be envisaged for double-bounded stochastic processes of interest.

Regardless of the type and parameters of the uncertainty distribution, the chance-constrained counterpart of the deterministic gas network optimization in (2) writes as

$$\min_{\tilde{\vartheta}, \tilde{\kappa}, \tilde{\varphi}, \tilde{\pi}} \mathbb{E}^{\mathbb{P}_\xi} [c_1^\top \tilde{\vartheta}(\xi) + \tilde{\vartheta}(\xi)^\top \text{diag}[c_2] \tilde{\vartheta}(\xi)] \quad (6a)$$

s.t.

$$\mathbb{P}_\xi \left[\begin{array}{l} A\tilde{\varphi}(\xi) = \tilde{\vartheta}(\xi) - B\tilde{\kappa}(\xi) - \tilde{\delta}(\xi), \\ \tilde{\varphi}(\xi) = \gamma_1 + \gamma_2\tilde{\pi}(\xi) + \gamma_3\tilde{\kappa}(\xi), \\ \tilde{\pi}_r(\xi) = \dot{\pi}_r \end{array} \right] \stackrel{\text{a.s.}}{=} 1, \quad (6b)$$

$$\mathbb{P}_\xi \left[\begin{array}{l} \bar{\pi} \leq \tilde{\pi}(\xi) \leq \bar{\pi}, \quad \underline{\vartheta} \leq \tilde{\vartheta}(\xi) \leq \bar{\vartheta}, \\ \underline{\kappa} \leq \tilde{\kappa}(\xi) \leq \bar{\kappa}, \quad \tilde{\varphi}_\ell(\xi) \geq 0, \quad \forall \ell \in \mathcal{E}_a \end{array} \right] \geq 1 - \varepsilon, \quad (6c)$$

which optimizes stochastic network variables $\tilde{\vartheta}, \tilde{\kappa}, \tilde{\varphi}$ and $\tilde{\pi}$ to minimize the expected value of the cost function (6a) subject to probabilistic constraints. The almost sure (a.s.) constraint (6b) requires the satisfaction of the gas conservation law and linearized Weymouth equation with probability 1, while the chance constraint (6c) ensures that the real-time pressures together with the injection, pressure regulation and flow rates remain within their technical limits. The prescribed violation probability $\varepsilon \in (0, 1)$ reflects the risk tolerance of the gas network operator towards the violation of network limits.

B. Control Policies and Network Response Model

The chance-constrained problem (6) is computationally intractable as it constitutes an infinite-dimensional optimization problem. To overcome its complexity, it has been proposed to approximate its solution by optimizing stochastic variables as affine, finite-dimensional functions of the random variable [4]. This functional dependency constitutes the model of the gas network response to uncertainty.

The *explicit* dependency on uncertainty is enforced on the controllable variables through the following affine policies

$$\tilde{\vartheta}(\xi) = \vartheta + \alpha\xi, \quad \tilde{\kappa}(\xi) = \kappa + \beta\xi, \quad (7a)$$

where ϑ and κ are the nominal (average) response, while $\alpha \in \mathbb{R}^{N \times N}$ and $\beta \in \mathbb{R}^{E \times N}$ are variable recourse decisions of the gas injections and pressure regulation by active pipelines, respectively. When optimized, policies (7a) provide *control inputs* for the network operator to meet the realization of random forecast errors ξ . As the state variables, such as flow rates and pressures, are coupled with the controllable variables through stochastic equations (6b), they *implicitly* depend on uncertainty through the control inputs.

Lemma 1: Under control policies (7a), the random gas pressures and flow rates are given by affine functions

$$\tilde{\pi}(\xi) = \pi + \gamma_2(\alpha - \gamma_3\beta - \text{diag}[\mathbf{1}])\xi, \quad (7b)$$

$$\tilde{\varphi}(\xi) = \varphi + (\gamma_2(\alpha - \text{diag}[\mathbf{1}]) - \gamma_3\beta)\xi, \quad (7c)$$

both including the nominal and random components, and where $\gamma_2, \hat{\gamma}_2, \dot{\gamma}_2, \gamma_3, \dot{\gamma}_3$ are constants of proper dimensions.

Equations (7) constitute the desired model of the network response to uncertainty. The model is said to be admissible if the stochastic gas conservation law and linearized Weymouth equation in (6b) hold with probability 1, i.e., for any realization of random variable ξ . This is achieved as follows.

Lemma 2: The model of the gas network response (7) is admissible if the nominal and recourse variables obey

$$A\varphi = \vartheta - B\kappa - \delta \quad (8a)$$

$$(\alpha - B\beta)^\top \mathbb{1} = \mathbb{1}, \quad (8b)$$

$$\varphi = \gamma_1 + \gamma_2\pi + \gamma_3\kappa, \quad (8c)$$

$$\pi_r = \dot{\pi}_r, [\alpha]_r^\top = \mathbb{0}, [\beta]_r^\top = \mathbb{0}. \quad (8d)$$

Remark 2: The model of the gas network response (7) does not make an assumption on the uncertainty distribution.

C. Expected Cost Reformulation

The expected value of the gas network cost function in (6a) is computationally intractable as it involves an optimization of infinite-dimensional random variable $\tilde{\vartheta}(\xi)$. Under control policy (7a), however, we show that the computation of the expected cost reduces to solving an SOCP problem.

Due to definition of $\tilde{\vartheta}(\xi)$, function (6a) rewrites as

$$\mathbb{E}^{\mathbb{P}_\xi}[c_1^\top (\vartheta + \alpha\xi) + (\vartheta + \alpha\xi)^\top \text{diag}[c_2](\vartheta + \alpha\xi)],$$

where the argument of the expectation operator is separable into nominal and random components. Due to the linearity of the expectation operator, it equivalently rewrites as

$$c_1^\top \vartheta + \vartheta^\top \text{diag}[c_2]\vartheta + \mathbb{E}^{\mathbb{P}_\xi}[c_1^\top \alpha\xi + (\alpha\xi)^\top \text{diag}[c_2]\alpha\xi].$$

A zero-mean assumption made on distribution \mathbb{P}_ξ factors out the first term under the expectation operator. The reformulation of the second term is made recalling that the expectation of the outer product of the zero-mean random variable yields its covariance, i.e., $\mathbb{E}[\xi\xi^\top] = \Sigma$. Thus, the expected value of cost function (6a) reduces to a computation of

$$c_1^\top \vartheta + \vartheta^\top \text{diag}[c_2]\vartheta + \text{Tr}[\alpha^\top \text{diag}[c_2]\alpha\Sigma],$$

which is a convex quadratic function in variables ϑ and α . To bring it to an SOCP form, let vectors $c^\vartheta \in \mathbb{R}^N$ and $c^\alpha \in \mathbb{R}^N$ substitute the quadratic terms of the gas injection and recourse costs. Moreover, let $F \in \mathbb{R}^{N \times N}$ be a factorization of covariance matrix Σ , such that $\Sigma = FF^\top$, and $\check{c}_2 \in \mathbb{R}^N$ be the factorization of vector c_2 , such that $\text{diag}[c_2] = \check{c}_2\check{c}_2^\top$. Then, for any fixed values of nominal ϑ and recourse α decisions, the expected value of the cost is retrieved by solving the following SOCP problem

$$\min_{c^\vartheta, c^\alpha} c_1^\top \vartheta + \mathbb{1}^\top c^\vartheta + \mathbb{1}^\top c^\alpha \quad (9a)$$

$$\text{s.t. } \|\check{c}_{2n}\vartheta_n\|^2 \leq c_n^\vartheta, \forall n \in \mathcal{N}, \quad (9b)$$

$$\|F[\alpha]_n^\top c_{2n}\|^2 \leq c_n^\alpha, \forall n \in \mathcal{N}, \quad (9c)$$

where (9b) and (9c) are rotated second-order cone constraints. Hence, the co-optimization of variables $\vartheta, \alpha, c^\vartheta$ and c^α results in the minimal expected cost. As problem (9) acts on

a distribution-free response model (Remark 2), it does not require any assumption on the uncertainty distribution.

D. Variance of State Variables

The optimization of response model (7) using the criterion of the minimum expected cost involves the risks of producing highly variable solutions for the state variables. See, for example, the evidences in the power system domain [21], [22]. However, since the state variables (7b) and (7c) are affine in control inputs, they can be optimized to provide the minimal-variance solution. To achieve the desired result, however, it is more suitable to optimize the standard deviations of the state variables as they admit conic formulations.

Let $s^\pi \in \mathbb{R}^N$ and $s^\varphi \in \mathbb{R}^E$ be the variables modeling the standard deviations of pressures and flow rates, respectively. For any fixed values of recourse decisions α and β , the standard deviations of pressures and flows rates are retrieved by solving the following SOCP problem

$$\min_{s^\pi, s^\varphi} \mathbb{1}^\top s^\pi + \mathbb{1}^\top s^\varphi \quad (10a)$$

$$\text{s.t. } \|F[\gamma_2(\alpha - \hat{\gamma}_3\beta - \text{diag}[\mathbb{1}])]_n^\top\| \leq s_n^\pi, \quad (10b)$$

$$\|F[\gamma_2(\alpha - \text{diag}[\mathbb{1}]) - \hat{\gamma}_3\beta]_\ell^\top\| \leq s_\ell^\varphi, \quad (10c)$$

$$\forall n \in \mathcal{N}, \forall \ell \in \mathcal{E},$$

where (10b) and (10c) are second-order cone constraints, which are tight at optimality. Therefore, the co-optimization of variables α, β, s^π and s^φ yields the optimized system response (7) that ensures the minimal-variance solution for the state variables. We finally note that this co-optimization is also distribution-free.

E. Tractable Chance-Constrained Formulation

It remains to reformulate the joint chance constraint (6c) to attain a tractable reformulation. Given network response model (7), one way to satisfy (6c) is to enforce all its N_\leq inequalities on a finite number of samples from \mathbb{P}_ξ [23]. The sample-based reformulation, however, does not explicitly parameterize the problem by the risk tolerance ε of the network operator. We thus proceed by enforcing individual chance constraints with the explicit analytic parameterization of the risk tolerance through individual violation probabilities $\hat{\varepsilon} \in \mathbb{R}_+^{N_\leq}$. This approach admits the Bonferroni approximation of the joint chance constraint in (6c) when $\mathbb{1}^\top \hat{\varepsilon} \leq \varepsilon$. The joint feasibility guarantee is provided even when the choice of the individual violation probabilities is sub-optimal [24], e.g. $\hat{\varepsilon}_i = \frac{\varepsilon}{N_\leq}, \forall i = 1, \dots, N_\leq$.

From [19] we know that a scalar chance constraint

$$\mathbb{P}_\xi[\xi^\top x \leq b] \geq 1 - \hat{\varepsilon} \quad (11a)$$

analytically translates into the second-order cone constraint

$$z_\varepsilon \|Fx\| \leq b - \mathbb{E}_\xi[\xi^\top x], \quad (11b)$$

where $z_\varepsilon \geq 0$ is a safety parameter in the sense of [19], and the left-hand side of (11b) is the margin that ensures constraint feasibility given the parameters of the forecast errors distribution. Consequently, larger safety parameter z_ε improves

system security. The choice of z_ε depends on the knowledge about distribution \mathbb{P}_ξ [19], yet it always increases as the risk tolerance $\hat{\varepsilon}$ reduces.

Given the network response model (7) and the reformulations in (8)–(11), a computationally tractable version of stochastic problem (6) with the variance awareness formulates as the following SOCP problem:

$$\min_{\mathcal{P}} c_1^\top \vartheta + \mathbf{1}^\top c^\vartheta + \mathbf{1}^\top c^\alpha + \psi^{\pi^\top} s^\pi + \psi^{\varphi^\top} s^\varphi \quad (12a)$$

$$\text{s.t. } \lambda^c : A\varphi = \vartheta - B\kappa - \delta, \quad (12b)$$

$$\lambda^r : (\alpha - B\beta)^\top \mathbf{1} = \mathbf{1}, \quad (12c)$$

$$\lambda^w : \varphi = \gamma_1 + \gamma_2 \pi + \gamma_3 \kappa, \pi_r = \dot{\pi}_r, \quad (12d)$$

$$\lambda_n^\pi : \|F[\check{\gamma}_2(\alpha - \hat{\gamma}_3\beta - \text{diag}[\mathbf{1}])]_n^\top\| \leq s_n^\pi, \quad (12e)$$

$$\lambda_\ell^\varphi : \|F[\check{\gamma}_2(\alpha - \text{diag}[\mathbf{1}]) - \hat{\gamma}_3\beta]_\ell^\top\| \leq s_\ell^\varphi, \quad (12f)$$

$$\lambda_n^{\bar{\pi}} : z_\varepsilon \|F[\check{\gamma}_2(\alpha - \hat{\gamma}_3\beta - \text{diag}[\mathbf{1}])]_n^\top\| \leq \bar{\pi}_n - \pi_n, \quad (12g)$$

$$\lambda_n^\pi : z_\varepsilon \|F[\check{\gamma}_2(\alpha - \hat{\gamma}_3\beta - \text{diag}[\mathbf{1}])]_n^\top\| \leq \pi_n - \underline{\pi}_n, \quad (12h)$$

$$\lambda_\ell^\varphi : z_\varepsilon \|F[\check{\gamma}_2(\alpha - \text{diag}[\mathbf{1}]) - \hat{\gamma}_3\beta]_\ell^\top\| \leq \varphi_\ell, \quad (12i)$$

$$\|\dot{c}_{2n}\vartheta_n\|^2 \leq c_n^\vartheta, \quad (12j)$$

$$\|F\dot{c}_{2n}[\alpha]_n^\top\|^2 \leq c_n^\alpha, \quad (12k)$$

$$z_\varepsilon \|F[\alpha]_n^\top\| \leq \bar{\vartheta}_n - \vartheta_n, \quad (12l)$$

$$z_\varepsilon \|F[\alpha]_n^\top\| \leq \vartheta_n - \underline{\vartheta}_n, \quad (12m)$$

$$z_\varepsilon \|F[\beta]_\ell^\top\| \leq \bar{\kappa}_\ell - \kappa_\ell, \quad (12n)$$

$$z_\varepsilon \|F[\beta]_\ell^\top\| \leq \kappa_\ell - \underline{\kappa}_\ell, \quad (12o)$$

$$\forall n \in \mathcal{N}, \forall \ell \in \mathcal{E}, \forall \ell \in \mathcal{E}_a,$$

in variables $\mathcal{P} = \{\vartheta, \kappa, \varphi, \pi, \alpha, \beta, c^\vartheta, c^\alpha, s^\pi, s^\varphi\}$. Problem (12) optimizes the system response model (7) to meet a trade-off between the expected cost and the standard deviation of the state variables up to the given penalties $\psi^\pi \in \mathbb{R}_+^N$ and $\psi^\varphi \in \mathbb{R}_+^E$ for pressures and gas flow rates, respectively. Notice, that the constraints on the optimal recourse with respect to the reference node in (8d) are implicitly accounted for through the conic constraints on the gas injection and pressure regulation (12l)–(12o).

In formulation (12), the Greek letters λ denote the dual variables of the coupling constraints. In the next Section IV, we invoke the SOCP duality theory to establish an efficient pricing scheme for gas networks under uncertainty.

F. Approximation Errors and Performance Guarantees

Lemma 1 hypothesizes the linear dependency of state variables on random forecast errors. Although the linear dependency enables a computationally tractable chance-constrained optimization in (12), it also leads to approximation errors due to non-convex relation between pressures, flows, and uncertain gas extraction rates. To ensure that the optimization of control policies in (7a) makes use of reliable state predictions, we develop *a priori* worst-case performance guarantees that the approximation errors do not exceed a certain threshold.

Since gas network congestions are mostly explained by pressure limits, we specifically focus on approximation errors associated with stochastic pressure variables. Let $\tilde{\pi}^*(\xi)$ be the vector of the optimized stochastic pressures in (7b), i.e.,

$$\tilde{\pi}^*(\xi) = \pi^* + \check{\gamma}_2(\alpha^* - \hat{\gamma}_3\beta^* - \text{diag}[\mathbf{1}])\xi, \quad (13)$$

which models the linear dependency on the optimal solution of problem (12), denoted by $*$, and random forecast error ξ .

For some realization ξ , let $\pi^*(\xi)$ be the actual pressure variables under control inputs from the optimized policies

$$\tilde{\vartheta}^*(\xi) = \vartheta^* + \alpha^*\xi, \quad \tilde{\kappa}^*(\xi) = \kappa^* + \beta^*\xi, \quad (14)$$

where the optimal values are from the solution of problem (12). Pressure variables $\pi^*(\xi)$ can be then retrieved by projecting the optimized control inputs from (14) to the non-convex feasible region specific to realization ξ , i.e, by solving

$$\pi^*(\xi) \in \underset{\vartheta, \kappa, \varphi, \pi}{\operatorname{argmin}} \|\tilde{\vartheta}^*(\xi) - \vartheta\| + \|\tilde{\kappa}^*(\xi) - \kappa\| \quad (15a)$$

$$\text{s.t. } A\varphi = \vartheta - B\kappa - (\delta + \xi), \quad (15b)$$

$$\varphi \circ |\varphi| = \text{diag}[w](A^\top \pi + \kappa), \quad (15c)$$

$$\text{Constraints (12d) -- (12e).} \quad (15d)$$

For any node $n \in \mathcal{N}$, the stochastic pressure approximation error can be then pre-computed as an Euclidean distance

$$\Delta\pi_n(\xi) = \|\tilde{\pi}_n^*(\xi) - \pi_n^*(\xi)\| \quad (16)$$

between the approximation $\tilde{\pi}_n^*(\xi)$ and the actual pressure variable $\pi_n^*(\xi)$ for some forecast error realization ξ .

To provide the worst-case bound on the approximation error, we formulate the following optimization problem

$$\min_t t \quad (17a)$$

$$\text{s.t. } \Delta\pi_n(\xi) - t \leq 0, \quad \forall \xi \in \mathbb{P}_\xi \quad (17b)$$

in single variable t , which identifies that realization ξ from \mathbb{P}_ξ , that results in the largest distance between the linear and non-convex stochastic pressure spaces. Observe, however, that constraint (17b) is infinite as it requires infinitely many samples from \mathbb{P}_ξ . Using a sample-based approach from [25], we provide the following finite counterpart of (17)

$$\min_t t \quad (18a)$$

$$\text{s.t. } \Delta\pi_n(\hat{\xi}_s) - t \leq 0, \quad \forall s = 1, \dots, S, \quad (18b)$$

where $\hat{\xi}_s$ is a discrete sample from \mathbb{P}_ξ , and constraint (18b) is enforced on a finite S number samples (sample complexity), which is chosen to provide probabilistic performance guarantees with high confidence, as per the following Lemma.

Lemma 3 (Adapted from Corollary 1 in [25]): For some $p \in [0, 1]$ and $v \in [0, 1]$, if sample complexity S is such that

$$S \geq \frac{1}{pv} - 1,$$

then with probability $(1-p)$ and confidence level $(1-v)$, the pressure approximation error at node n under the linear law in (7b) will not exceed the optimal solution t^* of problem (18).

IV. PRICING GAS NETWORKS UNDER UNCERTAINTY

From program (12), we know that network assets participate in the satisfaction of the gas network equations (12b)–(12d), in state variance reduction (12e)–(12f), and in ensuring the feasibility of the state variables (12g)–(12i). In this section, we establish a pricing scheme that remunerates network assets

based on the combination of the classic linear programming duality [26], [27] and the SOCP duality [22], [28]. We refer the interested reader to Appendix C for a brief overview on SOCP duality. For presentation clarity, however, we should stress that for each second-order cone constraint in (12e)–(12i) with a dual variable $\lambda \in \mathbb{R}^1$ there exists a vector of dual prices $u \in \mathbb{R}^N$, corresponding component-wise to random vector $\xi \in \mathbb{R}^N$, such that $\|u\| \leq \lambda$. With a set of prices λ, u_1, \dots, u_N , each conic coupling constraint becomes separable, thus enabling the revenue decomposition associated with constraints (12e)–(12i).

We first show that the primal and dual solutions of program (12) solve a *partial* competitive equilibrium. This equilibrium consists of a price-setting problem that seeks the optimal prices associated with the coupling constraints (12e)–(12i), a set of profit-maximizing problems of gas suppliers $n \in \mathcal{N}$, active pipelines $\ell \in \mathcal{E}_a$, and a rent-maximization problem solved by the network operator, as we establish in the proof of the following result; see Appendix D for details. Note, as program (12) does not model consumer preferences explicitly, we provide the results for partial equilibrium only.

Theorem 1 (Partial equilibrium payments): Let \mathcal{P} and \mathcal{D} be the sets of the optimal primal and dual solutions of problem (12), respectively. Then, both sets \mathcal{P} and \mathcal{D} solve a partial competitive network equilibrium with the following payments:

- Each gas supplier $n \in \mathcal{N}$ maximizes the expected profit when receiving the revenue of $\mathcal{R}_n^{\text{sup}}$ as in (19a).
- Each active pipeline $\ell \in \mathcal{E}_a$ maximizes the expected profit when receiving the revenue of $\mathcal{R}_\ell^{\text{act}}$ as in (19b).
- The network operator minimizes the expected network congestion rent, which amounts to $\mathcal{R}^{\text{rent}}$ as in (19c).
- The payment of each consumer $n \in \mathcal{N}$ is minimized when they are charged with $\mathcal{R}_n^{\text{con}}$ as in (19d).

Similarly to a deterministic market settlement, the nominal gas injection or extraction is priced by associated locational marginal price λ^c , while the nominal pressure regulation is priced by the dual variable λ^w of the Weymouth equation. The pricing scheme of Theorem 1, however, goes beyond the deterministic payments and provides three additional revenue streams for network assets (19). First, each network asset is paid with the dual variable λ^r to remunerate its contribution to the feasibility of the gas network equations for any realization of uncertainty; see Lemma 2. The dual variables of the reformulated chance constraints (12g)–(12i) are used to compensate network assets for maintaining gas pressures and flow rates within network limits. Observe, this revenue stream is proportional to the safety parameter z_ε , which increases as risk tolerance $\hat{\epsilon}$ reduces. The last revenue streams for network assets come from the satisfaction of the variance criteria set by the network operator. From the stationarity conditions (28e) from Appendix D, the variance prices are $\lambda^\pi = \psi^\pi$ and $\lambda^\varphi = \psi^\varphi$, and from the SOCP dual feasibility condition (24) from Appendix D we know that $\|[u^\pi]_n\| \leq \lambda_n^\pi$, $\|[u^\varphi]_\ell\| \leq \lambda_\ell^\varphi$, $\forall n \in \mathcal{N}, \ell \in \mathcal{E}$. Thus, these revenue streams are proportional to the variance penalties ψ^π and ψ^φ set by the network operator. The consumer charges, motivated by their individual contributions to uncertainty and state variance, are explained

similarly. Finally notice that, in contrast to the deterministic rent, revenue (19c) additionally includes the variance control rent, which is non-zero whenever constraints (12e)–(12f) are binding, i.e., $\psi^\pi, \psi^\varphi > 0$.

The results of Theorem 1, and thus the equivalence between the centralized optimization (12) and its equilibrium counterpart (25)–(27), hold under certain assumptions. First, there exists at least one strictly feasible solution to SOCP problem (12) or to its dual counterpart to ensure that Slater's condition holds [28]. Second, the market is perfectly competitive and the equilibrium agents act according to their true preferences, i.e., no exercise of market power. Finally, the information on the uncertainty distribution must be consistent among equilibrium problems [29]. Under these assumptions, we analyze the revenue adequacy and cost recovery of payments (19) and make them conditioned on the network design.

Corollary 1 (Revenue adequacy): Let $\gamma_1 = 0$ and $\underline{\pi} = 0$. Then, the payments established by Theorem 1 are revenue adequate, i.e., $\sum_{n=1}^N \mathcal{R}_n^{\text{con}} \geq \sum_{n=1}^N \mathcal{R}_n^{\text{sup}} + \sum_{\ell=1}^E \mathcal{R}_\ell^{\text{act}}$.

As a result, the natural gas system does not incur a financial loss when the payments are distributed from consumers to network assets. The first condition in Corollary 1 is motivated by the linearization of the Weymouth equation. If $\gamma_1 \neq 0$, there exists an extra revenue term $\lambda^w \gamma_1$. As consumers are inelastic, this payment can be thus allocated to consumer charges, however its distribution among the customers remains an open question. Finally, the second condition in Corollary 1 allows pressures to be zero at network nodes, which is too restrictive for practical purposes. In the next Section V we show that the revenue adequacy holds in practice even when this condition is not satisfied.

The surplus of consumer payments in Corollary 1 amounts to the congestion rent minimized by the network operator; see Appendix E for details. The consumer payments are thus implicitly minimized by problem (12) to only cover the congestion rent and compensate network assets for incurred costs. With our last result, we show that the cost recovery for network assets is also conditioned on the network design.

Corollary 2 (Cost recovery): Let $\vartheta = 0$, $\kappa_\ell = 0, \forall \ell \in \mathcal{E}_c$, and $\bar{\kappa}_\ell = 0, \forall \ell \in \mathcal{E}_v$. Then, the payments of Theorem 1 ensure cost recovery for suppliers and active pipelines, i.e., $\mathcal{R}_\ell^{\text{act}} \geq 0, \forall \ell \in \mathcal{E}_a$, and $\mathcal{R}_n^{\text{sup}} - c_{1n} \vartheta_n - c_n^\vartheta - c_n^\alpha \geq 0, \forall n \in \mathcal{N}$.

V. NUMERICAL EXPERIMENTS

We run numerical experiments using a 48-node natural gas network depicted in Fig. 1. The network parameters are sourced from [30] with a few modifications to enable large uncertainty and variability of gas extraction rates and provide more variance control opportunities. Specifically, the pressure limits at nodes 1 and 3 are homogenized with those at the rest of network nodes, two injections are added in the demand area at nodes 32 and 37, and two valves are installed in the pipelines connecting nodes (28, 29) and (43, 44). The 22 gas extractions are modeled as $\tilde{\delta}(\xi) = \delta + \xi$, where δ is the nominal extraction rate reported in [30] and ξ is the zero-mean normally distributed forecast error. The safety parameter z_ε is thus the inverse CDF of the standard Gaussian distribution

$$\mathcal{R}_n^{\text{sup}} \triangleq \underbrace{\lambda_n^c \vartheta_n}_{\text{nominal balance}} + \underbrace{[\lambda^r]^\top [\alpha_n]^\top}_{\text{recourse balance}} + \underbrace{z_{\hat{\varepsilon}} (\langle \check{\gamma}_2 \rangle_n^\top (u^{\bar{\pi}} + u^{\pi}) + \langle \hat{\gamma}_2 \rangle_n^\top u^{\varphi}) F[\alpha]_n^\top}_{\text{gas pressure and flow limits}} + \underbrace{(\langle \check{\gamma}_2 \rangle_n^\top u^{\pi} + \langle \hat{\gamma}_2 \rangle_n^\top u^{\varphi}) F[\alpha]_n^\top}_{\text{gas pressure and flow variance}} \quad (19a)$$

$$\mathcal{R}_{\ell}^{\text{act}} \triangleq \underbrace{((\gamma_3)^\top \lambda^w - \lambda^{c\top} \langle B \rangle_\ell) \kappa_\ell}_{\text{nominal pressure regulation}} - \underbrace{1^\top \langle B \rangle_\ell \lambda^{r\top} [\beta]_\ell^\top}_{\text{recourse balance}} - \underbrace{z_{\hat{\varepsilon}} (\langle \check{\gamma}_2 \hat{\gamma}_3 \rangle_\ell^\top (u^{\bar{\pi}} + u^{\pi}) + \langle \hat{\gamma}_3 \rangle_\ell^\top u^{\varphi}) F[\beta]_\ell^\top}_{\text{gas pressure and flow limits}} - \underbrace{(\langle \check{\gamma}_2 \hat{\gamma}_3 \rangle_\ell^\top u^{\pi} + \langle \hat{\gamma}_3 \rangle_\ell^\top u^{\varphi}) F[\beta]_\ell^\top}_{\text{gas pressure and flow variance}} \quad (19b)$$

$$\mathcal{R}^{\text{rent}} \triangleq \underbrace{(\lambda^{\varphi\top} - \lambda^{w\top} - \lambda^{c\top} A) \varphi}_{\text{flow congestion rent}} + \underbrace{(\lambda^{w\top} \gamma_2 + \lambda^{\pi\top} - \lambda^{\bar{\pi}\top}) \pi + \lambda^{\bar{\pi}\top} \bar{\pi} - \lambda^{\pi\top} \pi}_{\text{pressure congestion rent}} + \underbrace{\lambda^{\varphi\top} s^{\varphi} + \lambda^{\pi\top} s^{\pi}}_{\text{variance rent}} \quad (19c)$$

$$\mathcal{R}_n^{\text{con}} \triangleq \underbrace{\lambda_n^c \delta_n}_{\text{nominal balance}} + \underbrace{\lambda_n^r}_{\text{recourse balance}} + \underbrace{z_{\hat{\varepsilon}} [F]_n (u^{\varphi\top} \langle \check{\gamma}_2 \rangle_n + (u^{\bar{\pi}} + u^{\pi})^\top \langle \check{\gamma}_2 \rangle_n)}_{\text{gas pressure and flow limits}} + \underbrace{[F]_n (u^{\varphi\top} \langle \hat{\gamma}_2 \rangle_n + u^{\pi\top} \langle \check{\gamma}_2 \rangle_n)}_{\text{gas pressure and flow variance}} \quad (19d)$$

Table I
DETERMINISTIC VERSUS CHANCE-CONSTRAINED OPTIMIZATION OF CONTROL POLICIES

Parameter	Unit	Deterministic control policies	Chance-constrained control policies						
			Variance-agnostic	Pressure variance-aware, ψ^π			Flow variance-aware, ψ^φ		
				10^{-3}	10^{-2}	10^{-1}	1	10^1	10^2
Expected cost	\$1000	80.9	82.5 (100%)	100.5%	105.6%	113.8%	100.1%	102.5%	112.6%
$\sum_n \text{Var}[\tilde{\varrho}_n(\xi)]$	MPa ²	217.5	63.4 (100%)	44.2%	18.9%	12.8%	92.8%	46.7%	24.7%
$\sum_{\ell} \text{Var}[\tilde{\varphi}_{\ell}(\xi)]$	BMSCFD ²	26.1	58.0 (100%)	83.4%	64.1%	59.2%	93.4%	44.8%	25.9%
$\sum_{\ell \in \mathcal{E}_c} \sqrt{\kappa_{\ell}}$	kPa	1939	3914	3570	3734	3661	3914	4030	3888
$\sum_{\ell \in \mathcal{E}_v} \sqrt{\kappa_{\ell}}$	kPa	0	0	0	150	576	0	1	500
Constraint inf.	%	53.7	0.04	0.02	0.02	0.02	0.03	0.02	0.03
Average \mathcal{P}_{inj}	MMSCFD	960.91	0.01	0.03	0.02	0.02	0.02	0.04	0.04
Average \mathcal{P}_{act}	kPa	121.68	0.19	0.08	0.10	0.05	0.28	0.04	0.04

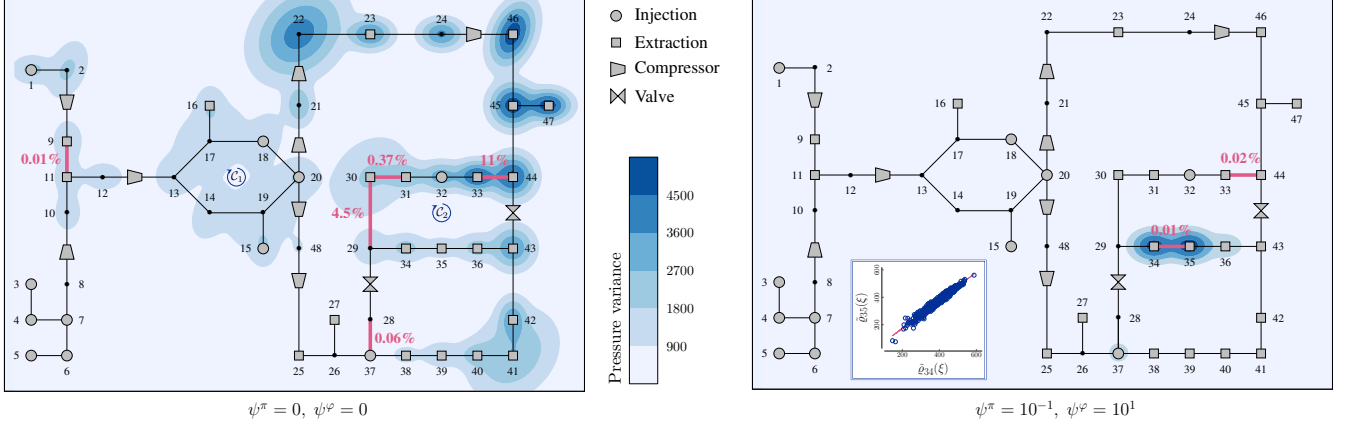


Figure 1. Comparison of the variance-agnostic (left) and the variance-aware (right) chance-constrained control policies in terms of the state variables variance for $\varepsilon = 10\%$. The red values show the probability of flow reversal. The inset plot shows the correlation between the pressures at nodes 34 and 35.

at $(1 - \hat{\varepsilon})$ -quantile [19]. The standard deviation of each gas extraction is set to 10% of the nominal rate. The joint constraint violation probability ε is set to 1% by default. To retrieve the stationary point in (4), the non-convex problem (2) is solved for the nominal gas extraction rates using the Ipopt solver [18]. The repository [31] contains the input data and code implementation in the JuMP package for Julia [32].

A. Analysis of the Optimized Network Response

We first study the optimized gas network response to uncertainty under deterministic and chance-constrained control

policies (7a). The deterministic policies are optimized by setting the safety factor $z_{\hat{\varepsilon}}$ in problem (12) to zero. The policies are compared in terms of the expected cost (9a), the aggregated variance of gas pressures and flow rates $\sum_n \text{Var}[\tilde{\varrho}_n(\xi)]$ and $\sum_{\ell} \text{Var}[\tilde{\varphi}_{\ell}(\xi)]$, respectively, and the total pressure regulation by compressors $\sum_{\ell \in \mathcal{E}_c} \sqrt{\kappa_{\ell}}$ and valves $\sum_{\ell \in \mathcal{E}_v} \sqrt{\kappa_{\ell}}$. Note, we discuss the natural pressure quantities, not their squared counterparts used in optimization. The policies are also compared in terms of network constraints satisfaction. We first sample control inputs from (7) for $S = 1,000$ realizations of forecast errors and count the violations of network limits (6c). Second, we assess the quality of the control inputs (7a) for the non-

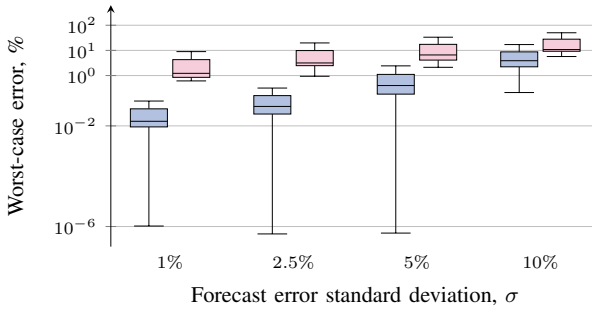


Figure 2. The worst-case stochastic pressure approximation errors summarized across 48 nodes, for $p = v = 0.9$ in Lemma 3, and for different uncertainty penetration levels. The blue boxplots \square summarize error statistics when the chance-constrained control policies are implemented, and red boxplots \blacksquare provide the summary of the deterministic solution.

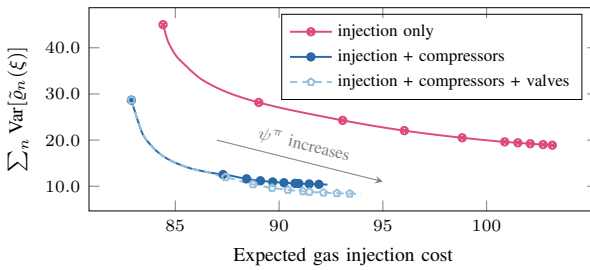


Figure 3. Expected cost versus pressure variance for different assignments of control polices to network assets. Pressure penalty $\psi^\pi \in [10^{-3}, 10^{-1}]$.

convex gas equations, by solving the projection problem (15) for all realizations $\xi_s, \forall s = 1, \dots, S$. A control input is considered feasible if (15a) is zero for a given realization. To characterize this infeasibility numerically, consider the average metrics $\mathcal{P}_{\text{inj}} = \sum_s \|\tilde{\vartheta}(\xi_s) - \vartheta_s\|/S$ for gas injections and $\mathcal{P}_{\text{act}} = \sum_s \|\tilde{\kappa}(\xi_s) - \kappa_s\|/S$ for active pipelines.

The results are reported in Table I. Disregarding uncertainty, the deterministic policies optimize the network operation for the nominal gas extraction rates and thus result in the minimum of cost at the operational planning stage. However, the produced control inputs are infeasible for most of the forecast error realizations. The projections \mathcal{P}_{inj} and \mathcal{P}_{act} of deterministic policies require the real-time correction of gas injections by 31.3% and the real-time correction of pressure regulation by active pipelines by 12.7% of the nominal rates on average. The chance-constrained policies, on the other hand, produce the control inputs that remain feasible with a probability at least $1 - \varepsilon = 99\%$ and require a minimal effort to restore the

real-time gas flow feasibility. This real-time effort is non-zero due to approximation errors induced by linear pressure and flow equations of Lemma 1. Figure 2 illustrates the *worst-case* stochastic pressure approximation errors obtained according to the approach in Section III-F. The errors significantly depend on the amount of uncertainty: with probability 90% and at high confidence, the errors approach 0% for a small uncertainty penetration level ($\sigma = 1\%$), and they will not exceed 5.8% on average for the extremely large uncertainty penetration ($\sigma = 10\%$). The errors under the deterministic solution, which ignores gas extraction uncertainty, are larger by at least an order of magnitude on average.

Table I further demonstrates that the variance-agnostic policy requires only a slight increase of the expected cost relative to the deterministic solution by 1.6%, while the variance-aware policies allow to trade-off the expected operational cost for the smaller variations of pressures and flow rates. The variance of gas pressures and flow rates can be reduced by 63.8% and 7.2%, respectively, without any substantial impact on the expected cost. Observe that the subsequent variance reduction is achieved also due to the activation of valves in two active pipelines, that are not operating in the deterministic and variance-agnostic solutions.

With the density plots in Fig. 1, we demonstrate the uncertainty propagation through the network. The variance-agnostic solution results in the large pressure variance in the eastern part of the network with a large concentration of stochastic gas extractions. This solution further allows the probability of the gas flows reversal up to 11% for certain pipelines, thus making the prediction of flow directions difficult. The variance-aware solution with the joint penalization of pressures and flows variance, in turn, drastically reduces the variation of the state variables and localizes the most of the variation only at nodes 34 and 35. Failure to minimize the pressure variance at these two nodes is due to relatively large approximation errors compared to the rest of the nodes (see the top quantiles of blue boxplots in Fig. 2). Although this variation remains large, the pressures at these nodes are highly correlated. Thus, by Weymouth equation (2c), the flow variance and the probability of flow reversal in edge (34, 35) remain small.

Next, we analyze the contribution of network assets to the variance control through the cost-variance trade-offs in Fig. 3. The figure illustrates these trade-offs when the control policies are assigned to gas injections only ($\alpha \in \text{free}, \beta = 0$), to gas injections and compressors ($\alpha, \beta \in \text{free}, [\beta]_\ell^\top = 0, \forall \ell \in \mathcal{E}_v$), and to all network assets including valves ($\alpha, \beta \in \text{free}$). Observe that the variance reduction is achieved more rapidly and at lower costs as more active pipelines are involved into uncertainty and variance control. Hence, the stochastic control becomes more available as the network operator deploys more pressure regulation action by compressors and valves.

Last, we analyze structural network impacts on the cost-variance trade-offs. We gradually break cycles \mathcal{C}_1 (by removing edges (13, 14) and (14, 19)) and \mathcal{C}_2 (by removing edge (29, 30)) in Fig. 1 to change the network to a tree-like topology, leaving only those cycles that are mandatory for feasible operation. Figure 4 summarizes the cost-variance trade-offs and points on the ambiguous role of network cycles. Breaking

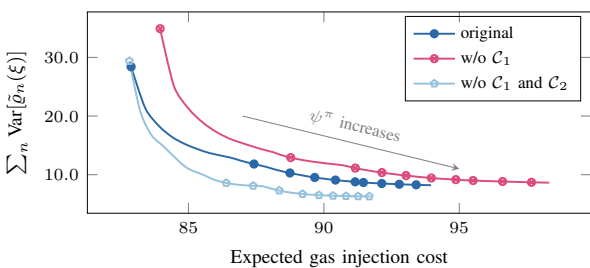


Figure 4. Expected cost versus pressure variance under three network structures. Pressure penalty $\psi^\pi \in [10^{-3}, 10^{-1}]$.

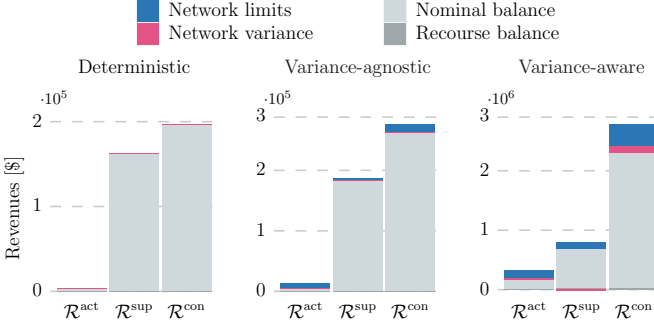


Figure 5. Total payments for active pipelines \mathcal{R}^{act} , suppliers \mathcal{R}^{sup} and consumers \mathcal{R}^{con} under deterministic, chance-constrained variance-agnostic and chance-constrained variance-aware ($\psi^\pi = 0.1, \psi^\varphi = 100$) policies.

cycle \mathcal{C}_1 in the supply concentration area causes congestion, which prevents deploying western suppliers to minimize the pressure variance in the east, substantially increasing the cost of operations. On the other hand, the subsequent removal of cycle \mathcal{C}_2 weakens the graph connectivity and allows for more economical and more drastic variance reduction in the east. This agrees with equation (7b), which relates pressures and forecast errors through parameters $\check{\gamma}_2$ and $\hat{\gamma}_3$, that encode graph connectivity. We notice, the trade-offs in Fig. 3 and 4 motivate the problem of the variance-aware network design.

B. Revenue Analysis

Figure 5 depicts the total revenues of active pipelines and gas injections as well as the total charges of gas consumers. It further shows their decomposition into revenue streams defined by the pricing scheme in (19). Relative to the deterministic payments, the chance-constrained policies lead to a substantial increase in payments that further increase due to the variance awareness. Besides the nominal supply revenues, the chance-constrained policies produce the compensations for the uncertainty and variance control that together exceed deterministic payments by 37.3%. Moreover, the payments for the nominal supply under stochastic policies also increase due to several reasons. First, as shown in Table I, the stochastic policies require a larger deployment of gas compressors and valves that extract an additional gas mass for fuel purposes, up to 4.2% of the network demand, thus increasing the marginal cost of gas suppliers. Second, to provide the security margins for chance constraints (12g)–(12i) and (12l)–(12o), the optimized policies require withholding less expensive injections from the purposes of the nominal supply. Last, with increasing assignments of penalty factors ψ^π and ψ^φ , the optimality of the nominal injection cost is altered in the interest of reduced variance of state variables. Finally, the mismatch between the consumer charges and the revenues of gas injections and active pipelines is non-negative, thus satisfying the revenue adequacy in all three instances.

VI. CONCLUSIONS & OUTLOOK

This work has established the stochastic control policies and pricing scheme for the non-convex steady-state gas network operations under gas extraction uncertainty. The work offers an uncertainty- and variance-aware policy optimization that

ensures the gas flow feasibility with a high probability and minimal variance of the state variables. Moreover, the work challenged the deterministic market settlement and offered financial remunerations to network assets for their contributions to uncertainty and variance control.

The definition and optimization of gas storage control policies under uncertainty constitute the relevant direction for a future work. In addition, a price-responsive modeling of stochastic gas extraction rates, by means of co-optimization of control policies and the stochastic gas consumption models, is a valid research direction. This would lead, for example, to uncertainty- and variance-aware coordination and financial contracts between the gas and power network operators.

APPENDIX

A. Proof of Lemma 1

The substitution of the linearized Weymouth equation from (6b) and policies (7a) into the gas conservation law in (6b) yields stochastic pressures as

$$\begin{aligned} A\tilde{\varphi}(\xi) &= \tilde{\vartheta}(\xi) - B\tilde{\kappa}(\xi) - \tilde{\delta}(\xi) \\ &\Leftrightarrow A(\gamma_1 + \gamma_2\tilde{\pi}(\xi) + \gamma_3(\kappa + \beta\xi)) \\ &\quad = \vartheta + \alpha\xi - B(\kappa + \beta\xi) - \delta - \xi \\ &\Leftrightarrow \underbrace{A\gamma_2}_{\check{\gamma}_2}\tilde{\pi}(\xi) = \underbrace{\vartheta - (B + A\gamma_3)\kappa - \delta - A\gamma_1}_{\text{from (2b),(4) : } A\gamma_2\pi = \hat{\gamma}_2\pi} \\ &\quad + (\alpha - \underbrace{(B + A\gamma_3)\beta - \text{diag}[1]}_{\hat{\gamma}_3})\xi \\ &\Leftrightarrow \hat{\gamma}_2\tilde{\pi}(\xi) = \hat{\gamma}_2\pi + (\alpha - \hat{\gamma}_3\beta - \text{diag}[1])\xi \\ &\Leftrightarrow \tilde{\pi}(\xi) = \pi + \hat{\gamma}_2^{-1}(\alpha - \hat{\gamma}_3\beta - \text{diag}[1])\xi, \end{aligned}$$

where $\hat{\gamma}_2 \in \mathbb{R}^{N \times N}$ and $\hat{\gamma}_3 \in \mathbb{R}^{N \times E}$ are auxiliary constants. As $\hat{\gamma}_2 = A\gamma_2$, it is only invertible for the tree network topology. For generality, consider a reference node (r), see Remark 1, and let $\hat{\gamma}_{2|r}$ be a reduced matrix $\hat{\gamma}_2$ without the rth row and column in $\hat{\gamma}_2$. The invertible counterpart of $\hat{\gamma}_2$ is

$$\check{\gamma}_2 = \begin{bmatrix} \hat{\gamma}_{2|r}^{-1} & \mathbf{0} \\ \mathbf{0}^\top & 0 \end{bmatrix},$$

and the stochastic pressures become

$$\tilde{\pi}(\xi) = \pi + \check{\gamma}_2(\alpha - \hat{\gamma}_3\beta - \text{diag}[1])\xi, \quad (20a)$$

$$\pi_r = \hat{\pi}_r, [\alpha]_r^\top = \mathbf{0}, [\beta]_r^\top = \mathbf{0}, \quad (20b)$$

for an arbitrary network topology. Here, equation (20b) is enforced to satisfy the reference node definition.

To obtain the stochastic flow rates, substitute (20a) into the linearized Weymouth equation in (6b) and rearrange, i.e.,

$$\begin{aligned} \tilde{\varphi}(\xi) &= \gamma_1 + \gamma_2\tilde{\pi}(\xi) + \gamma_3\tilde{\kappa}(\xi) \\ &\Leftrightarrow \tilde{\varphi}(\xi) = \underbrace{\gamma_1 + \gamma_2\pi + \gamma_3\kappa}_{\text{from (4) : } \varphi} + \underbrace{\gamma_2\hat{\gamma}_2}_{\hat{\gamma}_2}(\alpha - \text{diag}[1])\xi \\ &\quad - \underbrace{(\gamma_2\check{\gamma}_2\hat{\gamma}_3 - \gamma_3)\beta\xi}_{\hat{\gamma}_3} \\ &\Leftrightarrow \tilde{\varphi}(\xi) = \varphi + (\hat{\gamma}_2(\alpha - \text{diag}[1]) + \hat{\gamma}_3\beta)\xi, \end{aligned}$$

where $\hat{\gamma}_2 \in \mathbb{R}^{E \times N}$ and $\hat{\gamma}_3 \in \mathbb{R}^{E \times E}$ are constants.

B. Proof of Lemma 2

Consider the stochastic gas conservation law in (6b):

$$A\tilde{\varphi}(\xi) = \tilde{\vartheta}(\xi) - B\tilde{\kappa}(\xi) - \tilde{\delta}(\xi).$$

From the properties of the edge-node incidence matrix A , we know that $\mathbb{1}^\top A\tilde{\varphi}(\xi) = 0$. By summing up N equations above and by substituting equations (7a), we arrive to equation

$$\mathbb{1}^\top \vartheta - \mathbb{1}^\top B\kappa - \mathbb{1}^\top \delta + \mathbb{1}^\top \alpha\xi - \mathbb{1}^\top B\beta\xi - \mathbb{1}^\top \xi = 0,$$

which is separable into nominal and random components:

$$\mathbb{1}^\top \vartheta - \mathbb{1}^\top B\kappa - \mathbb{1}^\top \delta = 0, \quad (21a)$$

$$\mathbb{1}^\top \alpha\xi - \mathbb{1}^\top B\beta\xi - \mathbb{1}^\top \xi = 0, \quad (21b)$$

where equation (21a) is the deterministic gas conservation law, which is alternatively expressed through (1a), thus providing the first condition in (8a). The second condition in (8b) is provided from (21b), which holds for any realization of ξ if the recourse variables α and β obey $(\alpha - B\beta)^\top \mathbb{1} = 1$.

To obtain condition (8c), substitute (7) into the stochastic linearized Weymouth equation in (6b):

$$\begin{aligned} \varphi &= \gamma_1 + \gamma_2\pi + \gamma_3\kappa - \alpha(\dot{\gamma}_2 - \gamma_2\dot{\gamma}_2)\xi \\ &\quad + \beta(\dot{\gamma}_3 - \gamma_2\dot{\gamma}_2\hat{\gamma}_3 + \gamma_3)\xi + (\dot{\gamma}_2 - \gamma_2\dot{\gamma}_2)\text{diag}[\mathbb{1}]\xi \\ &= \gamma_1 + \gamma_2\pi + \gamma_3\kappa, \end{aligned}$$

yielding a deterministic equation due to the definition of constants $\dot{\gamma}_2$ and $\dot{\gamma}_3$. Finally, the stochastic equation for the reference node is satisfied by equations (20b).

C. Dualization of Conic Constraints

The results presented in this section are due to [28, Chapter 5]. Consider the SOCP problem of the form

$$\min_{x \in \mathbb{R}^n} c^\top x, \text{ s.t. } \|A_i x\| \leq b_i^\top x, \quad \forall i = 1, \dots, m, \quad (22a)$$

with $c \in \mathbb{R}^n$, $A_i \in \mathbb{R}^{n_i \times n}$, $b_i \in \mathbb{R}^n$. To dualize the second-order cone constraint, we use the fact that for any pair $\lambda_i \in \mathbb{R}^1$ and $u_i \in \mathbb{R}^{n_i}$ it holds that

$$\begin{aligned} \max_{\substack{u_i, \lambda_i: \\ \|u_i\| \leq \lambda_i}} -u_i^\top A_i x - \lambda_i b_i^\top x &= \max_{\lambda_i \geq 0} -\lambda_i (\|A_i x\| - b_i^\top x) \\ &= \begin{cases} 0, & \text{if } \|A_i x\| \leq b_i^\top x, \\ -\infty, & \text{otherwise.} \end{cases} \end{aligned} \quad (22b)$$

Therefore, the Lagrangian of the SOCP problem writes in variables $x \in \mathbb{R}^n$, $\lambda \in \mathbb{R}^m$ and $u \in \mathbb{R}^{n_i \times n}$ as

$$\max_{\|u_i\| \leq \lambda_i} \min_x \mathcal{L}(x, u, \lambda) = c^\top x - \sum_{i=1}^m (u_i^\top A_i x + \lambda_i b_i^\top x). \quad (22c)$$

Consider another SOCP problem of the form

$$\min_{x \in \mathbb{R}^n} c^\top x, \text{ s.t. } \|A_i x\|^2 \leq b_i^\top x, \quad \forall i = 1, \dots, m, \quad (22d)$$

with the *rotated* second-order cone constraint. To dualize this constraint, we use the fact that for any set of variables $\mu_i \in \mathbb{R}^1$, $\lambda_i \in \mathbb{R}^1$ and $u_i \in \mathbb{R}^{n_i}$ it holds that

$$\max_{\substack{u_i, \mu_i, \lambda_i: \\ \|u_i\|^2 \leq \mu_i \lambda_i}} -u_i^\top A_i x - 1/2\lambda_i - \mu_i b_i^\top x$$

$$= \max_{\lambda_i \geq 0} -\lambda_i (\|A_i x\|^2 - b_i^\top x) = \begin{cases} 0, & \text{if } \|A_i x\|^2 \leq b_i^\top x, \\ -\infty, & \text{otherwise.} \end{cases}$$

Therefore, the Lagrangian of the SOCP problem writes in variables $x \in \mathbb{R}^n$, $\mu, \lambda \in \mathbb{R}^m$ and $u \in \mathbb{R}^{n_i \times n}$ as

$$\begin{aligned} \max_{\|u_i\|^2 \leq \mu_i \lambda_i} \min_x \mathcal{L}(x, u, \mu, \lambda) &= c^\top x \\ &\quad - \sum_{i=1}^m (u_i^\top A_i x + 1/2\lambda_i + \mu_i b_i^\top x). \end{aligned} \quad (22e)$$

D. Proof of Theorem 1

Consider the problem of finding an equilibrium solution among the following set of agents. First, consider a price-setter who seeks the optimal prices to coupling constraints (12b)–(12i) in response to their slacks by solving

$$\begin{aligned} &\max_{\lambda^c, \lambda^r, \lambda^w, \lambda^\varphi, \lambda^\pi, \lambda^\vartheta, \lambda^\bar{\pi}, \lambda^\bar{\vartheta}} \lambda^{c^\top} (A\varphi - \vartheta + B\kappa + \delta) \\ &\quad + \lambda^{r^\top} (\mathbb{1} - (\alpha - B\beta)^\top \mathbb{1}) + \lambda^{w^\top} (\varphi - \gamma_1 - \gamma_2\pi - \gamma_3\kappa) \\ &\quad + \sum_{\ell=1}^E \lambda_\ell^\varphi (s_\ell^\varphi - \|F[\dot{\gamma}_2(\alpha - \text{diag}[\mathbb{1}]) - \dot{\gamma}_3\beta]_\ell^\top\|) \\ &\quad + \sum_{n=1}^N \lambda_n^\pi (s_n^\pi - \|F[\dot{\gamma}_2(\alpha - \hat{\gamma}_3\beta - \text{diag}[\mathbb{1}])]_n^\top\|) \\ &\quad + \sum_{\ell=1}^E \lambda_\ell^\vartheta (\varphi_\ell - z_\varepsilon \|F[\dot{\gamma}_2(\alpha - \text{diag}[\mathbb{1}]) - \dot{\gamma}_3\beta]_\ell^\top\|) \\ &\quad + \sum_{n=1}^N \lambda_n^{\bar{\pi}} (\bar{\pi}_n - \pi_n - z_\varepsilon \|F[\dot{\gamma}_2(\alpha - \hat{\gamma}_3\beta - \text{diag}[\mathbb{1}])]_n^\top\|) \\ &\quad + \sum_{n=1}^N \lambda_n^{\bar{\pi}} (\pi_n - \underline{\pi}_n - z_\varepsilon \|F[\dot{\gamma}_2(\alpha - \hat{\gamma}_3\beta - \text{diag}[\mathbb{1}])]_n^\top\|). \end{aligned} \quad (23)$$

Problem (23) adjusts the prices respecting the slack of each constraint, e.g., $\lambda^c \downarrow$ if $A\varphi - \vartheta + B\kappa > \delta$, and $\lambda^c \uparrow$ otherwise. From SOCP property (22b), we know that the last five terms associated with the conic constraints rewrite equivalently as

$$\begin{aligned} &- \lambda^{\varphi^\top} s^\varphi - \lambda^{\pi^\top} s^\pi - \lambda^{\vartheta^\top} \varphi - \lambda^{\bar{\pi}^\top} (\bar{\pi} - \pi) - \lambda^{\bar{\vartheta}^\top} (\pi - \underline{\pi}) \\ &- \sum_{\ell=1}^E [u^\varphi + z_\varepsilon u^\vartheta]_\ell F[\dot{\gamma}_2(\alpha - \text{diag}[\mathbb{1}]) - \dot{\gamma}_3\beta]_\ell^\top \\ &- \sum_{n=1}^N [u^\pi + z_\varepsilon u^{\bar{\pi}} + z_\varepsilon u^\pi]_n F[\dot{\gamma}_2(\alpha - \hat{\gamma}_3\beta - \text{diag}[\mathbb{1}])]_n^\top, \end{aligned}$$

which is linear and separable, and where the dual variables $u^\varphi, u^\vartheta \in \mathbb{R}^{E \times N}$ and $u^\pi, u^{\bar{\pi}}, u^\pi \in \mathbb{R}^{N \times N}$ are subject to the following dual feasibility conditions

$$\|[u^\pi]_n\| \leq \lambda_n^\pi, \|[u^{\bar{\pi}}]_n\| \leq \lambda_n^{\bar{\pi}}, \|[u^\pi]_n\| \leq \lambda_n^\pi, \quad (24a)$$

$$\|[u^\varphi]_\ell\| \leq \lambda_\ell^\varphi, \|[u^\vartheta]_\ell\| \leq \lambda_\ell^\vartheta, \forall n \in \mathcal{N}, \forall \ell \in \mathcal{E}. \quad (24b)$$

By separating the terms with respect to the variables of network assets, network operator, and free terms associated with each consumer, we obtain the revenue functions in (19). Consider next that each gas supplier $n \in \mathcal{N}$ solves

$$\max_{\vartheta_n, [\alpha]_n, c_n^\vartheta, c_n^\alpha} \mathcal{R}_n^{\text{sup}}(\vartheta_n, [\alpha]_n) - c_{1n}\vartheta_n - c_n^\vartheta - c_n^\alpha \quad (25a)$$

$$\text{s.t. } \lambda_n^\vartheta: \|\dot{c}_{2n}\vartheta_n\|^2 \leq c_n^\vartheta, \quad (25b)$$

$$\lambda_n^\alpha: \|F[\dot{c}_{2n}[\alpha]_n^\top]\|^2 \leq c_n^\alpha, \quad (25c)$$

$$\lambda_n^{\bar{\vartheta}}: z_\varepsilon \|F[\alpha]_n^\top\| \leq \bar{\vartheta}_n - \vartheta_n, \quad (25d)$$

$$\lambda_n^\vartheta: z_\varepsilon \|F[\alpha]_n^\top\| \leq \vartheta_n - \underline{\vartheta}_n, \quad (25e)$$

to maximize the profit in response to equilibrium prices. Next, consider that each active pipeline $\ell \in \mathcal{E}$ solves

$$\max_{\kappa_\ell, [\beta]_\ell} \mathcal{R}_\ell^{\text{act}}(\kappa_\ell, [\beta]_\ell) \quad (26a)$$

$$\text{s.t. } \lambda_{\ell}^{\bar{\kappa}} : z_{\varepsilon} \|F[\beta]_{\ell}^{\top}\| \leq \bar{\kappa}_{\ell} - \kappa_{\ell}, \quad (26b)$$

$$\lambda_{\ell}^{\underline{\kappa}} : z_{\varepsilon} \|F[\beta]_{\ell}^{\top}\| \leq \kappa_{\ell} - \underline{\kappa}_{\ell}, \quad (26c)$$

to maximize the revenue in response to equilibrium prices. Finally, consider a gas network operator which solves

$$\min_{\pi, \varphi, s^{\pi}, s^{\varphi}} \mathcal{R}^{\text{rent}}(\pi, \varphi, s^{\pi}, s^{\varphi}) \quad (27a)$$

$$\text{s.t. } \lambda_r^{\dot{\pi}} : \pi_r = \dot{\pi}_r \quad (27b)$$

to maximize the network rent in response to equilibrium prices. By taking the path outlined in Appendix C, the first-order optimality conditions (FOC) of equilibrium problems (25)–(27) are given by the following equalities

$$\vartheta : c_1 - u^{\vartheta} \circ \dot{c}_2 - \lambda^c + \lambda^{\bar{\vartheta}} - \lambda^{\underline{\vartheta}} = 0, \quad (28a)$$

$$\kappa : [\lambda^{c\top} B]^{\top} - [\lambda^{w\top} \gamma_3]^{\top} + \lambda^{\bar{\kappa}} - \lambda^{\underline{\kappa}} = 0, \quad (28b)$$

$$\pi : \lambda^{\bar{\pi}} - \lambda^{\underline{\pi}} - [\lambda^{w\top} \gamma_2]^{\top} - \mathbb{I}_r \circ \lambda^{\dot{\pi}} = 0, \quad (28c)$$

$$\varphi : [\lambda^{c\top} A]^{\top} + \lambda^w - \lambda^{\underline{\varphi}} = 0, \quad (28d)$$

$$s^{\pi} : \lambda^{\pi} = \psi^{\pi}, \quad s^{\varphi} : \lambda^{\varphi} = \psi^{\varphi}, \quad (28e)$$

$$c^{\vartheta} : \mu^{\vartheta} = 1, \quad c^{\alpha} : \mu^{\alpha} = 1, \quad (28f)$$

$$[\alpha]_n : F(u^{\varphi\top} \langle \gamma_2 \rangle_n + u^{\pi\top} \langle \gamma_2 \rangle_n + z_{\varepsilon}[u^{\bar{\vartheta}} + u^{\underline{\vartheta}}]_n^{\top}) \\ + F[u^{\alpha}]_n^{\top} \dot{c}_2 + \lambda^r = 0, \quad (28g)$$

$$[\beta]_{\ell} : F(u^{\varphi\top} \langle \gamma_3 \rangle_{\ell} + u^{\pi\top} \langle \gamma_2 \gamma_3 \rangle_{\ell} - z_{\varepsilon}[u^{\bar{\kappa}} + u^{\underline{\kappa}}]_{\ell}^{\top}) \\ + \mathbb{1}^{\top} \langle B \rangle_{\ell} \lambda^r = 0, \quad (28h)$$

where vector $\mathbb{I}_r \in \mathbb{R}^N$ takes 1 at position corresponding to the reference node, and 0 otherwise. Conditions (28) are identical to those of centralized problem (12), while the set of FOC of problem (23) yields primal constraints (12b)–(12i). Together with the primal constraints of problems (25)–(27), they are identical to the feasibility conditions of the centralized problem. Hence, problem (12) solves the competitive equilibrium.

E. Proof of Corollary 1

From the feasibility conditions (12b)–(12d) and complementarity slackness conditions associated with constraints (12e)–(12i), we know that the objective function of the price-setting problem in (23) is zero at optimum. By rearranging the terms of (23), we have

$$\sum_{n=1}^N \mathcal{R}_n^{\text{con}} - \sum_{n=1}^N \mathcal{R}_n^{\text{sup}} - \sum_{\ell=1}^E \mathcal{R}_{\ell}^{\text{act}} = \mathcal{R}^{\text{rent}} + \lambda^{w\top} \gamma_1.$$

If let $\gamma_1 = 0$, it remains to show that the congestion rent accumulated by the network is non-negative, i.e.,

$$\underbrace{(\lambda^{\underline{\varphi}\top} - \lambda^{w\top} - \lambda^{c\top} A) \varphi}_{\text{Term A}} + \underbrace{(\lambda^{w\top} \gamma_2 + \lambda^{\bar{\pi}\top} - \lambda^{\bar{\pi}\top}) \pi}_{\text{Term B}} \\ + \underbrace{\lambda^{\bar{\pi}\top} \bar{\pi} - \lambda^{\underline{\pi}\top} \underline{\pi}}_{\text{Term C}} + \underbrace{\lambda^{\varphi\top} s^{\varphi} + \lambda^{\pi\top} s^{\pi}}_{\text{Term D}} \geq 0.$$

From optimality condition (28d), we know that term A is zero. Due to (28c), the term B is zero for all nodes but the reference one, and for the reference node it is $\lambda^{\dot{\pi}\top} \dot{\pi} \geq 0$ from the dual objective function of problem (27). Term D is non-negative, because from (28e) we have that the dual prices λ^{φ} and λ^{π} are non-negative, and variables s^{φ} and s^{π} are lower-bounded

by zero as per (12e) and (12f). In term C, $\lambda^{\bar{\pi}\top} \bar{\pi}$ and $\lambda^{\underline{\pi}\top} \underline{\pi}$ are non-negative due conditions (24a). Thus, the rent is always non-negative if and only if the network design allows $\underline{\pi} = 0$.

F. Proof of Corollary 2

We need to show that the functions (25a) and (26a) are non-negative. Both (25a) and (26a) are lower bounded by their corresponding dual functions, i.e.,

$$(25a) \geq 1/2(\lambda_n^{\vartheta} + \lambda_n^{\alpha}) + \lambda_n^{\bar{\vartheta}} \bar{\vartheta}_n - \lambda_n^{\underline{\vartheta}} \underline{\vartheta}_n, \quad \forall n \in \mathcal{N},$$

$$(26a) \geq \lambda_{\ell}^{\bar{\kappa}} \bar{\kappa}_{\ell} - \lambda_{\ell}^{\underline{\kappa}} \underline{\kappa}_{\ell}, \quad \forall \ell \in \mathcal{E}_a.$$

From the complementary slackness of constraints in (25) and (26), we know that $\lambda^{\vartheta}, \lambda^{\alpha}, \lambda^{\bar{\vartheta}}, \lambda^{\underline{\vartheta}} \geq 0$ and $\lambda^{\bar{\kappa}}, \lambda^{\underline{\kappa}} \geq 0$. As injection limits are all non-negative, function (25a) is non-negative if and only if the network design allows $\underline{\vartheta} = 0$. As pressure regulation limits for compressors and valves are respectively non-negative and non-positive, function (26a) is non-negative if and only if the network design allows $\underline{\kappa}_{\ell} = 0, \forall \ell \in \mathcal{E}_c$ and $\bar{\kappa}_{\ell} = 0, \forall \ell \in \mathcal{E}_v$.

NOMENCLATURE

Sets

\mathcal{E} Set of pipelines.

$\mathcal{E}_a, \mathcal{E}_c, \mathcal{E}_v$ Set of active, compressor-, valve-hosting pipelines.

\mathcal{N} Set of nodes.

Parameters

δ Vector of nominal gas extraction rates.

$\gamma, \hat{\gamma}, \check{\gamma}, \bar{\gamma}$ Linearization coefficients (and their transformations) associated with the Weymouth equation.

\dot{c}_2 Factorization of the 2nd-order cost coefficients.

$\mathcal{R}(\cdot)$ Revenue associated with network agent (\cdot) .

ψ^{π} Vector of pressure variance penalty factors.

ψ^{φ} Vector of flow variance penalty factors.

Σ, F Forecast errors covariance matrix and its factorization.

$\underline{\kappa}, \bar{\kappa}$ Vectors of min. and max. squared regulation limits.

$\underline{\pi}, \bar{\pi}$ Vectors of min. and max. squared pressure limits.

$\rho, \bar{\rho}$ Vectors of min. and max. pressure limits.

$\underline{\vartheta}, \bar{\vartheta}$ Vectors of min. and max. gas injection limits.

$\varepsilon, \hat{\varepsilon}$ Joint and individual constraint violation parameters.

A Node-edge incidence matrix.

B Sending node - active pipeline incidence matrix.

b Vector of gas mass - pressure conversion factors.

c_1, c_2 Vectors of the 1st- and 2nd-order cost coefficients.

p Probability of violating performance guarantee.

S Sample complexity in out-of-sample analysis.

v Confidence level of performance guarantee.

w Vector of pipeline friction coefficients.

z_{ε} Safety parameter in chance constraint reformulation.

Variables

α Matrix of gas injection recourse decisions.

β Matrix of pressure regulation recourse decisions.

κ Vector of pressure regulation rates.

λ, u Vectors and matrices of dual variables.

π Vector of nodal pressures.

φ Vector of gas flows.

ϑ Vector of nodal gas injections.

- c^ϑ, c^α Vectors of 2nd-order nominal and recourse costs.
 s^π Vector of pressure standard deviations.
 s^φ Vector of flow standard deviations.

REFERENCES

- [1] BP Energy Outlook, “2019 edition,” *London, United Kingdom*, 2019.
- [2] PJM Interconnection, “Analysis of operational events and market impacts during the January 2014 cold weather events,” 2014.
- [3] R. Bent *et al.*, “Joint electricity and natural gas transmission planning with endogenous market feedbacks,” *IEEE Trans. Power Syst.*, vol. 33, no. 6, pp. 6397–6409, 2018.
- [4] A. Ben-Tal, L. El Ghaoui, and A. Nemirovski, *Robust optimization*, vol. 28. Princeton University Press, 2009.
- [5] A. Shapiro, D. Dentcheva, and A. Ruszczyński, *Lectures on stochastic programming: modeling and theory*. SIAM, 2014.
- [6] L. A. Roald *et al.*, “An uncertainty management framework for integrated gas-electric energy systems,” *Proc. IEEE*, 2020.
- [7] V. M. Zavala, “Stochastic optimal control model for natural gas networks,” *Comput. Chem. Eng.*, vol. 64, pp. 103 – 113, 2014.
- [8] C. Ordoudis, “Market-based approaches for the coordinated operation of electricity and natural gas systems,” *Ph.D. Thesis*, 2018. Technical University of Denmark.
- [9] A. Ratha *et al.*, “Affine policies for flexibility provision by natural gas networks to power systems,” *Electr. Power Syst. Res.*, vol. 189, 2020. Article no. 106565.
- [10] C. Ordoudis *et al.*, “Energy and reserve dispatch with distributionally robust joint chance constraints,” *Technical Report*, 2018. http://www.optimization-online.org/DB_FILE/2018/12/6962.pdf.
- [11] C. Wang *et al.*, “Strategic offering and equilibrium in coupled gas and electricity markets,” *IEEE Trans. Power Syst.*, vol. 33, no. 1, pp. 290–306, 2017.
- [12] C. Borraz-Sánchez *et al.*, “Convex relaxations for gas expansion planning,” *INFORMS J. Comput.*, vol. 28, no. 4, pp. 645–656, 2016.
- [13] M. K. Singh and V. Kekatos, “Natural gas flow solvers using convex relaxation,” *IEEE Trans. Control. Netw. Syst.*, 2020. to be published.
- [14] A. Zlotnik *et al.*, “Optimal control for scheduling and pricing intraday natural gas transport on pipeline networks,” in *2019 IEEE CDC*, pp. 4887–4884, 2019.
- [15] A. Zlotnik *et al.*, “Pipeline transient optimization for a gas-electric coordination decision support system,” in *PSIG Annual Meeting*, Pipeline Simulation Interest Group, Jun 2019.
- [16] A. Thorley and C. Tiley, “Unsteady and transient flow of compressible fluids in pipelines—a review of theoretical and some experimental studies,” *Int J Heat Fluid Flow*, vol. 8, no. 1, pp. 3–15, 1987.
- [17] M. K. Singh and V. Kekatos, “Natural gas flow equations: Uniqueness and an MI-SOCP solver,” in *2019 IEEE ACC*, pp. 2114–2120, 2019.
- [18] A. Wächter and L. T. Biegler, “On the implementation of an interior-point filter line-search algorithm for large-scale nonlinear programming,” *Math. Program.*, vol. 106, no. 1, pp. 25–57, 2006.
- [19] A. Nemirovski and A. Shapiro, “Convex approximations of chance constrained programs,” *SIAM J. Optim.*, vol. 17, no. 4, pp. 969–996, 2007.
- [20] K. N. Hasan, R. Preece, and J. V. Milanović, “Existing approaches and trends in uncertainty modelling and probabilistic stability analysis of power systems with renewable generation,” *Renewable and Sustainable Energy Reviews*, vol. 101, pp. 168–180, 2019.
- [21] D. Bienstock and A. Shukla, “Variance-aware optimal power flow: Addressing the tradeoff between cost, security, and variability,” *IEEE Trans. Control. Netw. Syst.*, vol. 6, no. 3, pp. 1185–1196, 2019.
- [22] R. Mieth, J. Kim, and Y. Dvorkin, “Risk-and variance-aware electricity pricing,” *Elecrt. Power Syst. Res.*, vol. 189, 2020. Article no. 106804.
- [23] M. C. Campi and S. Garatti, “The exact feasibility of randomized solutions of uncertain convex programs,” *SIAM J. Optim.*, vol. 19, no. 3, pp. 1211–1230, 2008.
- [24] W. Xie, S. Ahmed, and R. Jiang, “Optimized bonferroni approximations of distributionally robust joint chance constraints,” *Math. Program.*, pp. 1–34, 2019.
- [25] G. Calafiore and M. C. Campi, “Uncertain convex programs: randomized solutions and confidence levels,” *Mathematical Programming*, vol. 102, no. 1, pp. 25–46, 2005.
- [26] L. V. Kantorovich, “Mathematical methods of organizing and planning production,” *Manage. Sci.*, vol. 6, no. 4, pp. 366–422, 1960.
- [27] P. A. Samuelson, “Spatial price equilibrium and linear programming,” *The American Economic Review*, vol. 42, no. 3, pp. 283–303, 1952.
- [28] S. Boyd, S. P. Boyd, and L. Vandenberghe, *Convex optimization*. Cambridge university press, 2004.
- [29] V. Dvorkin Jr, J. Kazempour, and P. Pinson, “Electricity market equilibrium under information asymmetry,” *Oper. Res. Lett.*, vol. 47, no. 6, pp. 521–526, 2019.
- [30] S. Wu *et al.*, “Model relaxations for the fuel cost minimization of steady-state gas pipeline networks,” *Math. Comput. Modelling*, vol. 31, no. 2, pp. 197 – 220, 2000.
- [31] *Online repository: Stochastic Control and Pricing for Natural Gas Networks*, 2020 (accessed October 5, 2020). https://github.com/anubhavratha/ng_stochastic_control_and_pricing.
- [32] I. Dunning, J. Huchette, and M. Lubin, “Jump: A modeling language for mathematical optimization,” *SIAM Review*, vol. 59, no. 2, pp. 295–320, 2017.



Vladimir Dvorkin (S’18, M’21) received a Ph.D. degree from the Technical University of Denmark, Lyngby, Denmark, in 2021. He is currently a post-doctoral associate with MIT Energy Initiative and Laboratory for Information and Decision Systems of Massachusetts Institute of Technology, Cambridge, MA, USA. His research interests include economics, game theory, optimization, and their applications to energy systems and markets.



Anubhav Ratha (S’18), received his M.Sc. degree in energy science and technology from ETH Zurich and is currently pursuing his PhD with the Department of Electrical Engineering, Technical University of Denmark. His research focus is on the design of market mechanisms and products for integrated energy systems of the future. Before his PhD studies, he co-founded a startup leveraging behavioral demand response to develop solutions for the green transition of electricity systems.



Pierre Pinson (SM’13, F’20) received his M.Sc. degree in applied mathematics from the National Institute for Applied Sciences, Toulouse, France, and the Ph.D. degree in energetics from Ecole des Mines de Paris, Paris, France. He is a Professor of Operations Research at the Department of Technology, Management and Economics of the Technical University of Denmark, Lyngby, Denmark. His research interests include forecasting, uncertainty estimation, optimization under uncertainty, decision sciences, and renewable energies. He is the Editor-in-Chief for the International Journal of Forecasting.



Jalal Kazempour (SM’18) received the Ph.D. degree in electrical engineering from the University of Castilla-La Mancha, Ciudad Real, Spain, in 2013. He is currently an Associate Professor with the Department of Electrical Engineering, Technical University of Denmark, Lyngby, Denmark. His focus area is the intersection of multiple fields, including power and energy systems, electricity markets, optimization, and game theory.

Department of Electrical Engineering

Center for Electric Power and Energy (CEE)

Technical University of Denmark

Elektrovej, Building 325

DK-2800 Kgs. Lyngby

Denmark

www.elektro.dtu.dk/cee

Tel: (+45) 45 25 35 00

Fax: (+45) 45 88 61 11

E-mail: cee@elektro.dtu.dk